



UNIVERSITAT POLITÈCNICA DE CATALUNYA
BARCELONATECH

Departament d'Enginyeria Electrònica

**“ENERGY MANAGEMENT IN COLLABORATIVE POWER
ELECTRONICS-BASED MICROGRID INTEGRATED WITH
RENEWABLE ENERGIES”**

PhD Student: Navid Salehi

Advisors: Herminio Martínez-García

Guillermo Velasco-Quesada

Department of Electronic Engineering (EEL)

December, 2022

Acknowledgements

I would like to thank the directors of this PhD Thesis, Dr. Herminio Martinez-Garcia and Dr. Guillermo Velasco-Quesada, for the opportunity of being part of Energy Processing and Integrated Circuits (EPIC) research group. His guidance, support and knowledge during the evolution of this thesis has been essential to contribute my development as a researcher.

Thanks to the Universitat Politècnica de Catalunya (UPC), Col·legi d'Enginyers Industrials de Catalunya, and Fundació Caixa d'Enginyers for the 'Premi Beques per a Tesis Doctorals 2019' grant and for funding part of this Thesis.

Thanks to my parents for their everyday help and support during all these challenging years.

Resum

En aquesta tesi es presenta la recerca realitzada en aplicacions de microxarxes, especialment en mode de funcionament cooperatiu. La investigació es porta a terme considerant dos aspectes de l'operació de les microxarxes que han estat fonamentals durant els últims anys. El funcionament fiable i òptim de les microxarxes s'estudia centrant-se en els sistemes de gestió d'energia, específicament en el funcionament col·laboratiu de microxarxes i en les interfícies d'electrònica de potència robustes.

Aquesta tesi presenta una revisió exhaustiva dels mètodes d'optimització per a microxarxes individuals i comunitàries. A més, s'estudien diferents estratègies de control aplicades en sistemes de microxarxes. S'analitzen els avantatges i els inconvenients potencials de diverses estratègies de control i els estudis de fons aporten noves solucions per a un control òptim en una microxarxa connectada a la xarxa de distribució.

Es desenvolupa una estratègia d'agrupació basada en aprenentatge supervisat i no supervisat per controlar una microxarxa connectada a xarxa i formada per microxarxes industrials, comercials i residencials. Aquestes agrupacions es realitzen en funció de la demanda de càrrega màxima i de la reserva operativa de la microxarxa. A més, es presenta un procediment de dimensionament dels elements per a unitats distribuïbles en una microxarxa connectada a la xarxa. L'algorisme proposat avalua el dimensionat de l'element tenint en compte la reserva operativa de les microxarxes. Per disminuir l'efecte advers de la reducció de la mida dels elements sobre la fiabilitat de les microxarxes, el factor de reducció proposat es modifica atenent a la càrrega màxima i a la correlació del perfil de càrrega.

A continuació es presenten un funcionament òptim, una nova topologia i uns nous mètodes de control de diverses interfícies d'electrònica de potència per a la seva aplicació en microxarxes. El funcionament òptim del convertidor ressonant LLC s'investiga tenint en compte la variació de càrrega i la freqüència de commutació. A continuació, es proposa un convertidor DC-DC de font Z en cascada modificat d'alt guany en tensió i baixa tensió d'estres en els interruptors. Finalment, es presenta un nou mètode de control per a un inversor de font Z monofàsica. Una xarxa neuronal feed-

forward predu la resposta forçada del control predictiu generalitzat per millorar el rendiment transitori de l'inversor.

Resumen

En esta tesis se presenta la investigación realizada sobre aplicaciones de microrredes, especialmente en modo de operación cooperativa. La investigación se lleva a cabo considerando dos aspectos de la operación de microrredes que han sido fundamentales en los últimos años. El funcionamiento fiable y óptimo de las microrredes se estudia centrándose en los sistemas de gestión de la energía, específicamente en el funcionamiento colaborativo de las microrredes, y en las interfaces robustas de la electrónica de potencia.

Esta tesis presenta una revisión exhaustiva de los métodos de optimización para microrredes individuales y comunitarias. Además, se estudian diferentes estrategias de control aplicadas en sistemas de microrredes. Se analizan las ventajas y desventajas potenciales de varias estrategias de control, y los estudios de fondo aportan soluciones novedosas para un control óptimo en una microrred conectada a la red de distribución.

Se desarrolla una estrategia de agrupamiento basada en aprendizaje supervisado y no supervisado para controlar una microrred conectada a la red que consta de microrredes industriales, comerciales y residenciales. Estas agrupaciones se realizan en base a la máxima demanda de carga y reserva operativa de la microrred. Además, se presenta un procedimiento de dimensionado de componentes para las unidades despachables en una microrred conectada a la red. El algoritmo propuesto evalúa el dimensionado de cada componente considerando la reserva operativa de las microrredes. Para disminuir el efecto adverso de la reducción del tamaño de los componentes en la fiabilidad de las microrredes, el factor de reducción propuesto se modifica atendiendo a la carga máxima y la correlación del perfil de carga.

A continuación, se presenta el funcionamiento óptimo, la nueva topología y los nuevos métodos de control de varias interfaces de electrónica de potencia para su aplicación en microrredes. Se investiga el funcionamiento óptimo del convertidor resonante LLC considerando la variación de carga y la frecuencia de conmutación. Finalmente, se propone un convertidor CC-CC de fuente Z en cascada modificado de alta ganancia en tensión y baja tensión de estrés en los interruptores. Finalmente, se presenta un nuevo método de control para un inversor de fuente Z monofásico. Una red

neuronal de feed-forward predice la respuesta forzada del control predictivo generalizado para mejorar el rendimiento transitorio del inversor.

Summary

This thesis is introduced the research performed on microgrid applications, especially in cooperative operating mode. The research is conducted considering two main challenging aspects of microgrid operation over the last years. The reliable and optimum operation of microgrids is surveyed by focusing on: energy management systems, specifically in collaborative microgrid operation and robust power electronics interfaces.

This thesis presents a comprehensive review of optimization methods for individual and community microgrids. In addition, different control strategies applied in microgrid systems are studied. The potential pros and cons of various control strategies are analyzed, and the background studies bring brilliant and smart solutions for optimal control in a networked microgrid.

A supervised and unsupervised learning clustering is developed in order to control a networked microgrid consisting of industrial, commercial, and residential microgrids. The clustering algorithms are performed based on the maximum load demand and operating reserve of the microgrid. Furthermore, a component size procedure for dispatchable units in a networked microgrid is presented. The proposed algorithm evaluates the component size considering the operating reserve of microgrids. To diminish the adverse effect of component size reduction on microgrids' reliability, the proposed reduced factor is modified by the peak load and correlation of load profile.

Optimal operation, new topology, and new control methods for various power electronics interfaces for microgrid applications are presented in the following. The optimal operation of the LLC resonant converter is investigated considering the load variation and switching frequency. Then, a modified cascaded high step-up Z-source DC-DC converter with high voltage gain and low voltage stress is proposed. Eventually, a novel control method for a single-phase Z-source inverter is presented. A feed-forward neural network predicts the forced response of the generalized predictive control to enhance the transient performance of the inverter.

Table of Contents

| | |
|--|-----------|
| CHAPTER 1 Introduction | 1 |
| 1. Thesis Background..... | 3 |
| 1.1. Introduction | 3 |
| 1.2. Control Strategies | 6 |
| 1.3. Microgrid Planning | 13 |
| 1.4. Optimization Techniques for Microgrids | 15 |
| A. Probabilistic Methods | 17 |
| B. Deterministic Methods | 17 |
| C. Evolutionary Approaches | 19 |
| C.1. Penalty Function | 19 |
| C.2. Feasibility Method | 20 |
| C.3. Multi-Objective Optimization Methods | 21 |
| C.3.1. Decomposition Approaches | 22 |
| C.3.1.1. Weighted Sum | 22 |
| C.3.1.2. Weighted Metric Method | 23 |
| C.3.1.3. ε -Constraint | 24 |
| C.3.2. Direct Approach | 25 |
| D. Co-Evolutionary Approaches..... | 27 |
| 1.5. Feature Selection and Clustering Algorithms..... | 30 |
| 2. Power Electronics Interface for MGs..... | 32 |
| 2.1. Step-up DC-DC Converters..... | 34 |
| 3. Conclusion | 38 |
| 4. References | 39 |
| | |
| CHAPTER 2 Objective and Thesis Structure | 50 |
| 1. Thesis Objective and Methodology | 50 |
| 2. Thesis Contribution and Thesis Structure | 51 |
| | |
| CHAPTER 3 Networked Microgrid Energy Management Based on Unsupervised Learning Clustering | 54 |
| 3.1. Introduction..... | 54 |
| 3.2. Contributions to the State of Art..... | 54 |
| 3.3. References | 55 |
| 3.4. Journal Paper: Networked Microgrid Energy Management Based on Unsupervised Learning Clustering..... | 57 |
| 1. Introduction | 57 |
| 2. System Configuration, Clustering Methods, and System Operation..... | 59 |
| 2.1. System Configuration | 59 |
| 2.2. K-means Clustering Algorithm | 60 |
| 2.3. Self-organizing Map Algorithm | 61 |
| 2.4. Control Strategy and Energy Management Algorithm..... | 62 |
| 2.4.1. Load and Energy Generation Units Analysis | 62 |
| 2.4.2. MGs Clustering by K-means and SOM Algorithm..... | 64 |
| 2.5. MGs Clustering Optimization by EMS | 64 |
| 3. Results Analysis | 65 |
| 4. A Comparative Analysis..... | 67 |
| 5. Conclusion..... | 69 |

| | |
|--------------------|----|
| Nomenclature | 70 |
| References | 70 |

CHAPTER 4 Component Sizing of Isolated Networked Hybrid Microgrid Based on Operating Reserve Analysis72

| | |
|---|----|
| 4.1. Introduction | 72 |
| 4.2. Contributions to the State of Art | 72 |
| 4.3. References | 73 |
| 4.4. Journal Paper: Component Sizing of Isolated Networked Hybrid Microgrid Based on Operating Reserve Analysis | 75 |
| 1. Introduction | 75 |
| 2. Proposed Optimal Sizing Procedure of an NHMG | 77 |
| 2.1. Optimal Sizing of Hybrid Individual MGs..... | 79 |
| 2.2. Optimal Operation of HIMGs | 81 |
| 2.3. Evaluation of the HIMG Operation (RF Calculation)..... | 82 |
| 3. Evaluation and Simulation Results..... | 83 |
| 4. Verification of the Results in the NHMG..... | 85 |
| 4.1. Simulation Results..... | 86 |
| 4.2. Practical Results | 87 |
| 5. Conclusion..... | 89 |
| Nomenclature | 89 |
| References | 90 |

CHAPTER 5 A Comparative Study of Different Optimization Methods for Resonance Half-Bridge Converter92

| | |
|---|-----|
| 5.1. Introduction..... | 92 |
| 5.2. Contributions to the State of Art | 92 |
| 5.3. References | 93 |
| 5.4. Journal Paper: A Comparative Study of Different Optimization Methods for Resonance Half-Bridge Converter | 95 |
| 1. Introduction | 95 |
| 2. Operating Different Modes of LLC Resonant Converter..... | 96 |
| 3. LLC Resonant Half-Bridge Converter Design Procedure by FHA Technique | 97 |
| 4. Introducing Optimization Methods | 98 |
| 4.1. The Lagrangian Method | 99 |
| 4.2. Least Squares Quadratic (LSQ) Optimization | 99 |
| 4.3. Modified LSQ Optimization | 99 |
| 4.4. Monte Carlo Optimization..... | 100 |
| 5. Power-Loss Calculation..... | 100 |
| 6. Simulation Results..... | 101 |
| 7. Experimental Results..... | 106 |
| 8. Conclusions | 107 |
| Abbreviations | 107 |
| References | 107 |

CHAPTER 6 Modified Cascaded Z-Source High Step-Up Boost Converter109

| | |
|--|-----|
| 6.1. Introduction..... | 109 |
| 6.2. Contributions to the State of Art | 109 |
| 6.3. References..... | 110 |

| | |
|---|------------|
| 6.4. Journal Paper: Modified Cascaded Z-Source High Step-Up Boost Converter | 112 |
| 1. Introduction | 112 |
| 2. Proposed Converter and Principle of Operation | 114 |
| 3. The Proposed Converter Analysis and Design Considerations | 118 |
| 3.1. Conversion Ratio | 118 |
| 3.2. Voltage Stresses of Switch and Diodes | 120 |
| 3.3. Converter Analysis and Design Guideline | 121 |
| 3.4. High Step-up Converters Comparison..... | 121 |
| 4. Experimental Results..... | 122 |
| 5. Conclusion..... | 124 |
| References | 125 |
| | |
| CHAPTER 7 Neural Networks-Generalized Predictive Control for MIMO Grid-connected Z-source Inverter Model | 127 |
| 7.1. Introduction..... | 127 |
| 7.2. Contributions to the State of Art..... | 127 |
| 7.3. References..... | 129 |
| 7.4. Conference Paper: Neural Networks-Generalized Predictive Control for MIMO Grid-connected Z-source Inverter Model | 130 |
| Introduction | 130 |
| MIMO Z-source Inverter Model | 131 |
| Proposed Neural Networks-Generalized Predictive Model | 133 |
| Performance Evaluation and Simulation Results | 134 |
| Conclusion..... | 136 |
| References | 136 |
| | |
| CHAPTER 8 Conclusion and Future Work | 138 |
| | |
| CHAPTER 9 Publications | 142 |

List of Figures

| | |
|---|-----------|
| CHAPTER 1 Introduction | 1 |
| Fig. 1: Master-slave control structure..... | 7 |
| Fig. 2: P2P control structure | 8 |
| Fig. 3: Hierarchical control structure..... | 9 |
| Fig. 4: Planning and scheduling program in MGs..... | 14 |
| Fig. 5: Cost and profit functions in MGs..... | 14 |
| Fig. 6: Optimization problem classification | 16 |
| Fig. 7: Constraint optimization classification..... | 17 |
| Fig. 8: Sample Pareto-front for two objective functions | 21 |
| Fig. 9: Multi-objective optimization methods | 22 |
| Fig. 10: Co-evolutionary Algorithm..... | 28 |
| Fig. 11: Clustering methods..... | 31 |
| Fig. 12: Typical structure of a power electronics-based DC MG [182] | 33 |
| Fig. 13: Typical structure of a power electronics-based AC MG [182] | 33 |
| Fig. 14: structures of electronically-coupled DER units [182]..... | 34 |
| Fig. 15: Voltage boost techniques classification for DC-DC converters [190]..... | 35 |
| Fig. 16: Z-source converter structure [192]..... | 35 |
| Fig. 17: Different magnetically coupled impedance source networks, (a) Trans-Z-source, (b) Γ -source, (c) Y-source, (d) Quasi-Y-source [190] | 35 |
| Fig. 18: The proposed ZVT high step-up three level coupled-inductor-based boost converter [195] | 36 |
| Fig. 19: The schematic of the high step-up converter presented in [196] | 37 |
| Fig. 20: Flyback-boost converter topology [197]..... | 37 |
| Fig. 21: Flyback-boost converter with voltage multiplier topology [198] | 38 |
| | |
| CHAPTER 2 Objective and Thesis Structure | 50 |
| Fig. 1. Thesis structure | 53 |
| | |
| CHAPTER 3 Networked Microgrid Energy Management Based on Unsupervised Learning Clustering | 54 |
| Fig. 1. Star-connected configuration of NMG..... | 60 |
| Fig. 2. K-means algorithm..... | 61 |
| Fig. 3. SOM algorithm..... | 61 |
| Fig. 4. Control strategy of individual MGs | 63 |
| Fig. 5. Residential, commercial, and industrial load pattern | 63 |
| Fig. 6. K-means and SOM clustering for time steps 1, 8, and 16..... | 67 |
| Fig. 7. MLD and OR of MG1 and MG2 in individual and clustered operating mode | 68 |
| Figure 8. MLD and OR of MG3, MG5, MG6, and MG8 in individual and clustered operating mode | 68 |
| Figure 9. MLD and OR of MG4 and MG7 in individual and clustered operating mode | 69 |

CHAPTER 4 Component Sizing of Isolated Networked Hybrid Microgrid Based on Operating Reserve Analysis72

Fig. 1. This is a figure. Schemes follow the same formatting78
Fig. 2. Proposed algorithm of NMG optimal sizing78
Fig. 3. Power management algorithm for HIMG81
Fig. 4. Load profile for each MG of NMG82
Fig. 5. Optimal operation of HIMG, (a) MG₁, (b) MG₂, (c) MG₃.....84
Fig. 6. hybrid control strategy in NHMG85
Fig. 7. Optimal operation of HIMG, (a) MG₁, (b) MG₂, (c) MG₃.....86
Fig. 8. Implemented structure of the NHMG88
Fig. 9. Laboratory experiments configuration88
Fig. 10. Practical results of HIMG, (a) MG₁, (b) MG₂, (c) MG₃.....88

CHAPTER 5 A Comparative Study of Different Optimization Methods for Resonance Half-Bridge Converter92

Fig. 1. LLC resonant half-bridge converter97
Fig. 2. LLC resonant half-bridge converter97
Fig. 3. Equivalent circuit of LLC resonant converter98
Fig. 4. Optimization procedure of LLC resonant half-bridge converter102
Fig. 5. The efficiency at different load conditions105
Fig. 6. Photo of the implemented prototype106
Fig. 7. Input and output voltage and current of LLC resonant converter in CCMA106
Fig. 8. Measured optimized efficiency of the implemented prototype.....106

CHAPTER 6 Modified Cascaded Z-Source High Step-Up Boost Converter109

Fig. 1. Two cascaded Z-source high step-up converter114
Fig. 2. Modified converter by clamp capacitor114
Fig. 3. Circuit diagram of proposed converter with equivalent circuit of coupled-inductors115
Fig. 4. Equivalent circuits of the proposed converter for each operation mode.....116
Fig. 5. Theoretical waveforms of the proposed converter117
Fig. 6. Voltage gain of proposed converter for different turn ratio of coupled inductors119
Fig. 7. Voltage gain of proposed converter vs. converters in [12], [18]-[19].....119
Fig. 8. Voltage stress of the switch for different turn ratio of coupled inductors.....120
Fig. 9. Voltage stress of the switch in proposed converter and converters in [12], [18]-[19].....121
Fig. 10. Implemented prototype of the proposed converter122
Fig. 11. Input Voltage and current of the converter123
Fig. 12. Voltage and current waveform of the diode D₁.....123
Fig. 13. Voltage and current waveform of the switch Q123
Fig. 14: Voltage and current waveform of the diode D₄124
Fig. 15. Output voltage and current waveform of the high step-up converter124
Fig. 16. Efficiency plot of the implemented prototype under different load conditions124

CHAPTER 7 Neural Networks-Generalized Predictive Control for MIMO Grid-connected Z-source Inverter Model127

Fig. 7.1: Inverter classifications128
Fig. 1: Single-phase grid-connected z-source inverter132
Fig. 2: Pole and zero trajectories with system parameters variations133
Fig. 3: Neural networks structure to predict the control signals135
Fig. 4: Proposed NN-GPC135
Fig. 5: Simulation results of ZSI control by GPC136
Fig. 6: Simulation results of ZSI control by NN-GPC136

List of Tables

CHAPTER 1 Introduction1

| | |
|---|----|
| Table 1. Control strategies in MGC application..... | 11 |
| Table 2. Commercial software for MG's planning..... | 15 |
| Table 3. Violation and Optimization Problem..... | 19 |
| Table 4. Optimization in MGC application | 27 |
| Table 5. Optimization in MGC application | 28 |
| Table 6. Feature selection and clustering methods in multi-objective optimization | 31 |

CHAPTER 3 Networked Microgrid Energy Management Based on Unsupervised Learning Clustering54

| | |
|--|----|
| Table 1: Component size of MGs and VPP..... | 60 |
| Table 2: Maximum load demand (MLD) and operating reserve (OR) of MGs for different step time | 66 |
| Table 3: K-means and SOM clustering results | 66 |
| Table 4: Energy management comparison | 68 |

CHAPTER 4 Component Sizing of Isolated Networked Hybrid Microgrid Based on Operating Reserve Analysis72

| | |
|---|----|
| Table 1: Power output and cost function of power generation units in a HIMG | 79 |
| Table 2: Parameter definitions in Table 1 | 79 |
| Table. 3: HIMG optimal design by HOMER | 80 |
| Table 4: Economical and constraints parameters | 80 |
| Table. 5: HIMGs specifications | 84 |
| Table. 6: Optimal operation of NHMG | 87 |

CHAPTER 5 A Comparative Study of Different Optimization Methods for Resonance Half-Bridge Converter92

| | |
|--|-----|
| Table 1. Procedure of LLC resonant half-bridge converter design [14] | 98 |
| Table 2. Power-loss equations of LLC resonant half-bridge converter [12,23]..... | 100 |
| Table 3. Load condition, constraints and switching frequency range | 101 |
| Table 4. List of components | 102 |
| Table 5. Losses Profile of LLC resonant converter by Lagrangian optimization method | 103 |
| Table 6. Losses Profile of LLC resonant converter by LSQ optimization method..... | 103 |
| Table 7. Losses Profile of LLC resonant converter by modified LSQ optimization method..... | 104 |
| Table 8. Losses Profile of LLC resonant converter by Monte Carlo optimization method | 104 |

CHAPTER 6 Modified Cascaded Z-Source High Step-Up Boost Converter109

Table 1. Comparison of proposed converter with other z-source DC-DC converters ..122

Table 2. Important parameters of the implemented prototype123

CHAPTER 7 Neural Networks-Generalized Predictive Control for MIMO Grid-connected Z-source Inverter Model127

Table 1. Z-source inverter and NN-GPC specifications.....136

Table 2. Comparison of GPC and NN-GPC characteristics136

Chapter 1

Introduction

Over time, increasing the world's energy demand resulted in changes in the conventional power system by introducing the concept of distributed generation (DG) and microgrids. Microgrids are small-scale power systems involving generation systems and loads. With significant distance reduction in generation and consumption, power loss is reduced considerably in microgrids; however, the complexity of the power system rises, especially when the microgrid is integrated with renewable energies in order to suppress the environmental problems which are caused by traditional generation.

Microgrids are distinguished from two points of view, specifically: the capability of supplying their own demand loads – stand-alone operation mode—and the capability of transferring their surplus energy to the grid – grid-connected operation mode—. Moreover, microgrids can switch between these two states effectively in different operation conditions. Thus, in microgrid systems, the existence of an energy storage system is essential for diverse purposes, such as the immune transition between isolated and grid-connected modes, providing power balance, and reducing the impact of uncertainty in renewable energy generation.

Therefore, in order to increase the efficiency, reliability, and security of microgrid operation, applying an energy management system (EMS) is inevitable. The EMS is able to handle the power flow of microgrid components based on the defined algorithms to optimize the microgrid operation.

Furthermore, the EMS can be utilized intelligibly to coordinate several MGs, known as networked MG (NMG). However, the complexity of the EMS algorithm increases in NMG, and managing the surplus energy of each individual MG can bring multiple advantages to the NMG system for both grid-connected and stand-alone operation modes. Increasing reliability and decreasing capital, replacement, operational, and maintenance (O&M) costs are the main issues discussed in this thesis.

In addition, apart from efficient energy management algorithms in MG systems and their consequence advantages, power electronics converters are played a prominent role in the optimal and reliable operation of MGs. Inverters (DC/AC converters) are inevitably utilized in MGs integrated with renewable energies. Inverters are responsible

for providing the proper AC voltage for consumers for both grid-connected and isolated operation modes of MGs. Furthermore, in NMG operation mode the power-sharing amongst MGs makes the transient performance of inverters unfavorable. Therefore, in this thesis, a control method based on the model predictive control approach is presented to suppress the transient operation of the Z-source-based inverter in both grid-connected operation mode and MG's power exchange in NMG.

Moreover, isolated and non-isolated DC-DC converters are widely employed in low-power and medium-power hybrid MGs such as residential MGs. Although the parallel connection of PV panels in these MGs increase the efficiency and reliability of the PV system, the low voltage generation of panels leads to utilizing a power electronics interface to level up the voltage for inverter operation. In addition, in NMG the size of the components such as PV panels are prone to be reduced due to the possibility of energy sharing. Therefore, the parallel connection of PV panels and low-level voltage production of the PV system, inevitably make utilizing step-up converters mandatory. Consequently, efficient step-up converters are necessarily momentous in hybrid MGs.

This thesis consists of two main parts. Firstly, the various EMS methods and optimization algorithms for individual and collaborative MGs are elaborated and defined. An energy management system for NMG with the aid of artificial intelligence is proposed to increase the system's reliability. Then, an optimal component sizing in collaborative MGs is analyzed by considering the operating reserve of each individual MG.

It has to be mentioned that the introduction of the first part related to the energy management in networked microgrids involves the published paper by thesis author. This paper is entitled by 'A comprehensive review of control strategies and optimization methods for individual and community microgrids' published in IEEE Access in 2022.

Secondly, various novel topologies and control methods are discussed for AC-DC and DC-DC converters that are widely utilized as power electronics converters in MGs. An intelligence control algorithm for a Z-source grid-connected inverter is proposed to enhance the transient operation of the inverter. This inverter's control method can be effectively employed for NMG to suppress the voltage transient of inverters due to consecutive power references determined by EMS. Furthermore, a novel topology for a non-isolated high step-up converter with low-stress voltage for semiconductor devices

and high voltage gain is investigated in the second part. In addition, a comparative study for LLC resonant converters as a highly efficient isolated power electronics interface in MGs is presented. Utilizing isolated or non-isolated converters is depended on the norms and requirements of the MG system.

1. THESIS BACKGROUNG

1.1. INTRODUCTION

As a response to rapid energy consumption in recent years, microgrids (MGs) appear as an alternative solution in order to reduce the adverse effect of using fossil fuels in conventional power plants and their adverse consequences on the environment. The significant advances in the power electronics interfaces in MG applications led to integrating renewable energies (REs) such as PV, WT, and FC into MGs [1-3]. Therefore, MGs develop great changes in the paradigm of conventional power systems. The unilateral power flow between power plants and consumers has changed to the reciprocal power flow between the power system and MGs [4, 5].

Harvesting energy from renewable energy sources (RES) brings out multiple difficulties associated with the operation and reliability of MGs. Uncertainty and the intermittent nature of REs disrupt the conventional methods for planning the MGs operation. The investigation to suppress the difficulties has commenced from the first moments of MG's emergence. Utilizing an energy storage system (ESS) can effectively improve employing REs due to the controllability of energy storage units such as batteries and fuel cells (FC). The controllable energy generator units such as capacity storage and backup units like diesel generators (DGs) efficiently can maintain the balance between electricity supply and demand in MGs integrated with REs [6, 7].

MGs clustering is an advanced concept to take advantage of the cooperative operation of adjacent MGs. The possibility of mutual power-sharing among a community microgrid provides a number of interests for MGs. Increasing the penetration ratio of REs into the MGs and distribution network, achieving MGs' reliable and efficient operation, and providing backup power to prioritized critical loads are some features that can offer by the microgrid community (MGC) concept [8-10]. Moreover, MGC can provide certain profits from the distribution network and utility grid perspective. Providing convenient replication and scaling across any distribution

network and surrounding the distribution and substation area to provide reliable service for customers are the benefits can gain by MGC [11].

In order to achieve the expected goals, which are conceivable by MG and MGC concept, applying an energy management system (EMS) is inevitable [12]. EMS has to ensure the optimal and economical operation of MGs according to the defined MGs plan and schedule. The planning process must be addressed to economic feasibility regarding the geographical conditions, allocated area, and the existence of energy resources (PV, WT, DG, and ESS) [13, 14]. On the other hand, scheduling concentrates more on the available energy resources in order to minimize operational costs [15].

The EMS has to solve the optimization problem considering the short-term and long-term attributes in planning and scheduling program. From a short-term perspective avoiding mismatch in power demand and supply is the primary purpose. In grid-connected operation mode, the active and reactive power has to be controlled in order to balance the demand and supply, and voltage and frequency are determined by the main grid. However, in stand-alone operation mode, voltage and frequency also have to be controlled as well as active and reactive power to stabilize the system. Therefore, the control strategy in stand-alone operation is more intricate [16]. From a long-term perspective, economic issues play a more prominent role [17].

The optimization problem ascertains the optimal solutions for specific decision variables in EMS considering the practical and technical constraints, uncertainties, goals, and alternatives. Moreover, solving the optimization problem will be the more involved procedure by taking network communication delays into consideration [18, 19]. A wide variety of optimization methods could be exploited for EMS. However, using an appropriate method in order to fulfill the requirements is a challenging issue.

Various researches have been carried out associated with MG and MGC application in respect of the MGC architecture [20], control strategies [21], computational optimization [22], and communication strategies [23]. A comprehensive review of MG and virtual power plant concepts was conducted in [24], and scheduling problems associated with the formulation and objective functions, solving methods, uncertainty, reliability, reactive power, and demand response are studied. Samir et al. in [25] conducted a review on hybrid renewable MG optimization techniques considering the probabilistic, deterministic, iterative, and artificial intelligence (AI) methods. A survey on significant benefits and challenges related to the MGC operation and control is

presented in [8]. Carlos et al. reviewed the computational techniques applied to MG planning in [26]. Distributed communication network characteristics, classification of distributed control strategies, and communication reliability issues are discussed in [27]. A comprehensive study on the classification of optimized controller approaches concerning the RES integration into MGs and analyzing advanced and conventional optimization algorithms in MG applications is performed by M.A. Hannan et al. in [28].

According to the previous academic literature, with respect to the control strategies and EMS framework, the optimization technique and computational approaches play an important role in the efficient and reliable operation of MGs and MGC. Optimization problems cover a wide variety of methods and techniques in mathematics. In recent years, advanced algorithms have been applied to MGs optimization problems to gain the exquisite features of these algorithms. Evolutionary and co-evolutionary optimization methods are smart, reliable, accurate, and problem-independent approaches frequently apply in MG and MGC applications [29]. However, in most academic papers brief explanation of the applicable method is provided, and in some cases, essential information is skipped. This article focuses on the most practical and advanced algorithms applied in previous studies or are prone to exploit in future researches. The main contributions of the manuscript can be highlighted as:

- The comparison of the most practical control strategies in MGC and the inverter operation of the control schemes,
- Surveying the possible scheduling and planning problems in MGC,
- Studying applicable optimization methods in MG and MGC considering the planning problems.
- Overview of the advanced optimization algorithms in order to optimize the MG and MGC operation.

In this chapter, the control strategies in MGC are reviewed, and the inverter control schemes are investigated in section II by considering the most well-known control strategies. Then, the planning and scheduling programs in the MGs application are discussed in order to define the proper optimization problem. Section IV introduces the classification of optimization methods and analyzes the most relevant algorithms in the MG application. Single-objective and multi-objective optimization algorithms are expressed. Section V is dedicated to investigating the artificial intelligence (AI)

application on feather selection and clustering analysis. Eventually, section VI is expanded to conclude the chapter.

1.2. CONTROL STRATEGIES

Stability and efficiency are two main requirements in the control strategies, which are basically related to the dynamic of the systems. In conventional power systems, the synchronous generators (SGs) are the most crucial part of the system from the aspect of system stability [30]. Rotor angle, voltage, and frequency stability in conventional power systems are three main stabilities to maintain the regular operation of the system facing potential disturbances [31]. Identically, the inverters in MGs are the most significant part of keeping the system stable in transients. Compared with conventional power systems with inherent large inertia of SGs, especially in high power scale, the fast response and low overcurrent capacity of inverters resulted in significant changes in operation, control, and protection of MGs [32-33].

The control of individual MG is studied in multiple manuscripts. Among various proposed control approaches such as predictive control, intelligence control, the performance of sliding mode control, and H_∞ control proving more robust operation [34]. However, MGC control has received more attention recently due to increasing interest in the MGC concept. According to the researches, the MGC control strategy can be categorized as master-slave [35-37], peer-to-peer (P2P) [38-40], and hierarchical control [41-43].

In master-slave control, the master converter in voltage source mode is responsible for controlling the DC bus voltage, and slave converters in current source mode share the current according to the total load current [44]. Fig. 1 demonstrates the master-slave control strategy. The V/f controller in Fig. 1 is applied when the MG is in islanded operation mode, and the P/Q controller is for grid-connected mode. Droop control and V/f control are two voltage control strategies for master converter [45]. Different droop control methods with their potential advantages and disadvantages are discussed in [46-48]. The V/f control method, in comparison with droop control, suffers from a slow dynamic response [45]. The main disadvantage of master-slave control is the reliability dependency of the whole system to the master converter and consequently interruption of the whole system in case of master converter failure [35].

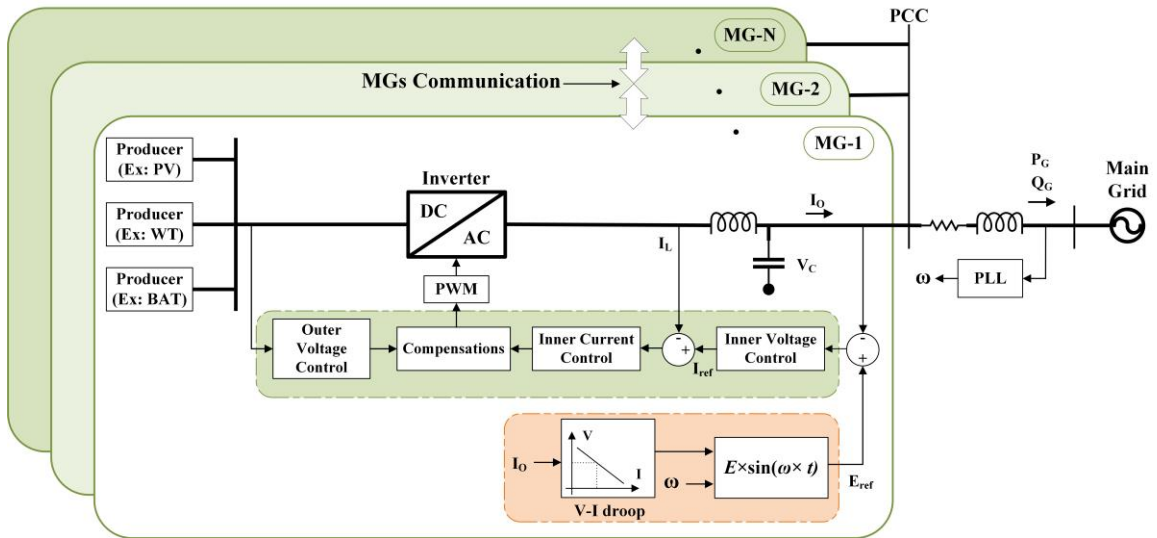


Fig. 2: P2P control structure

dynamic response of the V/f controller. In addition, a simple mixed droop-V/F control strategy for the master inverter is proposed in [52] to achieve seamless mode transfer in MG operation modes.

The hierarchical control strategy is the most adopted control structure due to providing seamless operation in transient between islanded and grid-connected modes. The hierarchical structure consists of primary, secondary, and tertiary control levels to manipulate the static and dynamic stability of MGs. Fig. 3 shows an overview of the incorporation of hierarchical control in a grid-connected individual MG. The primary control is in charge of voltage and frequency stability by regulating the active and reactive power. The deviation of output voltage and frequency in primary control compensates in secondary control. Eventually, the optimum power flow between the MGs and the utility grid is under control at the tertiary control level [53, 54].

The secondary control level in hierarchical control could hire centralized, decentralized, hybrid, and distributed controller architecture based on the communication topologies [55]. In the centralized framework, the central controller has to handle large amounts of data from other MGs to analyze the optimum operation of the whole system [56]. Time-consuming data analysis, complex communication network, and low reliability of system operation by a single-point failure in communication are some important drawbacks that make the centralized approach appropriate only for small-scale MGC. On the other hand, the decentralized approach is proposed to optimize the individual MG operation with no dependency on other adjacent MGs [57]. Although in this

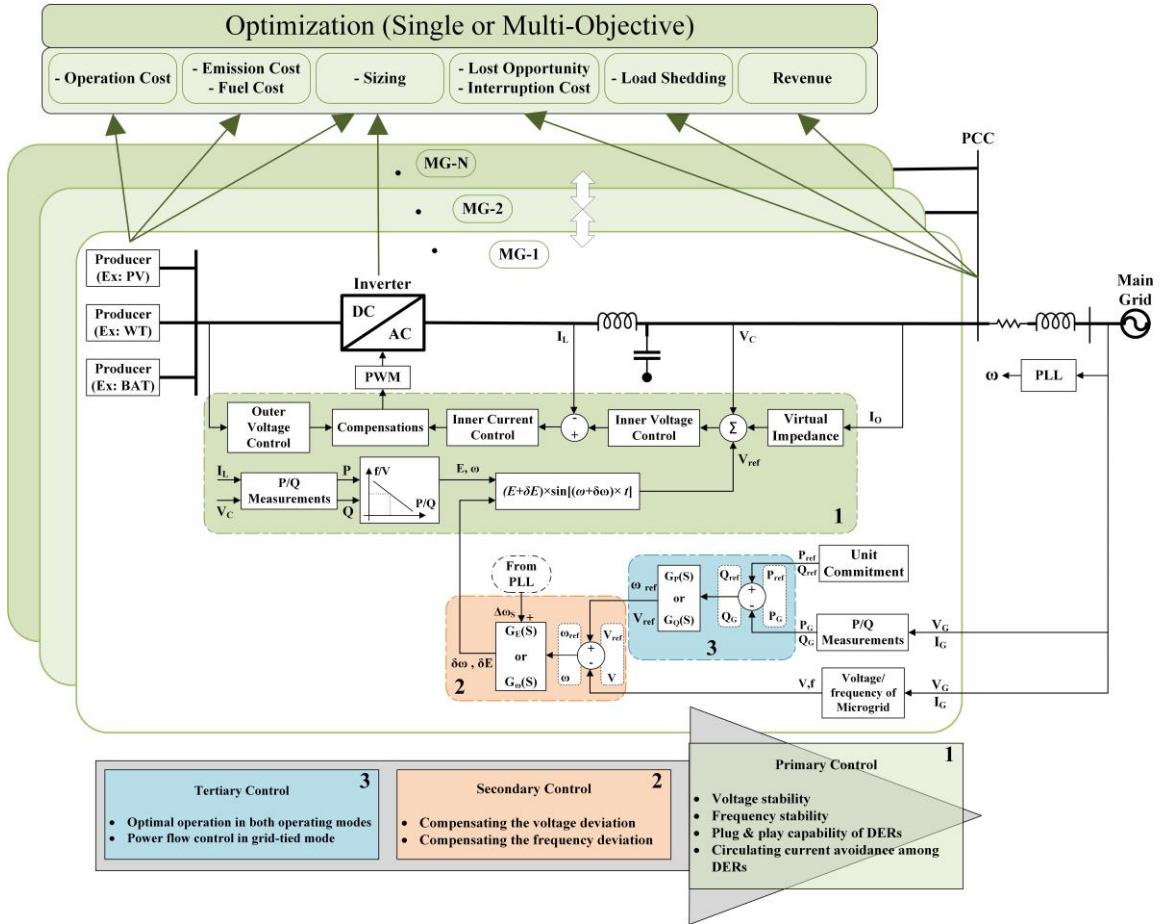


Fig. 3: Hierarchical control structure

approach, the optimization calculations reduce significantly, independent optimization of units cannot guarantee the optimum status of the whole system. In order to take advantage of the centralized and decentralized approaches, the hybrid method is introduced. Nevertheless, the drawbacks mentioned for the centralized framework is still persisted in the hybrid approach [58]. In recent years, the distributed control has drawn attention as a control scheme in MGC to tackle problems related to centralized and decentralized frameworks. In the distributed scheme, the computing burden is reduced significantly by sharing key information among MGs [59], making this control scheme appropriate for large-scale MGC.

Model predictive control (MPC) can effectively apply to the hierarchical architecture to handle the stochastic nature of REs and variable power demand based on the prediction [60-64]. In [60, 61], an overview of MPC in individual MGs and MGC corresponding to three levels of hierarchical strategy for converter-level and grid-level control is presented. MPC ordinarily is based on the system's future behavior and can make the system more robust against uncertainties by the feedback mechanism.

Centralized MPC (CMPC) requires complete information and an accurate centralized method. On the other hand, distributed MPC (DMPC) is proposed in order to reduce the data evaluation by sharing essential global information. In [65], a DMPC is applied to MGC to optimally coordinate the energy among MGs and DERs. The main contribution of this article is introducing a virtual two-level MGC, which DERs consider a virtual MG (VMG) with the possibility of power exchange with the main grid, and other MGs are virtually located in the lower level communicate with VMG. In this case, the MGs cannot directly exchange power with the utility grid; therefore, the decision variables are reduced, and computing speed increases.

Model predictive control (MPC) can effectively apply to the hierarchical architecture to handle the stochastic nature of REs and variable power demand based on the prediction [60-64]. In [60, 61], an overview of MPC in individual MGs and MGC corresponding to three levels of hierarchical strategy for converter-level and grid-level control is presented. MPC ordinarily is based on the system's future behavior and can make the system more robust against uncertainties by the feedback mechanism. Centralized MPC (CMPC) requires complete information and an accurate centralized method. On the other hand, distributed MPC (DMPC) is proposed in order to reduce the data evaluation by sharing essential global information. In [65], a DMPC is applied to MGC to optimally coordinate the energy among MGs and DERs. The main contribution of this article is introducing a virtual two-level MGC, which DERs consider a virtual MG (VMG) with the possibility of power exchange with the main grid, and other MGs are virtually located in the lower level communicate with VMG. In this case, the MGs cannot directly exchange power with the utility grid; therefore, the decision variables are reduced, and computing speed increases.

The multi-agent system (MAS) is another control scheme that effectively can adopt the hierarchical structure in order to enhance the voltage and frequency reliability, intelligence, scalability, redundancy, and economy in MGC. The main idea of MAS-based distributed control is dividing the complex and large-scale system into several subsystems with the possibility of mutual interaction. In [32], a comprehensive overview of MAS-based distributed coordination control and optimization in MG and MGC is surveyed. In addition, the control strategies in MAS, topology model, and mathematical model are discussed, and the pros and cons of these methods are compared.

The optimal configuration and control strategy in the MAS control approach requires a proper model. In recent publications, the graph model as a topology model and the non-cooperative game model, GA, and PSO algorithm as mathematical models are overviewed in [32]. The graph model is widely adopted in MAS due to its simple model structure and high redundancy. However, the system robustness is significantly affected by the graph [66]. Non cooperative and cooperative game theory approaches can also exploit in MGC optimization. Nash equilibrium in non-cooperative game theory is used as a stable strategy solution [67]. In [68], the game model analyzes the interactions between the agents and their actions to enhance the economic interest between MG and the utility grid by considering the uncertainty of RE power generations. The comparison of the non-cooperative and cooperative game model results in decreasing the total configuration capacities by 10% in a cooperative game. Despite non-cooperative games, players or agents in cooperative games are able to coordinate with each other to increase their profit from the game by constructing alliances among themselves [69]. In [70], cooperative game theory applications such as cost and benefit allocation, transmission pricing, projects ranking, and allocation of power losses in power systems are overviewed.

In Table I, an overview of the different control strategies in MGC applications is listed.

TABLE I
CONTROL STRATEGIES IN MGC APPLICATION

| No. | Ref | Control Strategy | Explanations | |
|-----|------|----------------------|--|---|
| 1 | [35] | Master-slave | Utility interface (UI) as control master for the energy gateways: 1) in grid-connected, UI performs as a grid-supporting to dispatch active and reactive power references; 2) in islanded operation: UI performs as a grid-forming voltage source to ensure power balance. | event-triggered control scheme to: 1) synchronize the voltage of multiple DERs to their desired value; 2) optimal load sharing for their economic operation. |
| 2 | [36] | Master-slave | Master-slave framework containing a two-layer voltage estimator to simultaneous achievement of accurate current sharing and current economical allocation, short time consumption and faster convergence, and robustness against uncertain communication environments. | Combined with the advantages of peer-to-peer control, an improved master-slave control strategy based on I-ΔV droop to control the smooth transition between grid-connected and island mode. |
| 3 | [37] | Master-slave | Distributed iterative | Improved V/f control strategy composed of two parts, feed-forward compensation and robust feedback control to enhance voltage output characteristics, dynamic characteristics and robustness in response to micro-source output power fluctuations, loads abrupt change or non- |
| 4 | [44] | Improved Maser-slave | | |
| 5 | [45] | Master-slave | | |

| | | | | | | | |
|----|------|-------------------|---|----|------|---------------------------------------|---|
| 6 | [52] | Master-slave | linear loads and unbalanced loads. Simple mixed droop-v/f control strategy for the master inverter of a MG to achieve seamless mode transfer between grid connected and autonomous islanding modes by means of: 1) a modified droop control in grid connected mode; 2) v/f control in islanding mode. | 14 | [41] | Hierarchical | Enhanced hierarchical control structure with multiple current loop damping schemes consisting of the |
| 7 | [38] | P2P | Decentralized control system, using the ICT concept of network overlays and P2P networks to eliminate single points of failure. | 15 | [43] | Hierarchical | A review of hierarchical control strategies that provide effective and robust control for a DC MG. |
| 8 | [39] | P2P + game theory | A hierarchical system architecture model to identify and categorize the key elements and technologies involved in P2P energy trading using game theory to improve the local balance of energy generation and consumption. | 16 | [53] | Hierarchical | A versatile tool in managing stationary and dynamic performance of MGs while incorporating economic aspects. |
| 9 | [40] | P2P + game theory | A two settlement P2P energy market framework for joint scheduling and trading of prosumers in MGC to provide price certainty and increase localized transaction volume of DERs. | 17 | [56] | Centralized | A mathematical model of the time-delay DC islanded MG to compensate the effect of the time-delay by three control strategies: stabilizing, robust, and robust-predictor. |
| 10 | [49] | P2P | An overlay P2P architecture for controlling and monitoring MGs in real time with satisfactory performance parameters proposed for MGs, such as latency and bandwidth, showing that P2P overlay networks are useful for energy grids in practice. | 18 | [57] | Decentralized | Decentralized economic power sharing strategy To improve the reliability, scalability, and economy of MGs. |
| 11 | [50] | P2P | A voltage control algorithm, based on P2P control and gossiping communication to operate in a distributed manner, with no central coordinator, thereby keeping all control local and eliminating any single point of failure. | 19 | [58] | Multilevel Distributed Hybrid Control | Overcome the drawbacks of centralized and decentralized control schemes. Ability of seamlessly switching between high bandwidth communication and low bandwidth communication channels of communications. |
| 12 | [51] | P2P | Distributed P2P enabled through broadcast gossip communication control scheme for voltage regulation and reactive power sharing of multiple inverter-based DERs. | 20 | [59] | Distributed control | A review of distributed control and management strategies for the next generation power system. |
| 13 | [41] | Hierarchical | A review of decentralized, distributed, and hierarchical control of grid-connected and islanded MGs. | 21 | [60] | Hierarchical + MPC | Comprehensive review of MPC in individual and interconnected MGs, including both converter-level and grid-level control strategies applied to three layers of the hierarchical control architecture. |
| | | | | 22 | [61] | MPC | A study on applying a MPC approach to the problem of efficiently optimizing MG operations while satisfying a time-varying request and operation constraints by using MILP. |
| | | | | 23 | [62] | MPC | To deal with uncertainties of renewable energy, demand and price signals in real-time MG operation, |
| | | | | 24 | [63] | MPC | An MPC for load frequency control of an interconnected power system based on a simplified system model of the Nordic power system taking into account limitations on |

| | | | | | | | |
|----|------|------|---|----|------|-------------------------|--|
| | | | tie-line power flow, generation capacity, and generation rate of change. | 28 | [68] | MAS + game theory | A structure of a MG based on MAS with a game-theory based optimization model for the capacity configuration of these agents, and economic interests between agents and their actions by the game model and the interactions between MG and power grid, and the uncertainty of wind power and solar power are taken into account. |
| 25 | [64] | CMPC | A coordinated control of PHEVs, PVs, and ESSs for frequency control in MG using a CMPC considering the variation of PHEV numbers to: 1) suppress the system frequency fluctuation; 2) minimize the surplus power of PV. | | | | |
| 26 | [65] | DMPC | A cooperative energy management scheme based on DMPC for grid-connected MGC to minimize the operation costs and maintain power balance. | 29 | [70] | Cooperative Game Theory | A review of cooperative game theory with theoretical background for the analysis of projects where participants can make collective actions to obtain mutual benefits. |
| 27 | [66] | MAS | Sign-consensus problems of general linear multi-agent systems by a signed directed graph. | | | | |

1.3. MICROGRID PLANNING

Planning and scheduling problems arise for economic purposes. Therefore, MG planning is no exception to this principle. The main goal in MG planning is to minimize the system's operation cost considering the practical and technical constraints. Practical constraints refer to some obligatory limitations with no alternatives. For example, the location and area of the construction site may not be debatable. In addition, the maximum solar irradiance and wind speed restrict the maximum harvesting energy from PV and WT. On the contrary, technical constraints are related to the incentive or punitive policies regarding the environmental impact, power quality, and reliability. Consequently, MG planning and scheduling can infer as an optimization problem subject to the corresponding constraints. In [26], the MG planning problem is examined firstly for possible configuration of different power generation types to meet the objectives such as cost-effectiveness, environmental concerns, and reliability. Secondly, the siting problem is discussed as a strategic level problem for the actual and potential customers. Eventually, scheduling as a tactical level problem is considered to minimize the operational costs according to the available energy sources. In [24], scheduling problem from various points of view is discussed. Fig. 4 depicts the correlation of explained scheduling problem in [24] and the MG planning problem defined in [26].

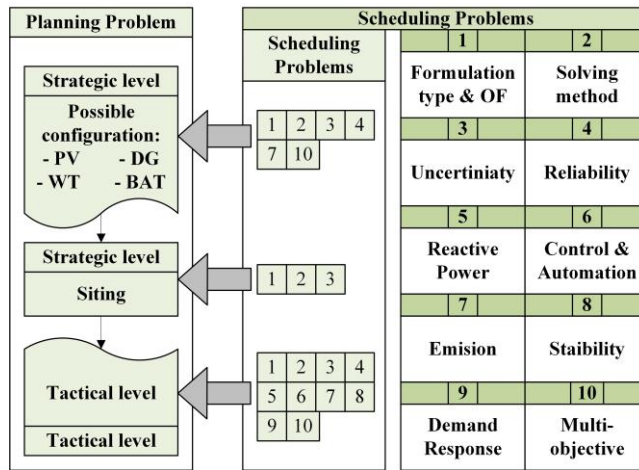


Fig. 4: Planning and scheduling program in MGs

The optimization problem is referred to as the minimization and maximization problem. In an optimization problem, costs tend to be minimized, and profits tend to be maximized. Fig. 5 represents a general categorization of optimization in MGs and MGC. As it can be seen from Fig. 5, most of the literature researches are related to the minimization problem by introducing a cost function. In [71, 72], the cost function is defined in order to minimize fuel cost. The operation cost is the primary concern of MGs in order to reduce the capital cost [73-75], replacement cost [76, 77], and operation and maintenance (O&M) cost [78, 79].

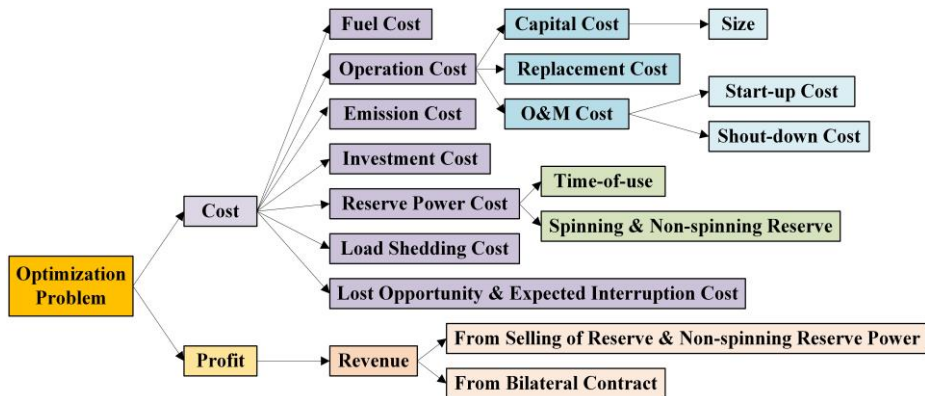


Fig. 5: Cost and profit functions in MGs

Moreover, capital cost as a strategic planning program in association with the size and the efficient combination of the generation units is one of the important optimization problems related to the component size [80]. Reserve power is another important topic, especially in islanded MGs, to optimize the time-of-use of stored energy in ESS [81]. In [82, 83], the spinning and non-spinning reserves are the main

objective function to be minimized. In [84], an algorithm is proposed to minimize the unmet load and consequently reduce the load shedding. Eventually, the cost of expected interruption and lost opportunity is considered a cost function in [85] to increase the system's reliability. On the other hand, the maximization problems are mostly related to maximizing the revenue from selling the spinning or non-spinning reserve power [86] or from a bilateral power exchange between MGs and the main grid [87]. Due to cost and profit functions similarity among articles, the most dominant objectives are mentioned in this section. A comprehensive study on cost and profit functions is surveyed in [88].

In addition, in recent years, several commercial software have been emerged in order to evaluate the MG's planning. HOMER, RETScreen, H2RES, DER-CAM, MDT, and MARKAL/TIMES are the most well-known software used in MG application. The scheduling program related to the RE accessibility, uncertainty, and technical limitation are considered and the optimal planning will be evaluated [27]. In Table II, the capabilities and characteristics of the most well-known software in this field are compared.

TABLE II
COMMERCIAL SOFTWARE FOR MG'S PLANNING

| Software | Grid-connected & Isolation mode analysis | User define power management strategy | Time step analysis | Optimization method |
|--------------|--|---------------------------------------|---------------------|---------------------|
| HOMER | Yes | Yes | Minute - hour | Exhaustive search |
| RETScreen | Yes | - | Day-month-year | Search scope |
| H2RES | Yes | Yes (partially) | Minute - hour | LP |
| DER-CAM | Yes | Yes | Minute - hour | MILP |
| MDT | Yes | Yes (partially) | - | MILP & GA |
| MARKAL/TIMES | Yes | Yes (partially) | Year-multiple years | LP/MIP, PE |

1.4. OPTIMIZATION TECHNIQUES FOR MICROGRIDS

According to the planning and scheduling problem, MG and MGC optimize operation is subjected to specify an objective function optimization problem. Optimization problems are widely used in computer science, economics, and engineering in order to find the minimum or maximum value among feasible solutions. Over the years, enormous optimization methods depending on the problem have been introduced. However, the most practical optimization methods regarding the MGs application are analyzed in this article. Linear programming (LP), non-linear programming (NLP), mixed-integer linear programming (MILP), mixed-integer non-linear programming (MINLP), quadratic programming, and linear least-square programming are the most popular optimization problem according to the features that

can be extracted from MGs application. To obtain the optimal solution of these programming, various commercial modeling platforms such as GAMS [89], AMPL [90], and AIMMS [91] have been nominated in recent years. These modeling platforms are armed with deterministic solvers such as IPOPT, CPLEX, SCIP, BARON, CONOPT, etc. [92]. MATLAB and Python environments also provide modeling platforms for some specific optimization problems, but this software provides the possibility of implementing optimization algorithms by programming.

Principally, optimization problems can be classified as unconstraint single-objective, constraint single-objective, unconstraint multi-objective, constraint multi-objective optimization. Fig. 6 shows these classifications. The planning and scheduling program inherently impose constraints to the problem; hence the unconstraint single-objective optimization is not a practical problem in MGs optimization.

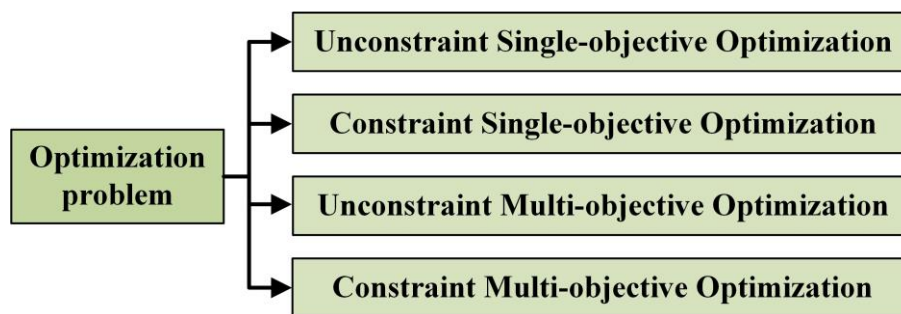


Fig. 6: Optimization problem classification

Accordingly, except for the unconstraint single-objective optimization, the other optimization methods can be converted to each other, i.e., there is the possibility of reducing the constraints space and add to the objective space and vice versa. The usual constraint optimization approaches in MGs application are investigated in this article. Fig. 7 shows the general classification of constraints problem approaches. As shown in Fig. 7, the constraint problems considering the scheduling programming in MG applications can be discussed in two distinct procedures: the probabilistic or stochastic problems or the deterministic or robust problem [24-25, 93].

| Constraints problems | | | |
|--|---|---|---|
| Probabilistic | Deterministic | | |
| <ul style="list-style-type: none"> • PEM (Point Estimate Method) • MCS (Monte Carlo Simulation) • Linear Discriminant • Linear Regressions | Classic | Heuristic & Meta-heuristic | |
| | <ul style="list-style-type: none"> • Lagrangian relaxation • Interior point • Newton's method • Sequential quadratic programming • Gradient descent • Simplex algorithm | Evolutionary | Co-evolutionary |
| | | <ul style="list-style-type: none"> • Penalty Function • Feasibility Method • Treating Constraints as Objectives (Multi-objective) • Evolutionary Computation (DE, GA, NSGA) • Swarm Intelligence (PSO, MOPSO, BE, BF, ACO) | <ul style="list-style-type: none"> • Dynamic Programming • Hybrid Meta-heuristic • Parallel Meta-heuristic |

Fig. 7: Constraint optimization classification

A. PROBABILISTIC METHODS

The probabilistic procedure could be applicable in systems with uncertainties. Principally, the uncertainties in power systems and MGs can be considered uncertainties regarding future conditions and uncertainties in computational modeling [94, 95]. Therefore, forecasting methods such as generalized predictive control (GPC) in model predictive control (MPC) like ARIMA, CARIMA, and ARIMAX can play an important role in diminishing the uncertainties related to wind speed, solar irradiance, load, and price forecasting. In addition, the more precise models of MG components, the more accurate estimation will be possible. Point estimated method (PEM) and Monte-Carlo simulation (MCS) are two statistical methods facing probabilistic problems, Fig 7. Nevertheless, linear discriminant and linear regressions are based on linearization and approximation methods. In [96], the PEM is applied for modeling the wind and solar power uncertainties, and a robust optimization technique is utilized to optimize an individual MG. Conventional MCS is an accurate method but time-consuming approach for uncertainty modeling. In [97], a new approach based on MCS with high precision and lower calculation time is proposed to optimize the investment and reliability of an islanded MG. The linearization and approximation methods are primarily used to discriminate or categorize the objectives to investigate linear combinations of variables that best explain the data [98, 99].

B. DETERMINISTIC METHODS

Deterministic methods are divided into classical methods and heuristic methods, Fig. 7. The classical methods are able to find the optimum solutions by means of analytical methods. Although these methods can guarantee the optimal solution, for large-scale and complex problems largely are not able to find the feasible solution

(problem-dependent). Regardless of the single variable or multivariable functions in classical methods, equality and inequality constraint problems can be handled effectively considering the objective functions. For equality constraints problem the Lagrange multiplier methods, and for inequality constraints, the Kuhn-Tucker conditions can be used to identify the optimum solution [100]. Furthermore, classical methods suffer from the initial point dependency, which makes divergence in case of inappropriate initial point selection.

On the other hand, the heuristic and meta-heuristic methods are faster methods, specifically in complicated large-scale problems. The performance of these methods is to explore the search space to find the optimum solution. Therefore, these methods cannot guarantee the exact optimum solution [101]. Unlike heuristic methods, the meta-heuristic approaches are not problem-dependent [102]. Meta-heuristics methods incorporate strategies and mechanisms to guide the search process and, most importantly, avoid getting trapped in confined areas of the search space. Considering the complexity of the problem, evolutionary or co-evolutionary approaches can be applied for optimization purposes.

The main idea to use evolutionary methods is achieving the best performance with minimum information about the problem. The evolutionary approaches can be distinguished into two classes, evolutionary algorithms and swarm intelligence. The main difference of these classes refers to the exploited algorithm in order to evolve a set point among the populations of search space [103]. The GA and DE are the most famous population-based meta-heuristic algorithm that the optimization procedure is based on an evolutionary process. The PSO, ACO, BE, and BF are the most famous swarm intelligence optimization methods based on a collaborative study of individuals' behavior and interactions with one another.

There is a multiplicity of classic methods that can be studied in various papers and book chapters. Therefore, in this chapter, the heuristic and meta-heuristic methods only are investigated specifically for multi-objective optimization problems. The problems are defined in minimization format, but the same procedure can be applied in maximization problems.

C. EVOLUTIONARY APPROACHES

C.1. PENALTY FUNCTION

In the penalty function method, the constraints of the problem aggregate to the objective function by considering a penalty factor. In fact, a constraints optimization problem converts to the unconstrained multi-objective problem in the penalty function method. In following this procedure is expressed [107]:

$$\min f(x) \quad x \in X \quad (1)$$

Subject to:

$$g_i(x) \leq g_0 \quad i = 1, 2, \dots, N \quad (2)$$

In this method, the constraints $g_i(x)$ replace by the violation function, and the unconstrained minimization problem is defined as:

$$\min \hat{f}(x) = f(x) - \sum_{i=1}^N \lambda_i v(x) \quad x \in X \quad (3)$$

where x is the state variable, and λ_i is the co-state. The λ_i variables can be extracted from an ancillary optimization procedure to enhance the performance of the optimization. However, a constant value for λ_i mostly results in a satisfactory achievement. The violation for inequality and equality constraints is defined in Table 1. In addition, the violation can be adopted to the primal problem $f(x)$ in the form of additive, multiplicative, and hybrid (additive-multiplicative or vice versa) [108]. These dual problems $\hat{f}(x)$ are described in Table III.

TABLE III
VIOLATION AND OPTIMIZATION PROBLEM

| Constraint | Violation | Optimization Problem | Formulation |
|-------------------|---|----------------------|--|
| $g_i(x) \geq g_0$ | $v(x) = \max\left(1 - \frac{g_i(x)}{g_{0,i}}, 0\right)$ | Additive | $\hat{f}(x) = f(x) + \lambda \sum \psi(v_i(x))$ |
| $g_i(x) \leq g_0$ | $v(x) = \max\left(\frac{g_i(x)}{g_{0,i}} - 1, 0\right)$ | Multiplicative | $\hat{f}(x) = f(x)(1 + \lambda \sum \psi(v_i(x)))$ |
| $g_i(x) = g_0$ | $v(x) = \left \frac{g_i(x)}{g_{0,i}} - 1 \right $ | Hybrid | $\hat{f}(x) = (f(x) + \lambda \sum \psi(v_i(x))) \times (1 + \gamma \sum \phi(v_j(x)))$ $\hat{f}(x) = f(x)(1 + \lambda \sum \psi(v_i(x))) + \gamma \sum \phi(v_j(x))$ |

The barrier function method, also known as the interior point method (IPM), is one of the approaches in constrained optimization problems that can effectively apply to the

penalty function method [109]. In barrier methods, a very high cost imposes on feasible points that lie so close to the boundary of the feasible solution region. A barrier function can hire continuous functions. However, the two most common barrier functions are logarithmic barrier function and inverse barrier function, which are described below:

$$\psi(x) = -\sum_{i=1}^N \log(-v_i(x)) \quad x \in X \quad (4)$$

$$\psi(x) = -\sum_{i=1}^N \frac{1}{v_i(x)} \quad x \in X \quad (5)$$

In (4), (5), the barrier function $\psi(x) \rightarrow \infty$, if $v_i(x) \rightarrow \infty$ for any i . In [65], the logarithmic barrier function is used to solve the distributed MPC problem with constraints.

C.2. FEASIBILITY METHOD

In the feasibility method, the response is endeavored to retain in an acceptable restriction area. This method is more applicable for the problem with equality constraints, although inequality constraints are also practical. Mathematically the feasibility method can be express as:

Suppose $x \in X$ is existed such that:

$$g_i(x) < 0 \quad i = 1, 2, \dots, N \quad (6)$$

$$Ax = B \quad (7)$$

Thus, the feasible solution can be found by solving:

$$\min_{x,f} \{f \mid g_i(x) \leq f\} \quad x \in X, i = 1, \dots, N, \quad (8)$$

subject to:

$$Ax = B \quad (9)$$

In this method, the best solution is discovered among the feasible solutions. However, in some problems determining the feasible area is complicated. It is worth mentioning that the barrier function also can be applied to this method. In [110], to enhance the MG system performance, a feasible range to obtain the optimal value of the virtual impedance of the droop-based control is determined.

C.3. MULTI-OBJECTIVE OPTIMIZATION METHODS

As mentioned previously, one of the approaches to dealing with constraints optimization problems is reducing constraints space and augmenting constraints to the objective space. Treating constraints as objectives make the cognition of multi-objective optimization methods essential. In this section, the most important multi-objective optimization methods are studied.

Instead of concentrating on a single goal, the optimization algorithms in multi-objective problems take several goals under evaluation simultaneously. Multi-objective optimization proposes a set of optimized solutions as Pareto-optimal solutions. Fig. 8 shows a sample Pareto-front with two objective functions. To produce the Pareto-optimal frontier, the non-dominated solutions are evaluated by the dominance concept [111]. In (10) dominance concept is stated:

$$x \text{ dom } y \Leftrightarrow \begin{cases} \forall i: & x_i \leq y_i \\ \exists i_0: & x_{i_0} < y_{i_0} \end{cases} \quad (10)$$

The relations in (10) state that x dominates y if solution x is no worse than y in all objectives, and solution x is strictly better than y in at least one objective. Fig. 8 shows a two-objective problem, the solid points represent the non-dominated solutions, and the hollow ones are the dominated solutions. The Pareto solution proposes a variety of optimum solutions. Therefore, to select a proper solution, the solutions have to be evaluated by considering the constraints. In the constraints problems, the limits of the constraints can be exploited to specify the best optimal value. For instance, as can be seen in Fig. 8, the closest solid point to the line $g(x) = g_0$ is the best acceptable solution

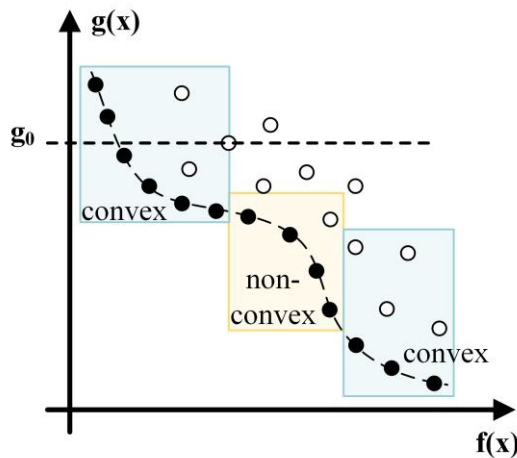


Fig. 8: Sample Pareto-front for two objective functions

to fulfill the constraint $g(x) < g_0$. Furthermore, the feature selection methods and clustering analysis can also be applied to determine the best solution in the Pareto-optimal solutions set.

Figure 9 demonstrates the general classification of multi-objective optimization methods. In decomposing approaches, the multi-objective problem converts to a single objective problem. Weighted sum, weighted metric sum, and ε -constraint are some decomposition approaches widely used in multi-objective optimizations and constraints problems. The main disadvantage of decomposition approaches is that the Pareto-front set will find after multiple iterations. On the other hand, direct solutions utilize a more complicated algorithm to find the Pareto-optimal solutions in only one single run considering all objective functions.

| Multi-objective Optimization Problem | |
|--|---|
| Decomposition | Direct solution |
| <ul style="list-style-type: none"> • Weighted Sum • Weighted Metric Method • ε-constraint | <ul style="list-style-type: none"> • NSGA-II • MOPSO • SPEA-II • MOEA/D • PESA-II |

Fig. 9: Multi-objective optimization methods

C.3.1. DECOMPOSITION APPROACHES

C.3.1.1. WEIGHTED SUM

This method is widely used in multi-optimization problems due to its simplicity and usability in convex objective functions. In the weighted sum method, a set of objective functions are scalarized into a single objective function considering different pre-multiplier weights for each objective function. Mathematically, the weighted sum method is expressed as [112]:

$$\min f_{ws}(x) = \sum_{i=1}^N W_i f_i(x) \quad x \in X, i \in \{1, 2, \dots, N\} \quad (11)$$

Subject to:

$$g_i(x) \leq g_0 \quad (12)$$

where the weights W_i determine the relative importance of the objective functions, $f(x)$ is the objective function, and N is the number of objective functions. There are two main disadvantages to using this method. Determine a weight vector set to obtain the Pareto-optimal solution in the desired region in the objective space is complex. Also, this method is not able to detect the Pareto-optimal solution for the non-convex part of the objective space. In the case of facing non-convex cost function in the MG application, the linearization methods can be used to obtain an approximate convex cost function. According to the constraints in (12), the best solution among the Pareto-optimal set can be determined. However, as discussed for the penalty function method, by considering the violation, the constraints can also integrate with the objective function:

$$\min \{f_{ws}(x) | g_i(x) \leq g_0\} \Rightarrow \min f_{ws}(x) + \frac{1}{n} \sum_{i=1}^n \psi(v_i(x)) \quad (13)$$

In [99], an incentive-based demand response program is implemented to achieve the optimal economic status. The multi-objective problem in this article involves maximizing the MGs' demand response program profit, minimizing the generator cost and trading cost. To produce the Pareto-optimal solutions, the weighted sum technique is applied in this chapter. In [113-116], also weighted sum method is used for multi-objective optimization.

C.3.1.2. WEIGHTED METRIC METHOD

This method combines multiple objective functions to minimize the distance metric between all solutions and an ideal solution T_0 . In (14), the formulation of this method is expressed:

$$\min f_{GP}(x) = \sum_{i=1}^N \left(W_i \|f_i(x) - T_{0i}\|_{P,W} \right)^{\frac{1}{P}} \quad x \in X, i \in \{1, 2, \dots, N\} \quad (14)$$

Subject to:

$$g_i(x) \leq g_0 \quad (15)$$

where W_i can effectively utilize to normalized the distance between objective functions and the target T_0 that this distance calculation method is dependent on P . If P is equal to 1, the distance calculates by city block distance norm, and if P is equal to 2, the distance calculates by Euclidean norm [117]. In these cases ($P = 1$ or 2), the weighted metric method is known as goal programming. In addition, if P tends to

infinity, the distance is considered the maximum distance between objective functions and T_0 , which this method is known as goal attainment or the Tchebycheff method [118]. Compared with the weighted sum technique, the main advantage of this method is producing the whole Pareto-optimal solution, either convex or non-convex problem, by ideal solution T_0 . However, knowledge about minimum or maximum objective values is required to choose a proper ideal solution T_0 .

In [119], a multi-objective optimization problem in order to maximize the investor's profit and MG operational cost considering the optimal storage power rating, energy capacity, and the year of installation is solved using a goal programming approach. Also, goal programming is applied in [120] to minimize the emission, storage operating, and startup/shutdown cost of DG units and maximize their efficiency. In [121], a multi-criteria decision analysis (MCDA) uses goal attainment programming to solve the multi-objective dispatch function for scheduling the dispatch in MGs. Goal programming and goal attainment are used in many articles for the purpose of optimization [122-125].

C.3.1.3. ε -CONSTRAINT

In this method, unlike the two previous methods, only one objective function keeps the main objective, and the rest of the objective functions are considered the constraints [126]. This method is expressed mathematically in (16):

$$\min f_M(x) \quad x \in X \quad (16)$$

Subject to:

$$f_i(x) \leq \varepsilon_i \quad i = 1, 2, \dots, N (N \neq M) \quad (17)$$

where $f_M(x)$ is the main objective function, and the other objective functions $f_i(x)$ are considered constraints restricted to ε_i . This method is also able to find all Pareto-optimal solutions for either convex or non-convex objective functions. However, the main disadvantage of this method is that the ε vector has to be chosen precisely considering the minimum and maximum values of the individual objective functions. In [127], an augmented ε -constraint method is implemented to solve the multi-objective optimization problem in order to achieve economic optimization and peak-load reduction of the combined cooling heating and power (CCHP) MGs model. In [128], an optimal energy management technique using the ε -constraint method for grid-tied and

stand-alone battery-based MGs is studied. The ϵ -constraint method is applied in further researches [129-133] as an optimization technique.

C.3.2. DIRECT APPROACH

The main difference between single-objective optimization algorithms like GA, PSO, DE, and multi-objective optimization algorithms like NSGA-II, MOPSO, PESA-II, SPEA-II, and MOEA/D is referred to the population sorting algorithm.

The non-dominated sorting genetic algorithm (NSGA) [134] is one of the first multi-optimization methods which produce a set of Pareto-optimal solutions in a single run. However, the high computational complexity of non-dominated sorting, lack of elitism, and need for specifying the sharing parameter led to proposing the modified version of this method as NSGA-II [135]. In this algorithm, in the initialization phase, the main population $P(t=0)$ is produced. The population $P(t)$ merges with offspring population $Q(t)$ and mutation population $R(t)$ in each iteration. Then, the merged population is sorted considering the rank and crowded distance of individuals to determine the non-dominated solution. NSGA-II is utilized in MG applications for different purposes. In [136], NSGA-II is used in order to establish a smart networked MG with the lowest operating cost and the most negligible pollutant emission. In [137], the membership functions (MFs) of a fuzzy logic-based energy management system (FEMS) are optimized by the NSGA-II algorithm. The proposed FEMS is responsible for reducing the average peak load and operating cost. Moreover, in [138], NSGA-II is applied to the controller of the inverters of distributed generators with inner and outer control loops to seamless transition operation between grid-connected and islanding mode. In [139-142] the more applications of NSGA-II are presented.

The Strength Pareto evolutionary algorithm (SPEA-II) is proposed by Zitzler and Thiele as an efficient algorithm to face multi-objective optimization. The second version of SPEA could eliminate the potential weaknesses of the first edition by improving the fitness assignment scheme, more accurate guidance of the search process by incorporating a nearest neighbor density estimation technique, and preserving boundary solutions by a new archive truncation method [143]. This algorithm presents an acceptable performance in terms of convergence and diversity by introducing the concept of strength for non-domination solutions. SPEA-II is applied in multiple studies in MG application [144-146]. In [147], SPEA-II is used in demand response

management (DRM) to meet the peak load demand and decreasing customer expenditure. In [148], a multi-level algorithm is proposed to optimize the revenue and expense while preserving the quality of service (QoS) of the data center and power network stability. The proposed algorithm uses SPEA-II for the multi-objective constrained optimization problem. A multi-objective algorithm based on the Six Sigma approach is proposed in [149] to solve the sizing problem of the hybrid MG system consists of multiple resources and multiple constraints. Among MOPSO, PESA-II, and SPEA-II, which are applied to the optimization algorithm, the results show SPEA-II has better performance in this article.

The Pareto envelope-based selection algorithm (PESA-II) uses the GA mechanism by applying hyper-grids to make the selections and create the next generation. The individuals-based selection in the first edition of PESA is replaced by the region-based selection in PESA-II for objective space [150]. This technique shows more sensitivity to ensure a good spread of development along the Pareto-front. In [151], the techno-economic objectives are optimized by the iterative-PESA-II algorithm to optimally sizing a stand-alone MG with PV and battery storage resources.

Multiple objective particle swarm optimization (MOPSO) is also one of the practical algorithms among swarm intelligence methods. MOPSO applied the same technique used in PESA-II by replacing GA with the PSO algorithm. In MOPSO, the particles dynamically change their position according to the velocity vector by considering the individuals' best and global best. In [152], the MOPSO algorithm is proposed by using an external repository of non-dominated vectors to guide the other particles in each iteration meanwhile maintaining the diversity. Multiple studies were carried out by applying MOPSO in order to optimize the multi-criteria objectives in MGs. In [153], MOPSO is used to find the best configuration and sizing the components of a hybrid PV, WT, DG, and battery storage system, considering a tradeoff between cost and reliability of the system. In [154], the energy management unit employed the MOPSO algorithm to ensure the maximum utilization of resources by maintaining the state of charge (SOC) in batteries to manage power exchange between MGs. In [155], MOPSO makes able the proposed EMS to minimize the operation cost of the MG concerning the renewable penetration, the fluctuation in the generated power, uncertainty in the power demand, and utility market price. More uses of MOPSO are investigated in MG application in various researches [156-159].

The multi-objective evolutionary algorithm based on decomposition (MOEA/D) is one of the algorithms in multi-objective optimization problems. The main difference between MOEA/D and the other algorithms discussed for direct approach solutions is not using the concept of dominance to produce the Pareto-frontier. In this algorithm, a multi-objective optimization problem decomposed into several scalar optimization sub-problems and optimized them simultaneously. Weighted sum, Tchebycheff, and boundary intersection (BI) are three approaches discussed in [160] to decompose a multi-objective optimization. Despite the weighted sum and weighed metric method discussed in the previous section, in the MOEA/D algorithm, the Pareto-front produces in only a single run. Multi-objective optimization using MOEA/D also draws attention to be used in MG applications. In [161], the optimal design of a hybrid MG system consists of PV, WT, DG, and storage devices considering load uncertainty is analyzed. MOED/D and transforming to a single objective function are two optimization methods applied in this article to optimize the loss of power supply probability (LPSP) and cost of electricity (COE). In [162], a three-level hierarchical control architecture is proposed in order to mitigate the unbalance currents through the MG's point of common coupling (PCC) and degradation of power factor (PF). The MOEA/D in the second level is employed to maximize the active power injection and minimize the currents unbalance into the main grid. MOEA/D is widely used for optimization purposes in distribution networks and MGs [163-166].

Table IV compares the performance of the direct approach algorithms discussed in this section.

TABLE IV
OPTIMIZATION IN MGC APPLICATION

| Algorithm | Time execution | Complexity | Accuracy & performance |
|-----------|-----------------|------------|------------------------|
| NSGA-II | High | High | High |
| SPEA-II | Relatively high | Moderate | Moderate |
| PESA-II | Relatively high | Moderate | Moderate |
| MOPSO | Relatively low | low | Relatively high |
| MOEA/D | High | High | Moderate |

D. CO-EVOLUTIONARY APPROACHES

In the case of facing an extremely complex problem, the evolutionary approaches may not be able to attain the solution with adequate accuracy. Therefore, co-evolutionary approaches proposed a computational procedure by converting a large problem to smaller ones and do parallel calculations by applying several optimization algorithms simultaneously. Fig. 10 illustrates the general performance of a co-

evolutionary approach. As it can be observed from Fig. 10, a meta-algorithm is in charge of coordinating other algorithms in order to obtain the optimum solution amongst the optimum feasible solutions by the sub-algorithms.

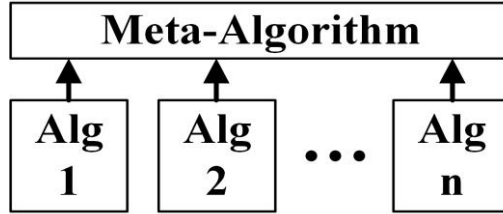


Fig. 10: Co-evolutionary Algorithm

Dynamic programming as the most popular co-evolutionary approach is a promising optimization method specifically in large-scale MGs and MGC to tackle dimensionality. In [104, 105], a dynamic programming method is developed to achieve the maximum profit from energy trading in a day. Furthermore, in the hybrid meta-heuristic approach, a heuristic algorithm combines with other optimization methods in order to exploit the complementary identity of different optimization methods. Vector evaluated genetic algorithm (VEGA) provides a robust search technique for a complicated multi-objective optimization problem. VEGA divides the population into multiple sub-population, and by considering Pareto dominance, only in the process of optimization, the individuals evolve toward the single objective. In consequence, the optimal non-dominated solution evaluates by a non-Pareto optimization algorithm [106]. The same policy is applied in parallel meta-heuristic approaches by taking advantage of multiple meta-heuristic algorithms.

In Table V, an overview of the different optimization methods in MGC applications is presented.

TABLE V
OPTIMIZATION IN MGC APPLICATION

| No. | Ref | Optimization Method | No. of OFs | Objective Functions |
|-----|----------------|---------------------------------|------------|--|
| 1 | [65] | logarithmic-barrier method | 4 | Minimizing the cost function of 4 MGs |
| 2 | [110] | Feasibility method + PSO | 1 | comprehensive assessment indices such as node voltage, power decoupling, system damping, and reactive power sharing |
| 3 | [99] | Weighted sum method | 3 | Maximizing MG's demand response program profit, minimizing generators cost and trading cost |
| 4 | [113] [114] | Weighted sum + Fuzzy techniques | 2 | Carbon emission and operation cost |
| 5 | [115] | Weighted sum + Fuzzy techniques | 3-4 | Loss minimization, minimizing apparent power transmitting, voltage deviation index (VDI), and system load balancing index (SLBI) |
| 6 | [116] | Weighted sum | 3 | Generation cost, pollutant gas emission and expected energy not supplied (EENS) |

| | | | | |
|----|-------|---|-----|--|
| 7 | [119] | Goal programming | 3 | Storage power rating, energy capacity, and the year of installation |
| 8 | [120] | Goal programming | 4 | Minimize the emission cost, the storage operating cost, startup/shutdown cost of the generation units, and maximizing their efficiency |
| 9 | [121] | MCD A + goal attainment | 3 | Cost of operation, peak load reduction, and emissions |
| 10 | [122] | Goal programming | 3 | Minimize the operational costs, the emissions produced, and the loss of life of assets exposed to excess temperatures |
| 11 | [123] | Goal programming | 4 | Minimize the deep discharge of battery, overcharging of battery, the curtailment amount of REs and Loads |
| 12 | [124] | Goal attainment | 3 | Minimize the energy cost, the active electrical losses, the natural gas losses |
| 13 | [125] | Weighted metric method | 2 | Minimizing fuel consumption and battery degradation costs |
| 14 | [127] | Augmented ϵ -constrain | 2 | Minimizing total cost and peak load |
| 15 | [128] | ϵ -constrain | 2 | Minimizing the MG total generation cost and the active power losses in the LCL filter of each inverter |
| 16 | [129] | ϵ -constrain | 2 | Minimization of total investment cost and loss of load expectation |
| 17 | [130] | Augmented ϵ -constrain | 2 | Minimizing the ship operating cost and gas emissions |
| 18 | [131] | ϵ -constrain | 2 | minimizing the cost of installing power/heat generation sources and the expected energy not served (EENS) |
| 19 | [132] | Augmented ϵ -constrain + fuzzy decision making | 2 | Economical (active and reactive power transfers from the external network, dispatchable distributed generations operations cost, degradation cost of plug-in electric vehicles battery), technical (Voltage deviation index) |
| 20 | [133] | ϵ -constrain | 2 | Minimizing operating cost, maximizing power quality |
| 21 | [136] | NSGA-II | 2 | Minimizing operating cost and the pollutants emission |
| 22 | [138] | NSGA-II | 2 | Optimally calculate the parameters of the system and the controllers by minimizing the maximum real part of the eigenvalues |
| 23 | [139] | Game theory + NSGA-II | N | Cost function of N microgrids (in this paper $N=10$) |
| 24 | [140] | NSGA-II | 2 | Minimizing total cost of electricity and the peak demand |
| 25 | [141] | NSGA-II | 3 | Minimization of operational cost, total emissions and power losses |
| 26 | [142] | NSGA-II | 2 | Minimize power generation cost and maximize the useful life of lead-acid batteries |
| 27 | [144] | Modified SPEA-II | 2 | Maximizes social welfare and minimizes losses |
| 28 | [146] | Improved SPEA-II | 3 | Minimizing economical cost, maximizing the average utilization rate of chargers and user's charging convenience |
| 29 | [147] | SPEA-II | 2 | Minimizing peak load demands and the expenditure to the costumers |
| 30 | [148] | SPEA-II | 2 | Maximizing revenue and minimizing expenses |
| 31 | [149] | MOPSO, PESA-II, SPEA-II | 3 | Minimizing the Net Present Cost, the penalty cost of emission and the quantity of the CO ₂ released into the atmosphere |
| 32 | [151] | PESA-II | 3 | Minimizing the loss of load probability, life cycle cost, and levelized cost of energy |
| 33 | [153] | MOPSO | 2 | Minimizing the Cost of Electricity (COE) and Loss of Power Supply Probability (LPSP) |
| 34 | [154] | MOPSO | 2 | Maximize the consistency of the generation system and maximum utilization of resources |
| 35 | [155] | MOPSO | 2 | Minimize the operation cost of the microgrid and maximize the generated power by each source |
| 36 | [156] | MOPSO | 2 | Minimizing the total cost of the system optimal design with hybrid REs in a smart microgrid to increase the availability |
| 37 | [157] | MOPSO | 3 | Minimizing annualized cost of the system, loss of load expected and loss of energy expected |
| 38 | [158] | MOPSO + fuzzy decision making | 2 | Optimal operation time (OT) and optimization constraints |
| 39 | [159] | MOPSO, | 2 | Minimizing the operation cost and pollution rate |

| | | | | |
|----|-------|--|---|--|
| 40 | [161] | NSGA-II MOEA/D | 2 | Minimizing the Loss of Power Supply Probability (LPSP) and Cost of Electricity (COE) |
| 41 | [162] | Cone-based multi-objective evolutionary algorithm based on decomposition | 2 | Maximize the active power injection by single-phase units, and minimize the currents unbalance into the main grid |
| 42 | [163] | Adaptive MOEA/D, MOEA/D | 3 | Minimizing the transmission losses, operating costs, and carbon emissions of multiple microgrid systems |
| 43 | [164] | Improved MOEA/D | 4 | Minimization of total operating cost, active network loss, voltage deviation and the total output reduction rate of renewable energy |
| 44 | [166] | MOEA/D | 2 | Maximizing the active power generation, minimizing the reactive power circulation and current unbalance |
| 45 | [104] | Dynamic programming | 5 | Maximizing Profit (Profit = Revenue – Cost) Cost = Generation cost + Start-up and Shut-down cost + Electric buying cost + Battery wear cost |
| 46 | [105] | Dynamic programming | 2 | Minimize the cash flow of the system and maximizing the net power import from the main grid |

1.5. FEATURE SELECTION AND CLUSTERING ALGORITHMS

In multi-objective optimization problems, a wide variety of optimum solutions are proposed by the algorithm. Therefore, a supplementary evaluation is typically essential to select the proper Pareto-front solution. Various methods can be applied to these problems in order to evaluate the Pareto-front solutions. The first and preliminary approach that could be utilized in these problems is exploiting the experience of the designer. For instance, in [167], a certain amount of Pareto-front solutions is tabulated for three different cases, and the results can be evaluated for each solution to select the final proper solution according to the best operation of the system. Moreover, the knee point for convex Pareto front is typically an appropriate solution as a trade-off between two or several objective extremes. In [78, 129], the knee point is used as a compromise solution.

A sort of intelligent approach has been introduced in recent years that can be effectively applied in selecting a proper solution amongst a set of optimal solutions presented in Pareto-front. Feature selection and clustering algorithms are two important approaches in data mining science that can apply in data analysis related to the Pareto-optimal set.

Artificial intelligence (AI) is a practical tool using in feature selection and clustering data analysis. Feature selection is a process of selecting a small subset of essential features from the data. On the other hand, in clustering analysis, the data points are assigned to belong to the clusters such that items in the same cluster are as similar as possible from the aspects of similarity measurement like distance, connectivity, and

intensity. Supervised learning artificial neural networks (ANN) such as multilayer perceptron (MLP), radial basis function (RBF), and unsupervised learning ANN like self-organized map (SOM) and Hopfield neural network are able to apply to the algorithms in feature selection or clustering applications. Support vector machines (SVM) are also a kind of neural network that, unlike MLP and RBF, minimizes the operational risk of classification or modeling instead of minimizing the error between system and model.

The k-means (KM) problem is also one of the famous clustering problems that can be solved by the Lloyd algorithm. In the k-means problem, the data partition to K cluster in which each data belongs to the nearest mean of the partitions [168]. Fuzzy clustering algorithms are another clustering method such that data points can belong in more than one cluster. Easier creating the fuzzy boundaries is the main advantage of this method from the computation point of view. In [127], a fuzzy clustering method is applied to the multi-optimization problem to deal with the large scale of the solution set. It is shown that the selection of the Pareto optimal set depends on the preference of the decision-maker. Fuzzy C-means (FCM) clustering is one of the most popular fuzzy clustering algorithms. FCM is very similar to the KM algorithm; however, FCM is extremely slower than KM due to iterative fuzzy calculation [169]. In [170], FCM clustering is utilized to reduce the total output scenarios generated by Latin hypercube sampling (LHS) to analyze the uncertainty of RE output. Fig 11 represents the different clustering methods. In Table VI, different methods to find the best compromise solution in multi-objective optimization for microgrids applications are reviewed.

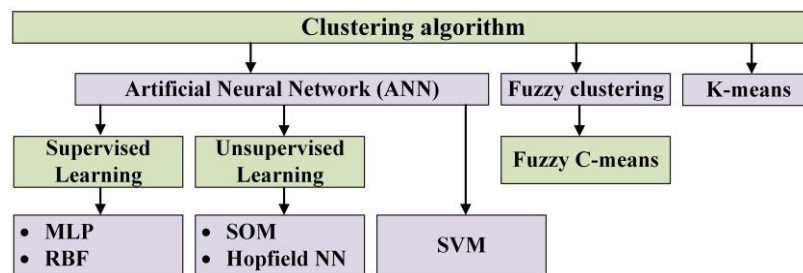


Fig. 11: Clustering methods

TABLE VI
FEATURE SELECTION AND CLUSTERING METHODS IN MULTI-OBJECTIVE OPTIMIZATION

| No. | Ref | Clustering Method | Explanations |
|-----|-------|-------------------|---|
| 1 | [171] | k-means | To significantly reduce the computation time by determining a representative load profile. |
| 2 | [172] | k-means | To generate typical daily load scenarios and used the upper and lower ranges to describe the load |

| | | | |
|----|------------------------|---|---|
| | | | and uncertainty to build a robust optimization model. |
| 3 | [173] | Wasserstein distance + k-means | To generate optimal scene and reflecting the random feature of distributed generation accurately. |
| 4 | [174] | Monte Carlo + k-means | To predict the load on the source-side and load-side. |
| 5 | [175] | Latin hypercube sampling (LHS) algorithm + k-means | To generate all uncertainties |
| 6 | [127] | Fuzzy clustering method | To select the final scheme according to the preference of decision maker. |
| 7 | [176] | Fuzzy satisfying technique | To determine the best solution among the obtained solutions. |
| 8 | [177] | Fuzzy clustering approach | To control the size of repository up to a limit range. |
| 9 | [178] | Fuzzy C-means clustering + grey relation projection | To identify the best compromise solutions from the entire solutions. |
| 10 | [179] | Fuzzy decision-making method | To enhance the decision makers obtain a solution from Pareto front. |
| 11 | [159] | Fuzzy decision-making | To choose a better solution from optimal solutions to manage the MG. |
| 12 | [148] | Two extremes and the middle of a Pareto front | To analyze the optimum solution |
| 13 | [162] | VIKOR multi-criteria decision-making methods | To select the solution that best suits the preferences of the Decision-Maker. |
| 14 | [164] | Fuzzy decision method | To select the best solution to be used in the scheduling scheme. |
| 15 | [129] | Knee point | Minimization of total investment cost and loss of load expectation |
| 16 | [78] | Knee point | To find the best compromise solution as a trade-off between two quality goals i.e. shifting and shrinking in convex curve. |
| 17 | [157] | Trade-off solution by fuzzy set | The best compromise solution is chosen based on the distance of non-dominated solutions and the nearest solution to the fuzzified origin. |
| 18 | [180] | R-NSGA-II | A combination of the classic NSGA-II with a multi-criteria decision-making approach to find a single optimal solution. |
| 19 | [137] | Fuzzy set | To determine the best compromise solution from the set of Pareto optimal solutions. |
| 20 | [113] | max-min fuzzy technique | To select the best solution which compromises both objective functions |
| 21 | [132],[99],[116],[181] | Fuzzy decision-making | To select the trade-off solution amid the obtained solutions |

2. POWER ELECTRONICS INTERFACE FOR MGs

By increasing the tendency of renewable energy resources penetration to the power system, inevitably the significance of power electronics interfaces in MGs is revealed. Depending on the MG system, various power electronics interfaces can be utilized in order to meet the system requirements. The typical structure of a power electronics-based DC and AC microgrid is depicted in Fig 12 and 13 respectively [182]. The cost and efficiency of DC MGs propose a superior performance compared with AC MGs. However, the application of DC MGs is limited to telecommunication systems [183], electric vehicles [184], and shipboard power systems [185].

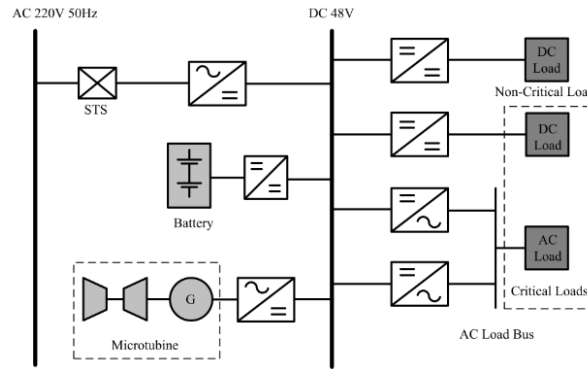


Fig. 12: Typical structure of a power electronics-based DC MG [182]

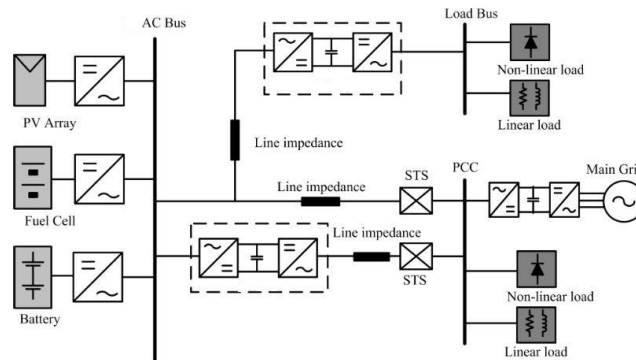


Fig. 13: Typical structure of a power electronics-based AC MG [182]

Accordingly, the electrical coupling of distributed energy resources (DERs) is illustrated in Fig. 14 [182]. Fig. 14. (a) represents an isolated single-stage power conversion system. This structure is normally utilized in high-power PV systems with series connections of panels to provide appropriate input voltage for the inverter. The bulky line frequency transformer is employed for power systems with isolation requirements [186]. Fig. 14. (b) depicts a non-isolated power conversion system with a DC-DC converter connected to RESs to step up the produced voltage and inverter operation [187]-[189]. Various non-isolated step-up converters with different voltage boost techniques are widely employed in this structure. Fig. 14. (c) demonstrates an isolated structure with a direct inverter connection to RESs and line frequency transformer with isolation purposes. Eventually, Fig. 14. (d) shows a popular structure with an isolated DC-DC converter to avoid using the line frequency transformer. The two-stage power conversion system is the most common structure, especially for low and medium MG systems. In this configuration, the first stage is used to extract the maximum power from RESs, step-up the generated voltage, and isolate the energy generation units in case of power system regulations.

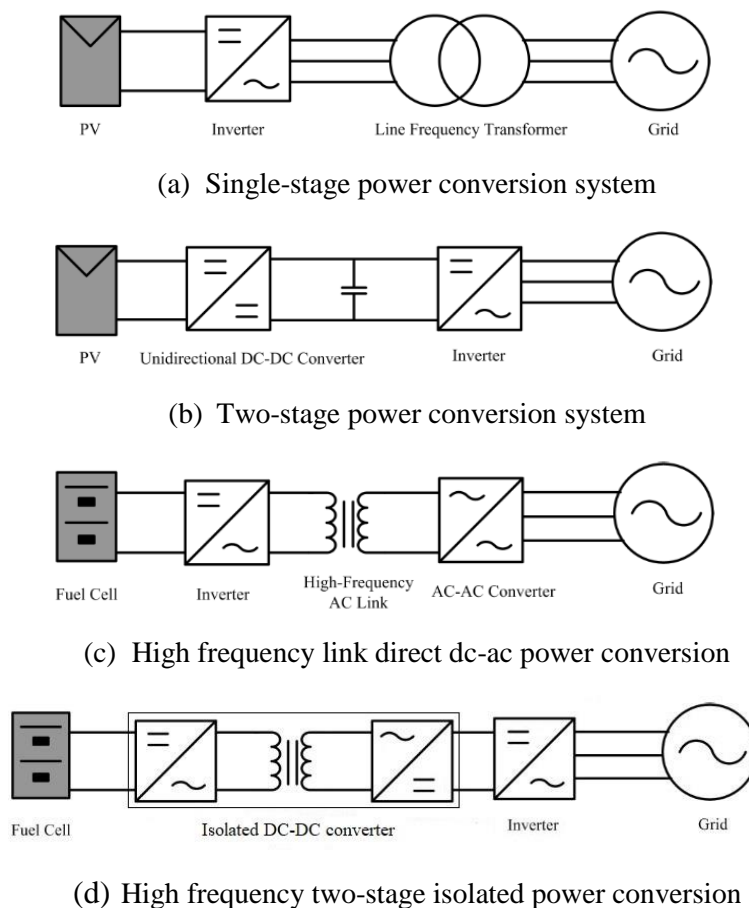


Fig. 14: structures of electronically-coupled DER units [182]

2.1. STEP-UP DC-DC CONVERTER

Step-up converters are widely used in hybrid MGs integrated with renewable energies especially by growing up the residential and small-scale MGs in the power system to increase the RE penetration. In recent years, different high step-up topologies are proposed in order to tackle the high-stress voltage and current of semiconductor devices and the reverse recovery problem of output diode. Therefore, the main challenge of high step-up converters is obtaining high gain voltage with a lower duty cycle. Accordingly, various voltage boost techniques are reviewed in [190]. Fig. 15 shows the voltage boost techniques classification for DC-DC converters.

In this thesis, LLC resonant converter as a high-efficiency isolated converter is studied. The high-frequency transformer of the LLC resonant converter is considered a magnetic coupling in order to step-up the voltage. Moreover, in [191] a novel high step-up interleaved LLC converter is proposed. The proposed topology consists of a two-phase interleaved full bridge with secondary and tertiary windings to increase the voltage gain.

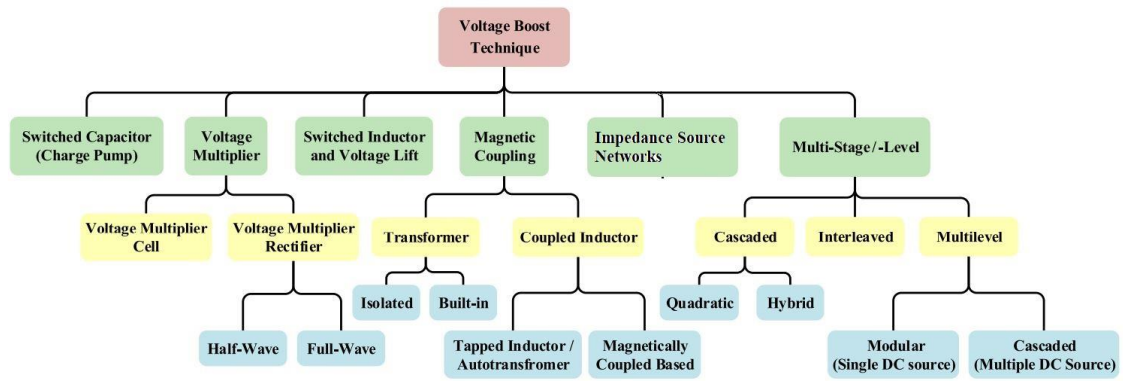


Fig. 15: Voltage boost techniques classification for DC-DC converters [190]

In addition, impedance source networks or Z-source converter is investigated in this thesis for both DC-DC and DC-AC converters. The z-source converter has been proposed by Fang Zheng Peng in 2002. These kinds of converters can be used for DC-DC, DC-AC, AC-DC, and AC-AC power conversion purposes [192]. Fig. 16 indicates the general structure of the z-source converter.

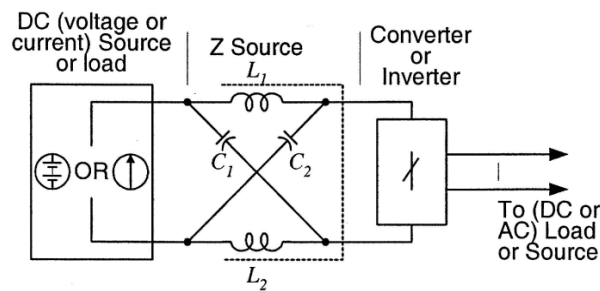


Fig. 16: Z-source converter structure [192]

Various impedance-network-based power converter with magnetic coupling technique has emerged in recent years. Fig. 17 depicts the most popular magnetically coupled impedance source network. Although the leakage inductance of coupled inductances can cause limitations for the normal operation of the converter, several methods such as switch cell capacitors are proposed in pieces of literature to eliminate this adverse effect.

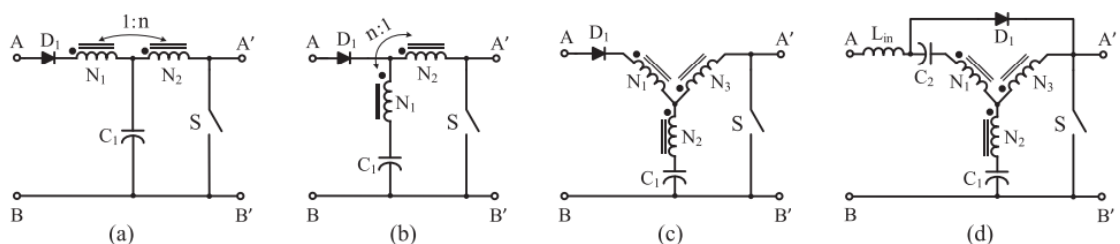


Fig. 17: Different magnetically coupled impedance source networks, (a) Trans-Z-source, (b) Γ -source, (c) Y-source, (d) Quasi-Y-source [190]

Fig. 17. (a) shows a trans-Z-source impedance network with a coupled inductor used to increase the voltage gain. A Γ -source impedance network that also exploits a coupled inductor is shown in Fig. 17 (b). The voltage gain of a trans-Z-source structure increases by increasing the turns ratio, while in a Γ -source structure gain increases by decreasing the turns ratio [190]. A three-winding coupled-inductor-based dc–dc converter that employs a novel impedance network is presented in [193]. Fig. 17. (c) shows a Y-source impedance network, which has more design degrees of freedom in comparison with Trans-Z-source topology. Fig. 17 (d) presents a continuous input current version of this converter, known as a quasi-Y-source dc–dc converter [194].

The variety of impedance source network topologies is not restricted to the proposed magnetically coupled inductor in Fig. 17. A zero-voltage switching high step-up three-level coupled inductor-based boost converter is proposed in [195]. Fig 18 represents the proposed structure of a high step-up converter. Three level structure of the proposed converter results in a significant reduction of the switches and diodes' voltage stress. The leakage inductance by coupled inductor leads to voltage ringing, the use of the active-clamp circuit in this structure eliminates the voltage ringing and makes all switches turn on and off under ZVS condition that results in improving the efficiency.

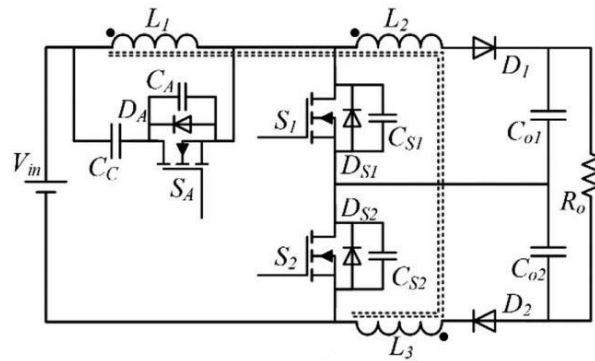


Fig. 18: The proposed ZVT high step-up three level coupled-inductor-based boost converter [195]

In [196], as can be seen in Figure 19, the proposed converter achieves high voltage gain and low switch voltage stress with a magnetic-coupling-based voltage multiplier technique. Also, due to a boost inductor at the input, the continuous input current is obtained, which is beneficial for battery, fuel cell, and photovoltaic applications. Moreover, zero voltage switching of the MOSFETs is achieved by utilizing an active

clamp technique, leading to low switching losses. Furthermore, zero DC bias of the coupled inductor is realized, resulting in small magnetic size and low core losses.

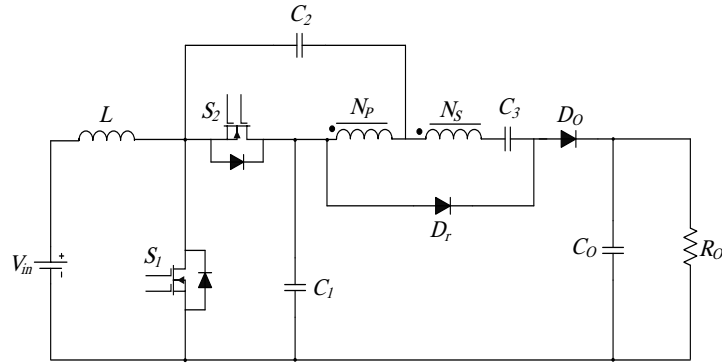


Fig. 19: The schematic of the high step-up converter presented in [196]

Flyback-boost converter with a coupled inductor is an attractive method for step-up converters. Fig. 20 shows a flyback-boost topology [197]. As can be observed in Fig. 20, the flyback converter transformer is combined with the output filter inductor of boost converter. It consists of two diodes D_{o1} and D_{o2} , one active switch S , and two output capacitors C_{o1} and C_{o2} . Generally, this converter works like the conventional boost or flyback converter. The energy is stored in the mutual core of the transformer when switch S is on and it is transferred to the output when switch S is off and diodes D_{o1} and D_{o2} are on.

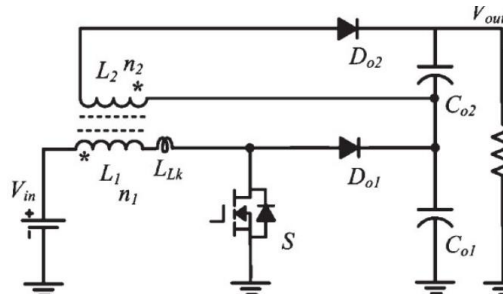


Fig. 20: Flyback-boost converter topology [197]

Fig. 21 shows another step-up topology employing a flyback boost converter [198]. As can be seen for the flyback-Boost converter with a coupled inductor, positive and negative voltage pulses have been applied across inductor L_1 when active switch S is turned on and off. Therefore, similar voltage pulses were induced across inductor L_2 , then these pulses were rectified with an output diode, and then this rectified voltage was used to charge the output capacitor. So negative pulses were just used to charge the output capacitor in the previous converter. However, in this converter, both positive and negative pulses are used to charge output capacitors.

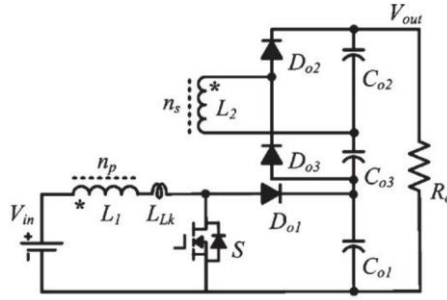


Fig. 21: Flyback-boost converter with voltage multiplier topology [198]

Various step-up topologies are proposed by researchers in order to enhance the performance of these converter. However, specific system requirements lead to evaluate the proposed structures with their potential pros and cons. A comprehensive review is conducted in [199]-[202].

3. CONCLUSION

According to the literature researches, master-slave, peer-to-peer, and hierarchical architecture are considered as the most prominent control strategies in grid-connected or isolated MGs. Each control strategy proposes specific features to MG and MGC operation from the efficiency and reliability perspective. The analysis verifies that the hierarchical structure could provide more reliable operation by employing different control strategies such as centralized, decentralized, hybrid, and distributed control. Furthermore, planning and scheduling programs for MGs are investigated in order to determine the practical and technical specifications of the operating system. Therefore, an energy management system is essentially required not only to guarantee the optimal operation and economic feasibility but also to follow specific practical and technical considerations determined by planning and scheduling. Consequently, the optimum operation assessment of MGs is the main purpose of energy management system in MGs. The optimum operation of MGs from the mathematics point of view is considered an optimization problem. Obviously, a more appropriate utilized optimizer results in a more reliable MG operation. To this end, this chapter concentrates on various optimization methods to fulfill the performance of MGs associated with practical and technical constraints, calculation burden, information communication delay, etc. A classification of optimization methods in order to solve the single objective and multi-objective problems is presented. Several multi-objective approaches are discussed, and it was observed that by applying the concept of dominance, the advanced single-

objective algorithms like GA, PSO, etc., turn to multi-objective algorithms like NSGA, MOPSO, etc. The multi-objective algorithms produced the Pareto-front set. Unlike single-objective optimization, in multi-objective optimization, a set of optimum solutions is offered by the algorithm. Therefore, the optimum solutions are required to be evaluated in order to select the proper solutions. Ultimately, various methods such as feature selection and clustering methods are proposed to analyze the Pareto-optimal solutions. The performance of the optimization algorithms can enhance by incorporating deep learning approaches. In this case, the optimal solutions can be produced properly employing deep learning algorithms. Therefore, the performance will be improved by reducing the calculation burden and obtaining more accurate solutions. This incorporation can be surveyed in future works.

On the other hand, by proposing an NMG system it is expected the size of the power generation units reduced. The low voltage generation of RESs units resulting from the parallel connection of RESs units makes using isolated or non-isolated step-up converters -depending on the power system requirements- essential to meet the required input voltage for inverters. Therefore, an overview of various step-up topologies is conducted in order to represent different voltage boost methods.

4. REFERENCES

- [1] Najafzadeh M, Ahmadihangar R, Husev O, Roasto I, Jalakas T, Blinov A. Recent Contributions, Future Prospects and Limitations of Interlinking Converter Control in Hybrid AC/DC Microgrids. *IEEE Access*. 2021 Jan 4;9:7960-84.
- [2] Peyghami S, Palensky P, Blaabjerg F. An overview on the reliability of modern power electronic based power systems. *IEEE Open Journal of Power Electronics*. 2020 Feb 14;1:34-50.
- [3] Wang F, Ji S. Benefits of high-voltage SiC-based power electronics in medium-voltage power-distribution grids. *Chinese Journal of Electrical Engineering*. 2021 Apr 6;7(1):1-26.
- [4] Kazerani M, Tehrani K. Grid of Hybrid AC/DC Microgrids: A New Paradigm for Smart City of Tomorrow. In 2020 IEEE 15th International Conference of System of Systems Engineering (SoSE) 2020 Jun 2 (pp. 175-180). IEEE.
- [5] Abdi H, Beigvand SD, La Scala M. A review of optimal power flow studies applied to smart grids and microgrids. *Renewable and Sustainable Energy Reviews*. 2017 May 1;71:742-66.
- [6] Faisal M, Hannan MA, Ker PJ, Hussain A, Mansor MB, Blaabjerg F. Review of energy storage system technologies in microgrid applications: Issues and challenges. *Ieee Access*. 2018 May 28;6:35143-64.
- [7] Sinha S, Bajpai P. Power management of hybrid energy storage system in a standalone DC microgrid. *Journal of Energy Storage*. 2020 Aug 1;30:101523.
- [8] Bandejas F, Pinheiro E, Gomes M, Coelho P, Fernandes J. Review of the cooperation and operation of microgrid clusters. *Renewable and Sustainable Energy Reviews*. 2020 Nov 1;133:110311.
- [9] Jena S, Padhy NP, Guerrero JM. Cyber-Resilient Cooperative Control of DC Microgrid Clusters. *IEEE Systems Journal*. 2021 Mar 22.
- [10] Wu L, Ortmeier T, Li J. The community microgrid distribution system of the future. *The Electricity Journal*. 2016 Dec 1;29(10):16-21.

- [11] Jadhav AM, Patne NR, Guerrero JM. A novel approach to neighborhood fair energy trading in a distribution network of multiple microgrid clusters. *IEEE Transactions on Industrial Electronics*. 2018 Mar 15;66(2):1520-31.
- [12] Vuddanti S, Salkuti SR. Review of Energy Management System Approaches in Microgrids. *Energies*. 2021 Jan;14(17):5459.
- [13] Al-Ismael FS. DC Microgrid Planning, Operation, and Control: A Comprehensive Review. *IEEE Access*. 2021 Mar 1;9:36154-72.
- [14] García Vera YE, Dufo-López R, Bernal-Agustín JL. Energy management in microgrids with renewable energy sources: A literature review. *Applied Sciences*. 2019 Jan;9(18):3854.
- [15] Hossain MA, Chakraborty RK, Ryan MJ, Pota HR. Energy management of community energy storage in grid-connected microgrid under uncertain real-time prices. *Sustainable Cities and Society*. 2021 Mar 1;66:102658.
- [16] Kumar PS, Chandrasena RP, Ramu V, Srinivas GN, Babu KV. Energy management system for small scale hybrid wind solar battery based microgrid. *IEEE Access*. 2020 Jan 6;8:8336-45.
- [17] Hemmati R, Saboori H, Siano P. Coordinated short-term scheduling and long-term expansion planning in microgrids incorporating renewable energy resources and energy storage systems. *Energy*. 2017 Sep 1;134:699-708.
- [18] Liu S, Wang X, Liu PX. Impact of communication delays on secondary frequency control in an islanded microgrid. *IEEE Transactions on Industrial Electronics*. 2014 Nov 5;62(4):2021-31.
- [19] Cao G, Lou G, Gu W, Sheng L. H_{∞} robustness for distributed control in autonomous microgrids considering cyber disturbances. *CSEE Journal of Power and Energy Systems*. 2021 Apr 30.
- [20] Zia MF, Benbouzid M, Elbouchikhi E, Muyeen SM, Techato K, Guerrero JM. Microgrid transactive energy: Review, architectures, distributed ledger technologies, and market analysis. *Ieee Access*. 2020 Jan 22;8:19410-32.
- [21] Nikam V, Kalkhambkar V. A review on control strategies for microgrids with distributed energy resources, energy storage systems, and electric vehicles. *International Transactions on Electrical Energy Systems*. 2021 Jan;31(1):e12607.
- [22] Zia MF, Elbouchikhi E, Benbouzid M. Microgrids energy management systems: A critical review on methods, solutions, and prospects. *Applied energy*. 2018 Jul 15;222:1033-55.
- [23] Chen B, Wang J, Lu X, Chen C, Zhao S. Networked microgrids for grid resilience, robustness, and efficiency: a review. *IEEE Transactions on Smart Grid*. 2020 Aug 18;12(1):18-32.
- [24] Nosratabadi SM, Hooshmand RA, Gholipour E. A comprehensive review on microgrid and virtual power plant concepts employed for distributed energy resources scheduling in power systems. *Renewable and Sustainable Energy Reviews*. 2017 Jan 1;67:341-63.
- [25] Dawoud SM, Lin X, Okba MI. Hybrid renewable microgrid optimization techniques: A review. *Renewable and Sustainable Energy Reviews*. 2018 Feb 1;82:2039-52.
- [26] Gamarra C, Guerrero JM. Computational optimization techniques applied to microgrids planning: A review. *Renewable and Sustainable Energy Reviews*. 2015 Aug 1;48:413-24.
- [27] Zhou Q, Shahidehpour M, Paaso A, Bahramirad S, Alabdulwahab A, Abusorrah A. Distributed control and communication strategies in networked microgrids. *IEEE Communications Surveys & Tutorials*. 2020 Sep 15;22(4):2586-633.
- [28] Hannan MA, Tan SY, Al-Shetwi AQ, Jern KP, Begum RA. Optimized controller for renewable energy sources integration into microgrid: Functions, constraints and suggestions. *Journal of Cleaner Production*. 2020 May 20;256:120419.
- [29] Emad D, El-Hameed MA, Yousef MT, El-Fergany AA. Computational methods for optimal planning of hybrid renewable microgrids: a comprehensive review and challenges. *Archives of Computational Methods in Engineering*. 2019 Jul 19:1-23.
- [30] Weiss G, Dörfler F, Levron Y. A stability theorem for networks containing synchronous generators. *Systems & Control Letters*. 2019 Dec 1;134:104561.
- [31] Shah R, Mithulananthan N, Bansal RC, Ramachandaramurthy VK. A review of key power system stability challenges for large-scale PV integration. *Renewable and Sustainable Energy Reviews*. 2015 Jan 1;41:1423-36.
- [32] Han Y, Zhang K, Li H, Coelho EA, Guerrero JM. MAS-based distributed coordinated control and optimization in microgrid and microgrid clusters: A comprehensive overview. *IEEE Transactions on Power Electronics*. 2017 Oct 9;33(8):6488-508.

- [33] Çelik D, Meral ME. A flexible control strategy with overcurrent limitation in distributed generation systems. *International Journal of Electrical Power & Energy Systems*. 2019 Jan 1;104:456-71.
- [34] Raeispour M, Atrianfar H, Baghaee HR, Gharehpetian GB. Robust Sliding Mode and Mixed H_2/H_∞ Output Feedback Primary Control of AC Microgrids. *IEEE Systems Journal*. 2020 Aug 31.
- [35] Caldognetto T, Tenti P. Microgrids operation based on master–slave cooperative control. *IEEE Journal of Emerging and Selected Topics in Power Electronics*. 2014 Jul 31;2(4):1081-8.
- [36] Lu X, Lai J, Liu GP. Master-slave cooperation for multi-DC-MGs via variable cyber networks. *IEEE Transactions on Cybernetics*. 2021 Apr 19.
- [37] Lai J, Lu X, Yu X, Yao W, Wen J, Cheng S. Distributed multi-DER cooperative control for master-slave-organized microgrid networks with limited communication bandwidth. *IEEE Transactions on Industrial Informatics*. 2018 Oct 16;15(6):3443-56.
- [38] Werth A, André A, Kawamoto D, Morita T, Tajima S, Tokoro M, Yanagidaira D, Tanaka K. Peer-to-peer control system for DC microgrids. *IEEE Transactions on Smart Grid*. 2016 Dec 12;9(4):3667-75.
- [39] Zhang C, Wu J, Zhou Y, Cheng M, Long C. Peer-to-Peer energy trading in a Microgrid. *Applied Energy*. 2018 Jun 15;220:1-2.
- [40] Zhang Z, Tang H, Ren J, Huang Q, Lee WJ. Strategic Prosumers based Peer-to-Peer Energy Market Design for Community Microgrids. *IEEE Transactions on Industry Applications*. 2021 Mar 8.
- [41] Han Y, Shen P, Zhao X, Guerrero JM. Control strategies for islanded microgrid using enhanced hierarchical control structure with multiple current-loop damping schemes. *IEEE Transactions on Smart Grid*. 2015 Sep 29;8(3):1139-53.
- [42] Guerrero JM, Chandorkar M, Lee TL, Loh PC. Advanced control architectures for intelligent microgrids—Part I: Decentralized and hierarchical control. *IEEE Transactions on Industrial Electronics*. 2012 Apr 16;60(4):1254-62.
- [43] Abhishek A, Ranjan A, Devassy S, Verma BK, Ram SK, Dhakar AK. Review of hierarchical control strategies for DC microgrid. *IET Renewable Power Generation*. 2020 Apr 21;14(10):1631-40.
- [44] Zhao W, Zhang X, Li Y, Qian N. Improved master-slave control for Smooth Transition Between Grid-connected and Islanded Operation of DC Microgrid Based on I- ΔV Droop. In 2020 IEEE 9th International Power Electronics and Motion Control Conference (IPEMC2020-ECCE Asia) (pp. 1194-1198). IEEE.
- [45] Wang C, Yang P, Ye C, Wang Y, Xu Z. Improved V/f control strategy for microgrids based on master–slave control mode. *IET Renewable Power Generation*. 2016 May 26;10(9):1356-65.
- [46] Tayab UB, Roslan MA, Hwai LJ, Kashif M. A review of droop control techniques for microgrid. *Renewable and Sustainable Energy Reviews*. 2017 Sep 1;76:717-27.
- [47] Wang S, Liu Z, Liu J, An R, Xin M. Breaking the boundary: A droop and master-slave hybrid control strategy for parallel inverters in islanded microgrids. In 2017 IEEE Energy Conversion Congress and Exposition (ECCE) 2017 Oct 1 (pp. 3345-3352). IEEE.
- [48] Cai N, Mitra J. A multi-level control architecture for master-slave organized microgrids with power electronic interfaces. *Electric Power Systems Research*. 2014 Apr 1;109:8-19.
- [49] Marzal S, Salas-Puente R, González-Medina R, Figueres E, Garcera G. Peer-to-peer decentralized control structure for real time monitoring and control of microgrids. In 2017 IEEE 26th International Symposium on Industrial Electronics (ISIE) 2017 Jun 19 (pp. 140-145). IEEE.
- [50] Engels J, Almasalma H, Deconinck G. A distributed gossip-based voltage control algorithm for peer-to-peer microgrids. In 2016 IEEE International Conference on Smart Grid Communications (SmartGridComm) 2016 Nov 6 (pp. 370-375). IEEE.
- [51] Lai J, Lu X, Wang F, Dehghanian P, Tang R. Broadcast gossip algorithms for distributed peer-to-peer control in AC microgrids. *IEEE Transactions on Industry Applications*. 2019 Feb 8;55(3):2241-51.
- [52] Chen J, Hou S, Chen J. Seamless mode transfer control for master–slave microgrid. *IET Power Electronics*. 2019 Jul 17;12(12):3158-65.
- [53] Bidram A, Davoudi A. Hierarchical structure of microgrids control system. *IEEE Transactions on Smart Grid*. 2012 May 18;3(4):1963-76.

- [54] Alam MN, Chakrabarti S, Ghosh A. Networked microgrids: State-of-the-art and future perspectives. *IEEE Transactions on Industrial Informatics*. 2018 Nov 15;15(3):1238-50.
- [55] Padhi PP, Mishra SP. Application of Control Strategy to DC Micro grids: A Survey. In 2021 7th International Conference on Electrical Energy Systems (ICEES) 2021 Feb 11 (pp. 377-384). IEEE.
- [56] Mehdi M, Kim CH, Saad M. Robust Centralized Control for DC Isolated Microgrid Considering Communication Network Delay. *IEEE Access*. 2020 Apr 23;8:77765-78.
- [57] Xu Q, Xiao J, Wang P, Wen C. A decentralized control strategy for economic operation of autonomous AC, DC, and hybrid AC/DC microgrids. *IEEE Transactions on Energy Conversion*. 2017 Apr 24;32(4):1345-55.
- [58] Mathew P, Madichetty S, Mishra S. A multilevel distributed hybrid control scheme for islanded DC microgrids. *IEEE Systems Journal*. 2019 Feb 21;13(4):4200-7.
- [59] Yazdani M, Mehrizi-Sani A. Distributed control techniques in microgrids. *IEEE Transactions on Smart Grid*. 2014 Aug 1;5(6):2901-9.
- [60] Hu J, Shan Y, Guerrero JM, Ioinovici A, Chan KW, Rodriguez J. Model predictive control of microgrids—An overview. *Renewable and Sustainable Energy Reviews*. 2021 Feb;136:110422.
- [61] Parisio A, Rikos E, Glielmo L. A model predictive control approach to microgrid operation optimization. *IEEE Transactions on Control Systems Technology*. 2014 Jan 9;22(5):1813-27.
- [62] Du Y, Pei W, Chen N, Ge X, Xiao H. Real-time microgrid economic dispatch based on model predictive control strategy. *Journal of Modern Power Systems and Clean Energy*. 2017 Sep;5(5):787-96.
- [63] Ersdal AM, Imsland L, Uhlen K. Model predictive load-frequency control. *IEEE Transactions on Power Systems*. 2015 Mar 23;31(1):777-85.
- [64] Pahasa J, Ngamroo I. Coordinated PHEV, PV, and ESS for microgrid frequency regulation using centralized model predictive control considering variation of PHEV number. *IEEE Access*. 2018 Nov 9;6:69151-61.
- [65] Xing X, Xie L, Meng H. Cooperative energy management optimization based on distributed MPC in grid-connected microgrids community. *International Journal of Electrical Power & Energy Systems*. 2019 May 1;107:186-99.
- [66] Jiang Y, Zhang H, Chen J. Sign-consensus of linear multi-agent systems over signed directed graphs. *IEEE Transactions on Industrial Electronics*. 2016 Dec 21;64(6):5075-83.
- [67] Nash JF. Equilibrium points in n-person games. *Proceedings of the national academy of sciences*. 1950 Jan 15;36(1):48-9.
- [68] Jin S, Wang S, Fang F. Game theoretical analysis on capacity configuration for microgrid based on multi-agent system. *International Journal of Electrical Power & Energy Systems*. 2021 Feb;125:106485.
- [69] Abdel-Raouf O, Elsisy M, Kelash E. A Survey of Game Theory Applications in Electrical Power Micro-Grid Systems. *International Journal of Computer Applications*. 2020;177(37):25-34.
- [70] Churkin A, Bialek J, Pozo D, Sauma E, Korgin N. Review of Cooperative Game Theory applications in power system expansion planning. *Renewable and Sustainable Energy Reviews*. 2021 Jul 1;145:111056.
- [71] Deckmyn C, Vandoorn TL, Moradzadeh M, Vandeveld L. Multi-objective optimization for environmental scheduling in microgrids. In 2014 IEEE PES General Meeting | Conference & Exposition 2014 Jul 27 (pp. 1-5). IEEE.
- [72] Bhattacharjee V, Khan I. A non-linear convex cost model for economic dispatch in microgrids. *Applied energy*. 2018 Jul 15;222:637-48.
- [73] Kumar M, Tyagi B. Capital cost based planning and optimal sizing of a small community smart microgrid. In 2020 12th International Conference on Knowledge and Smart Technology (KST) 2020 (pp. 121-126). IEEE.
- [74] Garg VK, Sharma S, Kumar D. Design and analysis of a microgrid system for reliable rural electrification. *International Transactions on Electrical Energy Systems*. 2021 Feb;31(2):e12734.
- [75] Motjoadi V, Adetunji KE, Joseph MK. Planning of a sustainable microgrid system using HOMER software. In 2020 Conference on Information Communications Technology and Society (ICTAS) 2020 Mar 11 (pp. 1-5). IEEE.

- [76] Ahamad NB, Othman M, Vasquez JC, Guerrero JM, Su CL. Optimal sizing and performance evaluation of a renewable energy based microgrid in future seaports. In 2018 IEEE International Conference on Industrial Technology (ICIT) 2018 Feb 20 (pp. 1043-1048). IEEE.
- [77] Hosseini Moghadam SM, Roghanian H, Dashtdar M, Razavi SM. Size optimization of distributed generation resources in microgrid based on scenario tree. In 2020 8th International conference on smart grid (icSmartGrid) 2020 Jun 17 (pp. 67-72). IEEE.
- [78] Çetinbaş, İpek, Bünyamin Tamyürek, and Mehmet Demirtaş. "Sizing optimization and design of an autonomous AC microgrid for commercial loads using Harris Hawks Optimization algorithm." *Energy Conversion and Management* 245 (2021): 114562.
- [79] Liu Z, Chen Y, Zhuo R, Jia H. Energy storage capacity optimization for autonomy microgrid considering CHP and EV scheduling. *Applied Energy*. 2018 Jan 15;210:1113-25.
- [80] Kaur R, Krishnasamy V, Kandasamy NK. Optimal sizing of wind-PV-based DC microgrid for telecom power supply in remote areas. *IET Renewable Power Generation*. 2018 Feb 8;12(7):859-66.
- [81] Imani MH, Niknejad P, Barzegaran MR. Implementing Time-of-Use Demand Response Program in microgrid considering energy storage unit participation and different capacities of installed wind power. *Electric Power Systems Research*. 2019 Oct 1;175:105916.
- [82] Fazlalipour P, Ehsan M, Mohammadi-Ivatloo B. Optimal participation of low voltage renewable micro-grids in energy and spinning reserve markets under price uncertainties. *International Journal of Electrical Power & Energy Systems*. 2018 Nov 1;102:84-96.
- [83] Contreras SF, Cortes CA, Myrzik JM. Optimal microgrid planning for enhancing ancillary service provision. *Journal of Modern Power Systems and Clean Energy*. 2019 Jul;7(4):862-75.
- [84] Jahangir H, Ahmadian A, Golkar MA. Optimal design of stand-alone microgrid resources based on proposed Monte-Carlo simulation. In 2015 IEEE Innovative Smart Grid Technologies-Asia (ISGT ASIA) 2015 Nov 3 (pp. 1-6). IEEE.
- [85] Morris GY, Abbey C, Wong S, Joós G. Evaluation of the costs and benefits of microgrids with consideration of services beyond energy supply. In 2012 IEEE Power and Energy Society General Meeting 2012 Jul 22 (pp. 1-9). IEEE.
- [86] Nelson JR, Johnson NG. Model predictive control of microgrids for real-time ancillary service market participation. *Applied Energy*. 2020 Jul 1;269:114963.
- [87] Cornélusse B, Savelli I, Paoletti S, Giannitrapani A, Vicino A. A community microgrid architecture with an internal local market. *Applied Energy*. 2019 May 15;242:547-60.
- [88] Fathima AH, Palanisamy K. Optimization in microgrids with hybrid energy systems—A review. *Renewable and Sustainable Energy Reviews*. 2015 May 1;45:431-46.
- [89] Bussieck MR, Meeraus A. General algebraic modeling system (GAMS). In *Modeling languages in mathematical optimization 2004* (pp. 137-157). Springer, Boston, MA.
- [90] Gay DM. The AMPL modeling language: An aid to formulating and solving optimization problems. In *Numerical analysis and optimization 2015* (pp. 95-116). Springer, Cham.
- [91] Bisschop J, Roelofs M. The modeling language AIMMS. In *Modeling Languages in Mathematical Optimization 2004* (pp. 71-104). Springer, Boston, MA.
- [92] Kronqvist J, Bernal DE, Lundell A, Grossmann IE. A review and comparison of solvers for convex MINLP. *Optimization and Engineering*. 2019 Jun;20(2):397-455.
- [93] Mashayekh S, Butler-Purry KL. A novel deterministic and probabilistic dynamic security assessment approach for isolated microgrids. In 2017 19th International Conference on Intelligent System Application to Power Systems (ISAP) 2017 Sep 17 (pp. 1-6). IEEE.
- [94] Alharbi W, Raahemifar K. Probabilistic coordination of microgrid energy resources operation considering uncertainties. *Electric Power Systems Research*. 2015 Nov 1;128:1-0.
- [95] Wang H, Yan Z, Xu X, He K. Probabilistic power flow analysis of microgrid with renewable energy. *International Journal of Electrical Power & Energy Systems*. 2020 Jan 1;114:105393.
- [96] Alavi SA, Ahmadian A, Aliakbar-Golkar M. Optimal probabilistic energy management in a typical micro-grid based-on robust optimization and point estimate method. *Energy Conversion and Management*. 2015 May 1;95:314-25.
- [97] Jahangir H, Ahmadian A, Golkar MA. Optimal design of stand-alone microgrid resources based on proposed Monte-Carlo simulation. In 2015 IEEE Innovative Smart Grid Technologies-Asia (ISGT ASIA) 2015 Nov 3 (pp. 1-6). IEEE.

- [98] Molavi A, Shi J, Wu Y, Lim GJ. Enabling smart ports through the integration of microgrids: A two-stage stochastic programming approach. *Applied Energy*. 2020 Jan 15;258:114022.
- [99] Khalili T, Nojavan S, Zare K. Optimal performance of microgrid in the presence of demand response exchange: A stochastic multi-objective model. *Computers & Electrical Engineering*. 2019 Mar 1;74:429-50.
- [100] Li M. Generalized Lagrange multiplier method and KKT conditions with an application to distributed optimization. *IEEE Transactions on Circuits and Systems II: Express Briefs*. 2018 May 30;66(2):252-6.
- [101] Trovão JP, Antunes CH. A comparative analysis of meta-heuristic methods for power management of a dual energy storage system for electric vehicles. *Energy conversion and management*. 2015 May 1;95:281-96.
- [102] Memmah MM, Lescourret F, Yao X, Lavigne C. Metaheuristics for agricultural land use optimization. A review. *Agronomy for sustainable development*. 2015 Jul;35(3):975-98.
- [103] Gao K, Cao Z, Zhang L, Chen Z, Han Y, Pan Q. A review on swarm intelligence and evolutionary algorithms for solving flexible job shop scheduling problems. *IEEE/CAA Journal of Automatica Sinica*. 2019 Jun 19;6(4):904-16.
- [104] Nguyen MY, Yoon YT, Choi NH. Dynamic programming formulation of micro-grid operation with heat and electricity constraints. In *2009 Transmission & Distribution Conference & Exposition: Asia and Pacific 2009* Oct 26 (pp. 1-4). IEEE.
- [105] An LN, Quoc-Tuan T. Optimal energy management for grid connected microgrid by using dynamic programming method. In *2015 IEEE Power & Energy Society General Meeting 2015* Jul 26 (pp. 1-5). IEEE.
- [106] He H, Haibo T, Hui Q, Wei F, Xiaofeng D. Optimization of Renewable Energy Big Data Transactions Based on Vector Evaluated Genetic Algorithm. In *2018 China International Conference on Electricity Distribution (CICED) 2018* Sep 17 (pp. 2756-2760). IEEE.
- [107] Yeniay Ö. Penalty function methods for constrained optimization with genetic algorithms. *Mathematical and computational Applications*. 2005 Apr;10(1):45-56.
- [108] Nanakorn P, Meesomklin K. An adaptive penalty function in genetic algorithms for structural design optimization. *Computers & Structures*. 2001 Nov 1;79(29-30):2527-39.
- [109] Hauser J, Saccon A. A barrier function method for the optimization of trajectory functionals with constraints. In *Proceedings of the 45th IEEE Conference on Decision and Control 2006* Dec 13 (pp. 864-869). IEEE.
- [110] Wu X, Shen C, Irvani R. Feasible range and optimal value of the virtual impedance for droop-based control of microgrids. *IEEE Transactions on Smart Grid*. 2016 Feb 3;8(3):1242-51.
- [111] Batista LS, Campelo F, Guimarães FG, Ramírez JA. A comparison of dominance criteria in many-objective optimization problems. In *2011 IEEE Congress of Evolutionary Computation (CEC) 2011* Jun 5 (pp. 2359-2366). IEEE.
- [112] Marler RT, Arora JS. The weighted sum method for multi-objective optimization: new insights. *Structural and multidisciplinary optimization*. 2010 Jun 1;41(6):853-62.
- [113] Saberi K, Pashaei-Didani H, Nourollahi R, Zare K, Nojavan S. Optimal performance of CCHP based microgrid considering environmental issue in the presence of real time demand response. *Sustainable cities and society*. 2019 Feb 1;45:596-606.
- [114] Conti S, Nicolosi R, Rizzo SA, Zeineldin HH. Optimal dispatching of distributed generators and storage systems for MV islanded microgrids. *IEEE Transactions on Power Delivery*. 2012 May 21;27(3):1243-51.
- [115] Khalili T, Hagh MT, Zadeh SG, Maleki S. Optimal reliable and resilient construction of dynamic self-adequate multi-microgrids under large-scale events. *IET Renewable Power Generation*. 2019 Apr 16;13(10):1750-60.
- [116] Pourghasem P, Sohrabi F, Abapour M, Mohammadi-Ivatloo B. Stochastic multi-objective dynamic dispatch of renewable and CHP-based islanded microgrids. *Electric Power Systems Research*. 2019 Aug 1;173:193-201.
- [117] Yang Z, Ye Q, Chen Q, Ma X, Fu L, Yang G, Yan H, Liu F. Robust discriminant feature selection via joint L2, 1-norm distance minimization and maximization. *Knowledge-Based Systems*. 2020 Nov 5;207:106090.
- [118] Mandal WA. Weighted Tchebycheff optimization technique under uncertainty. *Annals of Data Science*. 2020 Mar 23:1-23.

- [119] Alharbi H, Bhattacharya K. A Goal Programming Approach to Sizing and Timing of Third Party Investments in Storage System for Microgrids. In 2018 IEEE Electrical Power and Energy Conference (EPEC) 2018 Oct 10 (pp. 1-6). IEEE.
- [120] Hein K, Xu Y, Wilson G, Gupta AK. Coordinated multi-energy dispatch of ship microgrid with reefer system. In IECON 2020 The 46th Annual Conference of the IEEE Industrial Electronics Society 2020 Oct 18 (pp. 2370-2375). IEEE.
- [121] Panwar M, Suryanarayanan S, Hovsopian R. A multi-criteria decision analysis-based approach for dispatch of electric microgrids. *International Journal of Electrical Power & Energy Systems*. 2017 Jun 1; 88:99-107.
- [122] Choobineh M, Mohagheghi S. A multi-objective optimization framework for energy and asset management in an industrial Microgrid. *Journal of Cleaner Production*. 2016 Dec 15; 139:1326-38.
- [123] Hussain A, Kim HM. Goal-Programming-Based Multi-Objective Optimization in Off-Grid Microgrids. *Sustainability*. 2020 Jan;12(19):8119.
- [124] La Scala M, Vaccaro A, Zobaa AF. A goal programming methodology for multiobjective optimization of distributed energy hubs operation. *Applied Thermal Engineering*. 2014 Oct 22;71(2):658-66.
- [125] Chalise S, Sternhagen J, Hansen TM, Tonkoski R. Energy management of remote microgrids considering battery lifetime. *The Electricity Journal*. 2016 Jul 1;29(6):1-0.
- [126] Ehrgott M, Ruzika S. Improved ϵ -constraint method for multiobjective programming. *Journal of Optimization Theory and Applications*. 2008 Sep 1;138(3):375.
- [127] Yang X, Leng Z, Xu S, Yang C, Yang L, Liu K, Song Y, Zhang L. Multi-objective optimal scheduling for CCHP microgrids considering peak-load reduction by augmented ϵ -constraint method. *Renewable Energy*. 2021 Jul 1;172:408-23.
- [128] Agnoletto EJ, De Castro DS, Neves RV, Machado RQ, Oliveira VA. An Optimal Energy Management Technique Using the ϵ -Constraint Method for Grid-Tied and Stand-Alone Battery-Based Microgrids. *IEEE Access*. 2019 Nov 18;7:165928-42.
- [129] Nojavan S, Majidi M, Esfetanaj NN. An efficient cost-reliability optimization model for optimal siting and sizing of energy storage system in a microgrid in the presence of responsible load management. *Energy*. 2017 Nov 15;139:89-97.
- [130] Li Z, Xu Y, Fang S, Wang Y, Zheng X. Multiobjective coordinated energy dispatch and voyage scheduling for a multienergy ship microgrid. *IEEE Transactions on Industry Applications*. 2019 Nov 29;56(2):989-99.
- [131] Najafi J, Peiravi A, Anvari-Moghaddam A, Guerrero JM. Power-heat generation sources planning in microgrids to enhance resilience against islanding due to natural disasters. In 2019 IEEE 28th International Symposium on Industrial Electronics (ISIE) 2019 Jun 12 (pp. 2446-2451). IEEE.
- [132] Hamidi A, Nazarpour D, Golshannavaz S. Multiobjective scheduling of microgrids to harvest higher photovoltaic energy. *IEEE Transactions on Industrial Informatics*. 2017 Jun 21;14(1):47-57.
- [133] Shekari T, Golshannavaz S, Aminifar F. Techno-economic collaboration of PEV fleets in energy management of microgrids. *IEEE Transactions on Power Systems*. 2016 Dec 23;32(5):3833-41.
- [134] Srinivas N, Deb K. Multiobjective optimization using nondominated sorting in genetic algorithms. *Evolutionary computation*. 1994 Sep;2(3):221-48.
- [135] Deb K, Pratap A, Agarwal S, Meyarivan TA. A fast and elitist multiobjective genetic algorithm: NSGA-II. *IEEE transactions on evolutionary computation*. 2002 Aug 7;6(2):182-97.
- [136] Pooranian Z, Nikmehr N, Najafi-Ravadanegh S, Mahdin H, Abawajy J. Economical and environmental operation of smart networked microgrids under uncertainties using NSGA-II. In 2016 24th International Conference on Software, Telecommunications and Computer Networks (SoftCOM) 2016 Sep 22 (pp. 1-6). IEEE.
- [137] Teo TT, Logenthiran T, Woo WL, Abidi K, John T, Wade NS, Greenwood DM, Patsios C, Taylor PC. Optimization of Fuzzy Energy-Management System for Grid-Connected Microgrid Using NSGA-II. *IEEE Transactions on Cybernetics*. 2020 Nov 11.

- [138] Mahmoudi M, Fatehi A, Jafari H, Karimi E. Multi-objective micro-grid design by nsga-ii considering both islanded and grid-connected modes. In 2018 IEEE Texas Power and Energy Conference (TPEC) 2018 Feb 8 (pp. 1-6). IEEE.
- [139] Lin Y, Dong P, Sun X, Liu M. Two-level game algorithm for multi-microgrid in electricity market. *IET Renewable Power Generation*. 2017 Sep 5;11(14):1733-40.
- [140] Ray PK, Nandkeolyar S, Lim CS, Satiawan IN. Demand Response Management using Non-Dominated Sorting Genetic Algorithm II. In 2020 IEEE International Conference on Power Electronics, Smart Grid and Renewable Energy (PESGRE2020) 2020 Jan 2 (pp. 1-6). IEEE.
- [141] Vergara PP, Torquato R, Da Silva LC. Towards a real-time Energy Management System for a Microgrid using a multi-objective genetic algorithm. In 2015 IEEE Power & Energy Society General Meeting 2015 Jul 26 (pp. 1-5). IEEE.
- [142] Zhao B, Zhang X, Chen J, Wang C, Guo L. Operation optimization of standalone microgrids considering lifetime characteristics of battery energy storage system. *IEEE transactions on sustainable energy*. 2013 Sep 16;4(4):934-43.
- [143] Zitzler E, Laumanns M, Thiele L. SPEA2: Improving the strength Pareto evolutionary algorithm. *TIK-report*. 2001;103.
- [144] Khalid S, Ahmad I. Service Restoration Using Energy Donation in a Distribution System During Crisis. In 2020 International Conference on Smart Grids and Energy Systems (SGES) 2020 Nov 23 (pp. 562-567). IEEE.
- [145] Adinolfi G, Ciavarella R, Palladino V, Valenti M, Graditi G. A multi-objective optimization design tool for Smart Converters in photovoltaic applications. In 2018 International Symposium on Power Electronics, Electrical Drives, Automation and Motion (SPEEDAM) 2018 Jun 20 (pp. 793-798). IEEE.
- [146] Ruifeng S, Yang Y, Lee KY. Multi-objective EV charging stations planning based on a two-layer coding SPEA-II. In 2017 19th International Conference on Intelligent System Application to Power Systems (ISAP) 2017 Sep 17 (pp. 1-6). IEEE.
- [147] Ray PK, Nandkeolyar S, Subudhi B, Korkua SK. Multi-Objective Optimization for Demand Response Management. In 2019 International Conference on Information Technology (ICIT) 2019 Dec 19 (pp. 121-126). IEEE.
- [148] Khalid S, Ahmad I. QoS and power network stability aware simultaneous optimization of data center revenue and expenses. *Sustainable Computing: Informatics and Systems*. 2021 Jun 1;30:100459.
- [149] Kharrich M, Mohammed OH, Alshammari N, Akherraz M. Multi-objective optimization and the effect of the economic factors on the design of the microgrid hybrid system. *Sustainable Cities and Society*. 2021 Feb 1;65:102646.
- [150] Corne DW, Jerram NR, Knowles JD, Oates MJ. PESA-II: Region-based selection in evolutionary multiobjective optimization. In *Proceedings of the 3rd annual conference on genetic and evolutionary computation* 2001 Jul 7 (pp. 283-290).
- [151] Ridha HM, Gomes C, Hizam H, Ahmadipour M, Muhsen DH, Ethaib S. Optimum design of a standalone solar photovoltaic system based on novel integration of iterative-PESA-II and AHP-VIKOR methods. *Processes*. 2020 Mar;8(3):367.
- [152] Coello CA, Pulido GT, Lechuga MS. Handling multiple objectives with particle swarm optimization. *IEEE Transactions on evolutionary computation*. 2004 Jun 14;8(3):256-79.
- [153] Borhanazad H, Mekhilef S, Ganapathy VG, Modiri-Delshad M, Mirtaheri A. Optimization of micro-grid system using MOPSO. *Renewable Energy*. 2014 Nov 1;71:295-306.
- [154] Indragandhi V, Logesh R, Subramaniaswamy V, Vijayakumar V, Siarry P, Uden L. Multi-objective optimization and energy management in renewable based AC/DC microgrid. *Computers & Electrical Engineering*. 2018 Aug 1;70:179-98.
- [155] Elgammal A, El-Naggar M. Energy management in smart grids for the integration of hybrid wind-PV-FC-battery renewable energy resources using multi-objective particle swarm optimisation (MOPSO). *The Journal of Engineering*. 2018 Sep 21;2018(11):1806-16.
- [156] Ghiasi M. Detailed study, multi-objective optimization, and design of an AC-DC smart microgrid with hybrid renewable energy resources. *Energy*. 2019 Feb 15;169:496-507.
- [157] Baghaee HR, Mirsalim M, Gharehpetian GB. Multi-objective optimal power management and sizing of a reliable wind/PV microgrid with hydrogen energy storage using MOPSO. *Journal of Intelligent & Fuzzy Systems*. 2017 Jan 1;32(3):1753-73.

- [158] Baghaee HR, Mirsalim M, Gharehpetian GB, Talebi HA. MOPSO/FDMT-based Pareto-optimal solution for coordination of overcurrent relays in interconnected networks and multi-DER microgrids. *IET Generation, Transmission & Distribution*. 2018 Mar 22;12(12):2871-86.
- [159] Aghajani G, Ghadimi N. Multi-objective energy management in a micro-grid. *Energy Reports*. 2018 Nov 1;4:218-25.
- [160] Zhang Q, Li H. MOEA/D: A multiobjective evolutionary algorithm based on decomposition. *IEEE Transactions on evolutionary computation*. 2007 Nov 27;11(6):712-31.
- [161] Bouchekara HR, Javaid MS, Shaaban YA, Shahriar MS, Ramli MA, Latreche Y. Decomposition based multiobjective evolutionary algorithm for PV/Wind/Diesel Hybrid Microgrid System design considering load uncertainty. *Energy Reports*. 2021 Nov 1;7:52-69.
- [162] Ferreira WM, Meneghini IR, Brandao DI, Guimarães FG. Preference cone based multi-objective evolutionary algorithm to optimal management of distributed energy resources in microgrids. *Applied Energy*. 2020 Sep 15;274:115326.
- [163] Tan B, Chen H. Multi-objective energy management of multiple microgrids under random electric vehicle charging. *Energy*. 2020 Oct 1;208:118360.
- [164] Zhang J, Zhu X, Chen T, Yu Y, Xue W. Improved MOEA/D approach to many-objective day-ahead scheduling with consideration of adjustable outputs of renewable units and load reduction in active distribution networks. *Energy*. 2020 Nov 1;210:118524.
- [165] Martinez SZ, Coello CA. A multi-objective evolutionary algorithm based on decomposition for constrained multi-objective optimization. In 2014 IEEE Congress on evolutionary computation (CEC) 2014 Jul 6 (pp. 429-436). IEEE.
- [166] Brandao DI, Ferreira WM, Alonso AM, Tedeschi E, Marafão FP. Optimal Multiobjective Control of Low-Voltage AC Microgrids: Power Flow Regulation and Compensation of Reactive Power and Unbalance. *IEEE Transactions on Smart Grid*. 2019 Aug 7;11(2):1239-52.
- [167] Ramli, Makbul AM, H. R. E. H. Bouchekara, and Abdulsalam S. Alghamdi. "Optimal sizing of PV/wind/diesel hybrid microgrid system using multi-objective self-adaptive differential evolution algorithm." *Renewable energy* 121 (2018): 400-411.
- [168] Kapoor A, Singhal A. A comparative study of K-Means, K-Means++ and Fuzzy C-Means clustering algorithms. In 2017 3rd international conference on computational intelligence & communication technology (CICT) 2017 Feb 9 (pp. 1-6). IEEE.
- [169] Cebeci Z, Yildiz F. Comparison of k-means and fuzzy c-means algorithms on different cluster structures. *Agrárinformatika/journal of agricultural informatics*. 2015; 6(3):13-23.
- [170] Xiao, Jie, Xiangyu Kong, Dehong Liu, Ye Li, Delong Dong, and Yanan Qiao. "Multi-objective Optimization Scheduling Method for Integrated Energy System Considering Uncertainty." In 2019 22nd International Conference on Electrical Machines and Systems (ICEMS), pp. 1-5. IEEE, 2019.
- [171] Sachs, Julia, and Oliver Sawodny. "Multi-objective three stage design optimization for island microgrids." *Applied Energy* 165 (2016): 789-800.
- [172] Xinwei, Shen, Guo Qinglai, Xu Yinliang, and Sun Hongbin. "Robust planning of regional integrated energy system considering multi energy load uncertainty [J]." *Power system automation* 43, no. 07 (2019): 34-45.
- [173] Wu, Lizhen, Libo Jiang, and Xiaohong Hao. "Optimal scenario generation algorithm for multi-objective optimization operation of active distribution network." In 2017 36th Chinese Control Conference (CCC), pp. 2680-2685. IEEE, 2017.
- [174] Guo, Jiacheng, Peiwen Zhang, Di Wu, Zhijian Liu, Xuan Liu, Shicong Zhang, Xinyan Yang, and Hua Ge. "Multi-objective optimization design and multi-attribute decision-making method of a distributed energy system based on nearly zero-energy community load forecasting." *Energy* 239 (2022): 122124.
- [175] Hosseinnia, Hamed, Behnam Mohammadi-Ivatloo, and Mousa Mohammadpourfard. "Multi-objective configuration of an intelligent parking lot and combined hydrogen, heat and power (IPL-CHHP) based microgrid." *Sustainable Cities and Society* 76 (2022): 103433.
- [176] Nojavan, Sayyad, Majid Majidi, and Naser Nourani Esfetanaj. "An efficient cost-reliability optimization model for optimal siting and sizing of energy storage system in a microgrid in the presence of responsible load management." *Energy* 139 (2017): 89-97.

- [177] Moghaddam, Amjad Anvari, Alireza Seifi, Taher Niknam, and Mohammad Reza Alizadeh Pahlavani. "Multi-objective operation management of a renewable MG (micro-grid) with back-up micro-turbine/fuel cell/battery hybrid power source." *Energy* 36, no. 11 (2011): 6490-6507.
- [178] Li, Yang, Zhen Yang, Dongbo Zhao, Hangtian Lei, Bai Cui, and Shaoyan Li. "Incorporating energy storage and user experience in isolated microgrid dispatch using a multi-objective model." *IET Renewable Power Generation* 13, no. 6 (2019): 973-981.
- [179] Cao, Bin, Weinan Dong, Zhihan Lv, Yu Gu, Surjit Singh, and Pawan Kumar. "Hybrid microgrid many-objective sizing optimization with fuzzy decision." *IEEE Transactions on Fuzzy Systems* 28, no. 11 (2020): 2702-2710.
- [180] da Silva, Igor RS, Ricardo de AL Rabêlo, Joel JPC Rodrigues, Petar Solic, and Arthur Carvalho. "A preference-based demand response mechanism for energy management in a microgrid." *Journal of Cleaner Production* 255 (2020): 120034.
- [181] Nojavan, Sayyad, Majid Majidi, and Naser Nourani Esfetanaj. "An efficient cost-reliability optimization model for optimal siting and sizing of energy storage system in a microgrid in the presence of responsible load management." *Energy* 139 (2017): 89-97.
- [182] Wang, Xiongfei, Josep M. Guerrero, Frede Blaabjerg, and Zhe Chen. "A review of power electronics based microgrids." *International Journal of Power Electronics* 12, no. 1 (2012): 181-192.
- [183] Mizuguchi, K., S. Muroyama, Y. Kuwata, and Y. Ohashi. "A new decentralized dc power system for telecommunications systems." In *12th International Conference on Telecommunications Energy*, pp. 55-62. IEEE, 1990.
- [184] Ehsani, Mehrdad, Krishna Veer Singh, Hari Om Bansal, and Ramin Tafazzoli Mehrjardi. "State of the art and trends in electric and hybrid electric vehicles." *Proceedings of the IEEE* 109, no. 6 (2021): 967-984.
- [185] Ciezki, John G., and Robert W. Ashton. "Selection and stability issues associated with a navy shipboard DC zonal electric distribution system." *IEEE Transactions on power delivery* 15, no. 2 (2000): 665-669.
- [186] Kjaer, Soeren Baekhoej, John K. Pedersen, and Frede Blaabjerg. "A review of single-phase grid-connected inverters for photovoltaic modules." *IEEE transactions on industry applications* 41, no. 5 (2005): 1292-1306.
- [187] Kim, Jong-Soo, Gyu-Yeong Choe, Hyun-Soo Kang, and Byoung-Kuk Lee. "Robust low frequency current ripple elimination algorithm for grid-connected fuel cell systems with power balancing technique." *Renewable Energy* 36, no. 5 (2011): 1392-1400.
- [188] Ponnaluri, Srinivas, Gerhard O. Linhofer, Jurgen K. Steinke, and Peter K. Steimer. "Comparison of single and two stage topologies for interface of BESS or fuel cell system using the ABB standard power electronics building blocks." In *2005 European Conference on Power Electronics and Applications*, pp. 9-pp. IEEE, 2005.
- [189] Inoue, Shigenori, and Hirofumi Akagi. "A bidirectional isolated DC-DC converter as a core circuit of the next-generation medium-voltage power conversion system." *IEEE Transactions on Power Electronics* 22, no. 2 (2007): 535-542.
- [190] Forouzesh, Mojtaba, Yam P. Siwakoti, Saman A. Gorji, Frede Blaabjerg, and Brad Lehman. "Step-up DC-DC converters: a comprehensive review of voltage-boosting techniques, topologies, and applications." *IEEE transactions on power electronics* 32, no. 12 (2017): 9143-9178.
- [191] Amani, Danesh, Reza Beiranvand, and MohammadReza Zolghadri. "A new high step-up interleaved LLC converter." In *2021 12th Power Electronics, Drive Systems, and Technologies Conference (PEDSTC)*, pp. 1-6. IEEE, 2021.
- [192] Peng, Fang Zheng. "Z-source inverter." *IEEE Transactions on industry applications* 39, no. 2 (2003): 504-510.
- [193] Siwakoti, Yam P., Poh Chiang Loh, Frede Blaabjerg, Søren Juhl Andreasen, and Graham E. Town. "Y-source boost DC/DC converter for distributed generation." *IEEE Transactions on Industrial Electronics* 62, no. 2 (2014): 1059-1069.
- [194] Fang, Xupeng, Xiaokang Ding, Shixiang Zhong, and Yingying Tian. "Improved quasi-Y-source DC-DC converter for renewable energy." *CPSS transactions on Power Electronics and Applications* 4, no. 2 (2019): 163-170.

- [195] Salehi, Navid, Sayyed Mohammad Mehdi Mirtalaei, and Sayyed Hosein Mirenayat. "A high step-up DC–DC soft-switched converter using coupled inductor and switched capacitor." *International Journal of Electronics Letters* 6, no. 3 (2018): 260-271.
- [196] Zheng, Yifei, Benjamin Brown, Wenhao Xie, Shouxiang Li, and Keyue Smedley. "High step-up DC–DC converter with zero voltage switching and low input current ripple." *IEEE Transactions on Power Electronics* 35, no. 9 (2020): 9416-9429.
- [197] Liang, Tsorng-Juu, and K. C. Tseng. "Analysis of integrated boost-flyback step-up converter." *IEE Proceedings-Electric Power Applications* 152, no. 2 (2005): 217-225.
- [198] Baek, Ju-Won, Myung-Hyo Ryoo, Tae-Jin Kim, Dong-Wook Yoo, and Jong-Soo Kim. "High boost converter using voltage multiplier." In *31st Annual Conference of IEEE Industrial Electronics Society, 2005. IECON 2005.*, pp. 6-pp. IEEE, 2005.
- [199] Chub, Andrii, Dmitri Vinnikov, Frede Blaabjerg, and Fang Zheng Peng. "A review of galvanically isolated impedance-source DC–DC converters." *IEEE Transactions on Power Electronics* 31, no. 4 (2015): 2808-2828.
- [200] Siwakoti, Yam P., Fang Zheng Peng, Frede Blaabjerg, Poh Chiang Loh, and Graham E. Town. "Impedance-source networks for electric power conversion part I: A topological review." *IEEE Transactions on power electronics* 30, no. 2 (2014): 699-716.
- [201] Subhani, Nafis, Ramani Kannan, Apel Mahmud, and Frede Blaabjerg. "Z-source inverter topologies with switched Z-impedance networks: A review." *IET Power Electronics* 14, no. 4 (2021): 727-750.
- [202] Wu, Xiaogang, Jiulong Wang, Yun Zhang, Jiuyu Du, Zhengxin Liu, and Yu Chen. "Review of DC-DC Converter Topologies Based on Impedance Network with Wide Input Voltage Range and High Gain for Fuel Cell Vehicles." *Automotive Innovation* 4, no. 4 (2021): 351-372.

Chapter 2

Objectives and Thesis Structure

1. THESIS OBJECTIVES AND METHODOLOGY

The main objective of this thesis is to concentrate on the two main prominent subjects in the MGs system. The optimal operation of MGs systems is the most important and perpetual issue connecting with two subjects: energy management and power electronics interfaces. Advanced proposed energy management algorithms lead to cooperating multiple MGs with novel energy management methods. The concept of NMG is prone to provide several advantages to MGs' performance. The energy management system (EMS) in MGs is potentiated to control: the power generation, demand consumption, and energy storage system (ESS) in an optimal and economical manner. However, in NMG, the responsibility of EMS is expanded due to the possibility of energy sharing amongst MGs. Several EMS methods have emerged based on the data acquisition infrastructure over the last years, such as centralized, decentralized, and hybrid methods. However, recently distributed methods are developing more to cover previous methods' drawbacks.

In the collaborative operation mode of several MGs, the surplus and shortage of energy can be exchanged between MGs employing EMS. Therefore, it is expected the following consequents can be obtained in NMG operation mode:

- 1) Increasing the reliability of the whole system due to the possibility of supplying power demand from the collaborative MGs;
- 2) Improving the cost of power generators due to decreasing the capital cost, replacement cost, and O&M cost;
- 3) Enhancing the energy management system due to the possibility of controlling produced energy in each MG.

Furthermore, power electronics interfaces play a crucial role in MGs applications. DC-AC converters -known as inverters- are the most important part of grid-connected MGs. Providing proper voltage amplitude and frequency and coordinating the energy transfer between power lines are the main responsibility of inverters. On the other hand, standard available inverters require minimum input DC voltage for operation. However, the produced voltage of renewable energy sources (RESs) such as PVs and FCs are not

sufficient for normal inverter operation. Therefore, DC-DC converters are inevitably used in hybrid MGs.

Multiple DC-DC converters with various topologies are used in the MG system, primarily to step up the produced voltage of RESs and make them compatible for inverter operation. LLC resonant converter is one of the valuable DC-DC converters amongst power electronics interfaces. Parasitic elements of components can effectively exploit in this converter to achieve soft switching for MOSFETs and makes the converter able to operate at a higher frequency. Higher frequency resulted in smaller transformer volume. Therefore, optimal design of LLC converter leads to high-efficiency converter with ability power conversion at a smaller volume.

DC-DC converters usually suffer from high-stress voltage and current by increasing gain voltage. Consequently, various high step-up topologies have recently been proposed to suppress the drawbacks. A modified cascaded Z-source DC-DC converter is proposed in this thesis to obtain a high gain voltage; meanwhile, the stress voltage of semiconductor devices is low.

To sum up, the first part of this thesis focuses on the energy management algorithm and the benefits obtained from intelligent energy management for NMG. The second part is focused on the power electronics interfaces utilized in MGs systems.

2. THESIS CONTRIBUTION AND THESIS STRUCTURE

This PhD thesis is structured based on the published papers. The first part of the thesis involves the networked MG control strategies and energy management methods. The most prominent control strategies are discussed in chapter 1, and the optimization methods are reviewed for obtaining optimal operation of individual and networked MG. Accordingly, a novel networked microgrid energy management based on supervised and unsupervised learning clustering is proposed in chapter 3. The clustering in this method is performed by considering the maximum load demand (MLD) and operating reserve (OR). The k-means algorithm as an unsupervised clustering method and the self-organizing map (SOM) algorithm is utilized as a supervised clustering method.

Furthermore, a novel component sizing for dispatchable power generation units in hybrid MGs is surveyed in chapter 3. The proposed component sizing is based on the operating reserve of each individual MG. However, the possibility of power-sharing

amongst MGs results in introducing a method by considering the peak load intervals to reduce the size of dispatchable units.

The second part consists of a comparative study of different optimization methods for resonance half-bridge converter in chapter 5. The soft-switch operation of LLC resonance converters makes the converter operates at a higher switching frequency, and consequently, power density can increase; meanwhile, the passive components such as inductors and capacitors can decrease. Chapter 6 introduces a modified cascaded z-source high step-up boost converter. Two z-source networks are cascaded in this converter to create a quasi-z-source networked conventional boost converter. The gain voltage of the proposed topology is improved effectively; meanwhile, the stress voltage of semiconductor devices is decreased. Eventually, a neural networks-generalized predictive control for MIMO grid-connected z-source inverter is investigated in chapter 7. The proposed control methods for the z-source inverter enhance the converter performance when the current and voltage set points vary. This transient enhancement is obtained by predicting the state variables by means of the generalized predictive control (GPC) algorithm and providing the forced response for the model predictive control (MPC) method.

Figure 2.1. represents the general structure of the thesis. The main objectives of this PhD thesis are summarized as follows:

- Proposing a novel networked MG energy management employing artificial intelligence approaches such as k-means and self-organizing map (SOM) algorithm.
- Proposing a novel component sizing based on the operating reserve of dispatchable units, involving the laboratory results by analyzing the obtained results from three collaborative MGs.
- Studying the optimal operation of LLC resonant half-bridge converter for the different operating conditions, involving practical results.
- Proposing a modified high step-up Z-source boost converter with high voltage gain and low-stress voltage for semiconductor devices, involving practical results.
- Proposing a novel control algorithm based on model predictive control in order to enhance the transient operation of the Z-source inverter.

| | |
|--|--|
| Chapter 1: Introduction | 1. Introduction |
| | 2. Thesis back ground |
| Chapter 2: Objectives and thesis structure | 1. Thesis objectives and methodology |
| | 2. Thesis contribution & Thesis structure |
| Part 1: Networked Microgrid | |
| Chapter 3: Networked microgrid control strategies | Paper: Networked Microgrid Energy Management Based on Supervised and Unsupervised Learning Clustering |
| Chapter 4: Networked microgrid optimal component sizing | Paper: Component Sizing of Isolated Networked Hybrid Microgrid Based on Operating Reserve Analysis |
| Part 2: Power electronics interfaces in Microgrids | |
| Chapter 5: LLC resonant converters | Paper: A Comparative Study of Different Optimization Methods for Resonance Half-Bridge Converter |
| Chapter 6: Z-source converter | Paper: Modified Cascaded Z-Source High Step-Up Boost Converter |
| Chapter 7: Z-source control sterategy | Paper: Neural Networks-Generalized Predictive Control for MIMO Grid-connected Z-source Inverter Model |
| Chapter 8: Conclusion and future work | |

Fig. 1. Thesis structure

Chapter 3

Networked Microgrid Energy Management Based on Supervised and Unsupervised Learning Clustering

3.1. INTRODUCTION

By realizing the affirmative effect of MGs on the conventional power system, the idea of networked MG is raised to expand the potential pros of MGs operation. This chapter proposes energy management for a large-scale networked MG. MGs are clustered by considering two main factors: maximum load demand (MLD) and operating reserve (OR). Two clustering methods are exploited in order to cluster the MGs, considering MLD and OR. K-means algorithm as an unsupervised learning clustering and self-organizing map (SOM) algorithm as a supervised learning clustering is used for the proposed energy management. The results obtained from these two clustering methods are similar. However, SOM is a more powerful algorithm, especially if clustering criteria increase to more parameters such as SoC and DoD of batteries, etc.

3.2. CONTRIBUTIONS TO THE STATE OF ART

By emerging the concept of NMG, several energy management algorithms are investigated by researchers in order to enhance the performance of the whole system. Mainly, the proposed energy management for NMG pursues the following aims:

- Improving reliability, stability, and resiliency [1-3];
- Improving environmental benefits [3];
- Improving power quality [1], [3];
- Improving economic purposes [4].

A dynamic clustering scheme in a community home energy management system is conducted in [1] to improve the stability and resiliency of MGs. A sample population of 1000 residential consumers are clustered to study the proposed energy management based on time overlap criteria. The study is focused on electricity cost reduction for consumers and load profile peak to average ratio (PAR) curtailment for a large consumer population. Self-organization and decentralized energy management of an isolated microgrid cluster are proposed in [2]. The self-organization stage is responsible for deciding on whether to connect each MG to the cluster based on the available

generation resources. Then, decentralized energy management guarantees the energy reliability of critical loads and overall energy efficiency by managing the generation and storage resources of each MG. In addition to decentralized energy management, the two-level optimization model is an attractive method widely exploited in studies. An interactive model for energy management of clustered MGs is studied in [3]. A two-level optimization model consisting of the upper and lower level for the coordinated energy management between the distribution system and clustered MGs is proposed in this reference. The upper level deals with the operation of the distribution network, while the lower level considers the coordinated operation of multiple MGs. The proposed model demonstrates the improvement of power quality, reliability, and environmental benefits. Sixteen commercial MGs are considered in [4] to evaluate the proposed mathematical models for microgrid clusters using a transactive energy structure to manage energy exchange in the smart grid. The chance-constrained programming is employed in this reference to consider the uncertainties in balancing collective and individual interests under transactive energy management. In [5], a review of optimal energy management problems for industrial MGs is conducted.

In this chapter, a cluster of MGs involving residential, commercial, and industrial is under investigation. The MGs are connected to the grid by star connection topology. The main grid plays the role of energy trader. However, the shortage of energy can be compensated by the grid as well. Different load patterns of MGs result in facing different peak load demands at various time slots. Consequently, the maximum load demand (MLD) and operating reserve (OR) of each MG for the different intervals are evaluated for clustering purposes. Two well-known clustering methods are exploited to cluster the MGs in order to achieve a reliable and efficient operation for MGs.

3.3. REFERENCES

- [1]. Abbasi, Ayesha, Kiran Sultan, Muhammad Adnan Aziz, Adnan Umar Khan, Hassan Abdullah Khalid, Josep M. Guerrero, and Bassam A. Zafar. "A novel dynamic appliance clustering scheme in a community home energy management system for improved stability and resiliency of microgrids." *IEEE Access* 9 (2021): 142276-142288.
- [2]. He, Miao, and Michael Giesselmann. "Reliability-constrained self-organization and energy management towards a resilient microgrid cluster." In 2015 IEEE Power & Energy Society Innovative Smart Grid Technologies Conference (ISGT), pp. 1-5. IEEE, 2015.

- [3]. Lu, Tianguang, Zhaoyu Wang, Qian Ai, and Wei-Jen Lee. "Interactive model for energy management of clustered microgrids." *IEEE Transactions on Industry Applications* 53, no. 3 (2017): 1739-1750.
- [4]. Daneshvar, Mohammadreza, Behnam Mohammadi-Ivatloo, Somayeh Asadi, Amjad Anvari-Moghaddam, Mohammad Rasouli, Mehdi Abapour, and Gevork B. Gharehpetian. "Chance-constrained models for transactive energy management of interconnected microgrid clusters." *Journal of Cleaner Production* 271 (2020): 122177.
- [5]. Bektas, Zeynep, and Gülgün Kayakutlu. "Review and clustering of optimal energy management problem studies for industrial microgrids." *International Journal of Energy Research* 45, no. 1 (2021): 103-117.

3.4. JOURNAL PAPER



Article

Networked Microgrid Energy Management Based on Supervised and Unsupervised Learning Clustering

Navid Salehi , Herminio Martínez-García * and Guillermo Velasco-Quesada

Electronic Engineering Department, Universitat Politècnica de Catalunya—BarcelonaTech (UPC), 08019 Barcelona, Spain; navid.salehi@upc.edu (N.S.); guillermo.velasco@upc.edu (G.V.-Q.)

* Correspondence: herminio.martinez@upc.edu

Abstract: Networked microgrid (NMG) is a novel conceptual paradigm that can bring multiple advantages to the distributed system. Increasing renewable energy utilization, reliability and efficiency of system operation and flexibility of energy sharing amongst several microgrids (MGs) are some specific privileges of NMG. In this paper, residential MGs, commercial MGs, and industrial MGs are considered as a community of NMG. The loads' profiles are split into multiple sections to evaluate the maximum load demand (MLD). Based on the optimal operation of each MG, the operating reserve (OR) of the MGs is calculated for each section. Then, the self-organizing map as a supervised and a k-means algorithm as an unsupervised learning clustering method is utilized to cluster the MGs and effective energy-sharing. The clustering is based on the maximum load demand of MGs and the operating reserve of dispatchable energy sources, and the goal is to provide a more efficient system with high reliability. Eventually, the performance of this energy management and its benefits to the whole system is surveyed effectively. The proposed energy management system offers a more reliable system due to the possibility of reserved energy for MGs in case of power outage variation or shortage of power.

Keywords: networked microgrid; energy management; clustering; SOM algorithm; k-means algorithm



Citation: Salehi, N.; Martínez-García, H.; Velasco-Quesada, G. Networked Microgrid Energy Management Based on Supervised and Unsupervised Learning Clustering. *Energies* **2022**, *15*, 4915. <https://doi.org/10.3390/en15134915>

Academic Editors: Seleme Isaac Seleme Jr., Heverton Augusto Pereira and Allan Fagner Cupertino

Received: 13 June 2022

Accepted: 30 June 2022

Published: 5 July 2022

Publisher's Note: MDPI stays neutral with regard to jurisdictional claims in published maps and institutional affiliations.



Copyright: © 2022 by the authors. Licensee MDPI, Basel, Switzerland. This article is an open access article distributed under the terms and conditions of the Creative Commons Attribution (CC BY) license (<https://creativecommons.org/licenses/by/4.0/>).

1. Introduction

Microgrids (MGs) are inevitably a prominent part of the power system due to the capability of diminishing concerns related to rapid energy growth. Therefore, an optimal design of MGs has been one of the main issues between researchers and electricians. An optimal design can bring the following benefits to the system: lower investment cost, lower maintenance and operation cost, lower power loss, and higher reliability [1,2]. These benefits can be achieved by utilizing an energy management system (EMS) to coordinate the production and consumption energies optimally. After the achieved successes in MGs performance, the idea of networked MG (NMG) came up to enhance MGs' operation in grid-connected and specifically in an isolated system [3]. Although EMS in NMG is more complicated in comparison with individual MG, the flexibility of energy sharing amongst several MGs can offer extra benefits to the system. Increasing the reliability of the system, specifically in an isolated operation mode, and the possibility of power management in an interactive manner between MGs to provide the demand are some of the advantages that can be gained in NMG [4,5].

Besides MG and NMG, another structure to handle distributed energy resources (DERs) is known as a virtual power plant (VPP). Although a VPP is able to integrate demand response, renewable energy generation, and storage energy into the energy storage system (ESS) in the same way as MGs, there are some particular features in the association of VPP [6,7]:

- VPPs often are considered as grid-connected systems,
- Due to the non-isolated operation mode of VPP, the absence of ESS is possible in VPP,

- Due to the dependency of VPP on information technology and data analysis, a wide variety of energy resources can combine regardless of their deployment distance,
- Due to no particular restricted regulation being associated with VPP, they can participate in the wholesale trade market.

Like MGs and NMGs, the energy management system plays a crucial role in coordinating the power flows of various power generation units and power demand units in VPP. Several energy management strategies are proposed in the literature. Centralized and decentralized control are the most common strategies; however, distributed control schemes have recently received more attention [8,9]. A review of the cooperation and operation of microgrid clusters is performed in [10]. Several aspects of the interconnected MGs are investigated in this reference, such as control and energy-management strategies and architecture configurations in terms of layout, power conversion technology, and line frequency technology. Furthermore, energy trading and suitable energy-market designs for microgrids cluster implementation are addressed. In [11], the microgrid as a single entity and its possible interactions with external grids is defined. Moreover, the possible multi-microgrid architectures are defined in terms of layout, line technology, and interface technology. Parallel connected microgrids with an external grid, a grid of a series of interconnected microgrids, and mixed parallel-series connection are three layout architectures analyzed in [11]. Eventually, a comparison between the different architectures is performed from the aspect of cost, scalability, protection, reliability, stability, communications, and business models. A scalable and reconfigurable hybrid AC/DC microgrid clustering architecture is surveyed in [12]. The proposed energy networking unit (ENU) is used to interface the AC and DC subgrid in a single hybrid microgrid and also facilitates the connection with the external power grid. The ENU-based hybrid microgrid clustering architecture provides scalability, reconfigurability, and modularity architecture. Consequently, this architecture could realize flexible AC/DC interconnection between microgrids by the same converter modules with fewer power conversion units.

Based on the proposed energy management systems, various control methods for NMG and VPP have been presented recently. Blockchain technologies are utilized in [13] to optimize the financial and physical operations of power distribution systems by providing a powerful and reliable path for launching distributed data storage and management. The socioeconomic requirements of transactive energy management at the power distribution level are examined by blockchain technology. In addition, secure optimal energy transactions between networked microgrids and the local distribution grid are presented in [13].

A two-stage energy management strategy for networked microgrids with high renewable penetration is developed in [14]. In the first stage, a hierarchical hybrid control method is utilized for networked microgrids to minimize the system operation cost. In the second stage, the components in microgrids are adjusted optimally in order to minimize the imbalance cost between day-ahead and real-time markets. A cooperative energy management optimization based on distributed model predictive control (MPC) in grid-connected NMG is conducted in [15]. In this scheme, a virtual two-hierarchy NMG structure including MGs and distributed energy resources (DERs) is proposed such that all the DERs represent a virtual MG (VMG) as an upper level and the MGs belong to the lower level. The VMG can exchange power with the utility grid, and MGs at the lower level have to use VMS to share the energy. In [16], a three-level planning model for optimal sizing of networked microgrids is suggested. This research considers a trade-off between resilience and costs in the form of three levels. The first level is employed to tackle the normal sizing problem, while a time-coupled AC optimal power flow (OPF) is utilized to capture stability properties for accurate decision-making. The second and third levels are combined as a defender-attacker-defender model. First, the suggested adaptive genetic algorithm (AGA) is utilized to generate attacking plans that capture load profile uncertainty and contingencies for load shedding maximization. Then, a multi-objective optimization problem is suggested to obtain a trade-off between cost and resilience.

A novel cooperative MPC-based energy management for urban districts consisting of multiple microgrids is proposed in [17]. The proposed energy management coordinates the available flexibility sources of microgrids in order to obtain a common goal. MGs employ an MPC-based EMS to optimally control the loads and generation devices. The distributed proposed coordination algorithm guarantees cooperation amongst the microgrids. In [18], a community-based multi-party microgrid in grid-connected and islanded mode with different structures and a unique operating point is discussed. An iterative bi-level model simulates the interaction between the community microgrid operator and multiple parties for deriving good enough market-clearing results during the microgrid's normal operation status. A multi-agent framework for the energy optimization of NMG is proposed in [19]. The game theory optimization model is applied to this paper in order to optimize the capacity configuration of the agents. In [20], a comprehensive overview of a multi-agent system-(MAS) based distributed coordinated control in NMG is presented.

This paper proposes a novel control strategy for NMG based on MGs clustering. The residential, commercial, and industrial MGs with various load patterns are involved in the NMG. The NMG is structured as a star connection such that all MGs are connected to the VPP. Therefore, the whole system can operate in either grid-connected or isolated mode. A similar structure is presented in [15]. However, the collaborative MGs are considered as a single cluster. In this paper, MGs are clustered by employing two different clustering algorithms. The k-means and self-organizing map (SOM) algorithms are two well-known methods of unsupervised and supervised learning clustering. The MGs clustering is based on the maximum load demand (MLD) and operating reserve (OR) of dispatchable energy sources such as diesel generators (DGs) for each time step. By determining the MG clusters, the EMS is responsible for supplying the demand economically. By this approach, the MLD of the MGs in a particular cluster can be met by the operating reserve of the dispatchable energy sources. Consequently, the reliability of the system increased significantly, and it could be concluded that the peak load alleviation in the clustered MG results in efficient changes in the design of MGs from the capital, replacement, and maintenance and operation (M&O) cost perspective. The clustering approach makes the performance of EMS more efficient, especially in large-scale NMG, by concentrating on some specific MGs.

The rest of this paper is organized as follows: in Section 2, the system configuration of the NMG is presented. Moreover, the k-means algorithm and SOM clustering method are discussed in this section. In Section 2.4, the applied control strategy and EMS is analyzed. The simulation results are presented in Section 3, and a comparative analysis is performed in Section 4. The paper ends with a discussion of conclusions reached.

2. System Configuration, Clustering Methods, and System Operation

2.1. System Configuration

The NMG under study in this paper involves three residential MGs, two commercial MGs, three industrial MGs, and a VPP. In [21], different types of NMG configurations with their potential pros and cons are reviewed. Star-connected NMG, ring-connected NMG, and mesh-connected NMG are the three usual configurations in NMG. As shown in Figure 1, the star-connected configuration is used for the NMG. In this configuration, all MGs are connected to the VPP as the central point at the point of common coupling (PCC). Therefore, the power transaction amongst MGs can be realized through the VPP. As mentioned, the VPPs are usually grid-connected systems. Therefore, the discussed configuration is connected to the main grid through the VPP.

Moreover, each MG consists of renewable energy sources (RESs) like photovoltaic (PV) and wind turbine (WT) conventional energy sources such as DG, and energy storage systems (ESSs) like batteries. In addition, the VPP is considered to consist of only renewable energies like PV and WT, a battery bank, and a group of loads. In Table 1, the component size of each MG is listed. The HOMER is utilized to obtain the size of components. To this end, the load profiles and geographical location are introduced to evaluate the renewable resources production.

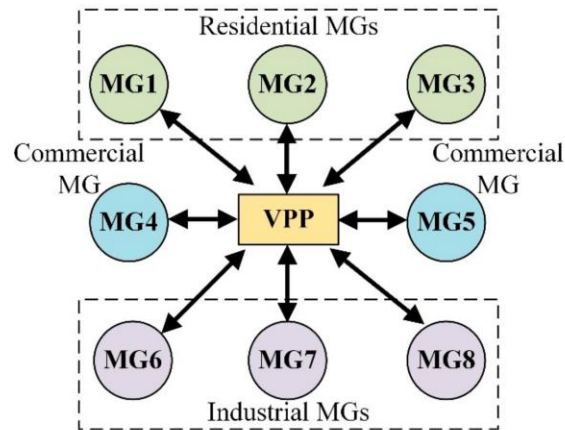


Figure 1. Star-Connected Configuration of NMG.

Table 1. Component size of MGs and VPP.

| | PV (kW) | WT (kW) | DG (kW) | Battery (kWh) |
|-----|---------|---------|---------|---------------|
| MG1 | 6.5 | 2 | 6.8 | 29 |
| MG2 | 8.31 | 3 | 9.1 | 38 |
| MG3 | 16.8 | 4 | 15 | 57 |
| MG4 | 29.1 | 0 | 17 | 86 |
| MG5 | 20 | 0 | 12 | 56 |
| MG6 | 20.6 | 0 | 24 | 36 |
| MG7 | 14.1 | 0 | 29 | 2 |
| MG8 | 19 | 0 | 23 | 30 |
| VPP | 15 | 2 | - | 10 |

2.2. K-Means Clustering Algorithm

Unsupervised learning is one of the significant problems in artificial intelligence and machine learning. Clustering-based methods, feature extraction-based methods, and artificial neural network-(ANN) based methods are the three main approaches to unsupervised learning. The k-means problem is one of the well-known algorithms widely used in clustering [22]. In this algorithm, the data are clustered based on similarity. It has to be noted that similarity is a general concept, and it can be inferred as distance, size, etc. Figure 2 illustrates the k-means algorithm. As can be seen from Figure 2, each data x is compared with the center of clusters, and the norm of the vector is calculated by the norm function block to evaluate the distance of data and the cluster's center. In this paper, the Euclidean norm is utilized as a distance metric. Therefore, the clustering problem can be stated as [22]:

$$\min E = \frac{1}{N} \sum_{i=1}^N \|x_i - c_k\|, \quad (1)$$

where N is the number of data, x is data, k is the number of clusters, and c_k is the center of the cluster. To minimize this problem, the k-means algorithm assumed that the following equation is established for each cluster S_k with the center of c_k :

$$c_k = \frac{1}{|S_k|} \sum_{x \in S_k} x \quad (2)$$

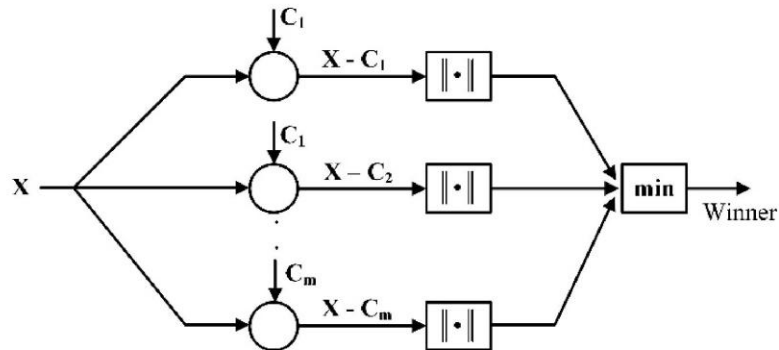


Figure 2. K-means algorithm.

The k-means algorithm employs two steps to solve the problem: the competition step and the update step. Each observation is assigned to the cluster in the competition step with the nearest mean. In addition, in the update step, the clusters' centers are updated with the mean value of the cluster's members. This algorithm proceeds in an iterative interaction until the converging by observing no significant change in the clusters. This algorithm does not guarantee the finding of optimum solutions. In addition, the initial random cluster's centers have a great effect on the final results. However, the k-means algorithm can provide a simple solution without mathematical complexity.

2.3. Self-Organizing Map Algorithm

The self-organizing map (SOM) is one of the artificial neural networks that, by employing supervised machine learning techniques, is widely used in clustering applications and dimension reduction of high-dimensional data [23]. Figure 3 presents the SOM algorithm structure. As observed, each data x is applied to the lattice involving a network of neurons. This stage is similar to the k-means algorithm at the phase of competition in order to evaluate the winner neuron. However, in SOM, the other neurons depending on the distance from the winner neuron will be stimulated as well. Eventually, the vector quantizer unit declares the winner neuron.

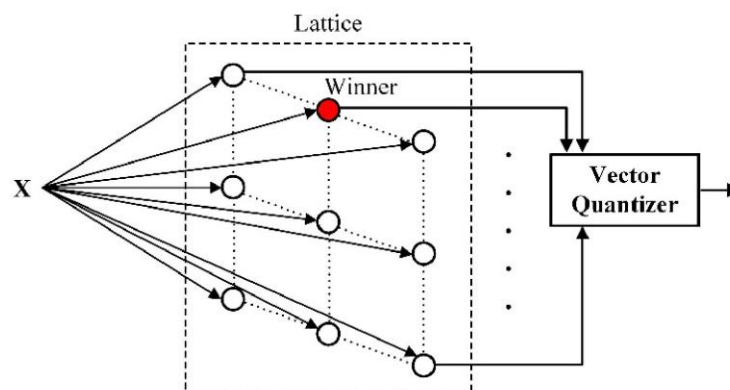


Figure 3. SOM algorithm.

Three main phases are involved in designing a SOM, the competitive, cooperative, and adaptation phases. In the competitive phase, the winner neuron is evaluated by comparing the similarity of data and neurons. In the cooperative phase, the effect of the winner neuron on other neurons is evaluated. The neurons with a smaller distance from the winner neuron are stimulated more in comparison with most far neurons. To this end, the Gaussian function is an appropriate function to assess the stimulation of neurons [23]:

$$h_{ij}(x, t) = \exp\left(-\frac{1}{2} \frac{d_{ij}^2}{\sigma(t)^2}\right), \quad (3)$$

where i is the index of the winner neuron, j is the index of other neurons, d is the distance of the winner neuron with others, and σ is the standard deviation.

The adaptation phase is based on the Kohonen Learning Rule. This rule determines the clusters' centers based on the winner neuron and the adjacent stimulation neurons as follows:

$$\omega_i(t+1) = \omega_i(t) - \eta h_{ij}(x, t) \times (x - \omega_i(t)), \quad (4)$$

where ω is the cluster's center, η is the Kohonen learning rate usually equal to 0.01, and the other parameters are defined in (3).

2.4. Control Strategy and Energy Management Algorithm

As mentioned, the proposed control strategy in this paper is based on MGs clustering by means of unsupervised and supervised algorithms. It means the MGs are clustered according to their similarities such that the MGs with higher load demand can be supplied by the operating reserve of dispatchable energy producers such as DGs and micro-gas turbines. Therefore, the MGs' similarities are maximum load demand and the operating reserve of dispatchable energy producers of each MG at each time slot. With this control strategy, the system's reliability will increase, and the size of energy production units will decrease as well. The proposed control strategy consists of three steps:

- (1) Load and energy generation units analysis in a certain time step;
- (2) MGs clustering by k-means and SOM algorithm;
- (3) MGs clustering optimization by EMS.

2.4.1. Load and Energy Generation Units Analysis

In each time step, the load and energy generation units are analyzed in order to evaluate the maximum load demand (MLD) and operating reserve (OR). MLD and OR amounts of each MG are essential data used by unsupervised and supervised learning clustering methods to cluster the MGs. The operating reserve is the difference between electric load and operating capacity. The maximum load for each time step can be obtained according to the MGs' load profile in Figure 4. However, to obtain the OR of dispatchable energy generation units, the optimal operation of each individual MG is evaluated according to the control strategy illustrated in Figure 5.

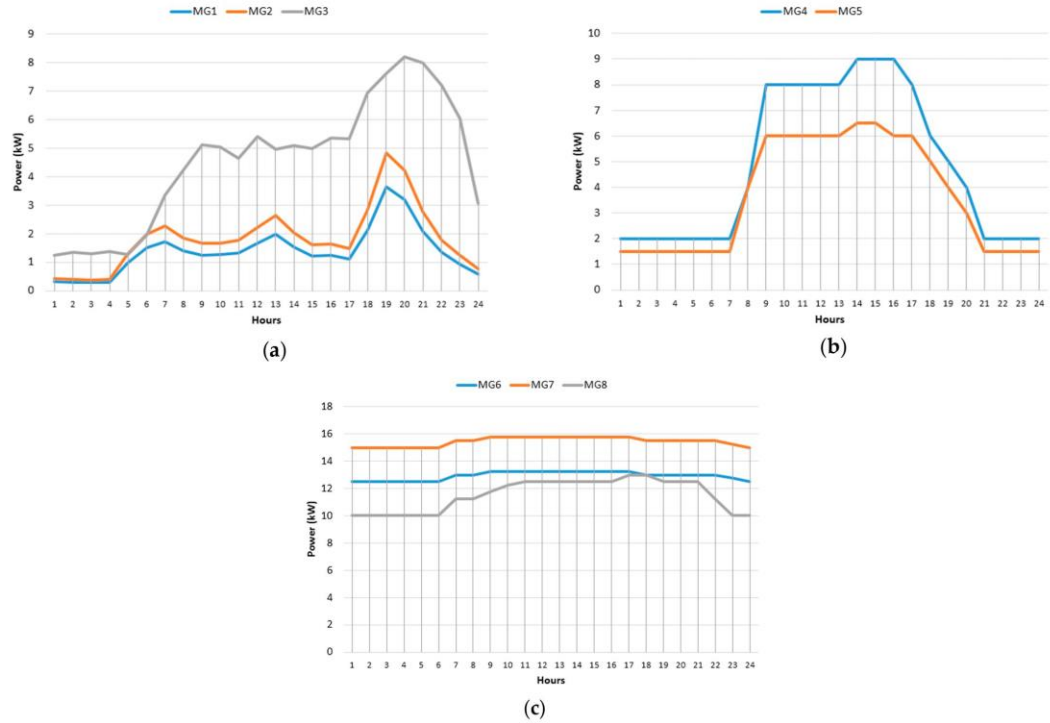


Figure 4. Residential, commercial, and industrial load pattern. (a) Residential load profile, (b) Commercial load profile, (c) Industrial load profile.

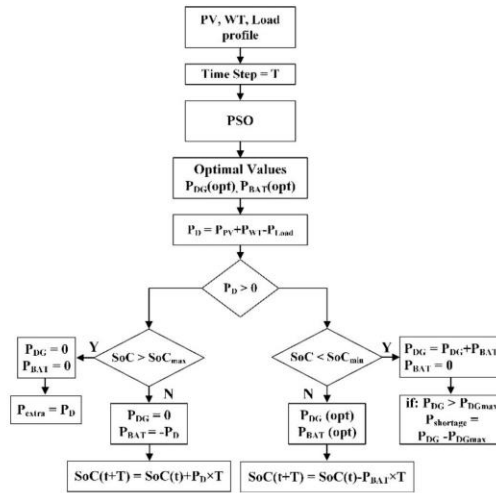


Figure 5. Control strategy of individual MGs.

As it can be seen from Figure 5, the optimal values of DG and Batteries of each MG are calculated by the PSO algorithm. In this control strategy, the loads are preferably met by renewable energies. However, in case of demanding more energy, the DG and battery power are used considering the state of charge (SoC) of batteries.

2.4.2. MGs Clustering by K-Means and SOM Algorithm

According to the MLD and OR of each MG obtained in the previous step, the k-means and SOM algorithms cluster the MGs in a manner that the MGs with higher MLD are clustered with the MGs with higher operating reserve. Therefore, the reliability of the system increases significantly due to the possibility of supplying the MLD by the operating reserve of the clustered MGs. The x for both supervised and unsupervised clustering methods introduced in this paper is considered (MLD, OR). However, the SOM algorithm is able to do the clustering by considering ultra-multi-criteria due to mapping the high dimensional data to reduce data. In order to enhance the performance of clustering algorithms, the MLD is normalized by considering the peak load (PL) of the load profile, as follows:

$$\overline{MLD} = \frac{MLD}{PL} \quad (5)$$

Furthermore, the clustering algorithms are based on similarities, and the similarity meters are the distance between the data. Euclidean distance is utilized for the clustering algorithms in this paper. Therefore, the ORs are applied to the clustering algorithm by means of the following equation:

$$\overline{OR} = 1 - \frac{OR}{OR_{\max}} \quad (6)$$

The maximum number of clusters is theoretically equal to the number of MGs. However, in this case, MGs operate individually. In this paper, the clusters' number is determined by considering the various load patterns in the NMG, i.e., three clusters.

2.5. MGs Clustering Optimization by EMS

An EMS is applied to each cluster in order to coordinate the MGs in an optimal manner. The EMS is responsible for supplying loads of the MGs involved in a particular cluster cost-effectively. Therefore, the performance of the EMS is based on the minimization of power generation cost functions. The optimization problem can be defined by the objective function below:

$$\min CF = \min \left\{ CF \left(\sum_{i \in C_n} PV_i \right) + CF \left(\sum_{i \in C_n} WT_i \right) + CF \left(\sum_{i \in C_n} DG_i \right) + CF \left(\sum_{i \in C_n} BAT_i \right) \right\} \quad (7)$$

This minimization is performed for the MGs involved in cluster C_n . The cost functions of the generation units are presented in [24,25]. Moreover, the optimization problem in MG applications is constrained to technical and practical considerations. These constraints are stated below:

$$\sum_{i \in C_n} P_{DG_i} + \sum_{i \in C_n} P_{BAT_i} + \sum_{i \in C_n} P_{PV_i} + \sum_{i \in C_n} P_{WT_i} + \sum VPP = \sum_{i \in C_n} P_{Load_i} \quad (8)$$

$$P_{DG}^{\min} \leq P_{DG} \leq P_{DG}^{\max} \quad (9)$$

$$0 \leq P_{BAT} \leq P_{DG}^{\max} \quad (10)$$

$$SoC^{\min} \leq SoC \leq SoC^{\max} \quad (11)$$

(8) represents the power balance in the clustered MG. In (9) and (10), the power restriction of diesel generators and batteries is presented, respectively. In (11), the state of

charge (SoC) restriction of batteries is stated. In addition, PV and WT also produce energy as non-dispatchable generators.

The minimization problem in (7) is solved using the particle swarm optimization (PSO) algorithm. Amongst different heuristic optimization methods, PSO proposes a robust and reliable solution over a short-time calculation. In the PSO algorithm, the particles are identified by position and velocity. At the initial phase, the particles' position and par best position are initialized. Then over the several iterations, the particles' position and velocity will be updated such that the particles propel toward the global best.

To apply the PSO, the introduced objective function (OF) in (7) has to convert to a closed-form formulation:

$$OF = \left\{ CF \left(\sum_{i \in C_n} DG_i \right) + CF \left(\sum_{i \in C_n} BAT_i \right) \right\} \times (1 + \alpha \times PBV), \quad (12)$$

where PBV is power balance violation:

$$PBV = \max \left[1 - \frac{\left(\sum_{i \in C_n} P_{DG_i} + P_{BAT_i} \right)}{\sum_{i \in C_n} (P_{Load_i} - P_{PV_i} - P_{WT_i})}, 0 \right] \quad (13)$$

The power balance violation is considered as a multiplicative term for the OF equation expressed in (12). In addition, α is the co-state variable that determines the amount of penalty imposed on the OF in the case of existing PBV . The co-state α can be defined as a constant value, or it could be defined as a variable value in an adaptive problem. Here, α is considered as a constant value equal to 1000.

Consequently, the EMS determines the optimal operation of each generation unit in the corresponding cluster. And the same happens to other clusters.

3. Results Analysis

In order to analyze the proposed control strategy, the simulations are performed in MATLAB. In this paper, to reduce the burden of calculations, the simulation time step is considered to be 1 h. For instance, for the first step, the load analysis is carried out to determine the MLD of each MG. Figure 4 shows the load profile of MGs. As can be seen, the load patterns are different for residential, commercial, and industrial MGs. Therefore, in each time step, the maximum load power of the MGs is distinct. Afterward, according to the optimal operation of MGs, the operating reserve of the MGs is evaluated. In Table 2, the MLD and OR of the MGs for 24 h are presented.

According to the evaluated MLD and OR, the k-means and SOM algorithms are applied to cluster the MGs. Because [MLD, OR] are applied to both k-means and SOM, therefore the obtained results of clustering for these methods are similar. However, as mentioned, the SOM algorithm is potential to cluster the MGs by considering more criteria such as the produced power of each power generation unit, SoC, and depth of discharge (DoD) of batteries.

Higher MLD and higher OR define the similarity criteria of clustered MGs. In this simulation, the number of clusters is considered to be three due to the existing three different load patterns. The k-means and SOM clustering results for 24 h are presented in Table 3. As can be seen from Table 3, over the 24 h simulation period, 9 different clusters appear. Figure 6 illustrates the MGs clustering based on the defined similarities for the time step 1, 8, and 16.

Table 2. Maximum load demand (MLD) and operating reserve (OR) of MGs for different step time.

| | | 1 | 2 | 3 | 4 | 5 | 6 | 7 | 8 | 9 | 10 | 11 | 12 | 13 | 14 | 15 | 16 | 17 | 18 | 19 | 20 | 21 | 22 | 23 | 24 |
|-----|-----|------|------|------|------|------|------|------|------|------|------|------|------|------|------|------|------|------|------|------|------|------|------|------|------|
| MG1 | MLD | 0.32 | 0.3 | 0.29 | 0.3 | 0.97 | 1.5 | 1.71 | 1.4 | 1.25 | 1.26 | 1.33 | 1.67 | 1.99 | 1.53 | 1.21 | 1.23 | 1.12 | 2.12 | 3.63 | 3.18 | 2.09 | 1.34 | 0.93 | 0.38 |
| | OR | 6.48 | 6.5 | 6.51 | 6.5 | 5.83 | 5.3 | 5.09 | 5.4 | 5.55 | 5.54 | 4.97 | 5.13 | 4.81 | 5.27 | 5.59 | 5.57 | 5.68 | 4.68 | 3.17 | 3.62 | 4.71 | 5.46 | 5.87 | 6.22 |
| MG2 | MLD | 0.42 | 0.4 | 0.38 | 0.4 | 1.29 | 1.99 | 2.27 | 1.86 | 1.66 | 1.67 | 1.77 | 2.22 | 2.65 | 2.04 | 1.61 | 1.64 | 1.49 | 2.82 | 4.83 | 4.23 | 2.78 | 1.78 | 1.24 | 0.77 |
| | OR | 8.68 | 8.7 | 8.72 | 8.7 | 7.81 | 7.11 | 6.83 | 7.24 | 7.44 | 7.43 | 7.33 | 6.88 | 6.45 | 7.06 | 7.49 | 7.46 | 7.61 | 6.28 | 4.27 | 4.87 | 6.32 | 7.32 | 7.86 | 8.33 |
| MG3 | MLD | 1.25 | 1.35 | 1.3 | 1.36 | 1.28 | 1.94 | 3.35 | 4.22 | 5.13 | 5.04 | 4.63 | 5.4 | 4.96 | 5.09 | 4.98 | 5.35 | 5.33 | 6.93 | 7.62 | 8.19 | 7.99 | 7.21 | 6.03 | 3.07 |
| | OR | 13.7 | 13.6 | 13.7 | 13.6 | 13.7 | 13 | 11.6 | 10.7 | 9.87 | 9.96 | 10.3 | 9.6 | 10 | 9.91 | 10 | 9.65 | 9.67 | 8.07 | 7.38 | 6.81 | 7.01 | 7.79 | 8.97 | 11.9 |
| MG4 | MLD | 2 | 2 | 2 | 2 | 2 | 2 | 2 | 4 | 8 | 8 | 8 | 8 | 8 | 9 | 9 | 9 | 8 | 6 | 5 | 4 | 2 | 2 | 2 | 2 |
| | OR | 15 | 15 | 15 | 15 | 15 | 15 | 15 | 13 | 9 | 9 | 9 | 9 | 9 | 9 | 8 | 8 | 8 | 9 | 11 | 12 | 13 | 15 | 15 | 15 |
| MG5 | MLD | 1.5 | 1.5 | 1.5 | 1.5 | 1.5 | 1.5 | 1.5 | 4 | 6 | 6 | 6 | 6 | 6 | 6 | 6.5 | 6.5 | 6 | 6 | 5 | 4 | 3 | 1.5 | 1.5 | 1.5 |
| | OR | 10.5 | 10.5 | 10.5 | 10.5 | 10.5 | 10.5 | 10.5 | 8 | 6 | 6 | 6 | 6 | 6 | 6 | 5.5 | 5.5 | 6 | 6 | 7 | 8 | 9 | 10.5 | 10.5 | 10.5 |
| MG6 | MLD | 12.5 | 12.5 | 12.5 | 12.5 | 12.5 | 12.5 | 13 | 13 | 13.2 | 13.2 | 13.2 | 13.2 | 13.2 | 13.2 | 13.2 | 13.2 | 13.2 | 13.2 | 13 | 13 | 13 | 13 | 13 | 13 |
| | OR | 11.5 | 11.5 | 11.5 | 11.5 | 11.5 | 11.5 | 11 | 11 | 10.8 | 10.8 | 10.8 | 10.8 | 10.8 | 10.8 | 10.8 | 10.8 | 10.8 | 10.8 | 11 | 11 | 11 | 11 | 11 | 11.5 |
| MG7 | MLD | 15 | 15 | 15 | 15 | 15 | 15 | 15.5 | 15.5 | 15.7 | 15.7 | 15.7 | 15.7 | 15.7 | 15.7 | 15.7 | 15.7 | 15.7 | 15.5 | 15.5 | 15.5 | 15.5 | 15.5 | 15.2 | 15 |
| | OR | 14 | 14 | 14 | 14 | 14 | 14 | 13.5 | 13.5 | 13.3 | 13.3 | 13.3 | 13.3 | 13.3 | 13.3 | 13.3 | 13.3 | 13.3 | 13.5 | 13.5 | 13.5 | 13.5 | 13.5 | 13.8 | 14 |
| MG8 | MLD | 10 | 10 | 10 | 10 | 10 | 10 | 11.2 | 11.2 | 11.7 | 11.2 | 12.5 | 12.5 | 12.5 | 12.5 | 12.5 | 12.5 | 12.5 | 13 | 13 | 12.5 | 12.5 | 12.5 | 11.2 | 10 |
| | OR | 13 | 13 | 13 | 13 | 13 | 13 | 11.8 | 11.8 | 11.3 | 11.8 | 10.5 | 10.5 | 10.5 | 10.5 | 10.5 | 10.5 | 10.5 | 10 | 10 | 10.5 | 10.5 | 10.5 | 11.8 | 13 |

Table 3. K-means and SOM clustering results.

| | | 1 | 2 | 3 | 4 | 5 | 6 | 7 | 8 | 9 | 10 | 11 | 12 | 13 | 14 | 15 | 16 | 17 | 18 | 19 | 20 | 21 | 22 | 23 | 24 |
|-----------|-----|-----|-----|-----|-----|-----|-----|-----|-----|-----|-----|-----|-----|-----|-----|-----|-----|-----|-----|-----|-----|-----|-----|-----|-----|
| Cluster 1 | MG1 | MG1 | MG1 | MG1 | MG1 | MG1 | MG1 | MG1 | MG1 | MG1 | MG1 | MG1 | MG1 | MG1 | MG1 | MG1 | MG1 | MG1 | MG1 | MG1 | MG1 | MG1 | MG1 | MG1 | MG1 |
| | MG2 | MG2 | MG2 | MG2 | MG2 | MG2 | MG2 | MG2 | MG2 | MG2 | MG2 | MG2 | MG2 | MG2 | MG2 | MG2 | MG2 | MG2 | MG2 | MG2 | MG2 | MG2 | MG2 | MG2 | MG2 |
| Cluster 2 | MG3 | MG3 | MG3 | MG3 | MG3 | MG3 | MG3 | MG3 | MG3 | MG3 | MG3 | MG3 | MG3 | MG3 | MG3 | MG3 | MG3 | MG3 | MG3 | MG3 | MG3 | MG3 | MG3 | MG3 | MG3 |
| | MG5 | MG5 | MG5 | MG5 | MG5 | MG5 | MG5 | MG5 | MG5 | MG5 | MG5 | MG5 | MG5 | MG5 | MG5 | MG5 | MG5 | MG5 | MG5 | MG5 | MG5 | MG5 | MG5 | MG5 | MG5 |
| Cluster 3 | MG4 | MG4 | MG4 | MG4 | MG4 | MG4 | MG4 | MG4 | MG4 | MG4 | MG4 | MG4 | MG4 | MG4 | MG4 | MG4 | MG4 | MG4 | MG4 | MG4 | MG4 | MG4 | MG4 | MG4 | MG4 |
| | MG7 | MG7 | MG7 | MG7 | MG7 | MG7 | MG7 | MG7 | MG7 | MG7 | MG7 | MG7 | MG7 | MG7 | MG7 | MG7 | MG7 | MG7 | MG7 | MG7 | MG7 | MG7 | MG7 | MG7 | MG7 |

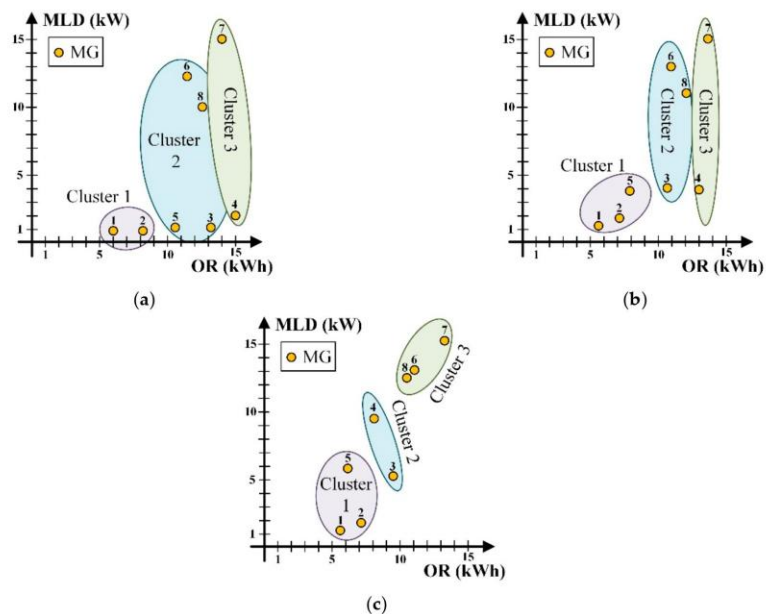


Figure 6. K-means and SOM clustering for time steps 1, 8, and 16. (a) Time step 1, (b) Time step 8, (c) Time step 16.

Eventually, an EMS is exploited for each cluster to optimize the operation of MGs. By this optimization approach, the MLD of MGs can be met by the operating reserve of the clustered MGs even if the MGs' power generation units are not capable of supplying the load. In other words, the reliability of the system increases significantly by clustering the MGs such that MGs with high MLD are grouped by MGs with high OR. To this end, the OR of individual MGs is compared with clustered MGs in next section. Moreover, increasing the reliability of the whole system can result in increasing the efficiency and enhancing the performance of NMG due to the possibility of reducing the component size of the power generation units and consequently reducing the capital, replacement, and M&O cost. However, the possibility of the effect of clustering on component sizing is not analyzed in this paper.

Furthermore, the virtual microgrid operates as an energy exchange node in this configuration. However, in the case of an existence shortage of energy or extra energy, the energy can be traded by the main grid.

Consequently, the proposed control strategy provides a reliable operation in NMG to supply the load. In this paradigm, even by accidentally losing the energy generators, the loads can supply efficiently by utilizing the operating reserve of adjacent MGs in the clustered MG.

4. A Comparative Analysis

The SOM clustering is able to cluster the MGs based on the multi-criteria considered in NMG. However, in this paper, the results of k-means and SOM are almost similar due to clustering 8 MGs and considering two criteria (MLD and OR) for both clustering methods. The PSO is utilized as an optimization method to obtain the optimal operation of MGs. The clustered MGs are able to exchange energy via VPP, and the extra energy or energy shortage can be compensated by VPP. In [14,15], the same structure is proposed to share the energy of MGs in the lower level via virtual MG as an upper level. In [10], an algorithm

is proposed to allow multiple MGs to exchange their excess energy when one or more MGs require a supply of energy. The scalable networked microgrids in [13] are able to offer reserves for their peers to reduce the probability of power outages in the utility grid. Table 4 presents a comparison of proposed energy management.

Table 4. Energy management comparison.

| | k-Means | SOM | Ref [15] | Ref [14] | Ref [10] | Ref [13] |
|---------------------|---------------------------|---------------------------|----------------------------|----------------------------------|---------------------------|-------------------------|
| Num. of MGs + VPP | 8 + 1 | 8 + 1 | 3 + 1 | 3 + 1 | 5 | 7 |
| Num. of clusters | 3 | 3 | 1 | 1 | 2 | 1 |
| Optimization method | PSO | PSO | Logarithmic-barrier method | Mixed integer linear programming | Linear programming | Blockchain technologies |
| Operation mode | Grid-connected & isolated | Grid-connected & isolated | Grid-connected | Grid-connected | Grid-connected & isolated | Grid-connected |

Moreover, in order to investigate the NMG operation from the reliability point of view, Figures 7–9 are provided to compare the operating reserve of MGs in individual operation mode and NMG operation mode. To this end, the OR is illustrated for the first time step. As can be seen from Figures 7–9, in clustered operating mode, the MLD is the maximum MLD of MGs that existed in the cluster. However, the OR is the summation of OR that existed in the cluster.

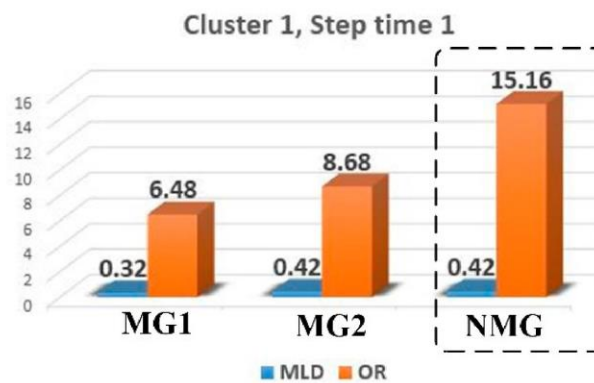


Figure 7. MLD and OR of MG1 and MG2 in individual and clustered operating mode.

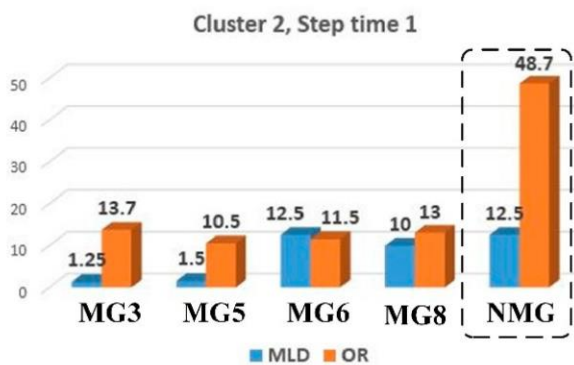


Figure 8. MLD and OR of MG3, MG5, MG6, and MG8 in individual and clustered operating mode.



Figure 9. MLD and OR of MG4 and MG7 in individual and clustered operating mode.

5. Conclusions

This paper applies supervised and unsupervised learning clustering to an NMG consisting of residential, commercial, and industrial MGs. By means of the SOM and k-means algorithm, the MGs are clustered such that the higher peak load MGs collaborate with higher operating reserve MGs in order to supply the loads efficiently. This control strategy can also affect component sizing and, consequently, the capital, replacement, and M&O cost of components by reducing the MGs' peak loads. The employed EMS offers several advantages to the system: the clustered MGs can perform effectively in this control strategy due to providing reliable and efficient operation for the clustered MGs even if losing power generation units accidentally; the efficiency, security, and dynamic in the proposed networked microgrids is improved due to contributing the MGs in case of encountering DER output variation; the system can expedite the restoration of electricity services in case of facing extreme event disruptions such as natural disasters and massive cyber or physical attacks.

Author Contributions: Conceptualization, N.S.; methodology, N.S., H.M.-G.; software, N.S.; validation, N.S., H.M.-G. and G.V.-Q.; investigation, N.S.; data curation, N.S., H.M.-G.; writing—original draft preparation, N.S.; writing—review and editing, N.S., H.M.-G. and G.V.-Q.; supervision, H.M.-G. and G.V.-Q. All authors have read and agreed to the published version of the manuscript.

Funding: Grant PGC2018-098946-B-I00 funded by: MCIN/AEI/10.13039/501100011033/ and by ERDF ERDF A way of making Europe.

Institutional Review Board Statement: Not applicable.

Informed Consent Statement: Not applicable.

Data Availability Statement: Not applicable.

Acknowledgments: The authors would like to thank the Spanish Ministerio de Ciencia, Innovación y Universidades (MICINN)-Agencia Estatal de Investigación (AEI) and the European Regional Development Funds (ERDF), by grant PGC2018-098946-B-I00 funded by MCIN/AEI/10.13039/501100011033/ and by ERDF A way of making Europe.

Conflicts of Interest: The authors declare no conflict of interest.

Nomenclature

The following abbreviations are used in this article:

| | |
|------|----------------------------------|
| AGA | Adaptive Genetic Algorithm |
| ANN | Artificial Neural Network |
| DER | Distributed Energy Resource |
| DG | Distributed Generation |
| DoD | Depth of Discharge |
| EMS | Energy Management System |
| ENU | Energy Networking Unit |
| ESS | Energy Storage System |
| MAS | Multi-agent System |
| MG | Microgrid |
| MILP | Mixed Integer Linear Programming |
| MLD | Maximum Load Demand |
| M&O | Maintenance and Operation |
| MPC | Model Predictive Control |
| NMG | Networked Microgrid |
| OF | Objective Function |
| OPF | Optimal Power Flow |
| OR | Operating Reserve |
| PBV | Power Balance Violation |
| PCC | Point of Common Coupling |
| PSO | Particle Swarm Optimization |
| PV | Photovoltaic |
| RES | Renewable Energy Source |
| SOM | Self-organizing Map |
| SoC | State of Charge |
| VPP | Virtual Power Plant |
| WT | Wind Turbine |

References

- Lou, G.; Gu, W.; Wang, J.; Sheng, W.; Sun, L. Optimal design for distributed secondary voltage control in islanded microgrids: Communication topology and controller. *IEEE Trans. Power Syst.* **2018**, *34*, 968–981. [\[CrossRef\]](#)
- Bracco, S.; Delfino, F.; Pampararo, F.; Robba, M.; Rossi, M. A mathematical model for the optimal operation of the University of Genoa Smart Polygeneration Microgrid: Evaluation of technical, economic and environmental performance indicators. *Energy* **2014**, *64*, 912–922. [\[CrossRef\]](#)
- Li, Z.; Shahidehpour, M.; Aminifar, F.; Alabdulwahab, A.; Al-Turki, Y. Networked microgrids for enhancing the power system resilience. *Proc. IEEE* **2017**, *105*, 1289–1310. [\[CrossRef\]](#)
- Schneider, K.P.; Miller, C.; Laval, S.; Du, W.; Ton, D. Networked Microgrid Operations: Supporting a Resilient Electric Power Infrastructure. *IEEE Electr. Mag.* **2020**, *8*, 70–79. [\[CrossRef\]](#)
- Ahmadi, S.E.; Rezaei, N.; Khayyam, H. Energy management system of networked microgrids through optimal reliability-oriented day-ahead self-healing scheduling. *Sustain. Energy Grids Netw.* **2020**, *23*, 100387. [\[CrossRef\]](#)
- Saboori, H.; Mohammadi, M.; Taghe, R. Virtual power plant (VPP), definition, concept, components and types. In Proceedings of the 2011 Asia-Pacific Power and Energy Engineering Conference, Wuhan, China, 25–28 March 2011; pp. 1–4.
- Othman, M.M.; Hegazy, Y.G.; Abdelaziz, A.Y. A Review of virtual power plant definitions, components, framework and optimization. *Int. Electr. Eng. J.* **2015**, *6*, 2010–2024.
- Salehi, N.; Martinez-Garcia, H.; Velasco-Quesada, G.; Guerrero, J.M. A Comprehensive Review of Control Strategies and Optimization Methods for Individual and Community Microgrids. *IEEE Access* **2022**, *10*, 15935–15955. [\[CrossRef\]](#)
- Querini, P.L.; Chiotti, O.; Fernández, E. Cooperative energy management system for networked microgrids. *Sustain. Energy Grids Netw.* **2020**, *23*, 100371. [\[CrossRef\]](#)
- Bandeiras, F.; Pinheiro, E.; Gomes, M.; Coelho, P.; Fernandes, J. Review of the cooperation and operation of microgrid clusters. *Renew. Sustain. Energy Rev.* **2020**, *133*, 110311. [\[CrossRef\]](#)
- Bullich-Massague, E.; Diaz-González, F.; Aragüés-Peñalba, M.; Girbau-Llistuella, F.; Olivella-Rosell, P.; Sumper, A. Microgrid clustering architectures. *Appl. Energy* **2018**, *212*, 340–361. [\[CrossRef\]](#)
- Yu, H.; Niu, S.; Shao, Z.; Jian, L. A scalable and reconfigurable hybrid AC/DC microgrid clustering architecture with decentralized control for coordinated operation. *Int. J. Electr. Power Energy Syst.* **2022**, *135*, 107476. [\[CrossRef\]](#)
- Li, Z.; Bahramirad, S.; Paaso, A.; Yan, M.; Shahidehpour, M. Blockchain for decentralized transactive energy management system in networked microgrids. *Electr. J.* **2019**, *32*, 58–72. [\[CrossRef\]](#)

14. Wang, D.; Qiu, J.; Reedman, L.; Meng, K.; Lai, L.L. Two-stage energy management for networked microgrids with high renewable penetration. *Appl. Energy* **2018**, *226*, 39–48. [[CrossRef](#)]
15. Xing, X.; Xie, L.; Meng, H. Cooperative energy management optimization based on distributed MPC in grid-connected microgrids community. *Int. J. Electr. Power Energy Syst.* **2018**, *107*, 186–199. [[CrossRef](#)]
16. Wang, Y.; Rousis, A.O.; Strbac, G. A Three-Level Planning Model for Optimal Sizing of Networked Microgrids Considering a Trade-Off Between Resilience and Cost. *IEEE Trans. Power Syst.* **2021**, *36*, 5657–5669. [[CrossRef](#)]
17. Parisio, A.; Wiezorek, C.; Kyntaja, T.; Elo, J.; Strunz, K.; Johansson, K.H. Cooperative MPC-based energy management for networked microgrids. *IEEE Trans. Smart Grid* **2017**, *8*, 3066–3074. [[CrossRef](#)]
18. Li, J.; Liu, Y.; Wu, L. Optimal operation for community-based multi-party microgrid in grid-connected and islanded modes. *IEEE Trans. Smart Grid* **2016**, *9*, 756–765. [[CrossRef](#)]
19. Jin, S.; Wang, S.; Fang, F. Game theoretical analysis on capacity configuration for microgrid based on multi-agent system. *Int. J. Electr. Power Energy Syst.* **2020**, *125*, 106485. [[CrossRef](#)]
20. Han, Y.; Zhang, K.; Li, H.; Coelho, E.A.A.; Guerrero, J.M. MAS-based distributed coordinated control and optimization in microgrid and microgrid clusters: A comprehensive overview. *IEEE Trans. Power Electron.* **2017**, *33*, 6488–6508. [[CrossRef](#)]
21. Islam, M.; Yang, F.; Amin, M. Control and optimisation of networked microgrids: A review. *IET Renew. Power Gener.* **2021**, *15*, 1133–1148. [[CrossRef](#)]
22. Sinaga, K.P.; Yang, M.-S. Unsupervised K-means clustering algorithm. *IEEE Access* **2020**, *8*, 80716–80727. [[CrossRef](#)]
23. Vesanto, J.; Alhoniemi, E. Clustering of the self-organizing map. *IEEE Trans. Neural Netw.* **2000**, *11*, 586–600. [[CrossRef](#)] [[PubMed](#)]
24. Ramli, M.A.; Boucekara, H.; Alghamdi, A.S. Optimal sizing of PV/wind/diesel hybrid microgrid system using multi-objective self-adaptive differential evolution algorithm. *Renew. Energy* **2018**, *121*, 400–411. [[CrossRef](#)]
25. Fueyo, N.; Sanz, Y.; Rodrigues, M.; Montañés, C.; Dopazo, C. The use of cost-generation curves for the analysis of wind electricity costs in Spain. *Appl. Energy* **2011**, *88*, 733–740. [[CrossRef](#)]

Chapter 4

Component Sizing of Isolated Networked Hybrid Microgrid Based on Operating Reserve Analysis

4.1. INTRODUCTION

Energy sharing amongst MGs in NMG is a promising solution introduced in the MG system in order to increase the reliability of the system. Energy management in NMG plays an important role in achieving a reliable, efficient, and economic system. Mainly, an efficient system is structured based on an optimization problem. Therefore, the primary duty of EMS is to achieve an optimal feasible solution for the system. Enormous energy management algorithms and optimization methods are proposed and studied in the literature. However, there are few pieces of research to propose a straightforward procedure to calculate the size of the components in NMG. With the possibility of energy sharing amongst MGs in NMG, the size of the components can be under effect accordingly. This chapter proposed a novel component sizing procedure based on the operating reserve of MGs. The introduced reduced factor (RF) affects the size of dispatchable units such as diesel generators and storage systems.

4.2. CONTRIBUTIONS TO THE STATE OF ART

Energy sharing in NMG usually is remarkable due to increasing the reliability of the whole system. However, NMG can introduce more advantages beyond reliability:

- Penetrating maximum renewable energies [1];
- Increasing lifetime of storage systems like batteries [2];
- Providing required energy for critical loads [3];

Moreover, the size of the components can reevaluate in NMG operation due to the possibility of using the stored energy of energy storage systems (ESS) in other adjacent MGs. In addition, the operating reserve (OR) of dispatchable units of each MG can effectively provide the shortage energy of other MGs. From the economic perspective, the stored energy of ESS and OR of dispatchable units can be traded based on the profitable algorithm.

In [4], the optimum sizing of the NMG is evaluated through the game theory technique. The capacities of generation resources and batteries are considered players,

and annual profit is the payoff. A three-level defender-attacker-defender model with decentralized control to realize a resilience-driven optimal sizing of mobile energy storage systems in NMG is developed in [5]. The upper level is respectively responsible for obtaining optimization results against a certain contingency. However, the middle and lower level problem jointly select a contingency that can cause the most severe damage. Another optimal energy storage sizing for NMG is conducted in [6]. The bi-level optimization model is responsible for both optimizing energy storage sizing problems aiming at maximizing annual profit and optimizing the operation under multiple operating scenarios. The results show that the required energy storage size can be reduced while the operating profit is improved by interconnecting the microgrids (MGs).

This chapter develops a novel component sizing for NMG consisting of three isolated hybrid MGs. The proposed component sizing is based on operating reserve analysis. Therefore, the component size reduction affects the dispatchable components such as diesel generators and storage systems like batteries. To this end, a reduced factor (RF) is introduced for each MG. In order to diminish the adverse effect of component size reduction on MG's reliability, the RF is moderated by the peak load (PL) and correlation of load profile. The results represent the effective size reduction for dispatchable units; consequently, the capital, operational, and M&O cost of MGs reduce.

4.3. REFERENCES

- [1]. Wang, Dongxiao, Jing Qiu, Luke Reedman, Ke Meng, and Loi Lei Lai. "Two-stage energy management for networked microgrids with high renewable penetration." *Applied Energy* 226 (2018): 39-48.
- [2]. Ali, Asfand Yar, Abdul Basit, Tanvir Ahmad, Affaq Qamar, and Javed Iqbal. "Optimizing coordinated control of distributed energy storage system in microgrid to improve battery life." *Computers & Electrical Engineering* 86 (2020): 106741.
- [3]. Yadav, Monika, Nitai Pal, and Devender Kumar Saini. "Microgrid control, storage, and communication strategies to enhance resiliency for survival of critical load." *IEEE Access* 8 (2020): 169047-169069.

- [4]. Ali, Liaqat, S. M. Muyeen, Hamed Bizhani, and Arindam Ghosh. "Comparative study on game-theoretic optimum sizing and economical analysis of a networked microgrid." *Energies* 12, no. 20 (2019): 4004.
- [5]. Wang, Y., A. Oulis Rousis, and G. Strbac. "Resilience-driven optimal sizing and pre-positioning of mobile energy storage systems in decentralized networked microgrids." *Applied Energy* 305 (2022): 117921.
- [6]. Xie, Hua, Xiaofei Teng, Yin Xu, and Ying Wang. "Optimal energy storage sizing for networked microgrids considering reliability and resilience." *IEEE Access* 7 (2019): 86336-86348.

4.4. JOURNAL PAPER



Article

Component Sizing of an Isolated Networked Hybrid Microgrid Based on Operating Reserve Analysis

Navid Salehi , Herminio Martínez-García * and Guillermo Velasco-Quesada

Electronic Engineering Department, Universitat Politècnica de Catalunya–BarcelonaTech (UPC),
08019 Barcelona, Spain

* Correspondence: herminio.martinez@upc.edu

Abstract: The power-sharing possibility amongst microgrids (MGs) in networked microgrids (NMGs) offers multiple profits to the NMG by employing an applicable energy management system. An efficient energy management system can provide an adequate compromise in terms of the component sizing of NMGs through MG collaboration. This paper proposes a procedure to size the component for an isolated networked hybrid microgrid. The proposed design procedure relies on the optimum operation of individual MGs. The defined Reduced Factor (RF) identifies the possible size reduction for the dispatchable components, such as diesel generators and the energy storage system of each MG. The introduced RF is based on the operating reserve evaluation obtained from the optimal operation of individual MGs and the correlation between load profiles. Eventually, the simulation and practical results of a networked hybrid MG consisting of three MGs are presented to verify the proposed component sizing procedure. The practical results verify the theoretical expectations. The results show that NPC and capital costs are reduced up to 13% and 17%, respectively.

Keywords: networked hybrid microgrid; operating reserve; peak load; component sizing; optimization



Citation: Salehi, N.; Martínez-García, H.; Velasco-Quesada, G. Component Sizing of an Isolated Networked Hybrid Microgrid Based on Operating Reserve Analysis. *Energies* **2022**, *15*, 6259. <https://doi.org/10.3390/en15176259>

Academic Editor: Dimitrios Katsaprakakis

Received: 14 July 2022

Accepted: 15 August 2022

Published: 27 August 2022

Publisher's Note: MDPI stays neutral with regard to jurisdictional claims in published maps and institutional affiliations.



Copyright: © 2022 by the authors. Licensee MDPI, Basel, Switzerland. This article is an open access article distributed under the terms and conditions of the Creative Commons Attribution (CC BY) license (<https://creativecommons.org/licenses/by/4.0/>).

1. Introduction

Conventional power systems have adopted microgrids (MGs) to address concerns about fossil fuel source depletion, environmental pollution, and climate change. Distributed energy resources (DERs) in an MG can consist of conventional power generators, such as diesel generators (DGs), or they can be integrated with renewable energy sources (RESs), such as photovoltaic (PV) and wind turbine (WT), as a hybrid MG (HMG). MGs propose valuable features to the power system, such as improving the operation and stability of the distributed system, reducing transmission line losses, and efficient harvesting of REs. These features can be obtained in both grid-connected and stand-alone MGs. However, the stand-alone operation mode in MGs is more delicate to provide the system's power balance due to the intermittency and uncertainty of RE sources (RESs). To this end, energy storage systems (ESSs), such as batteries and fuel cells, are inevitably utilized in the MGs. The ESS makes the system controllable to effectively manage the energy to supply the demand load. Therefore, the energy management system (EMS) is the other vital part of MGs, not only to provide the stability of the system but also to optimize the operation of the MG [1].

Accordingly, the configuration and the size of the components of the power generation units in an MG have attracted the attention of researchers in this industry to propose effective solutions for MGs. In [2], a multi-objective optimization problem was defined for an HMG to obtain the optimum size of the components. The net present cost (NPC), emission penalty cost, and CO₂ released quantity are three objective functions defined as a minimization problem. Moreover, the results from three multi-objective optimization—MOPSO, PESA-II, and SPEA-II—were analyzed to achieve the best solution to fulfill the objectives. A similar study was conducted in [3] to optimize the size of HMG components. The multi-objective self-adaptive differential evolution (MOSaDE) was assigned to the

optimization approach to propose the optimal HMG configuration. The loss-of-power supply probability (LPSP), the cost of electricity (COE), and the renewable factor are the three objective functions of the optimization problem that are restricted with HMG cost and reliability. The paper presented the optimally sized HMG components considering the load supply with a minimum energy cost and high reliability. Additionally, an optimal sizing methodology for an MG consists of a stand-alone photovoltaic system (SAPV), and the battery were studied in [4]. A mutation adaptive differential evolution (MADE) optimization algorithm was performed to optimize the configuration of the off-grid MG. The loss-of-load probability (LLP), leveled cost of energy (LCE), and life-cycle cost (LCC) are three objective functions that are normalized, weighted, and aggregated as a single objective for the optimization algorithm. In [5], the other HMG consists of renewable energies, and conventional energy sources were studied by considering the load uncertainty. To obtain the optimal configuration for the HMG, a decomposition-based multi-objective evolutionary algorithm (MOEA/D) was applied to minimize the LPSP and COE as the objective functions. In [6], the inconstancy and unpredictability of solar radiation were considered in the proposed hybrid optimization method of a SAPV/battery MG to optimize the configuration and size of the system.

Furthermore, some software tools have been introduced by several companies to plan the MG optimally. HOMER, RETScreen, H2RES, DER-CAM, and MARKAL/TIMES are several practical applications in MG design planning [7,8]. HOMER is widely used in MG applications to design the optimal MG consisting of renewable and non-renewable energy sources with different storage systems in grid-connected and isolation operation modes. In HOMER, the optimization procedure evaluates all possible configurations of energy generator units to meet the load. The simulation in HOMER carries out for a long time according to the cost function of the MG components. The results in HOMER present the most economic configurations with the lowest net total cost (NTC). In [9], HOMER develops an optimized grid-connected MG with PV and battery configuration. This study investigates the effect of the upsurge of grid failure frequency, and grid mean repair on the power price. Additionally, other studies have been conducted using HOMER to design HMG in remote areas, select and size power generators in rural MGs, and plan the micro-source generators to accommodate the high demand of RESs and environment policy [10,11]. RETScreen is more used to analyze the MG economically rather than operationally. The RETScreen can also be applicable for on-grid and off-grid MGs. The changes in parameters in RETScreen can provide a comparative analysis for the system under study considering the climate condition, RES availability, and load requirements [12]. The H2RES is also a balancing simulation tool that can effectively be used to design an MG integrated with RE. This tool checks the energy balance of the system hourly, considering the economic restriction [13]. The DER-CAM optimization is a customer-based model tool that monitors demand-side management and time-of-use under control by scheduling the DERs [14,15]. The MARKAL/TIMES energy system model can be applied to analyze the MG system as an energy sector. This tool evaluates the energy system in various time slices by considering the energy markets with a different objective function to obtain the least cost production units [16].

Recently, the concept of networked MG (NMG) has emerged to enhance the successful achievements of IMG. In NMGs, several MGs coordinate cooperatively to achieve the following goals:

- Increasing the reliability of the system due to increasing the possibility of power sharing and avoiding imbalanced power situation;
- Increasing the penetration ratio of REs into the MGs;
- Suppressing the uncertainties related to the RES employing the energy management system (EMS);
- Energy trading and ancillary service management.

On the other hand, the control strategies in NMGs are more complicated than in IMGs. In recent years, several control strategies have been introduced by researchers to control the

NMG effectively. Centralized, decentralized, hybrid, and distributed are some of the most prominent control strategies in NMGs. Each control strategy has its pros and cons, which, in several studies, are comprehensively surveyed [17,18]. However, briefly explained, in a centralized control scheme, all the MGs are controlled by a central controller; therefore, knowing the status of all MGs to analyze the system is mandatory. This control method is efficient and accurate. However, the enormous computing burden and dependency of the system on the central controller are the disadvantages of this method. In a decentralized control strategy, each MG controls separately to overcome the afore-mentioned drawbacks in the centralized method. However, optimizing the system without knowing other MGs' information reduces the system's efficiency. Therefore, in a hybrid strategy, the advantages of both centralized and decentralized methods are exploited. However, this method still suffers from the dependency on the central controller and the possibility of global failure in the system by any probable fault in the central controller. Finally, distributed control strategies have recently drawn more attention to increase the speed of analysis; meanwhile, the system's reliability increased as well.

In NHM, due to the possibility of power sharing amongst MGs, it is expected that the size of the components can be reduced effectively without significantly affecting the system's reliability. In [19], a three-level planning model for optimal sizing of NMG considering resilience and cost was proposed. An adaptive genetic algorithm was utilized for the normal sizing problem in the first level. However, load profile uncertainty and contingency for load shedding and a trade-off between cost and resilience were evaluated in the second and third levels, respectively. In [20], an optimal design of a hybrid distributed generation system to enhance the load and system reliability is conducted. The optimal sizing of the RE system considering electricity market interaction and reliability is presented in [21]. High renewables penetration considering demand response is investigated in [22] by proposing an optimal sizing and siting of smart MG components.

This paper proposes an optimal sizing components methodology for an isolated networked hybrid MG. The design procedure is based on IMG optimization. Consequently, according to the optimized operation of each IMG, a reduced factor (RF) identifies the possible component size reduction of each MG. This paper is organized as follows: In Section 2, the proposed NHMG configuration with RE and non-RE sources and load profiles are presented. Then, the optimal sizing of HIMG is investigated. To this end, HOMER is used to obtain the most economical configuration and component size for each IMG according to the energy sources and practical restrictions of the energy generator units. To evaluate the operation of the MGs, the optimal operation of each IMG is calculated for 24 h by considering the defined energy management algorithm. The RF calculation is conducted at the end of this section. In Section 3, the proposed sizing component algorithm is evaluated, and the simulation results will be presented in order to calculate the RF for each IMG. In Section 4, the verification of the proposed algorithm for an NHMG is analyzed according to the simulation and practical results. Finally, in Section 5, the conclusion of the paper is presented.

2. Proposed Optimal Sizing Procedure of an NHMG

The networked hybrid microgrid (NHMG), consisting of PV and WT with battery storage and DG, is investigated in this section. Figure 1 shows an HNMG of three MGs involving two residential and one industrial consumer. The MGs can exchange energy to provide a reliable operation to meet the loads according to the defined strategy. The load profiles are shown in Figure 4. As can be seen, the load profile of two residential consumers have the same pattern but with a different scale, and the load profile of industrial consumer has a different pattern. In this paper, to optimize the size of the components in HNMG, an algorithm is proposed. In this algorithm, the optimal design of the HNMG is based on the optimal design of each IMG. Figure 2 represents the proposed algorithm.

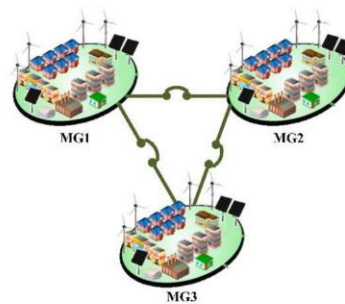


Figure 1. NMG consists of three residential MG and one industrial MG.

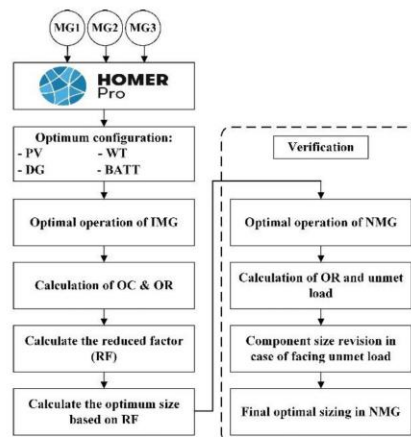


Figure 2. Proposed algorithm of NMG optimal sizing.

The optimal component size for each MG was obtained by HOMER Pro to evaluate the most economical configuration of potential candidate energy resources. According to the optimal sizing of each MG, power management was applied to the MGs to control the power production of dispatchable units, i.e., battery and DG. Moreover, the practical constraints and renewable energy intermittency were taken into consideration. Accordingly, the operating capacity (OC) and operating reserve (OR) of the individual MGs can be obtained. The calculation of OC and OR are essential due to the dependency of the optimization algorithm on these values. The OC and OR are defined as follows:

- Operating capacity (OC): the maximum amount of electrical generation capacity that is operating or is able to be produced at a moment's notice.
- Operating reserve (OR): the surplus operating capacity that can instantly respond to a sudden increase in the electric load or a sudden decrease in the renewable power output.

Peak load (PL) is an important factor with a significant impact on the component sizing in MGs. Demand-side management (DSM), integration of ESSs, and integration of electric vehicles (EVs) to the grid are considered as three methods in recent research as a solution for peak load shaving [23]. However, power sharing amongst MGs in NMGs results in the possibility of providing PL demand with the OR of adjacent MGs. The PLs and ORs are considered two main factors of MGs to define a reduced factor (RF) by the proposed algorithm in this paper. The RF represents the amount of energy that can be reduced when the MGs collaborate as an NMG. Consequently, the RFs assess the size of

dispatchable components while avoiding the reliability compromise due to OR reduction. Renewable energies exploit their maximum power due to utilizing maximum power point tracking (MPPT) to optimize the harvested energy.

2.1. Optimal Sizing of Hybrid Individual MGs

In order to obtain the optimal size of HIMGs, the power output and the cost function of power generator units have to be considered for each time step to supply the load in the most economical manner. The more precise power output model and cost function equations result in more accurate calculations. Tables 1 and 2 present the most well-known equations for power generation units and their cost functions. By considering the power output in Table 1, the optimization problem can be defined as:

$$\min CF = \{CF(PV) + CF(WT) + CF(DG) + CF(BAT)\} \tag{1}$$

Subject to:

$$P_{PV}(t) + P_{WT}(t) + P_{DG}(t) + P_{BAT}(t) = P_{Load}(t) \tag{2}$$

Equations (1) and (2) expressed that the total cost functions of generation units must be minimized considering the power balance of the system in each time step. Although only the power balance is stated as a constraint in this optimization problem, practically more constraints such as upper and lower limits for power generation units or battery SoC can be defined for this problem.

Table 1. Power output and cost function of power generation units in a HIMG.

| Gen Unit | Ref. | Power Output | Cost Function |
|----------|--------|--|---|
| PV | [3,24] | $P_{pv}(t) = P_{N-pv} \times \frac{G(t)}{G_{ref}} \times [1 + K_t((T_{amb} + (0.0256 \times G)) - T_{ref})]$ | $C_{PV} = \alpha I_{pv}^p P_{N-pv} + G_{pv}^E P_{N-pv}$ |
| WT | [5,24] | $P_{wt}(t) = \begin{cases} 0 & V < V_{cut-in}, V > V_{cut-in} \\ V^3(t) \left(\frac{P_r}{V_r^3 - V_{cut-in}^3} \right) - P_r \left(\frac{V_{cut-in}^3}{V_r^3 - V_{cut-in}^3} \right) & V_{cut-in} \leq V < V_{rated} \\ P_r & V_{rated} \leq V \leq V_{cut-out} \end{cases}$ | $C_{WT} = \alpha I_{pv}^p P_{N-r} + G_{wt}^E P_{N-r}$ |
| DG | [3] | $P_{DG}(t) = \frac{q(t) - bP_r}{a}$ | $C_{DG} = A + B \times P_{DG} + C \times P_{DG}^2$ |
| BAT | [2] | $P_{BATT}(T) = \frac{a}{T} \frac{E_L \cdot AD}{DOD \cdot \eta_{inv} \cdot \eta_b}$ | $C_{BAT} = \gamma + \xi \times P_{N-BAT}$ |

Table 2. Parameter definitions in Table 1.

| Parameter | Description | Parameter | Description |
|---------------|---|----------------------------|--|
| P_{pv} | output power of PV | a, b | fuel consumption coefficients (L/kW) [3] |
| P_{N-pv} | rated power under reference conditions | E_L | load power |
| G | solar radiation (W/m ²) | AD | autonomy days (typically 3–5 days) |
| G_{ref} | reference solar radiation (W/m ²) | DOD | depth of discharge |
| T_{ref} | 25 °C | η_{inv} | inverter efficiencies |
| K_t | -3.7×10^{-3} (1/°C) | η_b | battery efficiencies |
| P_{wt} | output power of WT | $A = r/[1 - (1 + r)^{-N}]$ | investment annuitization coefficient |
| P_r | rated power | r | interest rate |
| V_r | rated wind speed | N | investment lifetime |
| V_{cut-in} | cut-in wind speed | I^p | investment costs |
| $V_{cut-out}$ | cut-out wind speed | G^E | O&M cost for solar and wind generation [24] |
| $q(t)$ | fuel consumption (L/h) | A, B, C | generator coefficients |
| $P(t)$ | generated power (kW) | γ, ξ | coefficients to linearize the cost function of batteries according to the capital cost and operation cost of batteries |

HOMER Pro can effectively size the MG components consisting of the conventional power generation such as DGs, REs such as solar and wind energy, and energy storage systems (ESSs) such as batteries and fuel cells both in the grid-connected and stand-alone modes. HOMER analyzes all feasible solutions to meet the load and sorts them from the most economical configuration to the least one. To this end, the potential candidates for power generation have to be defined, and the cost of each unit must be determined. The cost in HOMER consists of capital cost, replacement cost, and operation and maintenance (O&M) cost. The capital cost is the initial investment to provide the power generation units. The replacement cost is the cost of replacing the units at the end of their lifetime. Additionally, the O&M cost is referred to as annual operation and maintenance cost. Moreover, cycling charging (CC) and load following (LF) are the two most common strategies in HOMER to control the power dispatch in the MG. The CC dispatch strategy is more economical when the RE generation consists of a lower portion of the total required energy. In this case, the dispatchable generators, such as DG, operate at full output power, and surplus energy charges the storage systems, such as batteries. On the other hand, in the LF strategy, the dispatchable units only produce the required power to supply the unmet load by REs, and REs can charge the storage systems if extra power is produced. The practical constraints for each power generation unit, operating reserve, and emission and environmental effects can be defined in HOMER effectively.

Table 3 represents the optimum design of the three MGs considering the load profiles in Figure 2 by HOMER Pro. The considered MGs are situated in the geographical coordinates of 41°23'04" N, 02°10'27" E (Barcelona City). The solar, wind, and temperature resources were loaded from NASA Prediction of Worldwide Energy Resources, and Table 4 presents the relevant costs. In order to increase the reliability of the MGs, the operating reserve for solar and wind power output and load in each current time step was considered and presented as the constraints in Table 4. Because forecasting solar radiation is more reliable than wind profile, the operating reserve for WT is usually greater than PV.

Table 3. HIMG optimal design by HOMER.

| | PV (kW) | WT (kW) | DG (kW) | BAT (kWh) | Converter (kW) | Dispatch | NPC (\$) | Unmet Electric Load | Capacity Shortage |
|-----|---------|---------|---------|-----------|----------------|----------|----------|---------------------|-------------------|
| MG1 | 6.5 | 2 | 6.8 | 29 | 2.95 | LF | 80,980 | 0 | 0 |
| MG2 | 8.31 | 3 | 9.1 | 38 | 4.03 | LF | 107,774 | 0 | 0 |
| MG3 | 16.8 | 4 | 15 | 57 | 9.71 | CC | 234,924 | 0 | 0 |

Table 4. Economical and constraints parameters.

| Gen Unit | Parameter | Value | Unit | Gen Unit | Parameter | Value | Unit |
|-----------|-----------------|-------|-------------|-------------|---------------------------|-------|-------------|
| PV | Capital | 2500 | USD/kW | WT | Capital | 3000 | USD/kW |
| | Replacement | 2500 | USD/kW | | Replacement | 3000 | USD/kW |
| | O&M | 10 | USD/kW/year | | O&M | 30 | USD/kW/year |
| | Derating Factor | 80 | % | | Hub Height | 17 | m |
| | Lifetime | 25 | year | | Lifetime | 20 | year |
| DG | Capital | 500 | USD/kW | BAT | Capital | 300 | USD/kW |
| | Replacement | 500 | USD/kW | | Replacement | 300 | USD/kW |
| | O&M | 0.03 | USD/kW/year | | O&M | 10 | USD/kW/year |
| | Fuel Price | 1 | USD/L | | Min SOC | 40 | - |
| | Lifetime | 15 k | hour | | Lifetime | 10 | year |
| CONVERTER | Capital | 300 | USD/kW | CONSTRAINTS | Load in current time step | 10% | |
| | Replacement | 300 | USD/kW | | Annual peak load | 0 | |
| | O&M | 0 | USD/kW/year | | Solar power output | 20% | |
| | Lifetime | 15 | year | | Wind power output | 50% | |

2.2. Optimal Operation of HIMGs

According to the obtained optimal size of HIMG, the optimal operation of the MGs over 24 h was performed to calculate the produced energy (PE) and OR of each power generator unit in the MGs. To this end, the cost functions in Table 1 were used. However, to achieve the maximum power from REs, it was supposed that a maximum power point tracking (MPPT) was applied to the PV and WT. Therefore, the DG and battery power as the decision variables and battery SoC as the state variable were defined for the optimizer in order to determine the most economical operation for MGs. Consequently, the optimization problem can be defined as cost function (CF) minimization of the total sum of DG and BAT:

$$\min\{CF(DG) + CF(BAT)\} \tag{3}$$

Subject to:

$$P_{DG}(t) + P_{BAT}(t) = P_{Load}(t) - P_{PV}(t) - P_{WT}(t) \tag{4}$$

$$P_{DGmin} \leq P_{DG} \leq P_{DGmax} \tag{5}$$

$$0 \leq P_{BAT} \leq P_{BATmax} \tag{6}$$

$$SoC_{min} \leq SoC(t) \leq SoC_{max} \tag{7}$$

where the SoC of the battery can be calculated by:

$$SoC(t + \Delta t) = SoC(t) + \frac{\Delta t}{C_{BAT}} P(t) \tag{8}$$

In (8), the power $P(t)$ can be positive or negative regarding the discharging or charging state of the battery.

To obtain the optimal operation for each MG, a power management unit has to be applied to the system. Figure 3 represents the power management in this paper.

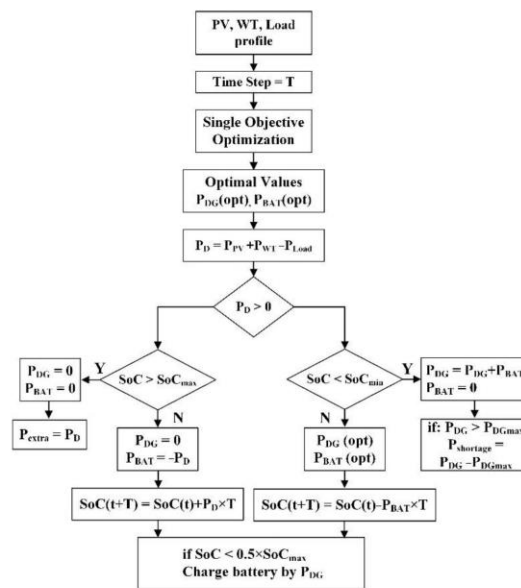


Figure 3. Power management algorithm for the HIMG.

As it can be seen from Figure 4, according to the power amounts of PV, WT, and Load at each time step, a single-objective optimization was employed to obtain the optimal values for DG and BAT considering the constraints in (4)–(7). If the REs meet the load, this difference power (PD) can charge the battery if the battery is not fully charged. On the contrary, if the battery is fully charged (SoCmax), then PD identifies as extra power. In this case, DG is not necessary to produce power to provide the power balance. On the other hand, if the REs are insufficient to supply the load, the DG and BAT participate economically to provide the required power for the load. In this case, the battery discharges if a portion of load demand is supplied by battery power. Supplementary battery management is also provided to check the SoC battery in each iteration. By evaluating the possibility of DG generation, the battery can be charged at least at the level of 50%.

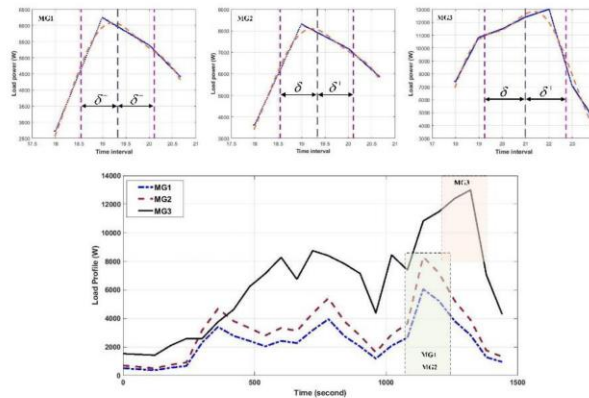


Figure 4. Load profile for each MG of the NMG.

Particle swarm optimization (PSO) was utilized in this paper as a single-objective optimization. However, other algorithms, such as differential evolution (DE), genetic algorithm (GA), and imperialist competitive algorithm (ICA), are also able to deal with this problem. PSO represents a robust, rapid, and reliable performance among different optimization algorithms. In the PSO algorithm, the particles are identified by position and velocity. At the initial phase, the particles position and particle best position are initialized. Then, over the iterations, the particles’ position and velocity are updated to propel the particles toward the global best [25].

2.3. Evaluation of the HIMG Operation (RF Calculation)

According to the optimal operation of the HIMG, the optimal produced energy of the energy generator units and consequently the OR of MGs can be calculated over a specific interval. Interactive transfer or receiving energy in the MG community results in higher OR in MGs. Therefore, optimal component sizing in the NMG can effectively reduce MGs’ capital, replacement, and M&O cost. The reduced factor proposed in this section was based on two main factors, the PL and correlation of load profile. Due to the dependency of the proposed RF to the OR of MGs, the RF affects the dispatchable components of the MGs. The RF is expressed in (9):

$$RF_{MG_i} = \frac{\left[OR_{MG_i} \times \frac{OC_{MG_i} - PL}{OC_{MG_i}} \right]_{MG_i} \|\delta_i^- - \delta_i^+\| \times \left(2 - \prod_{j=1}^N corr(MG_i, MG_j) \right)}{\left[OR_{MG_i} \times \frac{OC_{MG_i} - PL}{OC_{MG_i}} \right]_{MG_i} \|\delta_i^- - \delta_i^+\| + \frac{1}{N-1} \sum_{\substack{j=1 \\ j \neq i}}^N \left[OR_{MG_j} \times \frac{OC_{MG_j} - L_{max}}{OC_{MG_j}} \right]_{MG_j} \|\delta_j^- - \delta_j^+\|} \quad (9)$$

In (9), $|\delta^+ - \delta^-|$ represents the interval at which PL occurs, at $(\delta^+ + \delta^-)/2$, and the OR of other MGs are also calculated in this interval; therefore, only PL and the maximum load profile (L_{max}) are identical if the load patterns are similar. For instant, when the MG_1 and MG_2 are at PL, the MG_3 is not in its PL. In addition, N is the number of MGs that existed in the NHMG, and $corr$ represents the correlation of the load pattern among MGs. The Pearson's linear correlation coefficient was utilized to evaluate the correlation of the Load profile:

$$corr(MG_i, MG_j) = \frac{\sum_{k=1}^n (MG_{i,k} - \overline{MG_i})(MG_{j,k} - \overline{MG_j})}{\left\{ \sum_{k=1}^n (MG_{i,k} - \overline{MG_i})^2 \sum_{l=1}^n (MG_{j,k} - \overline{MG_j})^2 \right\}^{\frac{1}{2}}} \quad (10)$$

where \overline{MG} is the mean value of n data of MG's load profile. This correlation coefficient returns a value between -1 and 1 , if a perfect negative correlation and perfect positive correlation exists among the data, respectively. To obtain the δ for MGs, a Gaussian curve with a mean (μ) of PL ($\mu = PL$) was fitted to the load profile. The standard deviation of the fitted curve was considered as δ . Figure 4 demonstrates the Gaussian fitted curve to the MG load profiles. The following results can be deduced from (9):

- The calculations were based on the OR of a specific MG during the PL in the interval $|\delta^+ - \delta^-|$. This time interval is considered for the other MGs that exist in the NHMG. The ORs were calculated based on the optimal operation of HIMGs.
- The ORs are given importance by the factor of PL and OC difference. Therefore, the higher PL led to reducing lower OR in the NMG in order to increase the MG reliability.
- The correlation represents the PL coincidence of MGs. Therefore, the correlation with a value that is lower than the unity resulted in a higher RF due to the possibility of sharing OR of adjacent MGs.

3. Evaluation and Simulation Results

According to the optimal design of the HIMG with HOMER and the discussed power management algorithm in Figure 4, the ORs of HIMGs were calculated. To this end, the simulation was conducted in MATLAB. Eventually, according to Equation (9), the RFs were calculated in order to obtain the optimal design in the NHMG. Figure 5 shows the optimal operation of the HIMGs. The SoC of the batteries and extra and shortage power are also presented in Figure 5. The initial SoC of the batteries was set to 50%, and as can be observed, the extra power leads to charging the batteries completely.

The simulation was performed for 24 h, and the time step was set to 15 min to reduce the large quantity of data produced. The ORs were calculated for two different intervals $|\delta^+ - \delta^-|$. The PL of MG_1 and MG_2 is a coincidence at the same time, and the OR for MG_3 was also calculated during the PL of two other MGs. Furthermore, the OR during the PL of MG_3 was calculated for MG_1 and MG_2 to obtain the RF of MG_3 . To evaluate the battery power, the C-rate was considered as 5C. The correlation was calculated by using the "corr" function in MATLAB. The load profile of MG_1 and MG_2 are similar with different scales. Therefore, the correlation for these two MGs is unity. However, the correlation between MG_1 and MG_3 was obtained as 0.8727. Table 5 presents the HIMG specifications and RFs for the HIMGs. The RF represents the OR reduction percentage in each HIMG when the MGs are in collaborative operation as the NHMG. Therefore, in order to evaluate the optimal component size for the HNMG, the reduced power generation units were obtained as follows:

$$\min\{\alpha \times CF(DG) + \beta \times CF(BAT)\} \quad (11)$$

Subject to:

$$P_{MG_i}^{DG} + P_{MG_i}^{BAT} = \frac{RF_{MG_i} \times OR_{MG_i}}{\|\delta_i^- - \delta_i^+\|} \quad (12)$$

where DG and battery cost functions are defined in Table 1, and α and β weighed the priority of DG and battery cost functions, respectively. The reduced OR for MGs over the time interval $||\delta^+ - \delta^-||$ represents the amount of power. Eventually, the optimum result of DG and battery power from the minimization problem in (11) was deduced from the optimum results obtained from the algorithm in Figure 4. Due to the high M&O cost and the lower lifetime of batteries to produce energy, β was considered a higher value in this research in order to decrease the size of the more compared with DG. The optimum size of DG and batteries according to the proposed algorithm is presented in Table 5.

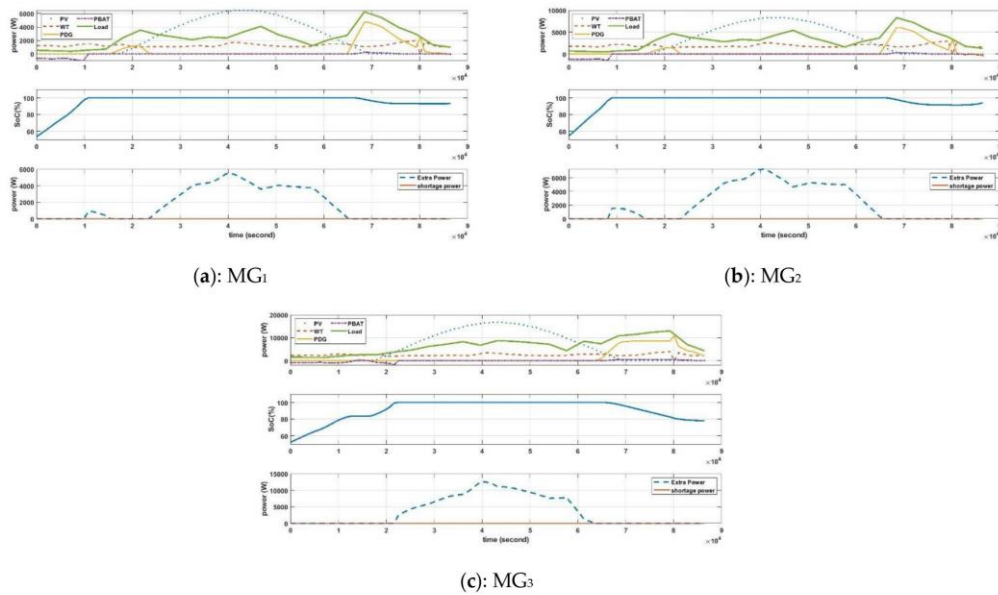


Figure 5. Optimal operation of the HIMGs: (a) MG₁, (b) MG₂, and (c) MG₃.

Table 5. HIMG specifications.

| | PGU | MG1 | MG2 | MG3 | Total |
|--|-----|--------|--------|--------|---------|
| OR (kWh) for MG ₁ and MG ₂ | DG | 4.4 | 6.45 | 13.44 | 24.29 |
| | BAT | 9.64 | 12.73 | 19.04 | 41.41 |
| OR (kWh) for MG ₃ | DG | 13.57 | 19.16 | 19.31 | 52.04 |
| | BAT | 14.92 | 19.79 | 28.56 | 63.27 |
| OC (kW) | DG | 6.8 | 9.1 | 15 | 30.9 |
| | BAT | 5.8 | 7.6 | 11.4 | 24.8 |
| Peak Load (kW) | | 6.2 | 8.3 | 13 | 27.5 |
| Electric Load (EL) (kWh/day) | | 237.83 | 316.49 | 630.46 | 1184.78 |
| Unmet load (kWh/day) | | 0 | 0 | 0 | 0 |
| Extra power (kWh/day) | | 160.02 | 216.99 | 351.73 | 728.74 |
| RF (%) | | 41 | 52 | 68 | - |
| DG (kW) | | 3.8 | 4.8 | 8.2 | - |
| BAT (kW) | | 3.2 | 3.8 | 6.4 | - |

4. Verification of the Results in the NHMG

To verify the results of the optimal and economical sizing components in an NMG, according to the calculated RF in Table 5, an algorithm to control the NHMG is proposed. The optimum operation of the NHMG was evaluated considering the hybrid control strategy defined in Figure 6. Hybrid control refers to the control strategies that take advantage of both centralized and decentralized control strategies. The centralized controller is applied in order to obtain the optimal operation of each HIMG. On the other hand, the decentralized controller is responsible for the optimum operation of the whole system by knowing the essential data from the centralized controller. As it can be observed from Figure 6, multi-objective optimization was utilized in the algorithm as a centralized controller for each HIMG.

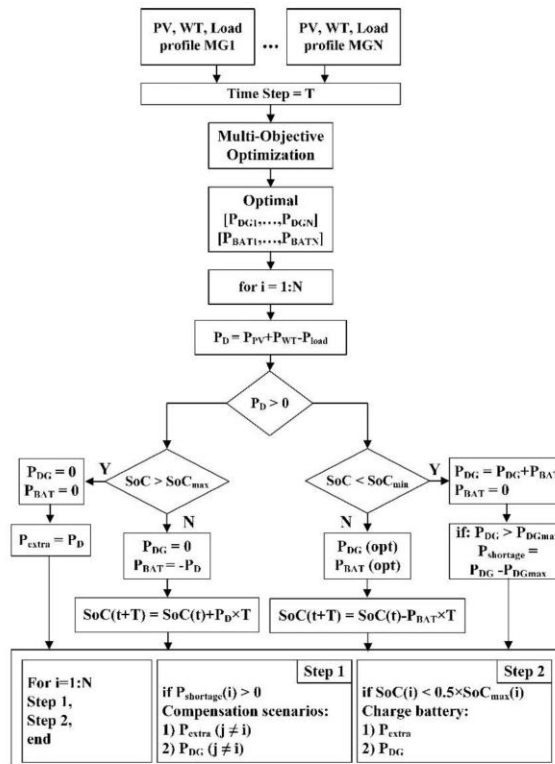


Figure 6. Hybrid control strategy in the NHMG.

The multi-objective optimization was implemented with the MOPSO and PESA-II algorithms in order to establish a comparison between these two optimization methods. MOPSO and PESA-II are technically similar. However, in PESA-II, the PSO algorithm is replaced with GA. In multi-objective optimization problems, the proposed algorithms utilize different methods to discover the non-dominated solutions and produce the Pareto frontier. The non-dominated solutions were produced using the concept of dominance in MOPSO and PESA-II. Moreover, both of the afore-mentioned optimization methods have region-based selection in leader and objective space in order to improve the diversity of the Pareto frontier [25].

Then, the essential information, i.e., DG and battery power, was obtained from the decentralized controller to provide an optimal operation for the NHMG. Compared with

the HIMG algorithm, a supplementary control to check the possibility of power sharing amongst MGs was applied to the algorithm in Figure 6. In this case, the extra power and shortage power can effectively interact through the MGs to have a reliable operation. To this end, two complementary steps were considered in order to take advantage of power sharing in the NHMG. At the first step, the MG with a power shortage attempts to meet the load first by the extra energy from other MGs, and if the extra energy does not exist or is sufficient to meet the power shortage, the DGs in MGs can assist by supplying the load completely. Moreover, in step 2, the SoC of the batteries check if they need charging if the SoC is less than 50% and extra energy and DG power exist to charge the batteries.

4.1. Simulation Results

In order to evaluate the operation of the NHMG by considering the sizing component design procedure in Section 3, the simulation was conducted according to the control algorithm in Figure 6. Two multi-objective optimization methods were implemented in MATLAB to optimize the operation of each HIMG, and the supplementary control was exploited to optimize the operation of the entire system. The multi-objective optimization proposed a set of optimal solutions as a Pareto frontier. To choose the proper solution, several methods can be applied to the problem. The evaluation of the solutions, feature selection, and clustering methods are usual methods to select a single or multi solution amongst several Pareto solutions.

In this simulation, k-means were applied to the problem to select the center of the cluster using Lloyd’s algorithm as a proper solution among the produced Pareto set. In Figure 7, the operation of the NHMG by MOPSO optimization is demonstrated. Moreover, Table 6 is provided in order to compare the obtained results from the two optimization algorithms.

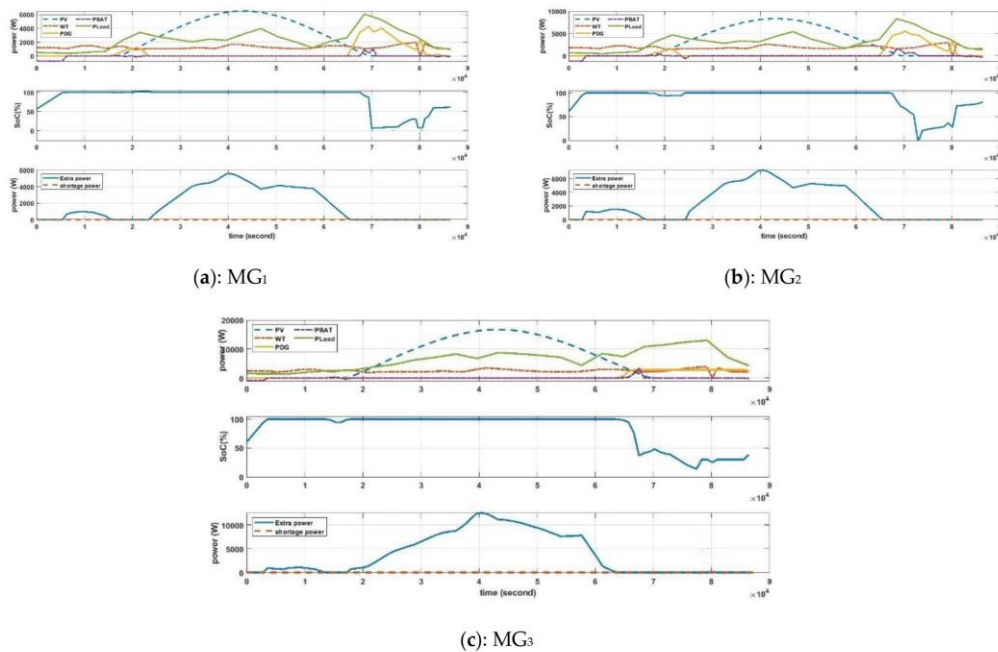


Figure 7. Optimal operation of the HNMGs: (a) MG₁, (b) MG₂, and (c) MG₃.

Table 6. Optimal operation of the NHMG.

| | MOPSO | | | | PESA-II | | |
|--|-------|-----------------|-----------------|-----------------|-----------------|-----------------|-----------------|
| | PGU | MG ₁ | MG ₂ | MG ₃ | MG ₁ | MG ₂ | MG ₃ |
| OR (kWh/day) for MG ₁ and MG ₂ | DG | 4.40 | 6.45 | 13.44 | 4.54 | 6.75 | 13.76 |
| | BAT | 9.64 | 12.73 | 19.04 | 9.50 | 12.43 | 18.84 |
| OR (kWh/day) for MG ₃ | DG | 13.57 | 19.16 | 19.31 | 13.87 | 19.36 | 19.50 |
| | BAT | 14.92 | 19.79 | 28.56 | 14.62 | 19.59 | 28.22 |
| Unmet load (kWh/day) | | 0 | 0 | 0 | 0 | 0 | 0 |
| Extra power (kWh/day) | | 160.02 | 216.99 | 351.73 | 159.74 | 216.55 | 350.66 |

To compare the performance of the two optimization algorithms, the simulation was conducted in one laptop set. The results obtained from PESA-II are slightly more accurate due to providing a more optimal solution. However, the performance of PESA-II is slower than that of MOPSO (about 8 min for MOPSO vs. 28 min for PESA-II). In addition, the initial parameters related to the PESA-II were more sensitive in order to be adjusted accurately.

4.2. Practical Results

The experiments were implemented using a GPIB communication protocol, and RS485 Modbus transmits the measured values. Figure 8 shows the implemented structure of the NHMG. To achieve the performance of the batteries and WT energy, the optimal results of the central controller affect the load profile. The solar radiation profile was applied to the solar array simulator (SAS) to emulate solar energy. Furthermore, it is essential to define the short circuit current (I_{sc}), maximum power point current (I_{mpp}), open-circuit voltage (V_{oc}), and maximum power point voltage (V_{mpp}) of the solar panel for SAS:

$$I_{sc} = I_{sc}^{ref} \times \left(\frac{G}{G_{ref}} \right) \quad (13)$$

$$I_{mpp} = I_{mpp}^{ref} \times \left(\frac{G}{G_{ref}} \right) \quad (14)$$

$$V_{oc} = V_{oc}^{ref} + \alpha \ln \left(\frac{G}{G_{ref}} \right) \quad (15)$$

$$V_{mpp} = V_{mpp}^{ref} - \beta (T_{ref} - T) \quad (16)$$

where G is the solar radiation (W/m^2), α is modified ideality factor ($\alpha = K \times Temp/q$, where K is the Boltzmann constant, $Temp$ is cell temperature, and q is electron charge), and β is the temperature coefficient. The temperature is considered constant, $T = T_{ref}$. Figure 9 shows the laboratory experiments' configuration of the three MGs. Figure 10 represents the optimal operation of the NMG according to the reduced component sizing calculated by the proposed algorithm. As can be observed, the produced energy by the power generator units can meet the load effectively.

As can be observed from Figure 10, the load is met by power generation units effectively, and the surplus energy is transferred to the main grid through the grid-connected inverter. The grid-connected inverter used in the laboratory has a 30 s delay in order to start working in synchronization with the main grid. This delay can be seen in the PV power generation graph in Figure 10.

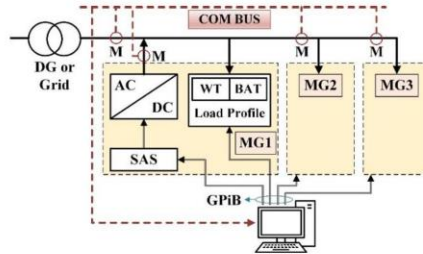


Figure 8. Implemented structure of the NHMG.

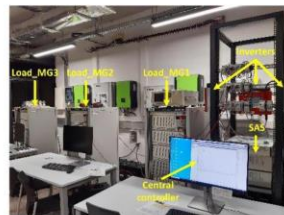
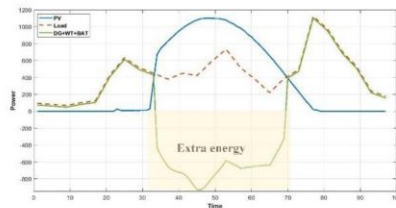
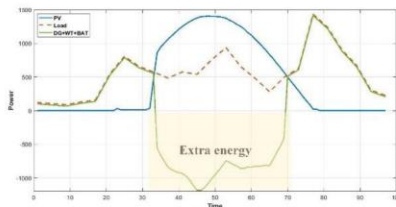


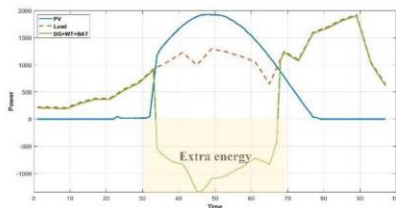
Figure 9. Laboratory experiments' configuration.



(a)



(b)



(c)

Figure 10. Practical results of the HIMGs: (a) MG₁, (b) MG₂, and (c) MG₃.

5. Conclusions

A component sizing procedure for a NHMG was proposed in this paper. The proposed algorithm was based on the OR and peak loads of MGs. To this end, the optimal operation of HIMGs was evaluated to obtain the optimal OR of each MG. Consequently, a reduced factor (RF) was presented in order to reduce the dispatchable component size of MGs. The RF was based on the OR, the peak load, and the correlation of load pattern. Therefore, NHMGs with different load patterns resulted in an RF increase and component size decrease. Due to the possibility of power sharing in NHMGs, the proposed algorithm did not affect the reliability of MGs by reducing the OR. The simulation results for the NHMG by using two different multi-objective optimizations, i.e., MOPSO and PESA-II, were analyzed. The results show that, in the NHMG, the size of the dispatchable generation units can decrease effectively. Therefore, the capital, operational, and M&O cost of the MGs can be reduced significantly. Finally, the results of the laboratory experiments were presented in order to verify the proposed algorithm.

Author Contributions: Conceptualization, N.S.; methodology, N.S. and H.M.-G.; software, N.S.; validation, N.S., H.M.-G. and G.V.-Q.; investigation, N.S.; data curation, N.S. and H.M.-G.; writing—original draft preparation, N.S. and H.M.-G.; writing—review and editing, N.S., H.M.-G. and G.V.-Q.; supervision, H.M.-G. and G.V.-Q. All authors have read and agreed to the published version of the manuscript.

Funding: Grant PGC2018-098946-B-I00, funded by: MCIN/AEI/10.13039/501100011033/and by ERDF A way of making Europe.

Institutional Review Board Statement: Not applicable.

Informed Consent Statement: Not applicable.

Data Availability Statement: Not applicable.

Acknowledgments: The authors would like to thank the Spanish Ministerio de Ciencia, Innovación y Universidades (MICINN)—Agencia Estatal de Investigación (AEI) and the European Regional Development Funds (ERDF) by grant PGC2018-098946-B-I00 funded by MCIN/AEI/10.13039/501100011033/and by ERDF A way of making Europe.

Conflicts of Interest: The authors declare no conflict of interest.

Nomenclature

| | |
|------|--|
| CC | Cycling Charging |
| CF | Cost Function |
| COE | Cost of Electricity |
| DE | Differential Evolution |
| DER | Distributed Energy Resources |
| DG | Diesel Generator |
| DSM | Demand-Side Management |
| EMS | Energy Management System |
| ESS | Energy Storage System |
| EV | Electric Vehicle |
| GA | Genetic Algorithm |
| HIMG | Hybrid Individual Microgrid |
| HMG | Hybrid Microgrid |
| ICA | Imperialist Competitive Algorithm |
| IMG | Individual Microgrid |
| LCC | Life-Cycle Cost |
| LCE | Levelized Cost of Energy |
| LF | Load Following |
| LLP | Loss-of-Load Probability |
| LPSP | Loss-of-Power Supply Probability |
| MADE | Mutation Adaptive Differential Evolution |

| | |
|---------|---|
| MG | Microgrid |
| MOEA/D | Multi-Objective Evolutionary Algorithm Based on Decomposition |
| MOSaDE | Multi-Objective Self-Adaptive Differential Evolution |
| MOPSO | Multi-Objective Particle Swarm Optimization |
| MPPT | Maximum Power Point Tracking |
| NHMG | Networked Hybrid Microgrid |
| NMG | Networked Microgrid |
| NPC | Net Present Cost |
| NTC | Net Total Cost |
| OC | Operating Capacity |
| OR | Operating Reserve |
| PE | Produced Energy |
| PESA-II | Pareto Envelop-based Selection Algorithm II |
| PL | Peak Load |
| PV | Photovoltaic |
| RE | Renewable Energy |
| RES | Renewable Energy Source |
| RF | Reduced Factor |
| SAS | Solar Array Simulator |
| SoC | State of Charge |
| SPEA-II | Strength Pareto Evolutionary Algorithm II |
| SAPV | Stand-Alone PV |
| WT | Wind Turbine |

References

- Kumar, P.S.; Chandrasena, R.P.S.; Ramu, V.; Srinivas, G.N.; Babu, K.V.S.M. Energy Management System for Small Scale Hybrid Wind Solar Battery Based Microgrid. *IEEE Access* **2020**, *8*, 8336–8345. [[CrossRef](#)]
- Mohammed, K.; Mohammed, O.H.; Alshammari, N.; Akherraz, M. Multi-objective optimization and the effect of the economic factors on the design of the microgrid hybrid system. *Sustain. Cities Soc.* **2021**, *65*, 102646.
- Ramli Makbul, A.M.; Bouchekara, H.R.E.H.; Alghamdi, A.S. Optimal sizing of PV/wind/diesel hybrid microgrid system using multi-objective self-adaptive differential evolution algorithm. *Renew. Energy* **2018**, *121*, 400–411. [[CrossRef](#)]
- Mohammed, R.H.; Gomes, C.; Hazim, H.; Ahmadipour, M. Sizing and implementing off-grid stand-alone photovoltaic/battery systems based on multi-objective optimization and techno-economic (MADE) analysis. *Energy* **2020**, *207*, 118163.
- Bouchekara, H.R.E.-H.; Javaid, M.S.; Shaaban, Y.A.; Shahriar, M.S.; Ramli, M.A.M.; Latreche, Y. Decomposition based multiobjective evolutionary algorithm for PV/Wind/Diesel Hybrid Microgrid System design considering load uncertainty. *Energy Rep.* **2020**, *7*, 52–69. [[CrossRef](#)]
- Ridha, H.M.; Gomes, C.; Hizam, H.; Ahmadipour, M.; Muhsen, D.H.; Ethaib, S. Optimum Design of a Standalone Solar Photovoltaic System Based on Novel Integration of Iterative-PESA-II and AHP-VIKOR Methods. *Processes* **2020**, *8*, 367. [[CrossRef](#)]
- Anderson Alexander, A.; Suryanarayanan, S. Review of energy management and planning of islanded microgrids. *CSEE J. Power Energy Syst.* **2019**, *6*, 329–343.
- Wei, F.; Jin, M.; Liu, X.; Bao, Y.; Mamay, C.; Yao, C.; Yu, J. A review of microgrid development in the United States—A decade of progress on policies, demonstrations, controls, and software tools. *Appl. Energy* **2018**, *228*, 1656–1668.
- Vinny, M.; Adetunji, K.E.; Joseph, M.K. Planning of a sustainable microgrid system using HOMER software. In Proceedings of the 2020 Conference on Information Communications Technology and Society (ICTAS), Durban, South Africa, 11–12 March 2020; pp. 1–5.
- Zahid, J.; Li, K.; Hassan, R.U.; Chen, J. Hybrid-microgrid planning, sizing and optimization for an industrial demand in Pakistan. *Teh. Vjesn.* **2020**, *27*, 781–792.
- Wencong, S.; Yuan, Z.; Chow, M. Microgrid planning and operation: Solar energy and wind energy. In Proceedings of the IEEE PES General Meeting, Providence, RI, USA, 25–29 July 2010; pp. 1–7.
- Yu, P.; Liu, L.; Zhu, T.; Zhang, T.; Zhang, J. Feasibility analysis on distributed energy system of Chongming County based on RETScreen software. *Energy* **2017**, *130*, 298–306.
- Gasparovic, G.; Krajačić, G.; Duić, N.; Baotić, M. New Energy Planning Software for Analysis of Island Energy Systems and Microgrid Operations – H2RES Software as a Tool to 100% Renewable Energy System. *Comput. Aid. Chem. Eng.* **2014**, *33*, 855–1860.
- Michalitsakos, P.; Mihet-Popa, L.; Xydis, G. A Hybrid RES Distributed Generation System for Autonomous Islands: A DER-CAM and Storage-Based Economic and Optimal Dispatch Analysis. *Sustainability* **2017**, *9*, 2010. [[CrossRef](#)]
- Essiet, I.O.; Sun, Y.; Wang, Z. Analysis of the Effect of Parameter Variation on a Dynamic Cost Function for Distributed Energy Resources: A DER-CAM Case Study. *Appl. Sci.* **2018**, *8*, 884. [[CrossRef](#)]

16. Comodi, G.; Cioccolanti, L.; Gargiulo, M. Municipal scale scenario: Analysis of an Italian seaside town with MarkAL-TIMES. *Energy Policy* **2012**, *41*, 303–315. [[CrossRef](#)]
17. Zia Muhammad, F.; Benbouzid, M.; Elbouchikhi, E.; Muyeen, S.M.; Techato, K.; Guerrero, J.M. Microgrid transactive energy: Review, architectures, distributed ledger technologies, and market analysis. *IEEE Access* **2020**, *8*, 19410–19432.
18. Islam, M.; Yang, F.; Amin, M. Control and optimisation of networked microgrids: A review. *IET Renew. Power Gener.* **2021**, *15*, 1133–1148. [[CrossRef](#)]
19. Yi, W.; Rousis, A.O.; Strbac, G. A Three-Level Planning Model for Optimal Sizing of Networked Microgrids Considering a Trade-Off Between Resilience and Cost. *IEEE Trans. Power Syst.* **2021**, *36*, 5657–5669.
20. Afolabi, Y.A.; AlMuhaini, M.; Heydt, G.T. Optimal design of hybrid DG systems for microgrid reliability enhancement. *IET Gener. Transm. Distrib.* **2020**, *14*, 815–823.
21. Hakimi, S.M.; Hasankhani, A.; Shafie-Khah, M.; Lotfi, M.; Catalão, J.P. Optimal sizing of renewable energy systems in a Microgrid considering electricity market interaction and reliability analysis. *Electr. Power Syst. Res.* **2021**, *203*, 107678. [[CrossRef](#)]
22. Hakimi, S.M.; Hasankhani, A.; Shafie-Khah, M.; Catalão, J.P. Optimal sizing and siting of smart microgrid components under high renewables penetration considering demand response. *IET Renew. Power Gener.* **2019**, *13*, 1809–1822. [[CrossRef](#)]
23. Moslem, U.; Romlie, M.F.; Abdullah, M.F.; Halim, S.A.; Kwang, T.C. A review on peak load shaving strategies. *Renew. Sustain. Energy Rev.* **2018**, *82*, 3323–3332.
24. Norberto, F.; Sanz, Y.; Rodrigues, M.; Montañés, C.; Dopazo, C. The use of cost-generation curves for the analysis of wind electricity costs in Spain. *Appl. Energy* **2011**, *88*, 733–740.
25. Navid, S.; Martinez-Garcia, H.; Velasco-Quesada, G.; Guerrero, J.M. A Comprehensive Review of Control Strategies and Optimization Methods for Individual and Community Microgrids. *IEEE Access* **2022**, *10*, 15935–15955.

Chapter 5

A Comparative Study of Different Optimization Methods for Resonance Half-Bridge Converter

5.1. INTRODUCTION

DC-DC converters are widely used in hybrid MGs and DC MGs due to existing DC generators such as PV, WT, FC, and Batteries. DC-DC converters are mainly applicable for several purposes like galvanic isolation, accurate voltage adjustment, accurate current adjustment, over-voltage, and over-current protection. Efficient power electronics interfaces utilize in MG applications result in reliable operation for MGs. LLC resonant converter is one of the most popular power electronics converters due to proposing various attractive advantages to researchers. Accurate design of LLC resonant converter leads to achieving a high efficiency and high-power density converter. In this chapter, a resonant half-bridge converter is studied for various operation modes. Different optimization methods are exploited for various operation modes of the converter to obtain the optimum operation for each operation mode.

5.2. CONTRIBUTIONS TO THE STATE OF ART

Various power electronics interfaces are used in the hybrid MGs to generate a proper voltage and high-quality power for the system. DC-DC and DC-AC converters are widely applied in MGs to make the generated voltage by renewable resources appropriate for consumers. LLC resonant converter is potentiated to utilize in MG application due to high efficiency and high-power density capability of topology. In a resonance converter, the power flow through a resonant tank. Consequently, the power flow can be controlled by frequency modulation. Therefore, the accurate design of the resonant tank element is essential to achieve an efficient converter. In [1], an overview of modulation strategies for LLC resonant converter is studied. The modulation strategies are categorized into three groups in this study: input voltage fundamental harmonic modulation, resonant tank elements modulation, and secondary equivalent impedance modulation. The pros and cons of each modulation strategy are summarized to compare the topology complexity, control complexity, and voltage gain range.

One of the exquisite features of the LLC resonant converter is magnetic integrity. The parasitic inductances of the magnetic transformer can effectively use as inductance

elements of the resonance tank. In [2], a front-end LLC resonant converter for distributed power system is investigated. Several integrated magnetic design is proposed in this study to achieve: reducing the number of components and reducing core loss by achieving the flux ripple cancellation. An LLC resonant converter with matrix transformer is introduced in [3]. A matrix transformer can reduce leakage inductance and the ac resistance of windings; therefore, the flux cancellation method can be utilized to reduce core size and loss.

In [4], a study is conducted to obtain a wide-range voltage source LLC resonant converter. Large resonant inductance increases output voltage adjustment range and conversion efficiency, especially at light loads. Soft switching is also analyzed for all operating conditions considering the effect of dead time and maximum switching frequency. Theoretical analysis and optimal design of LLC resonant converter are raised in [5]. DC characteristics and input-output response in the frequency domain are studied, and the equivalent circuit is derived by the first harmonic approximation (FHA) method. ZVS turn-on and ZCS turn-off of semiconductor devices for the whole operating range are also investigated.

In this chapter, the operation of the LLC resonant half-bridge converter is evaluated, and different operation modes of the resonant converter are introduced. It is observed that load variation and switching frequency create multiple operating modes for the converter. Therefore, different operating modes affect the converter's operating condition and efficiency. Consequently, to achieve a high-efficiency LLC resonant converter, different optimization methods are applied to evaluate the performance of the converter.

5.3. REFERENCES

- [1]. Wei, Yuqi, Quanming Luo, and Alan Mantooth. "Overview of modulation strategies for LLC resonant converter." *IEEE Transactions on Power Electronics* 35, no. 10 (2020): 10423-10443.
- [2]. Yang, Bo, Rengang Chen, and Fred C. Lee. "Integrated magnetic for LLC resonant converter." In *APEC. Seventeenth Annual IEEE Applied Power Electronics Conference and Exposition (Cat. No. 02CH37335)*, vol. 1, pp. 346-351. IEEE, 2002.
- [3]. Huang, Daocheng, Shu Ji, and Fred C. Lee. "LLC resonant converter with matrix transformer." *IEEE Transactions on Power Electronics* 29, no. 8 (2013): 4339-4347.

- [4]. Beiranvand, Reza, Bizhan Rashidian, Mohammad Reza Zolghadri, and Seyed Mohammad Hossein Alavi. "Using LLC resonant converter for designing wide-range voltage source." *IEEE Transactions on Industrial Electronics* 58, no. 5 (2010): 1746-1756.
- [5]. Jung, Jee-hoon, and Joong-gi Kwon. "Theoretical analysis and optimal design of LLC resonant converter." In *2007 European Conference on Power Electronics and Applications*, pp. 1-10. IEEE, 2007.

5.4. JOURNAL PAPER



Article

A Comparative Study of Different Optimization Methods for Resonance Half-Bridge Converter

Navid Salehi *, Herminio Martinez-Garcia and Guillermo Velasco-Quesada

Electronic Engineering Department, Universitat Politècnica de Catalunya (UPC)–BarcelonaTech, Escola d'Enginyeria de Barcelona Est (EEBE), E-08019 Barcelona, Spain; herminio.martinez@upc.edu (H.M.-G.); guillermo.velasco@upc.edu (G.V.-Q.)

* Correspondence: navid.salehi@upc.edu; Tel.: +34-698844553

Received: 31 October 2018; Accepted: 23 November 2018; Published: 2 December 2018



Abstract: The LLC resonance half-bridge converter is one of the most popular DC-DC converters and could easily inspire researchers to design a high-efficiency and high-power-density converter. LLC resonance converters have diverse operation modes based on switching frequency and load that cause designing and optimizing procedure to vary in different modes. In this paper, different operation modes of the LLC half-bridge converter that investigate different optimization procedures are introduced. The results of applying some usual optimization methods implies that for each operation mode some specific methods are more appropriate to achieve high efficiency. To verify the results of each optimization, numerous simulations are done by Pspice and MATLAB and the efficiencies are calculated to compare them. Finally, to verify the result of optimization, the experimental results of a laboratory prototype are provided.

Keywords: resonant converter; half-bridge converter; optimization; Lagrangian method; LSQ; Monte Carlo optimization

1. Introduction

The LLC resonant half-bridge converter is used widely in different industries and applications due to some important features such as high-power density, high efficiency, and cost effectiveness [1,2]. Zero voltage switching (ZVS) at turn-on and low turn-off current of MOSFETs in this converter makes the switching loss negligible, so switching frequency can be increased to produce a lightweight power supply for portable appliances [3].

One of the most popular methods for designing LLC resonant half-bridge converters is the first harmonic approximation (FHA) [4,5]. Though the FHA design procedure only considers the fundamental frequency harmonic and is not an accurate method to design an LLC resonant converter, the result in resonant frequency and above resonant frequency is acceptable [6]. Generally, the results of the FHA technique are considered as initial values for other optimization methods that need a starting point.

By increasing the popularity of LLC resonant converters in recent years, high-efficiency and optimum design have become more interesting for researchers. Different mathematical optimizations are applied to solve constrained or unconstrained non-linear programs with the aid of a computer. Most papers concentrate on optimizing a specific component. A study to optimize the performance of planar transformers by means of finite element analysis (FEA) is carried out in [7]. In [8] a framework for power system optimization with consideration of reliability and thermal and packaging limitation is proposed. There are other papers focusing on optimizing different aspects of converters, such as heat-sink design procedure [9], gate-drive circuitry [10] and the lowest possible inductance [11]. Generally, one of the common problems that apply to optimization procedures in the aforementioned

papers is that of time-consumption, because these approaches are based on an iterative procedure involving the trial of a wide range of parameters.

A comprehensive study to achieve high conversion efficiency for LLC series resonant converters with the development of numerical computational techniques by using non-linear programming to solve the steady-state equations of converter is done in [12]. In the aforementioned paper, a mode solver by using numerical procedure is proposed to predict LLC resonant behavior at different modes. However, there are some other methods that have different approaches to find the optimum results; optimal design based on peak gain placement is presented in [13]. This method maximizes efficiency while satisfying the gain requirement for the specified input voltage range, and by following this approach the converter can minimize the conduction loss.

All applied proposed procedures to optimize the resonant converter efficiency involve different operation modes; however, in discontinuous conduction mode (DCM), solving the LLC operation mode equations involves transcendental equations, which makes it difficult to induce an explicit expression of DC characteristics. Meanwhile continuous conduction mode (CCM) operation has a closed-form solution. Therefore, in this paper, different optimization procedures are applied to different operation modes to understand which method is most appropriate for different modes for achieving high efficiency. The applied optimizer procedures in this paper are Augmented LAGrangian (ALAG) penalty function technique, Least Squares Quadratic (LSQ), modified LSQ, and Monte Carlo optimization.

In this paper, after discussing different operation modes of LLC resonant converters, in Section 3 a design procedure by FHA technique is investigated to determine the initial values for other optimizers. In Section 4, the operational procedures of optimization methods are elaborated, and power-loss equations for the components of LLC resonant converters are discussed in Section 5. The simulation results are studied in Section 6 show which optimization methods lead to achieving high efficiency in LLC resonant converter. Finally, the experimental results of a real prototype are provided in Section 7 to verify the optimization methods and obtain maximum efficiency.

2. Operating Different Modes of LLC Resonant Converters

The LLC resonant half-bridge converter topology is shown in Figure 1. In this topology there are three reactive elements at the resonant tank, including two inductors and one capacitor. Consequently, there are two resonant frequencies in this converter f_{r1} and f_{r2} :

$$f_{r1} = \frac{1}{2\pi\sqrt{L_r C_r}}, \quad (1)$$

$$f_{r2} = \frac{1}{2\pi\sqrt{(L_r + L_m) C_r}}, \quad (2)$$

where L_r , L_m , and C_r are resonant inductor, magnetizing inductor, and resonant capacitor, respectively, and f_{r1} usually considers as resonant frequency (f_r). Depending on the switching frequency and load, the converter operates in different modes. Although all the operation modes cannot be practical in this converter due to MOSFET failure in capacitive mode [14], as a general classification it is possible to illustrate the diverse operation modes as shown in Figure 2, where f_{sw} is the switching frequency, and R_{crit} is a critical value that determine the input impedance of resonant tank ($Z_{in}(j\omega)$) is inductive ($R_L > R_{crit}$) or capacitive ($R_L < R_{crit}$), R_{crit} can be stated as $R_{crit} = \sqrt{Z_{o1} Z_{o2}}$, where Z_{o1} and Z_{o2} are resonant tank impedances with the source input short-circuited and open-circuited, respectively [15].

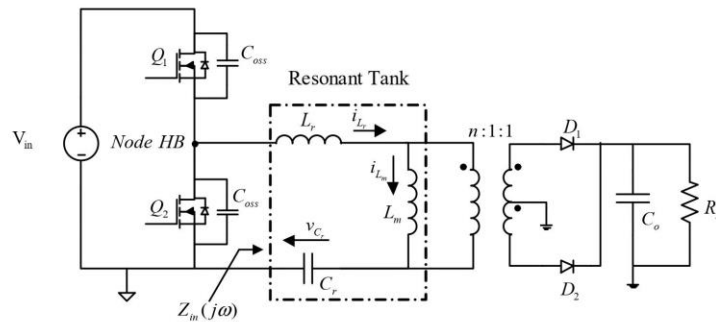


Figure 1. LLC resonant half-bridge converter.

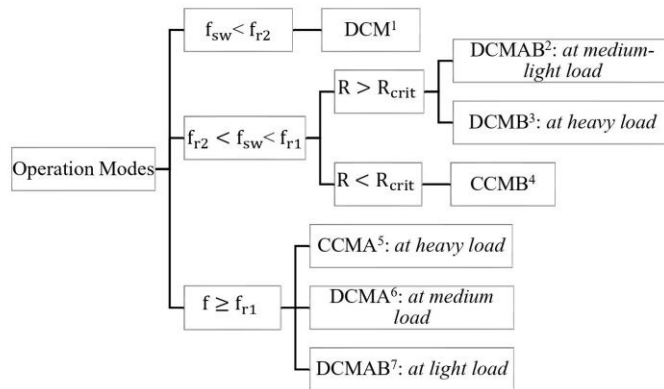


Figure 2. LLC resonant half-bridge converter.

3. LLC Resonant Half-Bridge Converter Design Procedure by FHA Technique

Figure 3 shows the equivalent circuit of an LLC resonant half-bridge converter at the half period in the continuous conduction mode above resonant frequency (CCMA) operation. This operation mode, as a popular mode in LLC resonant converters, can provide ZVS conditions for MOSFETs of the half-bridge converter; thus, the design procedure considers ZVS constraints. By considering the equivalent circuit voltage gain, the following equation can be obtained:

$$M = \frac{V_o}{V_s} = \frac{1}{(1 + \lambda - \frac{\lambda}{f_n}) + jQ_s(f_n - \frac{1}{f_n})} \tag{3}$$

where $\lambda = L_r/L_m$ is the inductance ratio, $f_n = f_{sw}/f_r$ is the normalized frequency, $Q_s = Z_s/R_{eq}$ is the quality factor, $Z_s = \sqrt{L_r/C_r}$ is the characteristic impedance, $R_{eq} = 8 n^2 V_o^2 / \pi^2 P_o$ is the effective resistive load that is transferred to the primary side of transformer, where n is the turn ratio of transformer, V_o is the output voltage, and P_o is output power. Although V_s is a square wave, in this calculation only the first harmonic of its Fourier is considered.

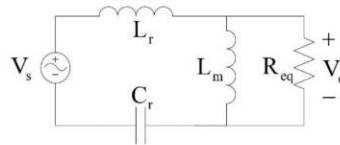


Figure 3. Equivalent circuit of LLC resonant converter.

Table 1 shows the procedure of the LLC resonant half-bridge converter design. Step 1 determines the turn ratio of the transformer by considering the nominal input voltage. Minimum and maximum voltage gain can be calculated by using Equation (3) in step 2. Steps 3 and 4 calculate the maximum normalized frequency and effective load resistance transfer to the primary side of the transformer, respectively. Also, by considering Equation (3), inductance ratio can be obtained; step 5 shows this value.

Table 1. Procedure of LLC resonant half-bridge converter design [14].

| Steps | Comments | Equations |
|---------|---|---|
| Step 1 | Calculating transformer turn ratio | $n = \frac{1}{2} \frac{V_{dc, min}}{V_{out}}$ |
| Step 2 | Calculating max. & min. voltage gain | $M_{max} = 2n \frac{V_{out}}{V_{dc, min}}, M_{min} = 2n \frac{V_{out}}{V_{dc, max}}$ |
| Step 3 | Calculating max. normalize frequency | $f_{n, max} = \frac{f_{max}}{f_r}$ |
| Step 4 | Calculating effective load resistance transfer to the primary side of transformer | $R_{eq} = \frac{8}{\pi^2} n^2 \frac{V_o^2}{P_o}$ |
| Step 5 | Calculating inductance ratio | $\lambda = \frac{1 - M_{min}}{M_{min}} \frac{f_{n, max}^2 - 1}{f_{n, max}^2}$ |
| Step 6 | Calculating the max Q to work at ZVS region at min. input voltage and full-load condition | $Q_{max} = \frac{\lambda}{M_{max}} \sqrt{\frac{1}{\lambda} + \frac{M_{max}^2}{1}}$ $Q_{ZVS,1} = 0.95 \times Q_{max}$ |
| Step 7 | Calculating the max. Q to work at ZVS region at no load condition and max. input voltage | $Q_{ZVS,2} = \frac{2}{\pi} \frac{\lambda f_{n, max}}{(\lambda + 1) f_{n, max} - \lambda} \frac{T_D}{R_{eq} C_{ZVS}}$ |
| Step 8 | Selecting max. Q for ZVS in the whole operation range | $Q_{ZVS} \leq \min\{Q_{ZVS,1}, Q_{ZVS,2}\}$ |
| Step 9 | Calculating the min. operation frequency at full load and min. input voltage | $f_{min} = f_r \sqrt{\frac{1}{1 + \frac{1}{\lambda} (1 - \frac{1}{M_{max}^2 (1 + (Q_{ZVS}^4)^{\frac{1}{\lambda}})})}}$ |
| Step 10 | Calculating the value of resonant tank's component | $Z_o = Q_{ZVS} R_{eq}, C_r = \frac{1}{2\pi f_r Z_o}, L_r = \frac{Z_o}{2\pi f_r}, L_m = \frac{L_r}{\lambda}$ |

Steps 6, 7, and 8 guarantee the ZVS constraints of primary MOSFETs at whole range load variations, where $C_{ZVS} = 2C_{OSS} + C_{stray}$ (C_{OSS} and C_{stray} are, respectively, the effective drain-source capacitance of the power MOSFETs and the total stray capacitance present across the resonant tank impedance at node HB). The converter could work properly at $V_{dc, min}$ and minimum frequency, and at $V_{dc, max}$ and maximum frequency. To find a minimum operating frequency in the ZVS operation mode, the converter should be analyzed in full-load and minimum input voltage conditions. Step 9 represents an approximate equation to find a minimum frequency [14]. Finally, in step 10, reactive elements of the resonant tank are calculated.

4. Introducing Optimization Methods

To achieve a high-efficiency converter, it is essential to consider a proper optimizer to determine the best values for different components of the converter. Generally, to achieve a high-efficiency converter, an optimization process tries to reduce the losses. Since the LLC resonant converter has non-linear behavior mostly in different modes, closed-form solutions are impossible to apply for solving equations. In this work, four usual optimization methods that can deal with non-linear equations are presented. The main aim of this paper is to determine proper optimization for each operation mode of the LLC resonant converter.

4.1. The Lagrangian Method

The Lagrangian method is one the most common mathematical solutions to find the extreme values of a function [16–18]. However, in our problem, of optimizing the efficiency by reducing the losses, the Lagrangian method tries to find a minimum feasible value by solving the optimization problem with linear and non-linear constraints. A complete optimization problem solved by the Lagrangian method can be defined as:

$$\begin{aligned} \min f(x_1, x_2, \dots, x_n) &= \min f(x), & (4) \\ \text{subject to} & \begin{cases} g_i(x_1, x_2, \dots, x_n) = 0 & i = 1, 2, \dots, k \\ h_j(x_1, x_2, \dots, x_n) \leq 0 & j = 1, 2, \dots, m \\ A_{eq}(x_1, x_2, \dots, x_n) = b_{eq} \\ A(x_1, x_2, \dots, x_n) \leq b \\ lb \leq x_n \leq ub \end{cases} \end{aligned}$$

To solve this optimization problem by the Lagrangian method, the Lagrangian is defined as:

$$L(x, \lambda_i, \mu_j) = f(x) + \sum_{i=1}^k \lambda_i g_i + \sum_{j=1}^m \mu_j h_j, \quad (5)$$

Finally, the optimization problem can be defined as:

$$\min L(x, \lambda_i, \mu_j), \quad (6)$$

In general, the Lagrangian is the sum of the original objective function and a term that involves the functional constraint and Lagrange multipliers such as λ_i and μ_j . In Equation (4), g_i is equality constraints, h_i is non-linear inequality constraints, m is the total number of non-linear constraints, k is the number of non-linear equality constraints, A_{eq} and b_{eq} are linear equalities, A and b are linear inequalities, lb is the lower boundary and ub is the upper boundary of variable x . In addition, $f(x_1, x_2, \dots, x_n)$ is the sum of loss equations of all components in the LLC resonant converter. Therefore, finding the accurate loss model for each component is very important in the final result of the optimization.

4.2. Least Squares Quadratic (LSQ) Optimization

The LSQ problem is based on iteratively calculating to meet some specific goals by adjusting different parameters [19]. The LSQ problem tries to minimize the total error:

$$\min E = \sqrt{\sum_{i=1}^n e_i}, \quad (7)$$

where E is the total error and e_i is the error of each parameter determined in the goal function. Therefore, in the LSQ method, the measurement goal is regularly compared with the goal to minimize the difference between these two values. Initial values play an important role in the LSQ optimizer. If the initial value will be close to a local minimum, it may not be an optimal solution. To find the global minimum solution, it may require extending the search space of starting points.

4.3. Modified LSQ Optimization

Modified LSQ is generally similar to the LSQ optimization [20]. However, it runs faster than LSQ for the sake of reducing the number of incremental adjustments into the goal. This optimizer can consider both constrained and unconstrained minimization problems. To implement the optimization procedure, two general algorithms are supposed to apply: least squares and minimization. Modified LSQ uses least squares algorithm when optimizing for more than one goal, then tries to reduce the

sum of the squares to zero. By increasing goals, it will be more complicated for the optimizer to reduce the sum of the squares to zero.

4.4. Monte Carlo Optimization

Monte Carlo optimization is one of the stochastic optimization methods that generates and uses random variables [21,22]. This optimization method relies on iteration as well as LSQ and modified LSQ. However, by using random values in the Monte Carlo method to solve the problem, the probability of getting stuck in an unacceptable local minimum is reduced. In this method, the initial values for the variables are not essential, but a domain of possible inputs need to be defined. Thus, a sample of a probability distribution for each variable produces numerous possible outputs. Generally, the Monte Carlo method follows the following steps:

1. Determine the statistical properties of possible inputs;
2. Generate many sets of possible inputs which follows the above properties;
3. Perform a deterministic calculation with these sets; and
4. Analyze statistically the results.

5. Power-Loss Calculation

Table 2 shows power-loss equations of each component using an LLC resonant converter. Since the switches usually turn on under ZVS condition, switching losses at turn-on can be neglected. In [12,23] the power-loss equations are elaborated specifically. The voltage and current of LLC resonant converters in different operation modes are presented in [12]; these voltage and currents are essential for loss calculation.

Table 2. Power-loss equations of LLC resonant half-bridge converter [12,23].

| Components | Loss Characteristic | Power-Loss Equations | |
|----------------------------|---|---|--|
| Half-Bridge MOSFETs | Conductive Loss | $P_{con} = R_{ds} \cdot I_{sw(rms)}^2$ | |
| | Switching Loss | At turn-on | 0 |
| | | At turn-off | $P_{sw_OFF} = \frac{(I_{th} \cdot T_f)^2}{12 \cdot C_{HB}} \cdot f_{sw}$ |
| | Driving Gate Loss | At turn-on | $P_{g_ON} = \frac{1}{2} \cdot \frac{V_{GS}^3}{V_{GS} - V_M} [Q_g - (Q_{gs} + Q_{gd})] \cdot f_{sw}$ |
| At turn-off | | $P_{g_OFF} = \frac{1}{2(V_{GS} - V_M)} [(V_{GS}^2 + V_M^2)(Q_g - Q_{gd}) - V_{GS}(V_{GS} + V_M)Q_{gs}] \cdot f_{sw}$ | |
| Transformer | Copper Loss | $P_{cu_Trans} = R_{AC} \cdot I_{RMS}^2$ | |
| | Core Loss | $P_{core} = V_e \cdot k \cdot f_s^{\alpha_{core}} \cdot \Delta B_m^{\beta_{core}}$ | |
| Secondary rectifier diodes | Conductive Loss of V_f | $P_{Vf} = V_f \cdot I_{dc,sec}$ | |
| | Conductive Loss of r_f | $P_{rf} = r_f \cdot I_{dc,sec}^2$ | |
| Capacitors Loss | Input capacitance Output capacitance Resonant capacitance | $P_c = R_{ESR} \cdot I_{RMS}^2$ | |

To calculate the conductive loss of switches, R_{ds} represents the drain-source on-state resistance, and $I_{sw(rms)}$ is the RMS value of switch current. Also, I_{R0} is the current of resonant tank at half period, which can be stated as:

$$I_{R0} = i_{Lr} \left(\frac{T_{sw}}{2} \right), \tag{8}$$

Moreover, CHB is considered to be a capacitor at node HB that involves the sum of C_{OSS} of MOSFETs and stray capacitance. T_f is the time that the current of each switch takes to become zero. To calculate the driving gate losses, Q_g , Q_{gs} , and Q_{gd} indicate total gate charge, gate-source charge, and gate-drain charge of the switch, respectively. Also, V_{GS} is the voltage level of the driving signal, and V_M is a plateau voltage value that lets MOSFET carry the specified current.

Furthermore, to compute the copper loss of transformer, AC resistance of wire (R_{AC}) and the RMS values of the primary and secondary side of the transformer (I_{RMS}) are necessary. The volume of transformer core (V_e), transformer flux density (B_m), and k , α_{core} , β_{core} that are Steinmetz coefficients, are essential for core loss calculation as well. Rectifier diodes losses comprise conduction losses

associated with forward voltage (V_f) and dynamic resistance (r_f). Finally, capacitor loss is calculated by considering the equivalent series resistance (R_{ESR}) and the RMS value of each capacitor current.

6. Simulation Results

The introduced optimization methods apply to different operation modes of the LLC resonant converter to obtaining a high-efficiency converter. In this paper, to perform the optimization procedures, different optimization engines in Pspice and solvers in MATLAB are employed. The solvers such as “fsolve” to solve the non-linear equation problem, and “fmincon” to find the minimum constrained non-linear multivariable function are used as the Lagrangian optimization method. In addition, the LSQ, modified LSQ and Monte Carlo optimizer engines in Pspice are used to employ an optimize LLC resonant converter.

To compare the results of different optimization methods, the same conditions such as input and output voltage, load condition, design variables, and initial values for optimizers are provided. Consequently, design variables will be computed by applying different optimization methods, and power loss of components are calculated to find out the minimum power loss.

The optimization procedures consider the switching frequency, resonant inductance, magnetizing inductance of transformer, resonant capacitance, and turn ratio of the transformer as design variables to find the optimum values. The following vector shows these design variables:

$$x = [f_{sw}, L_r, L_m, C_r, n], \quad (9)$$

Moreover, the lower and upper boundary of each variable is defined in Table 3 to obtain the possible components' values. Finally, to find the optimum values for design variables, the objective function $P_{loss}(x)$, i.e., the sum of the power-loss equation of each component, is minimized by considering the defined constraints:

$$\min P_{loss}(x), \quad (10)$$

Table 3. Load condition, constraints and switching frequency range.

| Variables | Lower Boundary | Upper Boundary | Operation Mode | Load Condition $V_{out}(V)$ & $I_{out}(A)$ | Switching Frequency |
|-----------|----------------|----------------|----------------|--|-----------------------------|
| L_r | 30 μ H | 250 μ H | DCMB | $V_{out} = 18, I_{out} = 8.44$ | 69 kHz < f_{sw} < 410 kHz |
| L_m | 30 μ H | 800 μ H | DCMAB | $V_{out} = 60, I_{out} = 2.53$ | 69 kHz < f_{sw} < 410 kHz |
| C_r | 5 nF | 100 nF | CCMA | $V_{out} = 20, I_{out} = 7.6$ | 31 kHz < f_{sw} < 410 kHz |
| n | 1 turn | 25 turns | DCMA | $V_{out} = 40, I_{out} = 3.8$ | 31 kHz < f_{sw} < 410 kHz |

To solve the problem with the Lagrangian method, the “fmincon(x)” solver of the MATLAB optimization toolbox is employed. The “fmincon(x)” tries to find a constrained minimum of a function of several variables at an initial estimate. The starting points are very important for the solver to converge the problem, and to find the feasible points.

The optimization procedure is shown in Figure 4. Based on the input/output specifications, the start points are calculated by the step-by-step design procedure in Table 1. Then, variables with lower and upper boundaries are determined. After applying the constraints to the solver, the optimization procedure starts. Therefore, efficiency can be calculated easily by knowing the output power of the converter and power losses by [(output power)/(output power + power losses)].

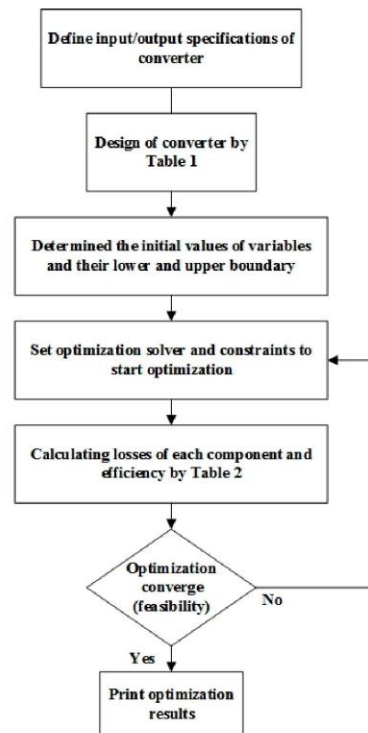


Figure 4. Optimization procedure of LLC resonant half-bridge converter.

Table 3 shows the load conditions and constraints of variables and the switching frequency range for four different operation modes. In addition, Table 4 shows the list of the components with their manufacturer information to calculate their losses.

Table 4. List of components.

| Components | Model | Description |
|--------------------|--------------------|---|
| MOSFET | IRFP460 | $V_{DS} = 500V$, $I_D = 20A$ |
| Transformer | EE3314 PC40 | Primary: 30×0.1 mm |
| Resonant inductor | EE28/11 PC40 | Secondary: 60×0.1 mm 30×0.1 mm |
| Rectifier diode | BYV42E | Dual center tap ultrafast rectifier $V_{RRM} = 100V$ |
| Resonant Capacitor | 10 – 45 nF, 1000 V | $I_{F(AV)} = 2 \times 15A$ |
| Output capacitor | 4.7 μF | MKP film cap MKT film cap |

Tables 5–8 show the power loss of each component, and the efficiency is calculated regarding optimum values of variables obtained by the different optimization procedures.

Table 5. Losses Profile of LLC resonant converter by Lagrangian optimization method.

| Optimum Values: $x=[f_{sw}(kHz), L_r(\mu H), L_m(\mu H), C_r(nF), n]$ | | $[f_{sw}, L_r, L_m, C_r, n]$ [80, 150, 420, 22, 9] | $[f_{sw}, L_r, L_m, C_r, n]$ [90, 140, 380, 18, 2.2] | $[f_{sw}, L_r, L_m, C_r, n]$ [115, 130, 330, 15, 7.5] | $[f_{sw}, L_r, L_m, C_r, n]$ [145, 95, 480, 15, 4] |
|--|--------------------------|---|---|--|---|
| Mode | | DCMB | DCMAB | CCMA | DCMA |
| Components | Power Losses | (W) | (W) | (W) | (W) |
| Transformer | core | 1.186 | 1.186 | 1.186 | 1.186 |
| | copper | 0.257 | 0.202 | 0.142 | 0.222 |
| Resonant inductor | core | 0.481 | 0.481 | 0.481 | 0.481 |
| | copper | 0.212 | 0.111 | 0.091 | 0.119 |
| MOSFETs | Conduction | 0.901 | 0.775 | 0.325 | 0.712 |
| | Gate driving | 0.019 | 0.019 | 0.019 | 0.019 |
| | Switching | 0.081 | 0.078 | 0.028 | 0.029 |
| Rectifier diodes | Conductive loss of V_F | 2.603 | 1.967 | 1.568 | 1.771 |
| | Conductive loss of r_F | 0.974 | 0.804 | 0.394 | 0.741 |
| Capacitors | Resonant capacitor | 0.161 | 0.098 | 0.078 | 0.092 |
| | Output capacitor | 0.188 | 0.181 | 0.171 | 0.177 |
| Total losses | | 7.063 | 5.902 | 4.483 | 5.549 |
| Efficiency | | 95.55% | 96.26% | 97.07% | 96.47% |

Table 6. Losses Profile of LLC resonant converter by LSQ optimization method.

| Optimum Values: $x=[f_{sw}(kHz), L_r(\mu H), L_m(\mu H), C_r(nF), n]$ | | $[f_{sw}, L_r, L_m, C_r, n]$ [67, 166, 470, 25, 8.5] | $[f_{sw}, L_r, L_m, C_r, n]$ [86, 140, 380, 18, 2.5] | $[f_{sw}, L_r, L_m, C_r, n]$ [150, 115, 380, 10, 8] | $[f_{sw}, L_r, L_m, C_r, n]$ [140, 100, 350, 19, 5.5] |
|--|--------------------------|---|---|--|--|
| Mode | | DCMB | DCMAB | CCMA | DCMA |
| Components | Power Losses | (W) | (W) | (W) | (W) |
| Transformer | core | 2.328 | 1.996 | 1.222 | 1.387 |
| | copper | 1.692 | 0.952 | 0.119 | 0.228 |
| Resonant inductor | core | 1.643 | 1.911 | 0.496 | 0.499 |
| | copper | 0.792 | 0.500 | 0.091 | 0.189 |
| MOSFETs | Conduction | 1.331 | 0.909 | 0.423 | 0.924 |
| | Gate driving | 0.019 | 0.019 | 0.019 | 0.019 |
| | Switching | 0.361 | 0.260 | 0.081 | 0.101 |
| Rectifier diodes | Conductive loss of V_F | 2.192 | 2.249 | 1.393 | 1.598 |
| | Conductive loss of r_F | 1.674 | 1.423 | 0.592 | 0.795 |
| Capacitors | Resonant capacitor | 0.366 | 0.279 | 0.192 | 0.310 |
| | Output capacitor | 0.261 | 0.181 | 0.110 | 0.293 |
| Total losses | | 12.659 | 10.679 | 4.738 | 6.343 |
| Efficiency | | 92.31% | 93.43% | 96.97% | 95.99% |

Table 7. Losses Profile of LLC resonant converter by modified LSQ optimization method.

| Optimum Values: $x=[f_{sw}(kHz), L_r(\mu H), L_m(\mu H), C_r(nF), n]$ | | $[f_{sw}, L_r, L_m, C_r, n]$ [70, 177, 455, 22, 9.5] | $[f_{sw}, L_r, L_m, C_r, n]$ [90, 155, 360, 15, 2.6] | $[f_{sw}, L_r, L_m, C_r, n]$ [135, 110, 370, 13, 8.8] | $[f_{sw}, L_r, L_m, C_r, n]$ [130, 120, 360, 15, 5.2] |
|--|--------------------------|---|---|--|--|
| Mode | | DCMB | DCMAB | CCMA | DCMA |
| Components | Power Losses | (W) | (W) | (W) | (W) |
| Transformer | core | 2.088 | 1.994 | 1.310 | 1.224 |
| | copper | 1.698 | 0.993 | 0.121 | 0.278 |
| Resonant inductor | core | 1.697 | 0.998 | 0.424 | 0.437 |
| | copper | 1.239 | 0.797 | 0.298 | 0.211 |
| MOSFETs | Conduction | 1.179 | 0.990 | 0.411 | 0.632 |
| | Gate driving | 0.019 | 0.019 | 0.019 | 0.019 |
| | Switching | 0.372 | 0.299 | 0.072 | 0.195 |
| Rectifier diodes | Conductive loss of V_F | 2.810 | 2.657 | 1.287 | 1.398 |
| | Conductive loss of r_F | 1.762 | 1.480 | 0.614 | 0.889 |
| Capacitors | Resonant capacitor | 0.398 | 0.298 | 0.162 | 0.292 |
| | Output capacitor | 0.297 | 0.254 | 0.103 | 0.203 |
| Total losses | | 13.559 | 10.779 | 4.821 | 5.778 |
| Efficiency | | 91.76% | 93.37% | 96.92% | 96.33% |

Table 8. Losses Profile of LLC resonant converter by Monte Carlo optimization method.

| Optimum Values: $x=[f_{sw}(kHz), L_r(\mu H), L_m(\mu H), C_r(nF), n]$ | | $[f_{sw}, L_r, L_m, C_r, n]$ [75, 155, 420, 22, 9] | $[f_{sw}, L_r, L_m, C_r, n]$ [85, 145, 380, 18, 2.8] | $[f_{sw}, L_r, L_m, C_r, n]$ [120, 130, 330, 15, 8.5] | $[f_{sw}, L_r, L_m, C_r, n]$ [135, 85, 390, 18, 4] |
|--|--------------------------|---|---|--|---|
| Mode | | DCMB | DCMAB | CCMA | DCMA |
| Components | Power Losses | (W) | (W) | (W) | (W) |
| Transformer | core | 1.691 | 1.212 | 1.090 | 1.328 |
| | copper | 0.397 | 0.183 | 0.122 | 0.298 |
| Resonant inductor | core | 0.599 | 0.410 | 0.599 | 0.582 |
| | copper | 0.329 | 0.143 | 0.102 | 0.169 |
| MOSFETs | Conduction | 0.892 | 0.693 | 0.391 | 0.690 |
| | Gate driving | 0.019 | 0.019 | 0.019 | 0.019 |
| | Switching | 0.096 | 0.067 | 0.027 | 0.030 |
| Rectifier diodes | Conductive loss of V_F | 2.174 | 1.779 | 1.633 | 1.907 |
| | Conductive loss of r_F | 0.899 | 0.785 | 0.654 | 1.008 |
| Capacitors | Resonant capacitor | 0.178 | 0.100 | 0.085 | 0.109 |
| | Output capacitor | 0.208 | 0.191 | 0.191 | 0.218 |
| Total losses | | 7.482 | 5.582 | 4.913 | 6.358 |
| Efficiency | | 95.30% | 96.45% | 96.86% | 95.98% |

The efficiency is calculated by the following:

$$\eta = \frac{P_{out}}{P_{out} + P_{loss}}, \tag{11}$$

As can be observed from simulation calculations in Tables 5–8, optimization by the Lagrangian method led to more possible efficiency in all different operation modes. However, this method is very time-consuming due to do many mathematical calculations in comparison with other optimizers. Moreover, the results of the LSQ and modified LSQ are quite similar, though for switching frequencies below the resonant frequency the LSQ optimizer is slightly more efficient than modified LSQ. On the other hand, by comparing the optimum results of Monte Carlo and LSQ, it can be seen that for the operating frequency below resonant frequency the optimum values of variables result in obtaining more efficiency by Monte Carlo optimization procedure, although for upper frequencies, from resonant frequency, the results of LSQ are more valuable.

To compare the efficiencies for different load ranges, Figures 5–8 are provided for each operation mode based on the optimum values which are calculated by different optimizers. The figures show that although efficiency decreased by reducing the load, the LLC resonant converter is suitable for high-efficiency power supply in a wide load range.

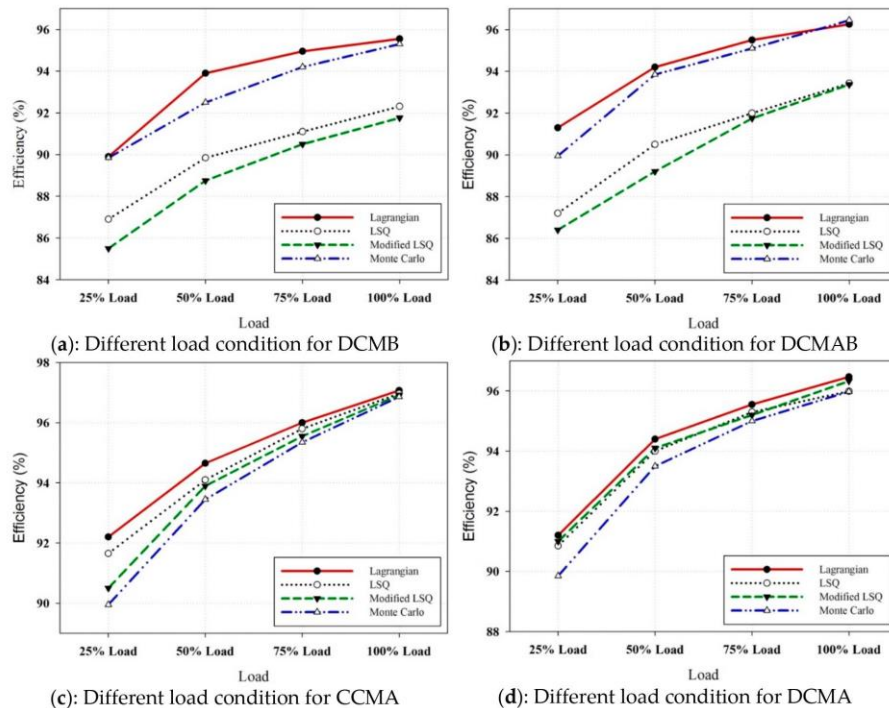


Figure 5. The efficiency at different load conditions.

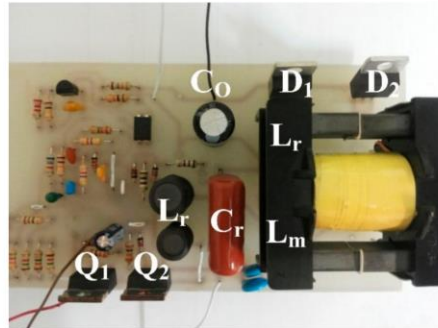


Figure 6. Photo of the implemented prototype.

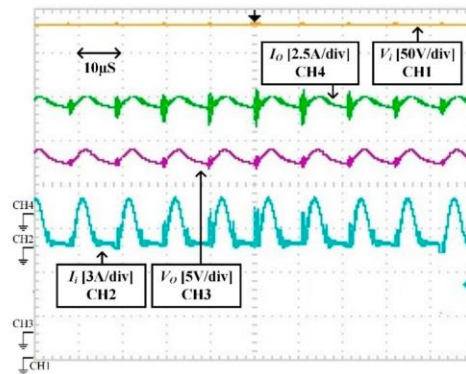


Figure 7. Input and output voltage and current of LLC resonant converter in CCMA.

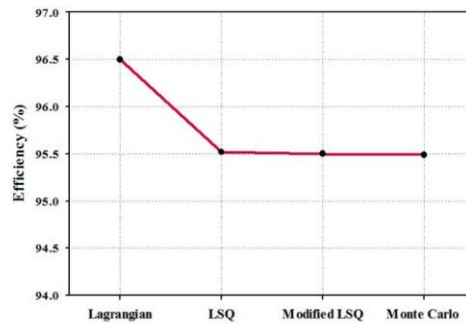


Figure 8. Measured optimized efficiency of the implemented prototype.

7. Experimental Results

A laboratory prototype of the LLC resonant converter is implemented to calculate the efficiency in different operation modes by the optimum values which are obtained by applying different optimizers. Figure 6 shows the implemented prototype and Figure 7 demonstrates the input and output voltage and current for CCMA operation mode. The efficiency for each operation mode is calculated by [average (output voltage × output current)] / [input voltage × average (input current)].

Figure 8 demonstrates the maximum measured efficiency which is possible based on the optimization results; therefore, for all optimization procedures the converter is designed for CCMA. The slight difference between practical result and simulation result refers to unconsidered power loss in the simulation such as printed circuit board (PCB) loss.

8. Conclusions

This paper presents different optimization methods to obtain a highly efficient LLC resonant half-bridge converter. Due to the operating frequency of converter and load condition, the LLC resonant converter can operate in different modes. In this paper, four common optimization methods are applied to the LLC resonant converter in different modes to determine the optimum values for resonant tank components and switching frequency. The results verified that the Lagrangian method is appropriate for all operation modes in LLC resonant converters, although more complicated mathematical calculation is required. However, the results for LSQ and modified LSQ are validated for operating frequency higher than resonant frequency; for below resonant frequency, Monte Carlo led to a more-efficient converter.

Author Contributions: Conceptualization, N.S.; methodology, N.S.; software, N.S.; validation, N.S., H.M.G. and G.V.Q.; investigation, N.S.; data curation, N.S.; writing—original draft preparation, N.S.; writing—review and editing, N.S., H.M.G. and G.V.Q.; supervision, H.M.G. and G.V.Q.

Funding: This research received no external funding.

Conflicts of Interest: The authors declare no conflict of interest.

Abbreviations

| | |
|-------|------------------------------|
| DCM | Discontinues Conduction Mode |
| DCMAB | DCM Above-Below Resonant |
| DCMB | DCM Below Resonant |
| CCMB | CCM Below Resonant |
| CCMA | CCM Above Resonant |
| DCMA | DCM Above Resonant |

References

1. Senthamil, L.S.; Ponvasanth, P.; Rajasekaran, V. Design and implementation of LLC resonant half bridge converter. In Proceedings of the 2012 International Conference on Advances in Engineering, Science and Management (ICAESM), Nagapattinam, India, 30–31 March 2012; pp. 84–87.
2. Park, H.P.; Choi, H.J.; Jung, J.H. Design and implementation of high switching frequency LLC resonant converter for high power density. In Proceedings of the 2015 9th International Conference on Power Electronics and ECCE Asia (ICPE-ECCE Asia), Seoul, Korea, 1–5 June 2015; pp. 502–507.
3. Guan, Y.; Wang, Y.; Xu, D.; Wang, W. A half-bridge resonant DC/DC converter with satisfactory soft-switching characteristics. *Int. J. Circuit Theory Appl.* **2017**, *45*, 120–132. [[CrossRef](#)]
4. Duerbaum, T. First harmonic approximation including design constraints. In Proceedings of the INTELEC—Telecommunications Energy Conference, San Francisco, CA, USA, 4–8 October 1998; pp. 321–328.
5. Lee, B.H.; Kim, M.Y.; Kim, C.E.; Park, K.B.; Moon, G.W. Analysis of LLC resonant converter considering effects of parasitic components. In Proceedings of the 31st International Telecommunications Energy Conference (INTELEC), Incheon, Korea, 18–22 October 2009; pp. 1–6.
6. Steigerwald, R.L. A comparison of half-bridge resonant converter topologies. *IEEE Trans. Power Electron.* **1988**, *3*, 174–182. [[CrossRef](#)]
7. Prieto, R.; Garcia, O.; Asensi, R.; Cobos, J.A.; Uceda, J. Optimizing the performance of planar transformers. In Proceedings of the Eleventh Annual Applied Power Electronics Conference and Exposition (APEC'96), San Jose, CA, USA, 3–7 March 1996; Volume 1, pp. 415–421.

8. Trivedi, M.; Shenai, K. Framework for power package design and optimization. In Proceedings of the IEEE International Workshop on Integrated Power Packaging, IWIPP, Chicago, IL, USA, 17–19 September 1998; pp. 35–38.
9. Gordon, M.H.; Stewart, M.B.; King, B.; Balda, J.C.; Olejniczak, K.J. Numerical optimization of a heat sink used for electric motor drives. In Proceedings of the Conference Record of the IAS'95 Industry Applications Conference, Thirtieth IAS Annual Meeting, 1995 IEEE, Orlando, FL, USA, 8–12 October 1995; Volume 2, pp. 967–970.
10. Kragh, H.; Blaabjerg, F.; Pedersen, J.K. An advanced tool for optimised design of power electronic circuits. In Proceedings of the Industry Applications Conference, Thirty-Third IAS Annual Meeting, St. Louis, MO, USA, 12–15 October 1998; Volume 2, pp. 991–998.
11. Piette, N.; Clavel, E.; Marechal, Y. Optimization of cabling in power electronics structure using inductance criterion. In Proceedings of the Industry Applications Conference, Thirty-Third IAS Annual Meeting, St. Louis, MO, USA, 12–15 October 1998; Volume 2, pp. 925–928.
12. Yu, R.; Ho, G.K.Y.; Pong, B.M.H.; Ling, B.W.K.; Lam, J. Computer-aided design and optimization of high-efficiency LLC series resonant converter. *IEEE Trans. Power Electron.* **2012**, *27*, 3243–3256. [[CrossRef](#)]
13. Fang, X.; Hu, H.; Shen, Z.J.; Batarseh, I. Operation mode analysis and peak gain approximation of the LLC resonant converter. *IEEE Trans. Power Electron.* **2012**, *27*, 1985–1995. [[CrossRef](#)]
14. De Simone, S.; Adragna, C.; Spini, C.; Gattavari, G. Design-oriented steady-state analysis of LLC resonant converters based on FHA. In Proceedings of the International Symposium on Power Electronics, Electrical Drives, Automation and Motion, SPEEDAM 2006, Taormina, Italy, 23–26 May 2006; pp. 200–207.
15. Erickson, R.W.; Maksimovic, D. *Fundamentals of Power Electronics*; Springer Science & Business Media: Berlin, Germany, 2007.
16. Bertsekas, D.P. *Constrained Optimization and Lagrange Multiplier Methods*; Academic Press: Cambridge, MA, USA, 2014.
17. Tourkhani, F.; Viarouge, P.; Meynard, T.A.; Gagnon, R. Power converter steady-state computation using the projected Lagrangian method. In Proceedings of the 28th Annual IEEE Power Electronics Specialists Conference, PESC'97 Record, Saint Louis, MO, USA, 27 June 1997; Volume 2, pp. 1359–1363.
18. Zhao, B.; Song, Q.; Liu, W. Efficiency characterization and optimization of isolated bidirectional DC–DC converter based on dual-phase-shift control for DC distribution application. *IEEE Trans. Power Electron.* **2013**, *28*, 1711–1727. [[CrossRef](#)]
19. Marquardt, D.W. An algorithm for least-squares estimation of nonlinear parameters. *J. Soc. Ind. Appl. Math.* **1963**, *11*, 431–441. [[CrossRef](#)]
20. Nye, W.; Riley, D.C.; Sangiovanni-Vincentelli, A.; Tits, A.L. DELIGHT. SPICE: An optimization-based system for the design of integrated circuits. *IEEE Trans. Comput. Aided Des. Integr. Circuits Syst.* **1988**, *7*, 501–519. [[CrossRef](#)]
21. Dickman, B.H.; Gilman, M.J. Monte carlo optimization. *J. Optim. Theory Appl.* **1989**, *60*, 149–157. [[CrossRef](#)]
22. Yang, G.; Dubus, P.; Sadarnac, D. Analysis of the load sharing characteristics of the series-parallel connected interleaved LLC resonant converter. In Proceedings of the 2012 13th International Conference on Optimization of Electrical and Electronic Equipment (OPTIM), Brasov, Romania, 24–26 May 2012; pp. 798–805.
23. Yang, C.H.; Liang, T.J.; Chen, K.H.; Li, J.S.; Lee, J.S. Loss analysis of half-bridge LLC resonant converter. In Proceedings of the 2013 1st International Future Energy Electronics Conference (IFEEEC), Tainan, Taiwan, 3–6 November 2013; pp. 155–160.



© 2018 by the authors. Licensee MDPI, Basel, Switzerland. This article is an open access article distributed under the terms and conditions of the Creative Commons Attribution (CC BY) license (<http://creativecommons.org/licenses/by/4.0/>).

Chapter 6

Modified Cascaded Z-Source High Step-Up Boost Converter

6.1. INTRODUCTION

By emerging the concept of MG and NMG afterward, the tendency to penetrate renewable resources increased substantially. The harvest of clean energy from renewable resources made the horizon of the future energy state bright regarding existing concerns about the future energy crisis. Although, intermittent availability of renewable resources is a challenging issue in MGs to continuously provide energy for consumers. However, energy management systems could tackle this issue. On the other hand, low voltage level production of renewable resources units like PV and fuel cells express extra issues, especially for AC MGs. AC MGs, either in a grid-connected or stand-alone system, inevitably employ an inverter to produce the proper AC voltage for consumers. However, the voltage level of renewable resources is significantly lower than the minimum required input voltage of inverters. There are various methods to tackle this problem. PV panels can connect in series for high-power MGs to increase the voltage. But, in case of failure in one panel, the whole string stops generating power. Therefore, the other solution is utilizing high step-up converters to elevate the voltage. This chapter proposed a high step-up converter for solar application.

6.2. CONTRIBUTIONS TO THE STATE OF ART

Step-up converters are introduced in power electronics to elevate the DC voltage. However, step-up converters' operation is usually restricted by increasing the duty cycle to obtain a higher voltage gain. The high-stress voltage of semiconductor devices and the reverse recovery problem of diodes restrict the operation of step-up converters at duty cycles close to unity. To overcome the drawbacks mentioned earlier, various high step-up converters with different topologies are introduced by researchers. An overview of non-isolated high step-up DC-DC converters is surveyed in [1-2]. Coupled inductor step-up converters, interleaved converters, integrated step-up converters, and converters with switched capacitors/inductors cells are the four main categories of high step-up converters.

Impedance source converters-known as z-source converters- proposed an attractive feature for DC-DC, DC-AC, AC-DC, and AC-AC converters in order to decrease voltage stress of semiconductor devices with a lower duty cycle of the switch and low reverse recovery problem of output diode. These converters employ a z-source network between the input source -that can be either voltage source or current source- and the main converter and result in various operating conditions for the main converter [3]. In [4], a non-isolated high step-up DC-DC converter with high voltage gain and low duty cycle is presented. The proposed topology makes the energy of leakage inductances absorbed and transferred to the load; therefore, the efficiency of the converter improves. In [5], a soft-switched non-isolated high step-up dc-dc converter based on the quasi-impedance-source structure is proposed. This study replaces the diode of the Z-source network with an active switch. Therefore, the conduction loss reduces, and zero voltage switching condition is provided for power switches. Moreover, the output diodes are switched under zero current switching, resulting in reduced reverse recovery loss. A review of impedance source galvanically isolated DC-DC converters for distributed generation systems with renewable energy sources is presented in [6].

In this chapter, cascaded technique is merged with the Z-source network in order to take advantage of both methods. The proposed topology provides high voltage gain while the voltage stress of semiconductor devices keeps low. High input current is addressed as one of the main intrinsic drawbacks of impedance source converters. However, the input current of the proposed topology is reduced significantly; therefore, the current stress of the input diode of the Z-source network decreases as well.

6.3. REFERENCES

- [1]. Koç, Yavuz, Yaşar Birbir, and Hacı Bodur. "Non-isolated high step-up DC/DC converters– An overview." *Alexandria Engineering Journal* 61, no. 2 (2022): 1091-1132.
- [2]. Turksoy, Arzu, Ahmet Teke, and Alkan Alkaya. "A comprehensive overview of the dc-dc converter-based battery charge balancing methods in electric vehicles." *Renewable and Sustainable Energy Reviews* 133 (2020): 110274.
- [3]. Forouzesh, Mojtaba, Yam P. Siwakoti, Saman A. Gorji, Frede Blaabjerg, and Brad Lehman. "Step-up DC–DC converters: a comprehensive review of voltage-boosting techniques, topologies, and applications." *IEEE transactions on power electronics* 32, no. 12 (2017): 9143-9178.


- [4]. Torkan, Arash, and Mehrdad Ehsani. "High step-up z-source dc-dc converter with flyback and voltage multiplier." In 2017 IEEE Applied Power Electronics Conference and Exposition (APEC), pp. 330-336. IEEE, 2017.
- [5]. Poorali, Behzad, and Ehsan Adib. "Soft-switched high step-up quasi-Z-source DC–DC converter." IEEE Transactions on Industrial Electronics 67, no. 6 (2019): 4547-4555.
- [6]. Chub, Andrii, Liisa Liivik, and Dmitri Vinnikov. "Impedance-source galvanically isolated DC/DC converters: State of the art and future challenges." In 2014 55th International Scientific Conference on Power and Electrical Engineering of Riga Technical University (RTUCON), pp. 67-74. IEEE, 2014.

6.4. JOURNAL PAPER



Article

Modified Cascaded Z-Source High Step-Up Boost Converter

Navid Salehi , Herminio Martínez-García *  and Guillermo Velasco-Quesada 

Department of Electronic Engineering, Eastern Barcelona School of Engineering, EEBE, Universitat Politècnica de Catalunya (UPC)—BarcelonaTech, E-08019 Barcelona, Spain; navid.salehi@upc.edu (N.S.); guillermo.velasco@upc.edu (G.V.-Q.)

* Correspondence: herminio.martinez@upc.edu; Tel.: +34-93-413-72-90

Received: 17 October 2020; Accepted: 11 November 2020; Published: 17 November 2020



Abstract: To improve the voltage gain of step-up converters, the cascaded technique is considered as a possible solution in this paper. By considering the concept of cascading two Z-source networks in a conventional boost converter, the proposed topology takes the advantages of both impedance source and cascaded converters. By applying some modifications, the proposed converter provides high voltage gain while the voltage stress of the switch and diodes is still low. Moreover, the low input current ripple of the converter makes it absolutely appropriate for photovoltaic applications in expanding the lifetime of PV panels. After analyzing the operation principles of the proposed converter, we present the simulation and experimental results of a 100 W prototype to verify the proposed converter performance.

Keywords: high step-up converter; impedance source converter; Z-source converter; cascaded technique

1. Introduction

Given the lack of energy and the climate changes due to increasing fossil fuel consumption over the last few decades, using renewable energies could be a way to help the planet Earth survive in a future energy crisis [1]. However, in order to utilize the renewable energies, power electronics converters are inevitably essential to produce the required voltage and current for different applications. Among different types of renewable energies, solar energy is more popular as a limitless source of energy, which is spread all over the world. Although the output voltage of photovoltaic (PV) cells are relatively low, applying high step-up DC–DC converters can lead to increasing the voltage level without connecting in series numerous PV panels to enhance the operation of photovoltaic systems, especially in low-power applications [2].

Research on high step-up converters in recent years has led to the present diverse topologies that are used to resolve existing drawbacks such as high voltage stress of semiconductor devices, reverse-recovery problem of diodes, and intense spike on switches which mostly appear in conventional boost converters by increasing the duty cycle [3,4]. Consequently, the topological alteration of the conventional boost converter was proposed by researchers to extend the input-to-output voltage ratio while the circuit operation is enhanced as well. To overcome the drawbacks of boost converters with high efficiency and their simple control scheme, boost converters based on different techniques were proposed by researchers, such as a coupled inductor based boost converter, switched-capacitor based boost converter, cascaded boost converter, and interleaved boost converter [5]. All introduced converters have some weaknesses and strengths that make them restricted for specific applications. A better performance of a high step-up converter may be obtained if it could be possible to apply different techniques in a converter.

Inserting coupled inductors into the DC–DC converters is an effective method to increase the voltage gain by adjusting the turn ratio between the windings in a topology. Although by increasing the leakage inductance, the reverse-recovery problem of diodes can be reduced effectively due to inserting coupled inductors, the leakage energy induces high voltage spikes across the semiconductor switches. One approach in order to solve this problem is employing a switched-capacitor technique as an active clamp circuit in order to recycle the leakage energy [6]. To reduce the topology complexity and cost, passive clamps are also considered as a possible solution. In [7], a passive clamp was replaced with an active clamp in a flyback converter to enhance the performance of the converter by alleviating the reverse-recovery problem and lowering the circulating current into the clamp circuit. Switched-capacitor converters are able to provide high voltage ratio for high power applications; however, the high input ripple current in these converters make them inappropriate for solar PV applications [5].

The other step-up converter topologies, such as cascaded boost converters, interleaved boost converters, and three-level boost converters, can effectively take the advantages of the mentioned techniques such as coupled inductors, switched capacitors, and switched-inductors to cover the mentioned weaknesses and improve their performance. For instance, the reverse-recovery problem of cascaded boost converters can be compromised with the coupled-inductor technique, although the converter efficiency in cascaded converters will be decreased due to the two-time energy processing [8–18]. Moreover, low input current ripple of interleaved converters can effectively employ switched-capacitor configurations to improve their static voltage gain and alleviate the adverse effect of their pulsating input current [9]. In [10], a three-level boost converter was proposed by employing coupled inductors to increase the voltage gain and an active clamp to recycle the leakage inductance energy of the coupled inductors. Consequently, it can be observed how incorporating step-up techniques can appropriately influence the operation of different step-up topologies.

Impedance source converters are the other recent popular methods that are used widely in power electronic converters by inserting an impedance network between the power source and main circuit. The first impedance source converter was proposed by authors in [11] in 2003 for implementing DC–AC, AC–DC, DC–DC, and AC–AC power conversion. The impedance source converters are able to totally change the operational characteristics of the main converter [11,12]. An impedance network could provide the following features for high step-up DC–DC converters [13]: high voltage gain, low voltage stress for semiconductor devices, inherent short circuit immunity, and inherent open circuit immunity. An impedance source network consists of inductors, capacitors, and diodes with different configurations, such as Z-source, Y-source, Δ -source, T-source, Γ -source, TZ-source, sigma-Z-source, and so on [14]. A Y-shaped impedance network by a coupled-inductor implementation in order to obtain high voltage gain in small duty ratio was presented in [15]. In [16], a Δ -source converter was investigated by employing three coupled inductors and comparing it with a Y-source impedance network. The investigation demonstrated that in a Δ -source converter, smaller magnetizing current and winding loss can be attained compared with a Y-source converter. Moreover, the adverse effect of leakage inductance caused by coupled inductors is reduced significantly in a Δ -source converter. In [19], the other Z-source high step-up converter was presented by utilizing two cores for two sets of coupled inductors. Although the voltage conversion ratio increased in the mentioned proposed converter in [19], the core loss of the ferrite reduced the efficiency of the converter. In [13], different topologies of a galvanically isolated impedance source DC–DC converter with a wide range of input voltage and load regulation for distributed generation systems were surveyed. By contrast, the operating principle of a common grounded Z-source DC–DC converter for photovoltaic applications was proposed in [17]. The proposed converter with a common ground for the input and output resulted in having a low cost and a small-sized step-up converter compared with the isolated ones.

Investigation in different types of high step-up converters resulted in the proposal of a novel impedance source converter by cascading two Z-source networks and employing switched-capacitor-inductor cells in order to obtain a converter with high voltage gain ratio, low voltage

stress on semiconductor devices, and low input current ripple, as expected from impedance source converters. However, the conventional configuration of cascading two Z-source networks between input source and main converter leads to the system suffering from very high input current ripple and high voltage stress for the switch. By modifying the proposed configuration, the converter can become appropriate for high step-up applications with low input current ripple. Furthermore, further research can be done to find out how cascading other impedance network configurations could affect the converter operation.

In this paper, after elaborating the topology of the proposed converter and investigating the operational modes in Section 2, the analysis and design consideration of the proposed converter are given in Section 3 in order to find out the voltage conversion ratio and voltage stresses of the switch and diodes. Finally, Section 4 presents the experimental results of a prototype converter to validate the theoretical analysis.

2. Proposed Converter and Principle of Operation

As it can be seen from Figure 1, the proposed high step-up DC-DC impedance source based boost converter includes two cascaded Z-source networks and two switched-capacitor-inductor cells. The converter hires a single ferrite core with six coupled inductors, which are part of the impedance network and cells. The very high input current ripple and the high voltage stress of the switch are two main problems in this converter. Therefore, some inevitable alterations are required in order to make the converter practically applicable. Although by adding a capacitor as shown in Figure 2, the voltage stress of the switch clamps at a specific value, the high input current ripple is still considered as a drawback in this converter. The dashed line in Figure 2 represents how the KVL (Kirchhoff’s Voltage Law) loop clamps the switch voltage at a specific value. Eventually, the final modification into the converter configuration resulted in obtaining a high step-up converter with low input current ripple and low voltage stress for semiconductor devices. Figure 3 shows the modified proposed high step-up impedance source converter with an equivalent circuit of coupled inductors. The proposed converter is composed of a single switch Q_1 ; one diode D_1 in the impedance network; two diodes in the cells D_2 and D_3 ; and one output diode D_4 ; six coupled inductors $L_1, L_2, L_3, L_4, L_5,$ and L_6 ; four capacitors $C_1, C_2, C_3,$ and C_4 in the impedance network; two switched-capacitors C_5 and C_6 ; and output capacitor C_7 .

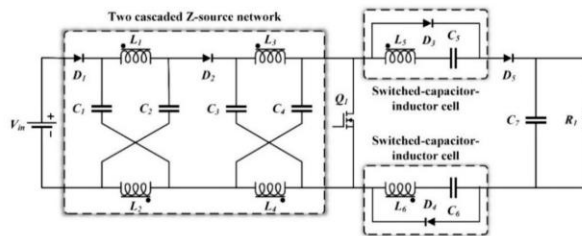


Figure 1. Two cascaded Z-source high step-up converter.

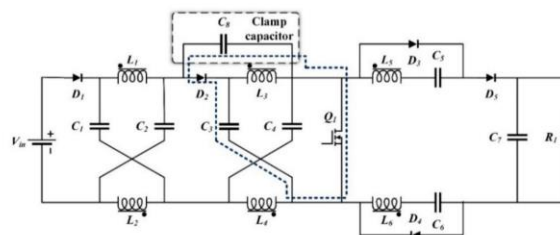


Figure 2. Modified converter by a clamp capacitor.

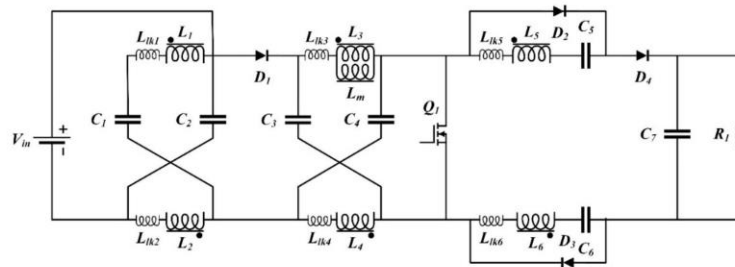


Figure 3. Circuit diagram of proposed converter with equivalent circuit of coupled inductors.

The converter has four time intervals within a switching cycle in the steady state operation. Figure 4 illustrates the equivalent circuits for each operating interval; the capacitor C_2 can be considered not in the circuit due to being in parallel with input voltage source, and Figure 5 is provided to show the theoretical waveforms of the proposed converter. To simplify the steady state analysis, the following assumptions are made:

- The converter operates in continuous conduction mode (CCM);
- The switch, diodes, and all inductors and capacitors are assumed ideal;
- The magnetizing inductance is large enough to ignore its current ripple;
- The leakage inductances of all windings are equal;
- The output capacitor C_7 is large enough to make the output voltage constant;
- The switching capacitors C_5 and C_6 are equal.

Operation Principles

Interval 1 [$t_0 < t < t_1$] (Figure 4a): Before the t_0 input, diode D_1 is conducting, and the other semiconductor devices are off. At t_0 , the switch Q turns on, diode D_1 becomes reverse-biased, and $(2 + n)V_C - V_{in}$ is applied across it. In addition, the current direction of capacitors C_3 and C_4 become reverse. In this operation mode, the capacitor voltage of C_3 and C_4 applies to inductors L_3 and L_4 , and consequently this voltage will be induced to other coupled inductors L_1, L_2, L_5 , and L_6 by considering the turn ratio. In this stage, the energy of leakage inductances L_1 and L_2 are recycled to the input voltage source, and the energy of leakage inductances L_5 and L_6 are absorbed by switched-capacitors C_5 and C_6 . The following equations are established in this time interval:

$$V_{C_3} = V_{C_4} = V_C, \tag{1}$$

$$V_{L_3} = V_{L_4} = V_C, \tag{2}$$

$$V_{L_1} = V_{L_2} = V_{L_5} = V_{L_6} = nV_C, \tag{3}$$

where n is the turn ratio of coupled inductors:

$$n = n_1/n_3 = n_2/n_3 = n_5/n_3 = n_6/n_3, \text{ and } n_3 = n_4 \tag{4}$$

$V_{C_5}(t_0)$ and $V_{C_6}(t_0)$ are less than the coupled inductor's voltage in their corresponding cells, so a resonance occurs between the leakage inductances and both C_4 and C_5 to charge the capacitors through D_2 and D_3 over the half resonance period. The current and voltage of capacitor C_5 can be expressed as:

$$i_{C_5}(t) = \frac{V_{C_5}(t_0) - nV_C}{Z_{res}} \sin \omega_{res}(t - t_0) \tag{5}$$

$$v_{C_5}(t) = nV_c + [V_{C_5}(t_0) - nV_c] \cos \omega_{res}(t - t_0) \tag{6}$$

where $\omega_{res} = 1/\sqrt{L_{lk}C_5}$ and $Z_{res} = \sqrt{L_{lk}/C_5}$.

The capacitor C_3 and switch Q current are determined as:

$$i_{C_3} = I_{L_m} + i_{L_3} = I_{L_m} + ni_{C_5} \tag{7}$$

$$i_Q = I_{L_m} + 2ni_{C_5} \tag{8}$$

where i_{C_5} is given by (5).

This mode ends after a half resonance period once the current direction changes. Therefore, the diodes D_2 and D_3 turn off at zero current.

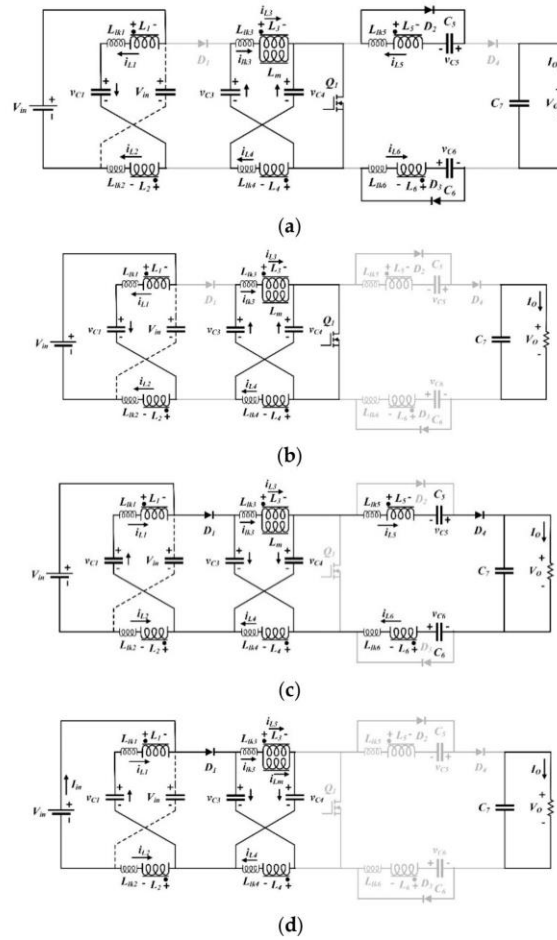


Figure 4. Equivalent circuits of the proposed converter for each operation mode. (a) interval 1, (b) interval 2, (c) interval 3, (d) interval 4.

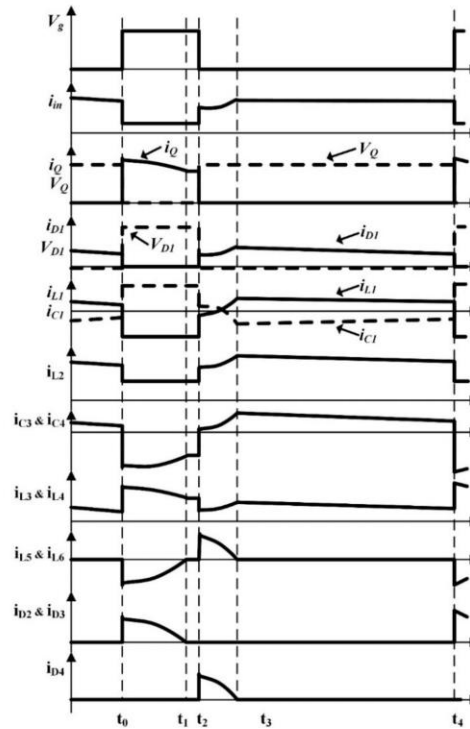


Figure 5. Theoretical waveforms of the proposed converter.

Interval 2 [$t_1 < t < t_2$] (Figure 4b): At this operation mode, the switch Q is still on and all diodes are at the off state. In addition, the magnetizing inductance L_m is still charging by C_3 and C_4 . Diodes D_2 and D_3 are off in this stage due to reversing the current of inductors L_5 and L_6 , which are blocked by diodes D_2 and D_3 , respectively. Therefore, the stored magnetic energy of the transformer leads to slightly increasing the current of other coupling windings. This mode ends when the switch Q turns off. The current of inductor L_1 can be expressed as:

$$i_{L_1}(t) = \frac{nV_C - V_{C_5}(t_1)}{Z'_{res}} \sin \omega'_{res}(t - t_1) + I_1 \cos \omega'_{res}(t - t_1) \quad (9)$$

where $\omega'_{res} = 1/\sqrt{2L_{lk}C_1}$, $Z'_{res} = \sqrt{2L_{lk}/C_1}$, and regarding Equation (5), I_1 is also equal to $i_{C_4}(t_1)$ by considering the turn ratio.

Interval 3 [$t_2 < t < t_3$] (Figure 4c): At $t = t_2$, the switch Q turns off, diodes D_1 and D_4 turn on, and the energy transfers from the input to the output during this stage. The stored energy of the magnetizing inductance and of capacitors C_5 and C_6 also transfers to the load, and capacitors C_3 and C_4 will be charged through diode D_1 ; however, capacitor C_1 is discharged in this operation mode. The resonance between leakage inductance L_5 and C_5 and also leakage inductance L_6 and C_6 occurs during the maximum time of the half-resonant interval. This stage ends when the resonant current of

i_{C5} becomes zero and provide the ZCS (zero current switching) turn-off for diode D_4 . In the following, the corresponding voltage and current equations are expressed:

$$i_{C5}(t) = \frac{V_{C5}(t_2) - nV_C}{Z_{res}} \sin \omega_{res}(t - t_2) \quad (10)$$

$$v_{C5}(t) = nV_C + [V_{C5}(t_2) - nV_C] \cos \omega_{res}(t - t_2) \quad (11)$$

$$i_{D1} = i_{L_m} + i_{L3} \quad (12)$$

Interval 4 [$t_3 < t < t_4$] (Figure 4d): In this stage, the switch is still off and the output diode D_4 is also off by reversing the current of L_5 , which occurred in the previous operation mode. However, the input diode D_1 remains on in this stage, which causes the capacitors C_3 and C_4 to keep their charging state on from the previous stage. In addition, capacitor C_1 is discharged the same way as operation mode 3. The current of L_1 can be stated as:

$$i_{L1}(t) = \frac{nV_C - V_{C5}(t_3)}{Z'_{res}} \sin \omega'_{res}(t - t_3) + I_3 \cos \omega'_{res}(t - t_3) \quad (13)$$

where I_3 is equal to $i_{C4}(t_3)$ by considering the turn ratio.

Moreover, the other current equations can be expressed as:

$$i_{D1} = I_{in} + i_{L1} \quad (14)$$

$$I_{L_m} = i_{C5} + i_{C4} - i_{L3} \quad (15)$$

This operation mode ends when the switch is turned on again.

3. The Proposed Converter Analysis and Design Considerations

In this section, different features of the proposed converter, such as voltage gain and voltage stresses of the switch and diodes, are discussed and compared with other high step-up converters. Then, in order to compare the performance of the proposed converter's features, some graphs and tables are provided.

3.1. Conversion Ratio

When the input diode D_1 is on, the capacitors C_3 and C_4 charge by the input voltage source through magnetizing inductance L_m . However, at the on-state of switch Q , the capacitors C_3 and C_4 discharge themselves to L_m , which causes the voltage gain of the converter to increase. By applying the magnetizing inductor L_m , the voltage-second balance equation V_C can be calculated as:

$$V_C = \frac{1 - D}{1 - (2 + n)D} V_{in} \quad (16)$$

According to interval 3, by applying a KVL the output voltage can be obtained as:

$$V_o = V_{in} + (V_{L3} + V_{L4}) + (V_{L2} + V_{L5} + V_{L6}) + (V_{C5} + V_{C6}) \quad (17)$$

where the V_{C5} and V_{C6} can be expressed as:

$$V_{C5} = V_{C6} = n \frac{(1 - D)}{1 - (2 + n)D} V_{in} \quad (18)$$

Therefore, the voltage gain of the proposed converter is equal to:

$$M = \frac{V_o}{V_{in}} = \frac{2n + 1}{1 - (2 + n)D} \tag{19}$$

Figure 6 shows the voltage gain of the proposed converter by variation of the duty cycle for different turn ratios of the coupled inductors. As it can be seen, although by increasing the turn ratio of the coupled inductors a larger voltage gain can be obtained at a lower duty cycle, the duty cycle range for the step-up purpose in the Z-source converter will be restricted. In fact, the following equation represents the range of duty cycle for the proposed impedance source converter in a step-up operation mode:

$$0 < D < \frac{1}{2 + n} \tag{20}$$

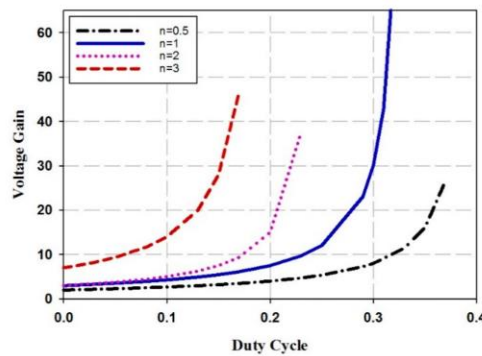


Figure 6. Voltage gain of the proposed converter for different turn ratio of coupled inductors.

Moreover, a higher turn ratio results in higher power loss due to increasing the leakage inductance of coupled inductors. Moreover in Figure 7, the voltage gain of the proposed converter is compared with converters in [12,18,19]. As it can be observed, the voltage gain of proposed converter is higher than that of the other three converters for variation of duty cycle from 0 to 0.33 due to considering the unity turn ratio of the coupled inductors.

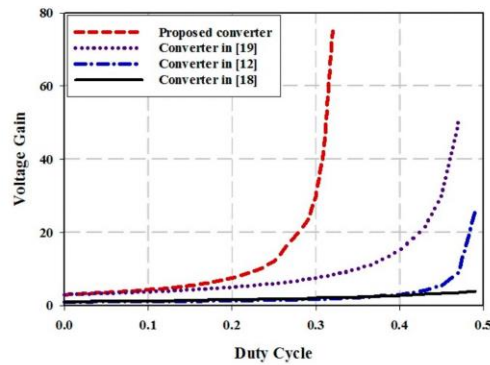


Figure 7. Voltage gain of the proposed converter vs. converters in [12,18,19].

3.2. Voltage Stresses of Switch and Diodes

By considering the corresponding time interval of the converter operation mode, the voltage stress of the semiconductor devices can be calculated. According to the interval 1, voltage stress of D_1 and D_4 can be determined as:

$$V_{D_1} = (2+n)V_C - V_{in} = \frac{1+n}{1-(2+n)D} V_{in} \quad (21)$$

$$V_{D_4} = V_O \quad (22)$$

In addition, the voltage stress of diodes D_2 and D_3 can be determined by considering interval 2 as:

$$V_{D_2} = V_{D_3} = \frac{V_O}{3} \quad (23)$$

To calculate the voltage stress of switch Q , a KVL is applied by considering interval 3; therefore, the following equation is obtained:

$$V_{sw} = 2V_{L_3} + nV_{L_3} + V_{in} = (2+n)\left(\frac{V_C - V_{in}}{1+n}\right) + V_{in} \quad (24)$$

According to Equation (16), the voltage stress of the switch can be expressed as:

$$V_{sw} = \frac{1}{1-(2+n)D} V_{in} \quad (25)$$

Figure 8 shows the voltage stress of the switch for different turn ratios of coupled inductors by varying the duty cycle; as it can be observed, by increasing the turn ratio, the voltage stress increases as well. Moreover, Figure 9 demonstrates the voltage stress of the proposed converter compared with converters in [12,18,19]. The voltage gain varies from 5 to 15, and the voltage stresses of the switch for the converters are compared with each other. As it can be seen from Figure 9, the stress voltage of the switch in the proposed converter and the converter in [19] is lower than that of the two other converters.

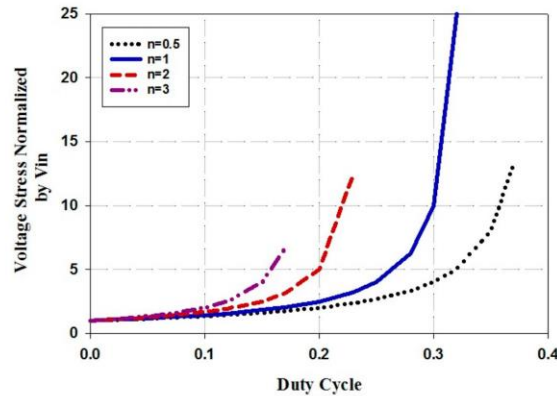


Figure 8. Voltage stress of the switch for different turn ratios of coupled inductors.

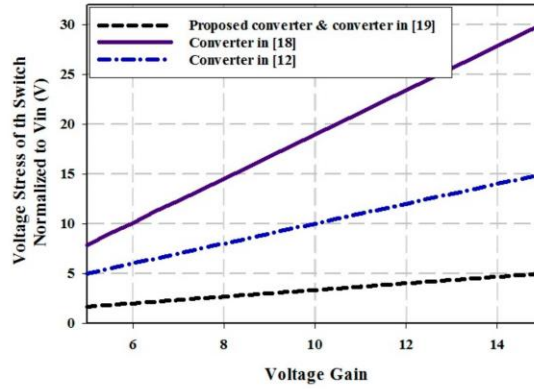


Figure 9. Voltage stress of the switch in the proposed converter and the converters in [12,18,19].

3.3. Converter Analysis and Design Guideline

The ZCS occurs for the diodes D_2, D_3 and D_4 for the sake of resonance between leakage inductances of L_5 (or L_6) and C_5 (or C_6). The full-resonance can be done if the following equation is satisfied:

$$\frac{T_{res}}{2} < DT_{SW} \quad (26)$$

In order to stabilize the input current, Equation (26) is not satisfied in the proposed converter. However, the ZCS condition is still established because even just the beginning part of the resonant waveform will be affected.

In addition, diode D_4 is conducting current only in time interval 3 ($t_2 < t < t_3$). Therefore, it can be concluded that the average current of D_4 is equal to the output current:

$$\langle I_{D_4} \rangle = I_O \quad (27)$$

Consequently, the leakage inductance can be calculated as:

$$L_{lk} = \frac{V_{C_5} - nV_C}{I_O} (1 - \cos \omega_{res}(t_3 - t_2)) \quad (28)$$

The duration $t_3 - t_2$ can be considered as the maximum DT_{SW} . In addition, the magnetizing inductance can be also calculated as the following by considering the desirable current ripple ΔI_L :

$$L_m = \frac{DV_C}{f_{SW} \Delta I_L} \quad (29)$$

Moreover, capacitor C_3 can be calculated with regard to the current flow over the switched-on interval:

$$C_3 = \frac{D(I_{L_m} + nI_{C_5})}{f_{SW} \Delta V_C} \quad (30)$$

The other capacitors in the impedance network have the same value as capacitor C_3 .

3.4. High Step-up Converters Comparison

In Table 1 the performance of the proposed converter is compared with the other high step-up converters in [12,18,19]. As observed, the proposed converter provides a higher voltage gain meanwhile the voltage stress of the switch is lower than that of others. Moreover, the proposed converter employs

a single ferrite core which make the converter more efficient due to reducing the core loss of the transformer in comparison with the converter in [18,19] with two ferrite cores and the converter in [12] with three ferrite core. In addition, the input current of proposed converter is continuous with a low current ripple; however, the input current of the other compared converters are discontinuous.

Table 1. Comparison of proposed converter with other Z-source DC–DC converters.

| Converter | Voltage Gain (M) | Switch Voltage Stress | Input Current | Number of Ferrite Core |
|----------------------------|-------------------------|-------------------------|---------------|------------------------|
| Conventional Z-source [12] | $1 - D/1 - 2D$ | $(2M - 1)V_{in}$ | Discontinuous | 3 |
| Converter in [18] | $1/(1 - D)^2$ | MV_{in} | Discontinuous | 2 |
| Converter in [19] | $2n + 1/1 - 2D$ | $V_{in}/(1 - 2D)$ | Discontinuous | 2 |
| Proposed Converter | $2n + 1/(1 - (2 + n)D)$ | $V_{in}/(1 - (2 + n)D)$ | Continuous | 1 |

4. Experimental Results

To compare the performance of the proposed converter in practice, a real prototype of the converter was implemented, and experimental results are provided in order to verify the theoretical analysis. Figure 10 shows the real implemented prototype. The implemented converter operated at 50 kHz to convert the 25 V input voltage to 300 V with a nominal power of 100 W for the load.

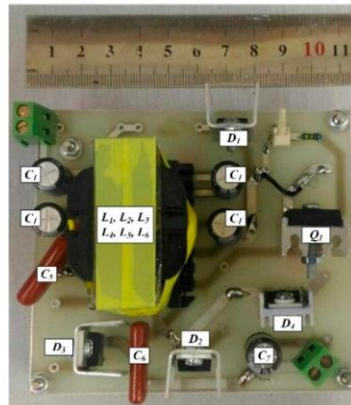


Figure 10. Implemented prototype of the proposed converter.

Table 2 reports the parameters of the designed converter. The drain-to-source breakdown voltage of the selected MOSFET was much lower than the output voltage, and therefore a low R_{DS} of the MOSFET resulted in low conduction power loss.

Experimental waveforms of the implemented prototype are illustrated in Figures 11–15. The input current and voltage of the converter are shown in Figure 11; the low input current ripple can be observed in this figure. Figure 12 shows the voltage and current of diode D_1 ; the voltage and current waveforms of the switch are shown in Figure 13. It can be seen that regarding the output voltage of 300 V, which is illustrated in Figure 15, the stress voltage of MOSFET is 100 V. Finally, the voltage and current of diode D_4 can be seen in Figure 14.

Table 2. Important parameters of the implemented prototype.

| Parameters | Value |
|---|------------------|
| Input voltage V_{in} | 25 V |
| Output voltage V_o | 300 V |
| Output power P_o | 100 W |
| Switching frequency (f_{sw}) | 50 kHz |
| Switch Q | IRFP3710 |
| Input diode D_1 | MUR880 |
| Diodes D_2, D_3, D_4 | MUR460 |
| Coupled inductors core | 380 μ H |
| $L_1, L_2, L_3, L_4, L_5, L_6$ | 90 turns |
| Turns of ($L_1 \dots L_6$) | 1 |
| Turns ratio n | 1 |
| Z-source network capacitors (C_1, C_2, C_3 and C_4) | 15 μ F/100 V |
| Switched capacitors C_6, C_7 | 560 nF/100 V |
| Output capacitors C_8 | 10 μ F/400 V |

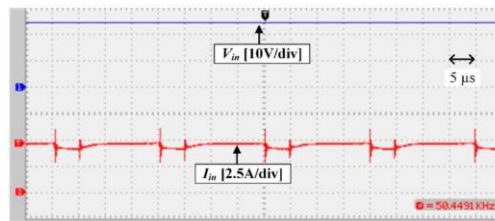


Figure 11. Input Voltage and current of the converter.

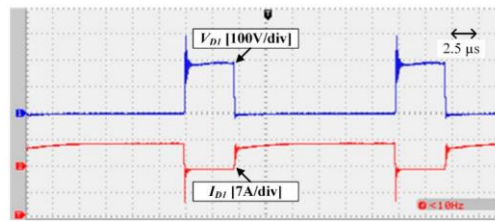


Figure 12. Voltage and current waveform of the diode D_1 .

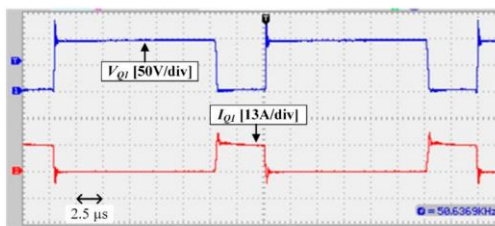


Figure 13. Voltage and current waveform of the switch Q.

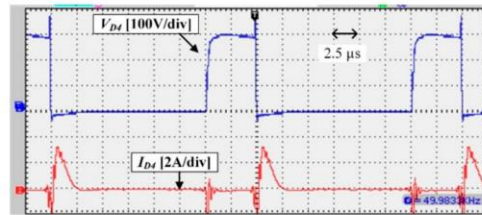


Figure 14. Voltage and current waveform of the diode D_4 .

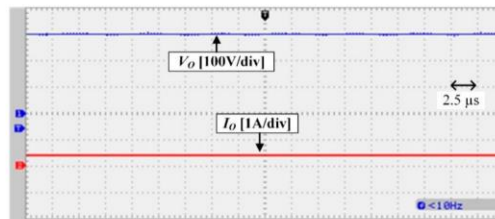


Figure 15. Output voltage and current waveform of the high step-up converter.

The efficiency of the proposed converter was calculated by measuring the input and output current and voltage of the converter by means of DC current and voltage meters, respectively. Figure 16 shows the efficiency of the implemented proposed converter from 50% to 100% of a full load condition and it is compared with the converter in [19]. As it can be observed, by increasing the output power, conduction losses increase as well and lead to dropping the efficiency slightly. Moreover, under a full load condition, the measured efficiency is 93%.

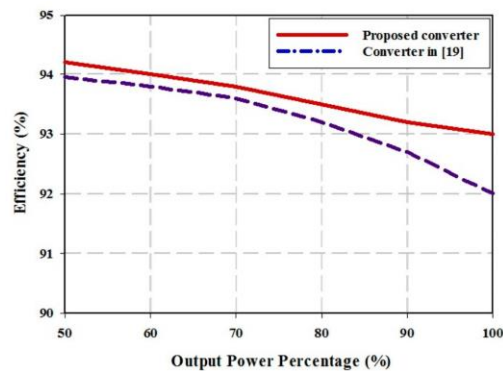


Figure 16. Efficiency plot of the implemented prototype under different load conditions.

5. Conclusions

Among the different step-up techniques that were applied on boost converters in order to improve the input-to-output voltage ratio, the cascaded technique was chosen in this paper in order to cascade two Z-source networks and take advantage of both the cascade and impedance source converters. All inductors were coupled together in the proposed converter; therefore, the voltage gain increased only by utilizing a single core in the proposed configuration. A low duty cycle of the switch lead to reducing the reverse-recovery problem of the output diode significantly and results in enhancing the efficiency

due to a reduction of power loss of the switch and diodes. Furthermore, diodes D_2 , D_3 , and D_4 turn off under a ZCS condition. The low input current ripple of this converter makes it appropriate to apply in renewable energy sources. A laboratory prototype of the proposed converter in order to justify the theoretic analysis was built, and experimental waveforms were presented for a 100 W output power converter.

Author Contributions: Conceptualization, N.S.; methodology, N.S.; software, N.S.; validation, N.S., H.M.-G., and G.V.-Q.; investigation, N.S.; data curation, N.S.; writing—original draft preparation, N.S.; writing—review and editing, N.S., H.M.-G., and G.V.-Q.; supervision, H.M.-G. and G.V.-Q. All authors have read and agreed to the published version of the manuscript.

Funding: This research and the APC was funded by the Spanish Ministerio de Ciencia, Innovación y Universidades (MICINN)-Agencia Estatal de Investigación (AEI) and the European Regional Development Funds (FEDER), by means of project PGC2018-098946-B-I00.

Conflicts of Interest: The authors declare no conflict of interest.

References

- Bugaje, I. Renewable energy for sustainable development in Africa: A review. *Renew. Sustain. Energy Rev.* **2006**, *10*, 603–612. [\[CrossRef\]](#)
- Wai, R.-J.; Wang, W.-H.; Lin, C.-Y. High-Performance Stand-Alone Photovoltaic Generation System. *IEEE Trans. Ind. Electron.* **2008**, *55*, 240–250. [\[CrossRef\]](#)
- Liu, H.; Hu, H.; Wu, H.; Xing, Y.; Batarseh, I. Overview of High-Step-Up Coupled-Inductor Boost Converters. *IEEE J. Emerg. Sel. Top. Power Electron.* **2016**, *4*, 689–704. [\[CrossRef\]](#)
- Forouzeh, M.; Siwakoti, Y.P.; Gorji, S.A.; Blaabjerg, F.; Lehman, B. Step-Up DC–DC Converters: A Comprehensive Review of Voltage-Boosting Techniques, Topologies, and Applications. *IEEE Trans. Power Electron.* **2017**, *32*, 9143–9178. [\[CrossRef\]](#)
- Tofoli, F.L.; De Paula, W.J.; Júnior, D.D.S.O.; Pereira, D.D.C. Survey on non-isolated high-voltage step-up dc–dc topologies based on the boost converter. *IET Power Electron.* **2015**, *8*, 2044–2057. [\[CrossRef\]](#)
- Salehi, N.; Mirtalaei, S.M.M.; Mirenayat, S.H. A high step-up DC–DC soft-switched converter using coupled inductor and switched capacitor. *Int. J. Electron. Lett.* **2017**, *6*, 260–271. [\[CrossRef\]](#)
- Zhao, Q.; Lee, F. High-efficiency, high step-up DC-DC converters. *IEEE Trans. Power Electron.* **2003**, *18*, 65–73. [\[CrossRef\]](#)
- Kim, K.-D.; Kim, J.-G.; Jung, Y.-C.; Won, C.-Y. Improved non-isolated high voltage gain boost converter using coupled inductors. In Proceedings of the 2011 International Conference on Electrical Machines and Systems, Beijing, China, 20–23 August 2011; pp. 1–6.
- Prudente, M.; Pfitscher, L.L.; Emmendoerfer, G.; Romaneli, E.F.; Gules, R. Voltage Multiplier Cells Applied to Non-Isolated DC–DC Converters. *IEEE Trans. Power Electron.* **2008**, *23*, 871–887. [\[CrossRef\]](#)
- Poorali, B.; Jazi, H.M.; Adib, E. Single-core soft-switching high step-up three-level boost converter with active clamp. *IET Power Electron.* **2016**, *9*, 2692–2699. [\[CrossRef\]](#)
- Peng, F.Z. Z-Source Inverters. *IEEE Trans. Ind. Appl.* **2003**, *39*, 504–510. [\[CrossRef\]](#)
- Galigekere, V.P.; Kazimierczuk, M.K. Analysis of PWM Z-Source DC-DC Converter in CCM for Steady State. *IEEE Trans. Circuits Syst. I Regul. Pap.* **2011**, *59*, 854–863. [\[CrossRef\]](#)
- Chub, A.; Vinnikov, D.; Blaabjerg, F.; Peng, F.Z. A Review of Galvanically Isolated Impedance-Source DC–DC Converters. *IEEE Trans. Power Electron.* **2015**, *31*, 2808–2828. [\[CrossRef\]](#)
- Siwakoti, Y.P.; Peng, F.Z.; Blaabjerg, F.; Loh, P.C.; Town, G.E. Impedance-Source Networks for Electric Power Conversion Part I: A Topological Review. *IEEE Trans. Power Electron.* **2014**, *30*, 699–716. [\[CrossRef\]](#)
- Siwakoti, Y.P.; Loh, P.C.; Blaabjerg, F.; Town, G.E. Y-source impedance network. In Proceedings of the 2014 IEEE Applied Power Electronics Conference and Exposition—APEC 2014, Fort Worth, TX, USA, 16–20 March 2014; pp. 3362–3366.
- Hakemi, A.; Sanatkar-Chayjani, M.; Monfared, M. Δ -Source Impedance Network. *IEEE Trans. Ind. Electron.* **2017**, *64*, 7842–7851. [\[CrossRef\]](#)
- Shen, H.; Zhang, B.; Qiu, D.; Zhou, L. A Common Grounded Z-Source DC–DC Converter With High Voltage Gain. *IEEE Trans. Ind. Electron.* **2016**, *63*, 2925–2935. [\[CrossRef\]](#)

18. Luo, F.; Ye, H. Positive output cascade boost converters. *IEE Proc. Electr. Power Appl.* **2004**, *151*, 590–606. [[CrossRef](#)]
19. Poorali, B.; Torkan, A.; Adib, E. High step-up Z-source DC–DC converter with coupled inductors and switched capacitor cell. *IET Power Electron.* **2015**, *8*, 1394–1402. [[CrossRef](#)]

Publisher’s Note: MDPI stays neutral with regard to jurisdictional claims in published maps and institutional affiliations.



© 2020 by the authors. Licensee MDPI, Basel, Switzerland. This article is an open access article distributed under the terms and conditions of the Creative Commons Attribution (CC BY) license (<http://creativecommons.org/licenses/by/4.0/>).

Chapter 7

Neural Networks-Generalized Predictive Control for MIMO Grid-connected Z-source Inverter Model

7.1. INTRODUCTION

The reliable operation of inverters has a great effect on the reliable operation of the MG system. Inverters play a crucial role in both grid-connected and stand-alone operation modes and especially at transient between these two modes. Accordingly, an appropriate control method enables the inverter to operate robustly, especially at transients when the set points change. In this chapter, a single-phase Z-source inverter is under investigation. The non-minimum phase characteristic of this converter resulted in proposing a novel control method to enhance the performance of the converter. Model predictive control (MPC) has been presented recently as a potential solution to improve the operation of non-minimum phase systems. MPC is based on predicting the state variables. Therefore, the intrinsic delay of the non-minimum system can be compensated by predicted signals. A novel MPC based on the transfer function of the converter is proposed in this chapter. The predicted signals are obtained by the neural networks approach. Consequently, more accurate predicted signals resulted in performance enhancement of the converter.

7.2. CONTRIBUTIONS TO THE STATE OF ART

Inverters are a vital component of MG in order to provide the appropriate energy and control energy flow in individual and networked MG systems. Inverters can be surveyed from a different point of view according to their applications in MGs. Fig 7.1. demonstrates a general classification of inverters based on input supply source and output produced state.

Employing Z-source inverters brings the advantage of the voltage source and current source exhibition in only one single-stage conversion. Furthermore, the non-minimum phase behavior of the Z-source inverter makes this control attractive for advanced control methods such as MPC-based controllers. A comprehensive study on Z-source inverters and topology improvements is conducted in [1]. In [2], different structures of switched Z-source networks with high boost capability are reviewed and categorized.

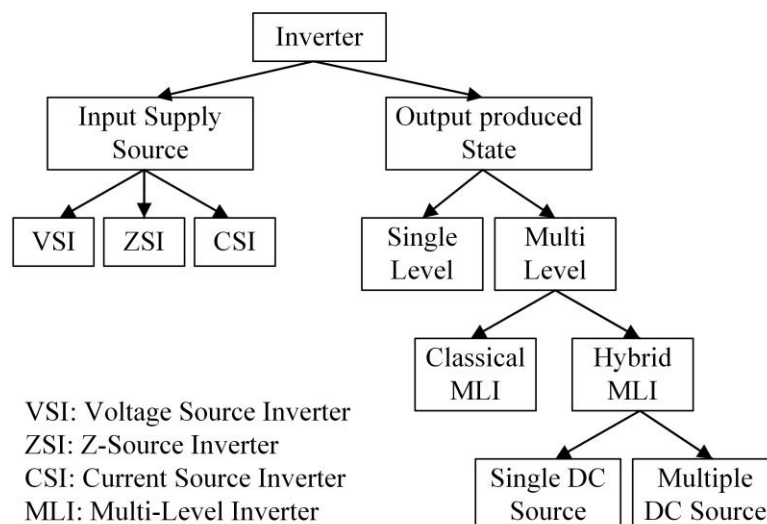


Fig. 7.1: Inverter classifications

Different control methods are applied to the Z-source inverter in order to obtain a robust performance due to the existing non-minimum phase characteristics of the converter. In [3], sliding mode control (SMC) is applied to a Z-source converter in continuous conduction operating mode to control the output DC voltage of the impedance network. A fuzzy logic controller (FLC) is presented in [4] to control a grid-connected photovoltaic system through a Z-source inverter. The proposed FLC is designed to improve the system's reliability. In [5], a model predictive control of dual-mode Z-source inverters with the capability to operate in grid-connected and stand-alone operation modes is developed. The proposed controller is addressed to mitigate the deviation in voltage and current due to mismatch in phase, frequency, and amplitude of voltages in the transition from island to grid-connected mode and vice versa.

This chapter applies a generalized predictive controller (GPC) to the single-phase Z-source grid-connected inverter. The GPC is one of the predictive controllers based on the transfer function of the system. Accordingly, the multi-input multi-output model of the converter is obtained. The GPC consists of two parts: free response related to past signals and forced response related to future signals. The forced response of the proposed controller in this chapter is replaced by feed-forward neural networks in order to predict future signals accurately. Therefore, the performance of the converter is enhanced, especially at set point transients. The performance of the converter is evaluated in MATLAB/SIMULINK.

7.3. REFERENCES

- [1]. Ellabban, Omar, and Haitham Abu-Rub. "Z-source inverter: Topology improvements review." *IEEE Industrial Electronics Magazine* 10, no. 1 (2016): 6-24.
- [2]. Hasan Babayi Nozadian, Mohsen, Ebrahim Babaei, Seyed Hossein Hosseini, and Elias Shokati Asl. "Switched Z-source networks: a review." *IET Power Electronics* 12, no. 7 (2019): 1616-1633.
- [3]. Rajaei, Amir Hossein, Shahriyar Kaboli, and Ali Emadi. "Sliding-mode control of Z-source inverter." In *2008 34th Annual Conference of IEEE Industrial Electronics*, pp. 947-952. IEEE, 2008.
- [4]. Mosalam, Hanan A., Ragab A. Amer, and G. A. Morsy. "Fuzzy logic control for a grid-connected PV array through Z-source-inverter using maximum constant boost control method." *Ain Shams Engineering Journal* 9, no. 4 (2018): 2931-2941.
- [5]. Sajadian, Sally, and Reza Ahmadi. "Model predictive control of dual-mode operations Z-source inverter: Islanded and grid-connected." *IEEE Transactions on Power Electronics* 33, no. 5 (2017): 4488-4497.

7.4. CONFERENCE PAPER

Neural Networks-Generalized Predictive Control for MIMO Grid-Connected Z-Source Inverter Model

Neural Networks-Generalized Predictive Control for MIMO Grid-Connected Z-Source Inverter Model

Navid Salehi, Herminio Martinez-Garcia, Guillermo Velasco-Quesada
 ELECTRONIC ENGINEERING DEPARTMENT, UNIVERSITAT POLITECTICA DE CATALUNYA – BarcelonaTech (UPC)
 Escola d'Enginyeria de Barcelona Est (EEBE), Av. Eduard Maristany, nº 16. E-08019
 Barcelona, Spain
 Tel.: +34.93.413.72.90
 E-Mail: navid.salehi@upc.edu, herminio.martinez@upc.edu, guillermo.velasco@upc.edu
 URL: <http://www.eel.upc.edu>

Acknowledgements

The authors would like to thank the Spanish Ministerio de Ciencia, Innovación y Universidades (MICINN)-Agencia Estatal de Investigación (AEI) and the European Regional Development Funds (ERDF), by grant PGC2018-098946-B-I00 funded by MCIN/AEI/10.13039/501100011033/ and by ERDF A way of making Europe.

Keywords

«Z-source», «MPC», «GPC», «ANN», «Non-minimum phase», «MIMO»

Abstract

This paper presents a neural network-generalized predictive control (NN-GPC) for a single-phase grid-connected z-source inverter. The NN forecasts the predictive horizon, and the conventional GPC algorithm calculates the control horizon. The results verify the proposed NN-GPC effectively enhances the dynamic operation of z-source inverter regarding the non-minimum phase characteristics of these converters.

Introduction

As a sustainable solution to provide the world's electrical energy, distributed energy resources (DERs) integrated with renewable energies (REs) are strongly regarded by researchers. Inverters in microgrids (MGs) and DERs systems provide standard AC electricity for customers and play a special role in the stability and optimal operation of the system. By introducing the concept of impedance source converters, z-source inverters (ZSI) are investigated rapidly in order to improve their performance. ZSI proposes a single-stage inverter with inherent buck-boost ability due to implementing an impedance network into the DC link. Therefore, the ZSI can operate as a voltage source inverter (VSI) and current source inverter (CSI) simultaneously by controlling the duty cycle of the converter. Although the reliability, efficiency, and cost-effectiveness are improved in ZSI, some weak points led to the proposal of different impedance network topologies [1]. The main disadvantages of impedance source converters are the high current and voltage stress of the input rectifier diode and the inability to inject reactive power into the grid [2]. Various topologies are proposed to alleviate these weaknesses. However, inherently impedance source converters suffer from the mentioned problems. In [3], a modified cascaded Z-source high step-up boost converter is proposed in order to obtain a high conversion ratio with low voltage stress of semiconductor devices. In addition, the results verify that the proposed topology operates at continuous current mode (CCM) with low current and voltage stress.

The control techniques in ZSI are normally deployed to control the capacitor voltage and inductor current of the impedance network and the inductor current of the inverter's AC side. However, the control strategies in ZSI are a challenging issue due to the existing right-half-plane (RHP) zero into the control to capacitor voltage transfer function of the impedance network. Accordingly, different control strategies are adopted to ZSI as a non-linear and non-minimum phase system [4]. The proportional-integral-derivative (PID) controller can be applied to the ZSI to control the converter around a specific operating point. Therefore, the converter operation is restricted, and the converter dynamic is affected by operating point variation. In [5], a PID-like fuzzy control strategy is established to control the peak dc-link voltage. The PID parameters are determined according to the fuzzy logic-based rule sets. The rule sets in this paper are modified based on the trajectory performance of the phase plane in order to enhance the transient performance. Sliding mode control, fuzzy logic controller, model predictive control (MPC), and neural networks control are some other controllers that can effectively apply to the ZSI. In [6], a neural networks control technique is exploited to control DC boost and AC output voltage of ZSI. The space vector pulse-width-modulation (SVPWM) is modified in this paper in order to control the shoot-through (ST) duty ratio to boost dc voltage.

Model predictive control (MPC) is also widely applied to the ZSI control scheme. In [7], MPC predicts the capacitor voltage, inductor current, and output load current of a switched-inductor quasi ZSI to compare with the corresponding reference values. Then, the switching states are selected to achieve the minimum cost function. In [8], MPC is used in islanded and grid-connected operation modes to achieve a seamless transition between operation modes, fast dynamic response, and small tracking error under the steady-state condition of controller objectives. In [9], MPC is applied to the quasi ZSI to reduce the inductor current ripple and the output current error. In recent years, different MPC algorithms based on the predictive process model and defined cost function have been introduced. Dynamic matrix control (DMC) and model algorithmic control (MAC) are two MPC algorithms based on system step response and impulse response. Moreover, generalized predictive control (GPC), which is based on the system's discrete transfer function, and predictive functional control (PFC) based on the system's state space are two advanced MPC algorithms. Neural networks MPC (NN-MPC) can also be used specifically in complicated systems that conventional system identification methods such as step response, impulse response, transfer function, or state space of the system cannot be applied straightforwardly. The NN-based MPC algorithms are not fast due to high burden calculations. Therefore, NN-MPC is not developed in recent years compared to other MPC algorithms.

In this paper, neural networks GPC (NN-GPC) is applied to the ZSI in order to predict the capacitor voltage and inductor current of the impedance network and output inductor current. In this algorithm, the forced response of the predictive control is obtained by neural networks. The analysis shows that the proposed MPC algorithm enhances the dynamic response of the ZSI without increasing the calculation burdens. To verify the theoretical analysis, the simulation results are compared with conventional GPC. The rest of the paper is structured as follows. First, the multi-input multi-output (MIMO) model of the ZSI is presented. Then, by obtaining the discrete transfer functions of the ZSI, the proposed NN-GPC is introduced. Eventually, the simulation results are shown in order to verify the theoretical analysis.

MIMO z-source inverter model

As it can be seen from Fig. 1, the single-phase Z-source inverter consists of an impedance network and an H-bridge inverter. The impedance network involves two inductors L_1 and L_2 , and two capacitors C_1 and C_2 . In addition, a rectifier diode is in series with the input DC voltage source. The impedance network components are symmetrical i.e. the inductors L_1 and L_2 , and capacitors C_1 and C_2 are equal ($L_1=L_2=L$ and $C_1=C_2=C$). Therefore, the inductor current and capacitor voltage are identical. Furthermore, the parasitic resistor of the inductors is considered in the inverter model. This inverter has three operating intervals over a complete duty cycle. In the first interval (T_{ON}), the switches Q_1 and Q_4 are conducted in a positive active switching state. During the second interval (T_{OFF}), the switches Q_2 and Q_3 are conducted in a negative active switching state. Finally, the third interval (T_{ST}) is related

to the shoot-through (ST) switching state that all switches are turned on simultaneously to boost the input voltage. According to the z-source converter operation and considering the inductor volt-seconds balance, the following relations are established in ZSI [10]:

$$V_{C1} = V_{C2} = V_C = \frac{1 - D_{ST}}{1 - 2D_{ST}} \times V_{DC} \quad (1)$$

$$V_{INV} = 2V_C - V_{DC} = \frac{1}{1 - 2D_{ST}} \times V_{DC}, \quad (2)$$

where D_{ST} is the shoot-through duty cycle ($D_{ST} = T_{ST}/T$). To obtain the state-space of the ZSI, the average model of the operation modes is considered in this paper. To this end, according to the operation modes of ZSI, the average of three different state-space are evaluated:

$$\dot{X} = A_{AVG}X + B_{AVG}U, \quad (3)$$

where X is the inductor current and capacitor voltage of impedance network, and inductor current of inverter AC side as the state variables, $X = [i_{L1}, V_{C1}, i_{LS}]$, and U is the input DC voltage and grid voltage, $U = [V_{DC}, V_{Grid}]$. Moreover, the A_{AVG} and B_{AVG} are defined as (A_{AVG} , A_{ON} , A_{OFF} , A_{ST} , B_{AVG} , B_{ON} , B_{OFF} , and B_{ST} are matrices):

$$A_{AVG} = \frac{1}{T} (T_{ON}A_{ON} + T_{OFF}A_{OFF} + T_{ST}A_{ST}) \quad (4)$$

$$B_{AVG} = \frac{1}{T} (T_{ON}B_{ON} + T_{OFF}B_{OFF} + T_{ST}B_{ST}), \quad (5)$$

where $T_{ON} = (\mu_m + 1 - D_{ST}/2) \times T$, $T_{OFF} = (1 - T_{ON} - T_{ST})$, and μ_m is amplitude modulation index. To obtain the state-space of ZSI, presented in Fig 1, the ZSI is simplified into two separated systems. The H-bridge, L_s , and grid are considered a simple switch and constant current source (I_s) in the first system. Therefore, the first system consists of the input voltage source, impedance network, and equivalent circuit of the switch and current source. Moreover, the second system involves the constant DC voltage (V_{INV}), H-bridge, grid impedance, and grid voltage. In [11-12], the state-space ZSI is analyzed with a similar procedure. Accordingly, the state-space of ZSI is obtained as:

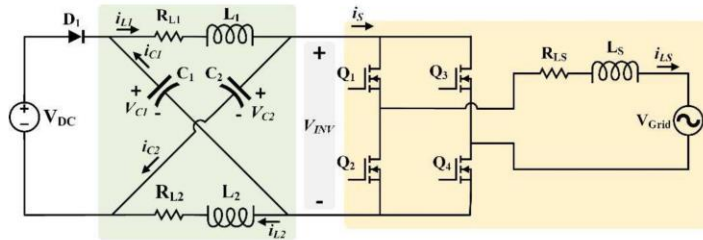


Fig. 1: Single-phase grid-connected z-source inverter

$$\begin{bmatrix} \dot{i}_{L1} \\ \dot{v}_{C1} \end{bmatrix} = \begin{bmatrix} \frac{-R_{L1}}{L} & -\frac{1}{L} + \frac{2}{L}D_{ST} \\ -\frac{1}{C} + \frac{2}{C}D_{ST} & 0 \end{bmatrix} \begin{bmatrix} i_{L1} \\ v_{C1} \end{bmatrix} + \begin{bmatrix} \frac{(2D_{sh} - 1)V_{DC} - 2R_{L1}I_s}{L(2D_{ST} - 1)^2} \\ \frac{2I_s}{C(2D_{ST} - 1)} \end{bmatrix} d_{ST} \quad (6)$$

$$\begin{bmatrix} \square \\ i_{LS} \end{bmatrix} = \begin{bmatrix} - \\ -\frac{R_{LS}}{L_S} \end{bmatrix} \begin{bmatrix} \\ i_{LS} \end{bmatrix} + \begin{bmatrix} \frac{2V_C - V_{DC}}{L_S} \\ \mu_m \end{bmatrix} \quad (7)$$

Therefore, the small-signal analysis can be performed in order to obtain the transfer functions of ZSI:

$$G_1(s) = \frac{i_L}{D_{ST}} = \frac{C(V_{DC} - 2D_{ST}V_{DC} - 2I_S r_L)s + (2 - 8D_{ST} + 8D_{ST}^2)I_S}{(2D_{ST} - 1)^2 (CLs^2 + Cr_L s + 4D_{ST}^2 - 4D_{ST} + 1)} \quad (8)$$

$$G_2(s) = \frac{v_C}{D_{ST}} = \frac{(2D_{ST} - 1)(2I_S L s + 4I_S r_L - (1 - 2D_{ST})V_{DC})}{C(V_{DC} - 2D_{ST}V_{DC} - 2I_S r_L)s + 2I_S + 8D_{ST}^2 I_S - 8D_{ST} I_S} \quad (9)$$

$$G_3(s) = \frac{i_{L_s}}{\mu_m} = \frac{2V_C - V_{DC}}{L_S s + r_{L_s}} \quad (10)$$

In $G_1(s)$ to $G_3(s)$, capital letters represents the variables at the operating point. Therefore, I_S and V_{DC} are the constant value at the operating point. As it can be seen, $G_2(s)$ represents a non-minimum phase system due to the existing RHP zero into the transfer function. Fig. 2 represents the pole and zero trajectories of control-to-capacitor with system parameter variations (C is considered constant and L is varied). Consequently, a MIMO ZSI is presented that the input variables (control variables) are shoot-through duty cycle (D_{ST}) and amplitude modulation index (μ_m), and the outputs are capacitor voltage of DC side and inductor current of inverter AC side.

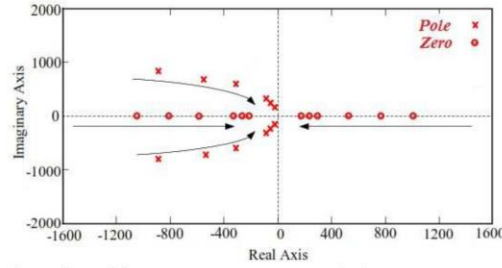


Fig. 2: Pole and zero trajectories with system parameters variations

Proposed neural networks-generalized predictive model

The GPC algorithm is exploited based on the transfer function that can possibly be a non-minimum phase and unstable system by considering the challenges regarding disturbances and noises. In MPC algorithms, the response is consists of free response and forced response. The free response refers to the signals in the past, and the forced response is related to the signals in the future. In this paper, controlled auto-regressive integrated moving average (CARIMA) is used to model the system in GPC:

$$A(z^{-1})y(t) = z^{-d}B(z^{-1})u(t-1) + C(z^{-1})\frac{e(t)}{(1-z^{-1})} \quad (11)$$

where d is the system delay, $e(t)$ is the noise that in this paper noise is not considered into the model, and $A(z^{-1})$ and $B(z^{-1})$ are obtained from the discrete-time model of transfer functions:

$$A(z^{-1}) = 1 + a_1 z^{-1} + a_2 z^{-2} + \dots + a_n z^{-n_a} \quad (12)$$

$$B(z^{-1}) = b_0 + b_1 z^{-1} + b_2 z^{-2} + \dots + b_n z^{-n_b} \quad (13)$$

According to the Diophantine equation in (13), the $E(z^{-1})$ and $F(z^{-1})$ can be calculated as a recursive relationship in (14) and (15) in order to predict the signals:

$$E_j(z^{-1})(1-z^{-1})A(z^{-1})+z^{-j}F_j(z^{-1})=1 \quad (14)$$

$$E_{j+1}(z^{-1})=E_j(z^{-1})+f_{j,0}z^{-j} \quad (15)$$

$$f_{j+1,i}=f_{j,i+1}-f_{j,0}\tilde{a}_{i+1} \quad i=0,1,\dots,n_{\tilde{a}}-1, \quad (16)$$

where j is the prediction horizon, and i represents the corresponding terms of the $F_j(z^{-1})$. In addition, \tilde{a}_i is i th term of $(1-z^{-1})A(z^{-1})$. Therefore, according to (10) and considering $e(t)=0$, the estimated outputs at the predictive horizon can be obtained:

$$\hat{y}(t+j|t)=B(z^{-1})E_j(z^{-1})(1-z^{-1})u(t+j-d-1)+F_j(z^{-1})y(t) \quad (17)$$

In (16), $F_j(z^{-1})y(t)$ is dependent on the past control signals. However,

$B(z^{-1})E_j(z^{-1})(1-z^{-1})u(t+j-d-1)$ is included both past and future control signals. In conventional GPC, the free response and forced response are separated by the following equation:

$$y=\Phi y_-+\Pi u_-+\Omega u \quad (18)$$

The first two terms in (17) are related to the past control signals, and the third term is related to the future control signals. The matrixes Φ , Π , and Ω are defined as below in the conventional GPC algorithm:

$$\Phi=\begin{bmatrix} f_{d+1,0} & \dots & f_{d+1,n_u} \\ \dots & \dots & \dots \\ f_{d+N,0} & \dots & f_{d+N,n_u} \end{bmatrix} \quad \Pi=\begin{bmatrix} g_{d+1,1} & \dots & g_{d+1,n_{g1}} \\ \dots & \dots & \dots \\ g_{d+N,N} & \dots & g_{d+N,n_{gN}} \end{bmatrix} \quad \Omega=\begin{bmatrix} g_{d+1,0} & 0 & 0 \\ \dots & \dots & \dots \\ g_{d+N,N-1} & \dots & g_{d+N,0} \end{bmatrix} \quad (19)$$

In the proposed NN-GPC algorithm, the forced response presented as Ωu in conventional GPC is replaced with feed-forward neural networks in order to predict the control signals. Therefore, the Ω matrix components are obtained by NN. In this algorithm, the GPC calculations reduce, instead the neural networks calculations are put in the algorithm. Fig. 3 represents the NN structure to predict the state variables. More accurate predicted state variables for the GPC enhance the algorithm operation and dynamic response of the ZSI. Fig. 4 shows the proposed NN-GPC. The inductor current and capacitor voltage of the impedance network and inductor current of inverter AC side as the feedback signals are inputs of the feed-forward NN and GPC. After algorithm calculations, the cost function units evaluate the optimum output control signals according to the predicted signals and reference signals. Eventually, the output control signals are applied to the gate drive to switch on or off the switches.

The cost function can be define as:

$$CF=(R-Y)^T(R-Y)+\alpha u^T u, \quad (20)$$

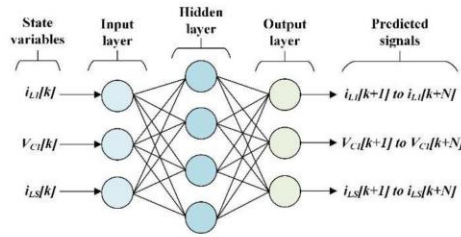


Fig. 3: Neural networks structure to predict the control signals

where R is the reference values $R=[R(t+d+1), R(t+d+2), \dots, R(t+d+N)]$, Y is defined in (17), and α is a constant value. Therefore, the optimum control signal can be stated:

$$u = (\Omega^T \Omega + \alpha I)^{-1} \Omega^T (R - \Phi y_- - \Pi u_-) \tag{21}$$

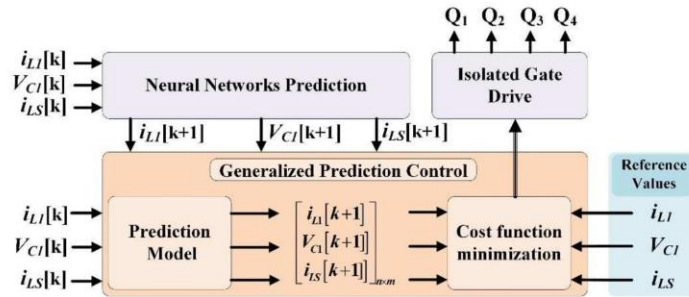


Fig. 4: Proposed NN-GPC

Performance evaluation and simulation results:

To evaluate the performance of the proposed NN-GPC on ZSI control, a ZSI with the specifications in Table I is considered. The NN is trained offline based on the obtained data of the ZSI simulation performance. Consequently, the NN offers the components of matrix Ω that are related to the future signals according to the instant values of state variables. On the other hand, the GPC algorithm evaluates the components of the matrices Φ and Π that are basically referred to the past signals. The NN parameters and GPC algorithm parameters are presented in Table I.

In order to evaluate the ZSI operation with the proposed NN-GPC, the simulation is carried out in MATLAB/ SIMULINK, and the results are compared with the conventional GPC. The neural networks toolbox is utilized to predict the state variables, and the GPC is set up by MATLAB codes. Eventually, the output signals of the cost function minimization are applied to the gate driver. The switching method in this simulation is the unipolar method. Figure 5 and 6 show the capacitor voltage and inductor current of the impedance network, coupling inductor current (L_s), and H-bridge inverter input voltage. It can be observed that the state variables follow their reference values effectively. In order to evaluate the dynamic response of ZSI in transients, the output current reference at 0.1ms is changed from 10A to 20A. The performance of NN-GPC and conventional GPC in transient can be seen in Fig. 5 and 6. The state variables in the conventional GPC are not able to trace the reference values in transition when the current reference is changed. However, the accurate prediction of state variables by feed-forward NN in NN-GPC makes the voltages and current track the reference values effectually. Although the MPC-GPC is also shown a favorable result in general specially comparing with PID controller, the proposed NN-GPC presents an effective performance specifically from the dynamic response perspective. Table II represents a characteristics comparison of GPC and NN-GPC.

Table I: Z-source inverter and NN-GPC specifications

| ZSI parameters | | NN specifications | NN-GPC parameters | |
|---------------------|--------------|--------------------|--------------------|----------------|
| V_{DC} | 100Vdc | | Input Data | 3×100 |
| V_{Grid} | 110Vrms | | Output Data | 3×100 |
| C_1 & C_2 | 1mF | | Training | 70% |
| L_1 & L_2 | 5.1mH | | Validation | 15% |
| R_{L1} & R_{L2} | 0.25Ω | | Testing | 15% |
| L_S | 5.1mH | GPC specifications | No. Hidden Neurons | 3 |
| R_{Ls} | 0.25Ω | | Sample T | $2\mu s$ |
| I_{OUT} | 20A | | Predictive horizon | 4 |
| V_{C1-ref} | 230V | | Control horizon | 4 |

Table II: Comparison of GPC and NN-GPC characteristics

| Specification | GPC | NN-GPC |
|------------------|---|---|
| System control | <ul style="list-style-type: none"> - Linear system - Nonlinear system - Minimum phase system - Non-minimum phase system | <ul style="list-style-type: none"> - Linear system - Nonlinear system - Minimum phase system - Non-minimum phase system |
| Complexity | Lower | Higher |
| Dynamic response | Lower | Higher |

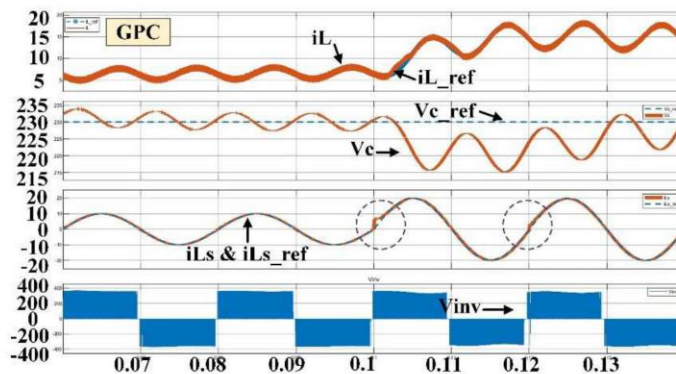


Fig. 5: Simulation results of ZSI control by GPC

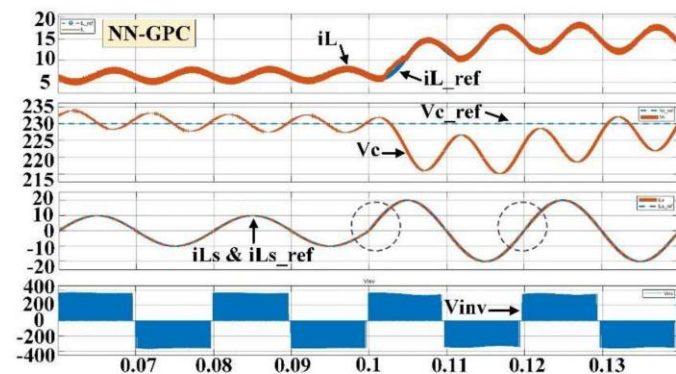


Fig. 6: Simulation results of ZSI control by NN-GPC

Conclusion

In this paper, an NN-GPC algorithm is proposed in order to control a ZSI. As discussed, the ZSI has non-minimum phase characteristics due to existing RHZ zero in control to capacitor voltage transfer function. Therefore, conventional linear control methods such as PID controllers make the ZSI operation unreliable and inefficient. The MPC algorithms as a promising control method for non-linear and non-minimum phase systems is considered recently to optimum control of ZSI. Eventually, the GPC algorithm is applied in this paper according to the MIMO model of ZSI. By deploying a feed-forward NN and improving the system identification to predict the state variables of the converter, the performance of the GPC algorithm is enhanced. Eventually, the simulation results for a specific ZSI are presented to verify the proposed NN-GPC algorithm.

Funding

Grant PGC2018-098946-B-I00 funded by: MCIN/ AEI /10.13039/501100011033/ and by ERDF ERDF A way of making Europe.

References

- [1] Hasan Babayi Nozadian, Mohsen, et al. "Switched Z-source networks: a review." *IET Power Electronics* 12.7 (2019): 1616-1633.
- [2] Nguyen, Minh-Khai, Young-Cheol Lim, and Sung-Jun Park. "Improved trans-Z-source inverter with continuous input current and boost inversion capability." *IEEE transactions on power electronics* 28.10 (2013): 4500-4510.
- [3] Salehi, Navid, Herminio Martínez-García, and Guillermo Velasco-Quesada. "Modified Cascaded Z-Source High Step-Up Boost Converter." *Electronics* 9.11 (2020): 1932.
- [4] Ellabban, Omar, Joeri Van Mierlo, and Philippe Lataire. "A comparative study of different control techniques for an induction motor fed by a Z-source inverter for electric vehicles." *2011 International Conference on Power Engineering, Energy and Electrical Drives*. IEEE, 2011.
- [5] Ding, Xiping, et al. "A direct DC-link boost voltage PID-like fuzzy control strategy in Z-source inverter." *2008 IEEE Power Electronics Specialists Conference*. IEEE, 2008.
- [6] Rostami, H., and D. A. Khaburi. "Neural networks controlling for both the DC boost and AC output voltage of Z-source inverter." *2010 1st Power Electronic & Drive Systems & Technologies Conference*. IEEE, 2010.
- [7] Bakeer, Abualkasim, et al. "Control of switched-inductor quasi Z-Source Inverter (SL-qZSI) based on model predictive control technique (MPC)." *2015 IEEE International Conference on Industrial Technology*. IEEE, 2015.
- [8] Sajadian, Sally, and Reza Ahmadi. "Model predictive control of dual-mode operations Z-source inverter: Islanded and grid-connected." *IEEE Transactions on Power Electronics* 33.5 (2017): 4488-4497.
- [9] Xu, Yuhao, et al. "Model Predictive Control Using Joint Voltage Vector for Quasi Z-Source Inverter with Ability of Suppressing Current Ripple." *IEEE Journal of Emerging and Selected Topics in Power Electronics* (2021).
- [10] Peng, Fang Zheng. "Z-source inverter." *IEEE Transactions on industry applications* 39, no. 2 (2003): 504-510.
- [11] Zakipour, Adel, Shokrollah Shokri-Kojori, and Mohammad Tavakoli Bina. "Sliding mode control of the nonminimum phase grid-connected Z-source inverter." *International Transactions on Electrical Energy Systems* 27, no. 11 (2017): e2398.
- [12] Loh, Poh Chiang, D. Mahinda Vilathgamuwa, Chandana Jayampathi Gajanayake, Yih Rong Lim, and Chern Wern Teo. "Transient modeling and analysis of pulse-width modulated Z-source inverter." *IEEE Transactions on Power Electronics* 22, no. 2 (2007): 498-507.

Chapter 8

Conclusion and Future Work

This PhD thesis addresses the conception, study, and development of two major points of view in MG and NMG systems. Energy management for networked MG and the consequence pros of sharing energy in networked MG is developed in the first part. Moreover, new topology and control methods for practical power electronics interfaces in MGs are expanded in the second part.

The major achievements of this PhD thesis are:

- **Networked MG energy management**

This study proposed a supervised and unsupervised learning clustering to cluster a number of residential, commercial, and industrial MGs. The clustering is based on the maximum load demand (MLD) and operating reserve (OR) of each MG evaluated for each interval considered for the load profile. Different load profile pattern of MGs lead to cluster the MGs such that the reliability of MGs increase. The proposed energy management is implemented for three residential MGs, two commercial MGs, and three industrial MGs. The performance of the proposed energy management is evaluated by MATLAB. The results represent that reliability of MGs and the whole system increased due to the possibility of sharing the operating reserve of MGs.

- **Component sizing for Networked MG**

This work presents a component sizing procedure for NMG. The proposed algorithm is based on the operating reserve of dispatchable units existing in MGs. Therefore, the proposed algorithm affects only the size of the dispatchable units. The size of the dispatchable units is reduced by a factor introduced as the Reduced Factor (RF). The peak load (PL) and correlation of load profiles are effective on RF. The proposed algorithm is evaluated for three MGs by simulation and practically at the laboratory. The results show that the size of dispatchable units can decrease significantly for the sake of the possibility of operating reserve sharing amongst MGs.

- **Optimum design of LLC resonant half-bridge converter**

This work addresses a practical optimum design procedure for LLC resonant half-bridge converters. LLC resonant converter proposes a galvanic isolated topology with

the possibility of voltage boosting by adjusting the turn ratio of the high-frequency transformer. Step-up converters are more applicable for MGs with low-power RESs generation such as low-scale PV systems. In this case, the PV panels are connected in series in order to provide a higher efficiency and reliability system. Moreover, networked MG systems result in a smaller size of energy generation units. Therefore, employing step-up converters is mandatory to meet the inverter input voltage. On the other hand, depending on the power system requirement, galvanic isolation of power generation units is obligatory by standards. LLC resonant converters are able to have different operation modes based on switching frequency and load demand. Accordingly, different operation modes indicate an exclusive performance of the converter. Different optimization methods are exploited in this study to investigate the best operation of the converter in various operation modes. To evaluate the proposed design procedure, the theoretical analysis is performed for the optimization methods and all operation modes of the converter. A real prototype of the LLC resonant half-bridge converter is also built to verify the obtained results of the proposed design procedure.

- **Z-source DC-DC high step-up converter**

This work presents a non-isolated high step-up DC-DC converter for hybrid MGs applications. Step-up converters are widely used for PV applications specifically for low-power PV systems with series connection of panels. Non-isolated converters can offer high efficiency and simple control solution for power systems with no galvanic isolation requirements. The proposed topology takes advantage of the cascading technique for two Z-source networks. The cascaded network leads to decreasing the input current peak and current stress of the Z-source network input diode. In addition, the Z-source networks provide low voltage stress for semiconductor devices with high gain voltage. The theoretical analysis is performed in this study to obtain the voltage gain and voltage stress of devices equations as a function of the duty cycle. The results of a laboratory prototype are obtained to validate the theoretical analysis. The results represent that the proposed topology is suitable for PV application in order to elevate the voltage at a proper level for grid-connected or isolated inverters.

- **Control method for grid-connected Z-source inverter**

This study addresses the non-minimum phase behaviour of the Z-source inverter. The control of non-minimum phase systems is challenging due to the existence of

intrinsic delay of state variables. The proposed control method is based on generalized-predictive control (GPC). However, the forced response of GPC is replaced by a feed-forward neural network in order to predict the state variables. The results show the enhancement of converter operation, especially at transients. Therefore, the proposed control methods make the inverter operation appropriate for grid-connected and NMG applications with multiple power reference changes due to energy sharing amongst MGs.

Future Work

The reliability of MG is a challenging topic, especially in hybrid MG integrated with renewable energies. This thesis has been developed to address challenging issues such as energy management in networked MG, the effect of energy sharing on the size of the components, the step-up converters to elevate the voltage level of renewable energies, and enhanced control method for Z-source inverter to improve the performance of the converter in transients.

However, the following topics can be addressed as future work:

- **Novel control strategies and energy management based on machine learning strategies:** microgrid clustering and associated tasks such as the integration of a considerable number of heterogeneous devices, real-time support, information processing, massive storage capabilities, security considerations, and advanced optimization techniques usage could take place in an autonomous and scalable energy management system architecture under a machine learning perspective.
- **Analyzing the effect of energy sharing on non-dispatchable units for grid-connected and isolation operating mode in NMG:** efficient energy management can propose an accurate procedure to evaluate the renewable energy generation economically in order to survey the possibility of RE size reduction in NMG.
- **Analyzing and investigating Z-source topologies to tackle the inherent restrictions:** Z-source converters propose a high voltage gain with low voltage stress for semiconductor devices; however, the high input current level and unidirectional operation of these converters make their application restricted for some specific purposes.
- **Investigation on multi-port converters for NMG:** multi-port converters are prone to propose an efficient solution for networked MG in order to share the energy amongst MGs. Multiple advanced control method such as MPC algorithms can exploit in these converters to enhance the converter operation.

Chapter 9

Publications

- **Neural Networks-Generalized Predictive Control for MIMO Grid Connected Z-Source Inverter Model**

Authors: Navid Salehi, Herminio Martínez-García, Guillermo Velasco-Quesada

Conference: EPE

Publication Date: 2022

- **Component Sizing of an Isolated Networked Hybrid Microgrid Based on Operating Reserve Analysis**

Authors: Navid Salehi, Herminio Martínez-García, Guillermo Velasco-Quesada

Journal: Energies

Special Issue "Development Strategies of Distributed Power Generation"

Publication Date: 2022/08/27

Journal Rank: CiteScore – Q1

Impact Factor: 3.252 (2021); 5-Year Impact Factor: 3.333 (2021)

- **Networked Microgrid Energy Management Based on Supervised and Unsupervised Learning Clustering**

Authors: Navid Salehi, Herminio Martínez-García, Guillermo Velasco-Quesada

Journal: Energies

Publication Date: 2022/07/05

Journal Rank: CiteScore – Q1

Impact Factor: 3.252 (2021); 5-Year Impact Factor: 3.333 (2021)

- **A comprehensive review of control strategies and optimization methods for individual and community microgrids**

Authors: Navid Salehi, Herminio Martínez-García, Guillermo Velasco-Quesada, Josep M Guerrero

Journal: IEEE Access

Publication Date: 2022/01/13

Journal Rank: CiteScore – Q1

Impact Factor: 3.476

- **A Novel Component Sizing Procedure in Off-grid Networked Microgrids**

Authors: Navid Salehi, Herminio Martínez-García, Guillermo Velasco-Quesada

Conference: 2021 International Conference on Electrical, Computer and Energy Technologies (ICECET)

Publisher: IEEE

Publication Date: 2021/12/09

- **Inverter Control Analysis in a Microgrid Community Based on Droop Control Strategy**

Authors: Navid Salehi, Herminio Martínez-García, Guillermo Velasco-Quesada, Encarnación García-Vílchez

Conference: 19th International Conference on Renewable Energies and Power Quality (ICREPQ'21)

Publication Date: 2021/09/01

- **Optimization of a Microgrid Integrated with Renewable Energies Using PSO**

Authors: Navid Salehi, Herminio Martínez-García, Guillermo Velasco-Quesada, Encarnación García-Vílchez

Conference: E3S Web of Conferences (ICREN 2020)

Publisher: EDP Sciences

Publication Date: 2021

- **Modified Cascaded Z-source High Step-up Boost Converter**

Authors: Navid Salehi, Herminio Martínez-García, Guillermo Velasco-Quesada

Journal: Electronics

Publication Date: 2020/11/17

Journal Rank: CiteScore – Q2

Impact Factor: 2.690 (2021); 5-Year Impact Factor: 2.657 (2021)

- **A Comparative Study of Different Optimization Methods for Resonance Half-Bridge Converter**

Authors: Navid Salehi, Herminio Martínez-García, Guillermo Velasco-Quesada

Journal: Electronics

Publication Date: 2018/12/02

Journal Rank: CiteScore – Q2

Impact Factor: 2.690 (2021); 5-Year Impact Factor: 2.657 (2021)

- **A Novel High Step-up Secondary Side Impedance Source Full-Bridge Converter**

Authors: Navid Salehi, Herminio Martínez-García, Guillermo Velasco-Quesada

Conference: SAAEI 2018: 25 Seminario Anual de Automática, Electrónica Industrial e Instrumentación

Publisher: International Centre for Numerical Methods in Engineering (CIMNE)

Publication Date: 2018